Letter from the Editors

Dear readers of *Acta Naturae*!

We are delighted to bring you the 26th issue of the *Acta Naturae* journal.

We kept to the traditional arrangement of the material and are publishing a number of reviews, research articles, and materials in the Forum section. The last one was written by a group of authors under the guidance of the head of the expert group "Life Sciences" of the Federal Targeted Program of Research and Development for 2014–2020, Andrey V. Lisitsa. The publication is devoted to the priority areas of development of the Russian scientific and technological complex and related issues of targeted funding of particular areas. The authors analyzed the various directions followed by researchers based on research proposals and projects submitted to the Ministry of Education and Science of the Russian Federation in 2013–2014. Undoubtedly, this publication will be of interest to the scientific community. The authors of the concept identified the following four lines of development: (1) personal genomics and post-genomic technologies; (2) possibility of integrating devices and materials with the body; (3) memory and brain plasticity; (4) bioactive substances. Apparently, we can expect the announcement of appropriate competitions in these topics in the future.

The reviews published in this issue are devoted to very topical areas of modern molecular biology and biomedicine. We publish a review by P.G. Georgiev et al. dedicated to optimizing conditions for the expression of recombinant proteins in eukaryotic systems. The review has both a fundamental and, obviously, applied significance and is closely in line with the data of a research article by N.B. Gasanov et al. devoted to the optimization of the expression of protein genes in Chinese hamster cells. This journal is largely focused on the issues of molecular oncology. A review by M.P. Kirpichnikov et al. (issues of PARP1 inhibitor design) and research articles by S.M. Deev et al. and O.E. Andreeva et al. deal with the issues of interaction between ligands and the HER2/neu receptor. We address the problems of regenerative medicine (review by E.S. Petrova) and innate immunity (article by T.V. Ovchinnikova et al.). We also do not ignore the issues of biochemistry and enzymology. In this regard, we recommend the classic article by V.I. Tishkov et al. devoted to formate dehydrogenases. In recent years, a number of authors have paid close attention to extracellular nucleic acids. There is evidence to suggest that these acids are important in the diagnosis of cancers at early stages. A review by P.P. Laktionova et al. is dedicated to extracellular nucleic acids in the urine. This issue also features articles concerned with topical issues such as HIV infection (S.N. Kochetkov et al.) and nootropics (S.B. Seredenin et al.).

The journal, in 6 years of its existence, has gained a degree of popularity among the scientific community. According to Thomson Reuters, the 2014 journal's impact factor is 1. This is a very good indicator for a Russian journal with a three-year history of open access for readers in the PubMed system. We strive to maintain these gains. We expect to announce the acceptance of short communications, including medical reports. At the same time, we ask authors to be very meticulous regarding the quality of submitted manuscripts and focus on important aspects of evidence-based medicine. We will also continue publishing articles in the field of classical biochemistry and molecular biology. The Editorial Council and Editorial Board recently adopted a decision to carry out preliminary selection of articles from new submissions. Therefore, we cannot guarantee complete reviewing of all submitted manuscripts. Some of them will be rejected at the stage of preliminary review by the Editorial Board.

We look forward to receiving your papers and guarantee a fair and impartial review. ●

The Editorial Council
Editorial Board

INNOVATION RUSSIA

Discussion club

We create a dialogue between all socially active groups of people: students, scientists, lecturers, businessmen, managers, innovators, investors, designers, art critics, architects, photographs.

Learn more at WWW.STRF.RU

Everyone with something to say and ideas to share is welcome to visit our events

Tel.: +7 (495) 930-87-07, 930-88-50
E-mail: seminar@strf.ru

Additivity of the Stabilization Effect of Single Amino Acid Substitutions in Triple Mutants of Recombinant Formate Dehydrogenase from the *Glycine Max* Soybean

A. A. Alekseeva, I. S. Kargov, S. Yu. Kleimenov, S. S. Savin, V. I. Tishkov

Recently, we demonstrated that amino acid substitutions A267M and A267M/I272V, as well as F290D, F290N, and F290S, in recombinant formate dehydrogenase from the *Glycine max* soybean (SoyFDH) lead to a 30- to100-fold increase in the thermal stability of the enzyme. Substitutions F290D, F290N, and F290S were introduced into double mutant SoyFDH A267M/I272V. Combinations of three substitutions did not lead to a noticeable change in k_{cat} and K_M. The stability of the mutants was studied using thermal inactivation kinetics and DSC. The stability of the new mutant SoyFDHs was shown to be much higher than that of their precursors. The obtained results indicate the great synergistic contribution of single substitutions to enzyme stabilization.

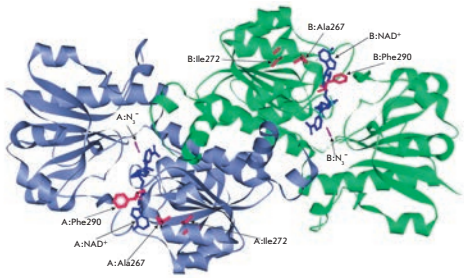

Three-dimensional structure of a ternary complex [SoyFDH-NAD$^+$-N_3^-]

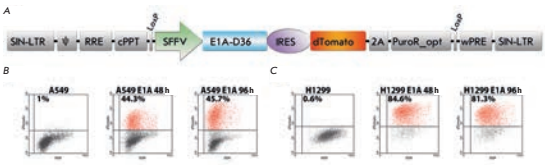

Model cell lines

Regulation of Human Adenovirus Replication by RNA Interference

N. A. Nikitenko, T. Speiseder, E. Lam, P. M. Rubtsov, Kh. D. Tonaeva, S. A. Borzenok, T. Dobner, V. S. Prassolov

Adenoviruses cause a wide variety of human infectious diseases. Currently, there are no selective anti-adenoviral drugs. Potential targets in developing therapeutic agents are human adenovirus early genes, such as the DNA polymerase gene *E2B* and *E1A* gene, which play an important role in viral DNA replication. The present paper suggests an approach to effective down regulation of the replication of human adenoviruses using RNA interference.

Internalization and Recycling of the HER2 Receptor in Interaction of the Target Phototoxic Protein DARPin-miniSOG with Human Breast Adenocarcinoma Cells

O. N. Shilova, G. M. Proshkina, E. N. Lebedenko, S. M. Deev

Elucidation of the mechanisms of interaction between target proteins and receptors of cancer cells is an important prerequisite for the development of effective methods of cancer therapy. The interaction of the recombinant phototoxin DARPin-miniSOG with human breast adenocarcinoma cells overexpressing the human epidermal growth factor receptor 2 (HER2) was studied. DARPin-miniSOG was found to bind specifically to the HER2 receptor and cause its internalization, followed by slow return of the receptor onto the cell membrane.

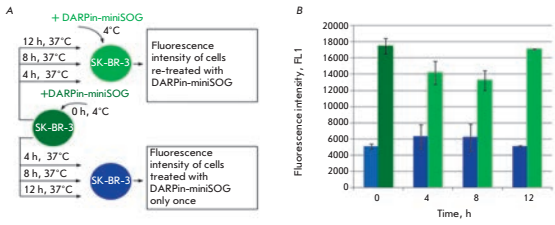

Interaction between the protein DARPin-miniSOG and the HER2 receptor of SK-BR-3 cells

ActaNaturae
JULY—SEPTEMBER 2015 VOL. 7 № 3 (26)

Founders
Ministry of Education and
Science of the Russian Federation,
Lomonosov Moscow State University,
Park Media Ltd

Address: 119234 Moscow, Russia, Leninskiye Gory, Nauchny
Park MGU, vlad.1, stroeniye 75G.
Phone/Fax: +7 (495) 727 38 60
E-mail: vera.knorre@gmail.com, mmorozova@strf.ru,
actanaturae@gmail.com

Номер подписан в печать 30 сентября 2015 г.
Тираж 200 экз. Цена свободная.
Отпечатано в типографии «МЕДИА-ГРАНД»

Indexed in Pubmed, Web of Science, Scopus, and RISC

CONTENTS

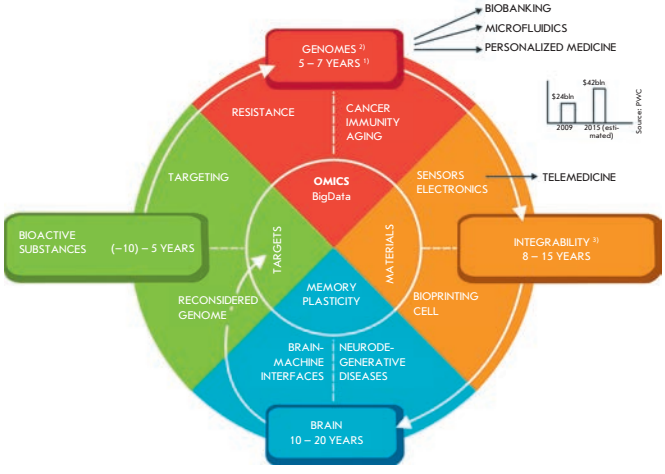

IMAGE ON THE COVER PAGE
Life sciences in Russia: a concept of research and development for 2014–2020. (See an article by Miroshnichenko *et al.*)

Life Sciences in Russia: Priorities in 2014-2020

Yu. V. Miroshnichenko[1]*, M. A. Prostova[2], A. V. Kvetinskaya[3], A. V. Lisitsa[1]
[1]Institute of Biomedical Chemistry, Pogodinskaya Str., 10/8, Moscow, 119121, Russia
[2]Chumakov Institute of Poliomyelitis and Viral Encephalitides, Kievskoe Shosse, 27 km, Moscow Region, 142782, Russia
[3]Non-commercial Partnership "Technology Platform – Medicine of the Future", Akademicheskiy Prosp., 8/8, Tomsk, 634055, Russia
*E-mail: yuliana.miroshnichenko@gmail.com

ABSTRACT **Life sciences are a priority in scientific development in Russia. The scientific interests of Russian research teams working in this area cover a range from the design of devices to sophisticated molecular biological experiments. The concept of implementation of the Life Sciences was developed based on proposals for research topics and projects submitted to the Ministry of Education and Science of the Russian Federation in 2013–2014. The concept defines four major directions of developments: (1) personal genomics and post-genomic technologies; (2) integrating devices and materials with the body; (3) memory and brain plasticity; and (4) bioactive substances.**

KEYWORDS **big data, biomaterials, implantable devices, sciences, neurosciences, postgenome technologies.**

ABBREVIATIONS **Programme – Federal Programme for Research and Developments in of Russian; Proposal – proposal for research topics and projects under the Federal Programme for Research and Developments in of Russian; Call – competitive offer for conducting applied research under the Federal Programme for Research and Developments in of Russian.**

In accordance with the Order of the President of the Russian Federation, applied research has been financed from the Federal Programme for Research and Developments in of Russia (hereinafter the Programme). The Programme supports projects focused on achieving clear characteristics of the developed products, meeting a specific consumer of these products, and a business partner ready to co-finance the development and sell the product in the future [1].

The Expert Group for the Life Sciences (hereinafter the Expert Group), in collaboration with the Russian Ministry of Education and Science, Directorate of Scientific and Technical Programmes, and Technological Platforms "Medicine of the Future" and "BioTech2030," has established promising research directions for the Russian Federation. The directions were unified into The Concept of Life Sciences in 2014–2020 (hereinafter Concept).

The Concept was developed based on an analysis of proposals for research topics and projects collected by the Russian Ministry of Education and Science (hereinafter Proposals) with alignment with modern research trends. The Expert Group identified effective research teams capable of conducting advanced research and obtaining results in cooperation with a business partner. These research teams should have a significant history of publications as proof of experience and groundwork and be competent to prepare a design and technical documentation in accordance with the requirements of The Unified System of Technological Documentation. Otherwise, the project results will be unsuitable for further practical use, which means ineffective spending of budget funds.

This article presents the basic directions of Life Sciences and summarizes examples encountered in the work of the Expert Group.

MECHANISMS USED BY THE EXPERT GROUP TO ANALYZE PROPOSALS

The Expert Group is composed of researchers and engineers. Representatives of technology platforms, the business community, universities, and state customers of the Programme were included in the Expert Group as well. Members of the group were chosen based on bibliometric indicators but also on their willingness to make quick decisions and remain permanently involved in the group's activity, all of which was dictated by the large number of proposals (over 50 per month) submitted for consideration. For example, the processing time by a scientist with a h-index above 40 exceeds the Programme's allotted time. The following ten-

dency was observed: the higher the expert's h-index, the lower the expert's activity is during the analytical assessment of proposals that are outside the scope of his narrow competence. Within the sphere of the expert's competence, the only result of the expert activity in the vast majority of criticism of potential competitors.

One of the main activities of the Expert Group is selection and preparation of topics for competitive calls to conduct applied research and experimental developments (hereinafter Call). Preparation of a Call is carried out on the basis of consideration of the Proposals registered in the information system of the Programme (http://tematika.fcpir.ru). When submitting a Proposal, the initiator should provide basic information about the project, which includes substantiation of the project implementation and the need for funding from the federal budget; a list of publications reflecting the scientific level of the expected results and characterizing the technological background conducted by the team in the field of research.

During the preparation of the Call, members of the Expert Group need to assess the possible risks associated with the subsequent implementation/non-fulfillment of work at the expense of federal budget funds. Therefore, a crowdsourcing mechanism was used. The Proposals that were deemed to be the most promising were posted on the web site of the Expert Group (http://rgls.wikivote.ru/), which is used as a tool to discuss expert opinions. There, the Proposals were accompanied by a brief description of the planned activities, publications supporting scientific and technological experience, and draft of the project statement.

The validity and feasibility of the topic was proved by publications in journals with an impact factor of at least 0.8 for the last 5 years. Proposals that were not supported by related publications of Russian teams were excluded, since this situation indicated a lack of competencies in the Russian Federation required for implementation of the project. Also, we excluded Proposals whose project statement did not contain numerical indicators of achieved results, or lacked a comparison with experimental (published article or patent) and/or industry analogues (or the absence of analogues was indicated).

The Expert Group analyzed the Proposals received under the arrangements 1.2 and 1.3 of the Programme[1] and rejected about 20% of them because of a lack of references to applicants' publications confirming the scientific potential in the area of the proposed research topic. PubMed search was used to reveal any experience of the initiators in the field of life sciences.

Other Proposals were rejected because of a lack of the information necessary for an objective peer review. Despite compliance with the formal requirements for preparation, consistent presentation, and seemingly outstanding ideas, their relation to experimental work and feasibility of the project implementation raised doubts. We may assume that these Proposals were prepared by persons not related to practical research. The amount of requested funds in many Proposals, including those satisfying the basic requirements, often exceeded the actual capabilities of the Programme. In this regard, the Proposal selection principles were developed and included in the main document (Concept) underlying the Expert Group's activity.

According to these principles, promising topics were brought up for discussion by the Expert Group, and their initiators made a report to substantiate the key positions of the stated topic. The main decision criteria were as follows: 1) compliance with modern international scientific trends, 2) result that has potential impact on the economy, 3) availability of an industrial partner interested in the result, 4) availability of Russian research teams working in the particular field, and 5) support of a specific technology platform[2].

Proposals were voted on by experts of the group and were numerically scored. Seventy-two per cent of the Proposals picked up for discussion received a positive score. In this case, generalization of the initial topic formulation and objective were performed at the stage of preparing the Call. This was done due to the requirement of the Russian Ministry of Education and Science for competition of several research teams. In other words, the Expert Group generated Call so that they could fit a rather broad interpretation of the requirements necessary to achieve the result. This approach enabled the participation of many teams in competitions held by the Russian Ministry of Education and Science and, thereby, expanded the possible range of participants from the scientific community to select the most competitive contractors. It's worth noting that the selection of contractors was carried out without participation of the Expert Group.

Generally, 341 Proposals under the 1.2 arrangement (research) and 214 Proposals under the 1.3 ar-

[1] *The arrangement 1.2 means conducting applied research for the development of industries. The arrangement 1.3 means conducting applied research and developments aimed at creating products and technologies.*

[2] *The technology platform is a communication tool aimed at intensifying efforts to develop advanced commercial technologies, new products (services), attracting additional resources for research and development through the participation of all stakeholders (government, business, science and education), as well as improving the legal framework in the field of scientific and technological development and innovation (source: www.hse.ru).*

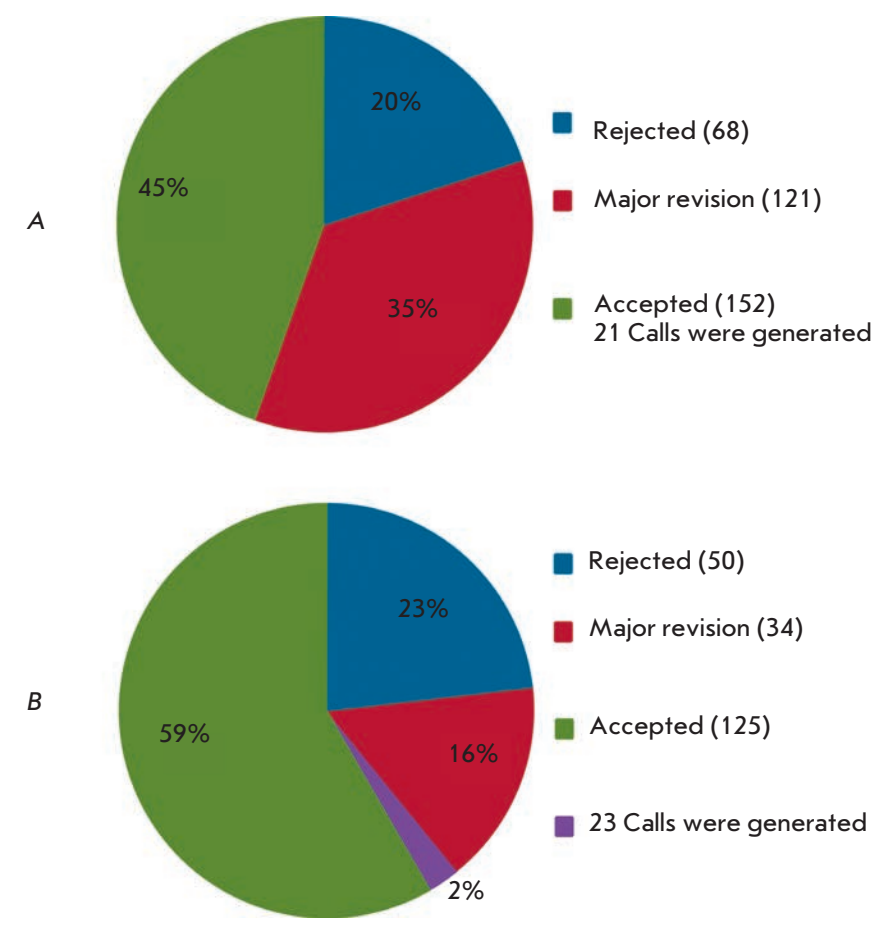

Fig. 1. The distribution of submitted Proposals: (A) research, (B) research and development

rangement (research and developments) were processed in the period from November 2013 to the end of 2014. On the basis of 152 Proposals (45% of the total), 21 research Calls were issued. On the basis of 125 Proposals (59% of the total), 23 research and development Calls were produced. The Proposal distribution is shown in *Fig. 1.*

THE CONCEPT ROLE IN THE SCIENTIFIC AND TECHNOLOGICAL DEVELOPMENT

The spectrum of Proposals submitted to the Expert Group was used to formulate the strategic directions (*Fig. 2*). The selected directions were considered topical to the Programme for the following reasons:

1) availability of recent publications on the topics of each area in peer-reviewed journals;

2) availability of Russian strong, dynamic research teams engaged in the appropriate areas, whose expertise is confirmed by publications; and

3) a set of particular products for a real sector of the economy[1] are expected as a result of the implementation of projects in these areas.

The submitted Proposals may be divided into two categories: medical sciences and life sciences. Despite division is artificial, it was necessary because the Expert Group should not implement tasks that are under the cognizance of the Ministry of Health of the Russian Federation. Therefore, the development of medical technology, medical devices, and pharmaceuticals was not included in the Concept. This separation is also due to the specialization of members of the Expert Group. Inclusion of researchers with a high h-index in the Expert Group naturally led to a shift in emphasis towards molecular and cellular biology.

The diagram in *Fig. 2* depicts four sectors corresponding to the strategic directions of the Concept: Genomes, Integrability, Brain, and Bioactive substances. The first strategic direction of the Concept, Genomes, is dedicated to post-genomic technologies. It includes large-scale studies of genomes/transcriptomes/proteomes that offer a selection of strategies for individual diagnosis and/or therapy. The sector is characterized by priority issues, such as the resistance of tumors and infections to treatment, carcinogenesis, immune system disorders, and aging. It is important to emphasize that the prioritization within the sector is not related to the social significance of diseases but indicates models where post-genomic research should demonstrate its effectiveness.

Let us illustrate the logic of the application of the priorities of the Genomes sector with the example of carcinogenesis. A project whose stated aim was to reduce incidence and mortality from cancers or choice of individual chemotherapy would not match the Concept. The quality of implementation of these clinical problems should be monitored by the relevant executive authority, i.e. by the Ministry of Health. On the other hand, a project aimed at decoding tumor genomes and identifying mutations specific to the Russian population is entire-

[1] *A real sector of the economy is a set of industries that produce tangible and intangible goods and services, excepting financial, credit, and exchange operations. This is a footnote*

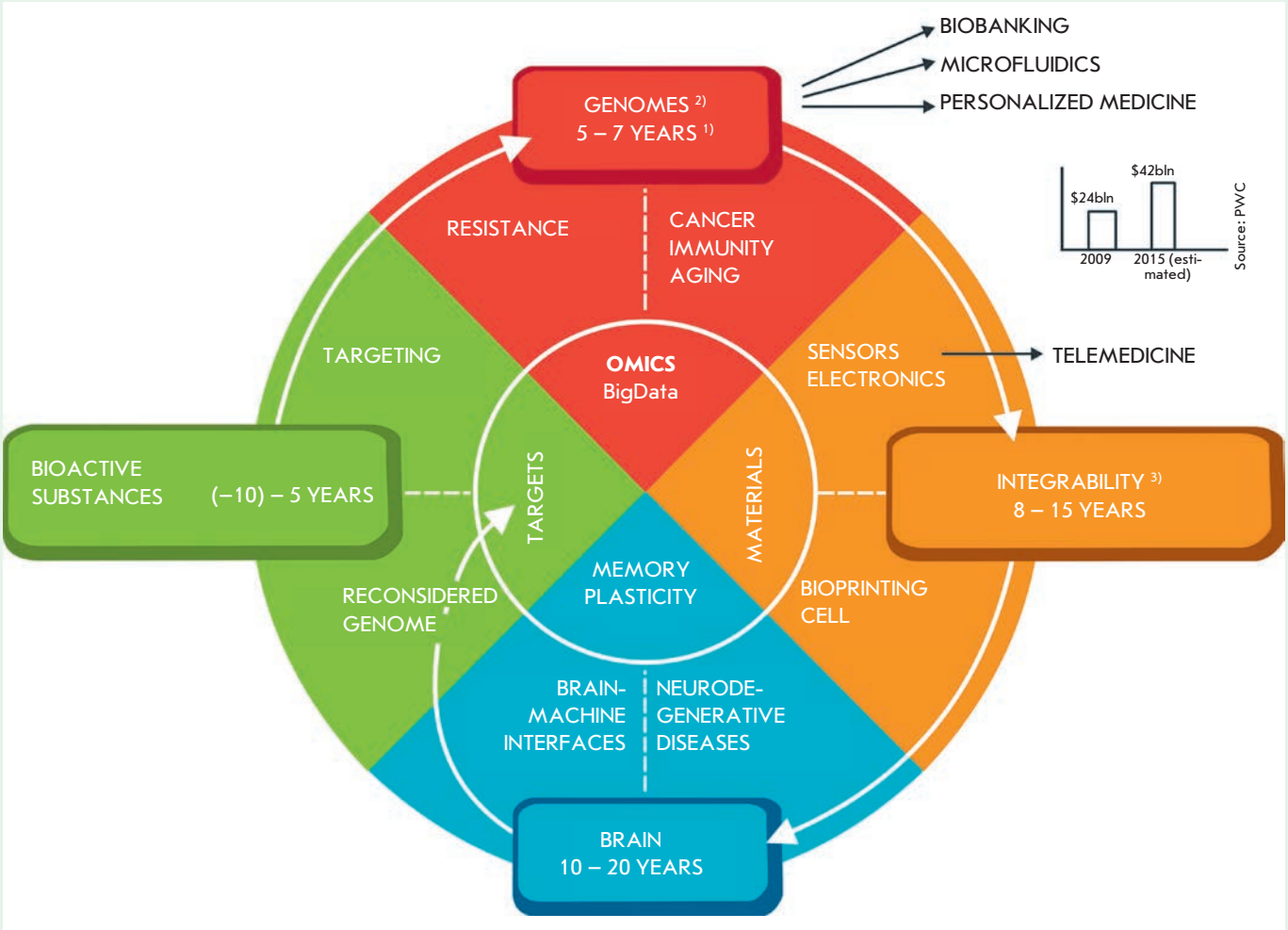

Fig. 2. The Concept of Life Sciences in 2014–2020. (1) Periods of the anticipated economic effect are depicted. (2) Personal genomics and post-genomic technologies. (3) Implantable devices and materials

ly consistent with the Concept. In this case, the result of the project will be a verified database of specific mutations, i.e. a tool for solving the previously mentioned clinical problems of oncological diseas. The quality of the result, in turn, will be evaluated by an industrial partner interested in the transition from applied research to the commercial product. Since a database of oncogenes can be used to solve diverse problems, it will be the case of implementation of the principle of multi-disciplinary development, which is in line with world trends in the development of medical sciences [2].

We emphasize that the Programme is open also for clinical studies: the prescriptive way is provided for this purpose based on an agreement between the Russian Ministry of Education and Science and another interested executive authority (in life sciences, it is primarily the Ministry of Health and Ministry of Agriculture of the Russian Federation). A Call is announced for a specific topic proposed by a federal authority. Many scientific directions were excluded from the Concept due to the presence of a prescriptive way to form such Calls. These include devices for diagnosis and treatment, medical technologies, clinical, preclinical and epidemiological studies, and software and hardware for medicine and health. Also, the Concept did not include analytical instrumentation, biodiversity and bioremediation, monitoring and protection of the environment, and functional foods and GMOs. Studies in these areas are initiated by the relevant authorities, but not by the Expert Group.

The Genomes sector (*Fig. 2*) also illustrates well the principles of practical implementation of the Concept. For example, a biobanking project cannot serve as a topic of the Call, because this is a large-scale infrastructure task. At the same time, any well-designed project to study biological material using genomic and post-genomic technologies will contribute to the standardization of the protocols of the sampling, transportation and storage of materials. Similarly, the need for automation and unification of sample preparation stages will contribute to the development of microfluidic devices. Finally, the results of applied research in the Genomes sector are expected to be used in the field of personalized medicine. According to a prognosis by Price Waterhouse Coopers, the personalized medicine market will be worth 42 billion US dollars by 2016.

For understanding the Concept's structure it is important to account for the trends of modern biotechnology. A biotechnology company has no access to the market of medical services or medical devices, since this sector is occupied by large corporations. It is impossible to compete with corporations like Pfizer, AstraZeneca, Bayer, etc., since the entire federal budget of the Life Sciences is less than 1% of the pharmaceutical industry's expenditure on research and development. However, there is no need for such competition, since growth in the biotechnology sector in the biopharmaceutics and biomedicine areas in the XXI century is achieved through the development and improvement of technologies. Human genome mapping has led to the creation of 310,000 new jobs and created, with the investment of 3.8 billion dollars, a market 10 times larger [3]. In this case, the genome, in terms of medicine, was in demand in rather limited use. Today, genome mapping technologies are more interesting to IT companies than to physicians: for example, Google has launched its Baseline Study project [4].

What is the output of the Programme in the area of Life Sciences? It would be speculation to say that it is people's health or the treatment of patients. It takes decades to implement a real result of clinical application. This matches neither the time nor financial frameworks of the Programme. Any Proposal of this kind is automatically qualified as not matching the format of the Programme and is rejected.

At the same time, Proposals of an exploratory kind also do not match the format of the Programme, which requires an application-oriented deliverable. Things useful for research may be such an intermediate result. In fact, the product is "a set of tubes" and the instruction on how to use this set to conduct scientific research. Actually, a high market growth rate is attributable to such reagent kits but not to "test kits for early cancer detection" or "medications for the cardiovascular system." For example, Luminex company provides dynamic capital growth of 30–40% (this means that if you bought the company shares for 100 thousand rubles in 2014, you could sell them for 130–140 thousand rubles in 2015). Turning to the 2013 Luminex financial statement (http://investor.luminexcorp.com), we see that much of its growth (72%) came from orders for reagent kits, while plate reader sales and the sector of health services accounted for about 10 and 5%, respectively. In the letter case, innovative medical services are provided in the CLIA format (www.cdc.gov/clia/), which is the system of health services registration. Russia has no analogues of such a system.

The narrow window of opportunities available to Russia in the field of genomic and post-genomic technologies is based on the related concepts of "big data" and "omics-science" (*Fig. 2*). The concepts are based on the paradigm of processing someone else's information, rather than on generating original datasets. A fundamentally important contribution to the development of post-genomic data processing was made by Yandex company [5], which provided long-term "buoyancy" of Russian developments in the field of bioinformatics.

The second strategic direction of the Concept is "Integrability" (*Fig. 2*). This sector represents a tendency to implant artificially created stuffs in to the human body. This sector includes cellular technologies, microelectronics, and micro- and nanoelectromechanical systems (MEMS and NEMS, respectively). An example of a development that would have been appropriate in the sector 3–4 years ago is a micro-device converting the heart's motion energy into electrical energy [6]. Currently, the gap in the bio MEMS area is not critical for Russian science, so the Expert Group considers projects from this area within the Concept.

Reprogrammed cells are of interest as a part of projects on tissue engineering, and this process should be performed on bioresorbable matrices formed by bioprinting [7]. Within this task, the Expert Group gave up on stem cells and the development of prostheses for orthopedics and maxillofacial surgery. Similar projects were substantially funded by the 2009–2013 Programme and are currently funded under the federal targeted programme Pharma 2020. Therefore, they were excluded from the Concept.

As in the sector of Genomes, in the sector of Integrability is marked by the basic technology – materials, where Russia can compete. Demand for this area depends on whether

researchers developing new materials can switch to a new format where a clinical problem, which is solved through creation of a high-technology device, applies the requirements to the properties of new materials. But not vice versa, when medical challenges are adjusted to the possibilities of creating new materials. This approach is relevant not only in materials science. The Concept means that advances in chemistry and physics are not what should define life sciences, but on the contrary, life sciences should specify the problem for nanotechnology, laser physics, high energy physics, as well as for electronics and circuit engineering. For professionals who are not biologists (e.g., materials scientists), this approach is a paradigm shift. In fact, they cannot be project leaders in life sciences but should limit themselves to the role of subcontractors.

The third strategic direction of the Concept, "Brain," was formed under the influence of the largest projects of our time: the American Connectome project [8] and the European Brain project [9]. The horizon of implementation of this key area is 20–30 years, i.e. the main experts living in this country will reach retirement age by the time of project implementation.

Investment into this research area in America, Europe, and Japan exceeds Russian expenses by more than 2 orders of magnitude. In the Russian Federation, there is experience of investment into the field of drug treatment of neurodegenerative diseases that is limited to two products: Dimebon (withdrawn from clinical trials by Pfizer [10]) and Semax, which was not interesting to major pharmaceutical companies, although the first publication dates back to 2000 [11].

The terms of memory and plasticity were taken as the basis of the strategic Brain direction in the described Concept. Investigation of the brain's properties will allow us to, if not close then, at least not widen the gap with more advanced countries. The direction became part of the priority research problems set forth by the Russian Ministry of Education and Science [12]. Brain sector Calls are oriented toward the development of tools to study and manage the living brain activity. Currently, there is a Russian research group that has learned and implemented optogenetic techniques in freely moving animals [13]. The next step is the development of tools for simultaneous transmitting and recording of a signal upon studying the mechanisms of memory and other cognitive processes. The brain responses recorded for different activities of a freely moving organism will form a large data array requiring supercomputers with a new architecture [14]. Today's markets in the field of eye-brain-computer neurointerfaces for game consoles and managing "a smart home" have already been formed [15, 16]. Brain activity reading will also be crucial for assessing the quality of presenting audio and video advertising (neuromarketing), training and coordinating co-working teams, and accelerated foreign language training [16].

The fourth strategic direction of the Concept is "Bioactive substances." In Russia, there are a number of professional companies committed to the biotechnology market and with the necessary capabilities. These include Biocad, R-Pharm, Generium, Microgen, and PharmEco, and others. Within the Programme, biotechnology companies can be involved only in inventions that are based on the molecular mechanisms of interactions of proteins, antibodies and peptides with living cell. Nontargeted drug delivery, creation of liposomal forms, development of long-acting biopolymer-based systems, gene therapy, investigation of small molecules, and screening of combinatorial libraries are areas of high patent activity, which means that developments in these areas should either be implemented under the federal targeted programme Pharma 2020 or be excluded from the priorities of scientific and technological development.

DEMAND FOR APPLICATION-ORIENTED RESULTS IN THE FIELD OF LIFE SCIENCES

The field of Life Sciences is a multisided area that can be characterized as "an infinitely small point" between the public tasks of the scientific institutions of the Federal Agency for Scientific Organizations and Ministry of Health and Ministry of Agriculture of the Russian Federation, as well as between the federal targeted programme Pharma 2020 supervised by the Russian Ministry of Industry and the programme Basic Research for Medicine of the Russian Academy of Sciences and grants of the Russian Foundation for Basic Research in the areas of medicine and biology. This "small point"can be transformed to the field of development of the scientific and technological potential when teams confirming their qualification by publications. In biomedical sciences, publication of well-cited papers in high impact factor journals is a basic skill [17].

The Proposals analyzed by the Expert Group reflect, to some extent, the current state of the Russian scientific community: the presence of great academic ideas but a lack of skills in structuring, planning, and achieving the desired result. It should be stressed that the Expert Group treats publications not as the assessment of the scientific viability of the project idea but as proof that the project's initiator is able not only to begin research, but also to bring it to conclusion.

The process of selection of the project topics under the Pro-

gramme is based on crowdsourcing combined with expert evaluation of results. Formulation of the described strategic directions of the Concept depended on the number of Proposals received from the scientific community. The expert could not add an idea to the Concept if it did not have three or four Proposals in the information system. Most Proposals that were submitted and then discussed at a meeting of the Expert Group were not relevant due to the impossibility of constructive analysis of the submitted information.

The result of applied research of the Programme should be specific products capable of competing worldvide. This requires efficient interaction of the scientific community with designers and engineers to transit from the searching science format to the applied science format. Involvement of technology platforms with an internal system of topic consideration facilitates the formation of the researcher + engineer + industrial partner = applied result.

Getting an applied result is economically justified if there is an interested business who is capable to use the result. Who is this industrial partner? The Programme is opened to companies that are consumers of the technological result, e.g. Evrogen, Syntol, or DNA Technology. The annual turnover of business partners of Programme projects ranges from tens to hundreds of millions of rubles. So we are not talking about huge company, vertical holdings, or about contribution to the development of entire industries. In life sciences, the market in the next 10–20 years will be a niche market and success in this market will depend on the capacity to master intelligent production technologies.

Prediction of the development of new market niches can be achieved by analyzing global databases, such as the database of the scientific publications Web of Science (WoS) and the Orbit patent database [18]. Keyword search reveals the dynamics of publication and quotation activity, i.e. provides an idea whether interest of the world scientific community in a given topic is growing or declining. The dynamics of patent applications filed and patents issued indicates technological trends. The analysis provides an assessment of the potential for entering the real economy by comparing the number of patents owned by universities and companies.

The problem of automatic foresight adoption is the dependence of the result on the way of formulation of keyword search. The results of an analysis are equally uninformative in the case of both wide and too narrow search patterns. In this case, co-operation with experts who offer variants for correcting of keyword search, as exemplified in *Fig. 3*, turned out to be effective. The initial version of the Lot received 20 out of 100 possible points. After correction of keyword search, the rating amounted to 55 out of 100 points.

According to the results of an analysis of topics proposed by the Expert Group, it can be concluded that drugs, diagnostic tools, and other products for medical and agricultural purposes cannot be the Programme's priority. The Programme, as a part of the Life Sciences area, offers a unique opportunity to develop something essential to the applicant for further self-development. Then, there is a chance that the development will be in demand not only to the applicant but also from other groups working around the world. If practical implementation of the project results is not planned after its completion, that does not qualify to the current Programme requirements.

PERSPECTIVES OF THE CONCEPT

Comparing the Concept with a technological development overview published by the Massachusetts Institute of Technology [19], it is possible to identify coincidence of the strategic directions of the Concept with key trends: modeling the brain, predictive medicine, bioprinting, BigData, digital medicine, and mobile health. This indicates that there are Russian researchers capable of capturing future trends. At the same time, most actively and successfully working in their fields specialists although "catch" breakthrough direction, but do not admit implementation of a breakthrough without personal involvement and control.

In life sciences, the situation of self-setting the problem (appropriate for the Russian Foundation for Basic Research and Russian Scientific Foundation but unacceptable for the target method of Programme implementation) can be solved through the mechanism of multiple "umbrella" Calls offered by the Ministry of Education and Science of the Russian Federation. These Calls are designed for several winners (contractors). The Call topic, for which there is no competition, should be considered inconsistent. For example, if a single application is filed for the Call, then this competition was likely created artificially, without regard for the possibility of further development of the proposed idea. Unfortunately, such examples appeared in 2014 (in particular, competitions aimed at studying single cells (single-cell-omics), creating non-invasive neurostimulators, and deciphering animal genomes).

The information system of the Programme continues to receive Proposals that are analyzed by experts of the group. The Concept will be changed based on newly received Proposals and the permanently changing picture of the develop-

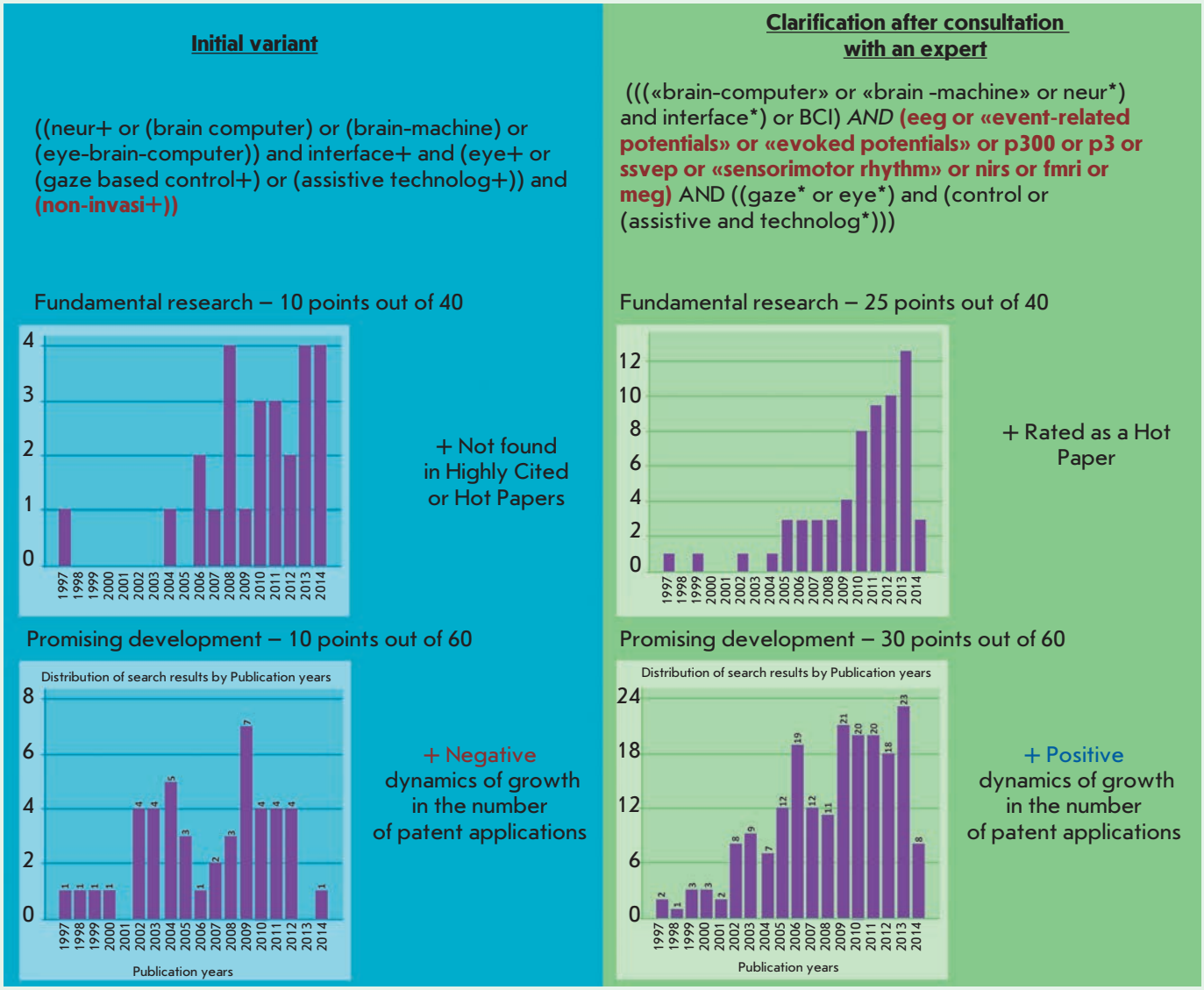

Fig. 3. The effect of keyword search on the results of an analysis of the databases Web of Science (Fundamental research) and Orbit (Promising development)

ment of modern science. On the basis of the analytical capabilities of some scientists to predict far in advance, it is possible to form general topics, since they become landmarks for submitting subsequent Proposals, to support in the framework of these topics not only (or even mainly) leading teams with an established reputation, but also second-tier groups that are ready to enter new areas. Selection among the latter is made based on the quality of Proposal preparation. The training of qualified second-tier professionals requires additional stabilizing efforts in the period of Programme execution, since the conditions of formation of research topics and projects should remain unchanged during the next few years. ●

The authors thank N.G. Kurakova, head of the Department of Scientific and Technological Forecasting in the Field of Biomedicine of the Federal Research Institute for Health Organization and Informatics of the Ministry of Health of the Russian Federation, for assistance in working with the database of scientific publications Web of Science (WoS) and the Orbit patent database; V.V. Burov, Chairman of the Board of Directors of WikiVote!, for provision of an electronic platform for Expert Group activities.

REFERENCES
1. Shatalova N. “The advantages of the new format. Changes in the Federal Targeted Programme did it good”. // Weekly newspaper of the scientific community “Search”. 2014. № 29–30.
2. The Directive of the Government of the Russian Federation of 28.12.2012 № 2580-r “On approval of the Strategy of development of medical sciences in the Russian Federation for the period till 2025”.
3. Hood L.E., Omenn G.S., Moritz R.L., Aebersold R., Yamamoto K.R., Amos M., Hunter-Cevera J., Locascio L. // Proteomics. 2012. V. 18. № 12. P. 2773–2783.
4. Esakova P. “Google launched a project to study human genetics”. // Information Agency RBC. URL: http://top.rbc.ru/society/25/07/2014/938993.shtml (accessed: 26.07.2014).
5. School of data analysis by Yandex. URL: https://yandexdataschool.com/ (accessed: 26.07.2014).
6. Dagdeviren C., Yang B.D., Su Y., Tran P.L., Joe P., Anderson E., Xia J., Doraiswamy V., Dehdashti B., Feng X. et al. // Proc. Natl. Acad. Sci. USA. 2014. V. 5. № 111. P. 1927–1932.
7. Bertassoni L.E., Cecconi M., Manoharan V., Nikkhah M., Hjortnaes J., Cristino A.L., Barabaschi G., Demarchi D., Dokmeci M.R., Yang Y. et al. // Lab on a Chip. 2014. V. 13. № 14. P. 2202–2211.
8. Human Connectome Project. URL: www.humanconnectomeproject.org/ (accessed: 26.07.2014).
9. Human Brain Project. URL: https://www.humanbrainproject.eu/ (accessed: 26.07.2014).
10. “Medivation and Pfizer Announce Results from Phase 3 Concert Trial of Dimebon in Alzheimer’s Disease”. // Pfizer 16.01.2012. URL: http://www.pfizer.com/news/press-release/press-release-detail/medivation_and_pfizer_announce_results_from_phase_3_concert_trial_of_dimebon_in_alzheimer_s_disease (accessed: 18.06.2015).
11. Levitskaya N.G., Sebentsova E.A., Glazova N.Yu., Voskresenskaya O.G., Andreeva L.A., Alfeeva L.Yu., Kamenskii A.A., Myasoedov N.F. // Dokl. Biological Sciences. 2000. V. 372. № 1–6. P. 243–246.
12. The list of priority scientific problems whose solution requires the use of the Federal centers for collective use of scientific equipment. URL: http://government.ru/orders/10326 (accessed: 26.07.2014).
13. Doronina-Amitonova L.V., Fedotov I.V., Ivashkina O.I., Zots M.A., Fedotov A.V., Anokhin K.V., Zheltikov A.M. // Scientific Reports. 2013. V. 3: 3265.
14. Gorbunov V., Elizarov S., Korneev V., Latsis A. // Supercomputers. 2014. V. 17. № 1. P. 24–28.
15. Marsman J.B., Renken R., Velichkovsky B.M., Hooymans J.M., Cornelissen F.W. // Human Brain Mapping. 2012. V. 33. № 2. P. 307–318.
16. Mokienko O.A., Chervyakov A.V., Kulikova S.N., Bobrov P.D., Chernikova L.A., Frolov A.A., Piradov M.A. // Frontiers in Computational Neuroscience. 2013. V. 7. P. 168.
17. Girsh E. “The victory of molecular biology over common sense”. // Polit.ru. URL: http://polit.ru/article/2013/12/12/hirsch_about_hirsch/ (accessed: 26.07.2014).
18. Bykova N. “Scientific review will be performed automatically”. // Science & Technology of the Russian Federation. URL: http://strf.ru/material.aspx?CatalogId=223&d_no=81544#.VYLyzEYppun (accessed: 26.07.2014).
19. MIT: 2013 Emerging Trends Report. // Special Issue. MIT Technology Review. Open Innovations Forum and Exhibition. 2013. URL: http://oneglobalonline.com/k/docs/MIT_Technology_Review_2013.pdf (accessed: 22.09.2015).

Regulatory Elements in Vectors for Efficient Generation of Cell Lines Producing Target Proteins

O. Maksimenko, N. B. Gasanov, P. Georgiev*
Institute of Gene Biology, Russian Academy of Sciences, Vavilova str. 34/5, 119334, Moscow, Russia
*E-mail: georgiev_p@mail.ru
Received 14.04.2015

ABSTRACT To date, there has been an increasing number of drugs produced in mammalian cell cultures. In order to enhance the expression level and stability of target recombinant proteins in cell cultures, various regulatory elements with poorly studied mechanisms of action are used. In this review, we summarize and discuss the potential mechanisms of action of such regulatory elements.
KEYWORDS insulators, recombinant proteins, protein production in mammalian cells, UCOE, S/MAR, STAR.
ABBREVIATIONS AND TERMS RP – recombinant protein; CHO – Chinese hamster ovary cells; UTR – untranslated gene region; kbp – a kilobase pair, a unit of length of nucleic acids equal to 1,000 base pairs; S/MAR – DNA sequences corresponding to nuclear matrix-attachment regions; insulators – regulatory elements that block interaction between enhancer and promoter; UCOE –regulatory elements containing strong promoters of housekeeping genes; STAR – regulatory elements protecting from HP1-dependent repression; MSX –L-methionine sulphoximine; MTX – methotrexate.

INTRODUCTION

Therapeutic proteins are major structural and regulatory molecules essential for a normal functioning of the human body. Part of recombinant proteins that are small in size and do not require additional modifications are produced in the most economical bioreactor – *E.coli* cells. However, the production of proteins in bacteria is associated with a number of limitations: disrupted folding of some proteins, absence of crucial modifications, and the inability to produce larger molecules [1, 2]. Some of these limitations are avoided when using yeast cells, which can produce high-quality recombinant proteins at sufficiently low cost. However, many recombinant human proteins require specific modifications that can only be obtained in higher eukaryotic cells [3]. Therefore, nowadays there is an increasing number of drugs obtained from mammalian cell cultures grown in bioreactors, mostly Chinese hamster ovary (CHO) cells [4, 5]. CHO cells were first isolated in 1957 [6]. It soon became evident that these cells are ideal for biomass scaling during the generation of recombinant proteins at the bioreactor level, since they are undemanding vis-a-vis growth conditions. Several lines were obtained from the initial clone of CHO cells, among which the CHO-K1 line became the most commonly used [7]. Optimal conditions for providing high growth density of CHO cells in bioreactors were selected using this cell line, enabling a significant increase in the product (target protein) yield alongside a reduced chance of human virus transmission [1, 4, 5]. Yet, the main problem in recombinant protein production in cultured cells is the extremely low product cost; therefore, there is a constant effort to reduce the expenses on obtaining high-producing cell cultures and elevate the yield of the protein product by enhancing the expression level of the target protein, cell culture density, and decreasing cell death. One of such approaches is vector improvement for obtaining transgenes, which can significantly reduce expenses in the generation of producing cell cultures. This paper presents an overview of the regulatory elements used in vector constructs for the generation of transgenic lines.

VECTOR CONSTRUCTS FOR GENERATION OF TARGET PROTEIN-EXPRESSING CELL LINES

The most widely used method in industrial biotechnology is transfection with linearized plasmid DNA [3, 8], which allows one to obtain cell lines containing multiple copies of the expression vector that are usually integrated in one or, rarely, several genomic sites. The mechanism of vector construct integration into the genome has not yet been fully elucidated. Introduction of

linear DNA into the nucleus results in the activation of reparation systems that provide cross-linking of linear DNA ends through two main mechanisms: homologous recombination and ligation of nonhomologous DNA ends [9–11]. As a result, long linear DNA molecules are formed bearing several copies of the vector construct capable of integrating into the genome with some probability. Linear DNA can integrate a genomic region that already contains other copies of the same DNA through the mechanism of homologous recombination, which leads to an increase in the copy number of the construct integrated in a specific genomic site [12]. Thus, one genomic site can bear up to several hundreds of integrated copies of a vector construct.

In order to enhance the producing capacity of clones, selective increase in the number of construct copies, which results in target protein expression, is used in industrial biotechnology [8]. This is achieved by decreasing the functional activity of the reporter gene encoding enzyme dihydrofolate reductase (DHFR), which catalyzes conversion of dihydrofolate to tetrahydrofolate and is essential for the synthesis of glycine, purines, and thymidine acid [13, 14]. DHF-auxotrophic cell lines can grow in media that necessarily contain glycine, as well as a source of purines (hypoxanthine) and thymidine. The derivative line CHO-DG44 with mutations of both alleles of the dihydrofolate reductase gene was obtained by random mutagenesis of the CHO-K1line quite a long time ago [15, 16]. It enabled to use dihydrofolate reductase as a selection gene for the generation of producing cell lines. Furthermore, in order to selectively increase the number of expression vector copies, which usually correlates with an increase in the target protein level, methotrexate (MTX) is used, which is able to selectively inhibit dihydrofolate to tetrahydrofolate conversion [2]. Treatment of transfected cell lines with MTX results in the survival only of cells with a significantly elevated level of dihydrofolate reductase. In most cases, this is caused by an increase in the copy number of the *dhfr* gene included in the construct and, as a result, of the gene encoding the target protein. Another frequently used selectable marker is the gene encoding glutamine synthetase (GS). The CHO-K1 cell line, which contains mutated allele of *gs*, is used when working with this marker. In this case, *L*-methionine sulphoximine (MSX) is used as a selective agent facilitating the selection of the most effective clones [2].

Clone selection can be conducted using other reporter genes, as well. The most promising options are the ones that do not require selection of a mutant cell line. Fluorescent protein technology, which allows one to select cells with maximum expression of a target gene based on emission at a particular wavelength, can be considered [17, 18]. Such an approach can be used for the generation of stable cell lines, which, in contrast to mutant derivatives deficient in *dhfr* and *gs*, exhibit a higher proliferative potential and viability. Among the disadvantages of using fluorescent protein genes as selectable markers is the inability to amplify the copy number, which in most cases would lead to increased producing capacity of a cell clone.

Recently, the application of special robots capable of selecting individual cell clones with the most efficient expression of the target protein, which is identified using antibodies, has become widespread [4]. Alongside with other advantages, this technology enables to avoid using markers the expression of which does not always correlate with the target protein level.

Vector constructs have also been developed based on viruses, mobile elements, bacterial anti-phage protection system, and recombination systems in phages and yeasts [3, 19]. Application of such vectors in several cases enables single insertions of a target gene into a specific genomic region, which is commonly used in gene therapy when generating transgenic cell lines and animals in order to obtain model systems for the study of gene expression regulation processes [20].

The main challenge in obtaining producing cell lines containing multiple expression vector copies is heterochromatin formation of repeated sequences of vector constructs, which usually enhances upon cell proliferation. The main role in heterochromatin formation of a repeated DNA sequence is played by RNA interference and noncoding RNAs that can stimulate repressive chromatin zone formation at promoters, as well as methylation of CpG sites in promoter regions, which decreases the efficacy of transcriptional factor binding in such regions [21–23]. This can result in a significant decrease in the target protein level after the obtainment of highly producing cell lines for some period. Moreover, heterochromatin formation at repeated copies of a vector construct can negatively affect the activity of adjacent cellular genes, which often leads to a decreased viability of producing cell lines. Repression of transcription from integrated repeats of a vector construct is caused by the cellular response to the introduction of foreign information, the expression of which should be suppressed, into the genome. Thus, application of regulatory elements capable of supporting efficient performance of the target protein gene alongside isolating regulatory elements of a vector construct from genomic regulatory elements seems to be extremely important.

USE OF PROMOTERS AND ENHANCERS FOR GENERATION OF CELL LINES PRODUCING TARGET PROTEINS

Strong viral promoters, such as the cytomegalovirus (CMV) promoter and the early promoter of SV40,

as well as strong cellular promoters of housekeeping genes, such as β-actin and factor EF1α genes, are usually used for transgene expression [24].

Strong viral or cellular promoters contain a minimal promoter of approximately 100 bp, which serves as the transcription start site (TSS), and a strong enhancer located in close vicinity to the promoter. For instance, the most widely used CMV promoter bears a core region located between positions −62 and −1 bp from TSS and the enhancer (−544 through −63 bp) [25]. There are several motifs in the region of the minimal promoter that determine the association with various components of the core transcription complex (TFIID): TATA [26], INR [27], DPE [28], BRE [29], DCE [30], and MTE [31]. However, such regions are not essential, since most strong promoters do not contain these elements or belong to the class of GC-rich promoters. One can assume the existence of a practically unexplored group of so-called architectural proteins determining the capacity of the core promoter to recruit the TFIID complex [32]. Unfortunately, the promoter architecture has not been studied deeply enough to determine, based on the sequence of a minimal promoter, its capacity to effectively bind the core transcription factors necessary for the performance of a strong promoter.

One of the approaches in applying effective promoters in biotechnology is identification of strong promoters directly in the cell cultures that are further to be utilized for the generation of target protein-producing lines. Thus, total genome screening of the strongest promoters in CHO cells that are most commonly used as the expression system in mammalian cells has been performed [33–35]. As expected, the most effective promoters appeared to be the promoters of housekeeping genes, including some ribosomal genes. However, the pitfall of this approach is a significantly high chance that the promoters identified by a genome-wide analysis may perform effectively only when located in a certain genomic region (the position effect) or when containing a complicated regulatory region, which significantly decreases the attractiveness of using such promoters in expression systems for obtaining target proteins from transgenic CHO cell lines.

One of the solutions to the position effect is using long regulatory sequences of actively transcribed housekeeping genes located on both sides of the coding region of the gene. Thus, a high expression level of target proteins (6–35 times the level of expression from a standard CMV promoter) has been obtained for vectors bearing a 12 kbp regulatory region or a 4 kbp 3'-region of the Chinese hamster *EF1α* gene [36]. One of the problems in utilizing long regulatory sequences for target protein expression is the instability of large vectors and decreased efficiency in generating multicopy lines that predominantly bear full constructs capable of expressing a target protein. The perspective model is the construct that includes long regulatory DNA regions from terminal repeats of the Epstein-Barr virus, which provides an order increase in efficiency in obtaining stably transfected cells [37].

Artificial modification of promoters is another promising approach to enhance their activity. For instance, a strong CMV promoter has been demonstrated to undergo negative regulation resulting in methylation of GC regions at transcription factor (TF) binding sites comprising promoters and, as a consequence, inhibition of TF recruitment to the promoter. As a result, the activity of the CMV promoter is greatly decreased. Such a negative affect can be avoided by integrating between the enhancer and core elements of the CMV promoter a regulatory sequence that binds transcriptional factors suppressing the DNA methylation process [38]. An effective promoter consisting of two divergent core elements with a single CMV enhancer integrated between them has been developed based on two CMV promoters [39]. This bidirectional promoter is able to express two divergent genes with approximately the same efficiency, which plays an important role in the production of proteins consisting of two different subunits (e.g., monoclonal antibodies).

A novel means to increasing a target protein expression is artificial recruitment of effective transcription-associated complexes to the promoter [40, 41]. For instance, histone acetyltransferase p300 binds active enhancers and promoters and also participates in the stimulation of transcription [42]. Recruitment of p300 to promoters significantly enhances efficiency in generating stable cell clones with a high level of a reporter gene expression [43]. It is worth mentioning that opposite results have been obtained in similar experiments with the Brahma remodeling complex, which provides increased mobility of nucleosomes and is capable of positively/negatively regulating transcription depending on a particular gene.

In order to enhance reporter gene transcription and reduce transgene expression dependence on the surrounding chromatin, strong cellular enhancers are used [44, 45]. One of the most frequently used enhancers is LCR (Locus Control Region), which controls the expression of human β-globin locus genes [46]. The main disadvantage of using enhancers for elevating transgene expression is due to their specificity, i.e. the ability to function only in certain cell lines, which imposes certain restrictions on their use as a general regulatory element. The search for the enhancers most efficient in the cell lines that are used for the generation of proteins at an industrial scale seems to be a promising trend in this direction [47].

PROSPECTIVE USE OF INSULATORS FOR ENHANCING THE EFFICIENCY OF TARGET GENE EXPRESSION IN PRODUCING CELL LINES

In order to increase the efficiency and stability of target protein expression, known insulators are used [41, 48-51]. Insulators are regulatory elements that block interaction between the enhancer and promoter if interposed between them [52, 53]. In addition, insulators do not directly affect an enhancer's and promoter's activity, which means that the promoter can be activated by any other enhancer, and the enhancer, in its turn, is capable of activating any other promoter. In addition, some insulators can serve as boundary elements between transcriptionally active chromatin and heterochromatin. The best-studied examples are insulators of fruit fly Drosophila and vertebrates. Initially, it was assumed that insulators determine the borders of transcriptional domains within which gene expression does not depend on the negative effects of the surrounding genome [54, 55]. However, it has been later demonstrated that insulator proteins are considerably more flexibly integrated into the gene regulatory system [52, 53].

Recently, certain insulator proteins have been shown to participate in the organization of specific, long-range interactions between distal regions of chromatin [56–59]. Insulator proteins can support interactions between enhancers and promoters, boundaries of transcriptional domains which are usually located up to several hundreds of kbp away [34, 60–62]. The obtained results allowed one to refer the class of insulator proteins to chromatin architectural proteins [32, 53].

To date, insulator architectural proteins (IAP) of Drosophila remain poorly described, which is largely due to the ease of generating transgenic lines of flies. The study of insulator properties in Drosophila transgenic lines showed that each insulator binds several IAP, which in turn determine the specificity of long-range interactions [32, 53]. As a result, two identical insulators can provide sufficient specific ultra long-distance interactions between regulatory elements in Drosophila transgenic lines [63, 64], which allowed researcher to propose a model in which IAP associated with specific binding sites, comprising regulatory elements, create a code, which in turn determines how effective a long-range interaction established between these regulatory elements will be (*Fig. 1A*) [32].

Usually, transgenic Drosophila lines are obtained by injecting a vector that contains P element ends flanking the transgenic construct alongside the gene encoding transposase essential for construct integration into the genome [65]. Cases have been described of highly specific integration of the P element that includes an insulator or a strong promoter into a certain genomic region containing the cognate endogenous regulatory element [66, 67]. Such highly specific integration of the P element called *homing* can be explained by the recruitment of IAP to the regulatory element that comprises the P element upon introduction of the construct into an embryo. This results in specific interaction between the P element and the cognate endogenous regulatory element, with further integration of transposon into a certain region at the chromosome (*Fig. 1B*).

Genome-wide studies of IAP-binding site distribution unambiguously demonstrated that insulators are not fixed boundaries between transcriptional domains [62, 68]. Two mechanisms of enhancer activity suppression by insulators have been described in Drosophila transgenic lines, cell cultures, and *in vitro* [53]. The first

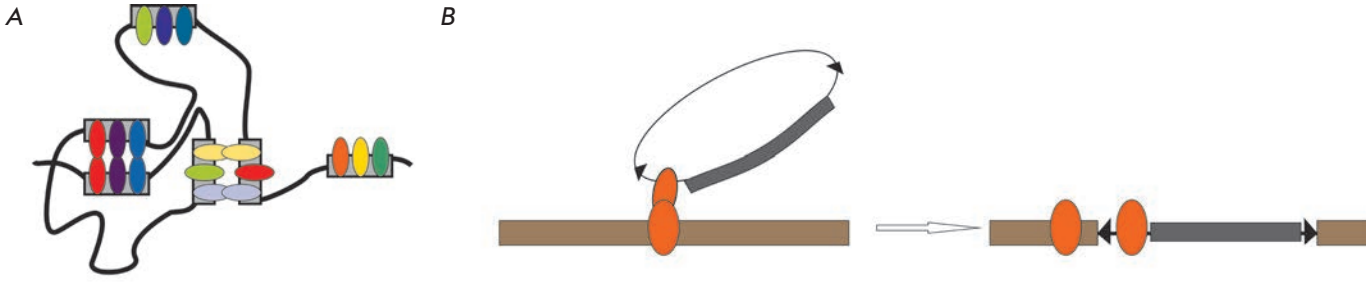

Fig. 1. *A* – Model of establishing specific long-range interactions between regulatory elements. Several IAP (insulator architectural proteins) bind with each element. As a result, two identical elements are capable of providing highly specific and efficient ultra long-range interactions between regulatory elements, but only weak contacts are formed upon partial overlap of IAP-binding sites in regulatory elements. Grey rectangles represent regulatory elements binding with IAP; colored ellipses depict combinations of IAP that specifically bind their own sites and interact with each other. *B* – Specific integration of a transgenic construct into a particular genomic region. The transgenic construct is presented as a circle. Black triangles correspond to P element end repeats; grey rectangle, –elements comprising a transgenic construct. Orange ellipses –regulatory elements that bind with IAP. Brown rectangle – a genome region

mechanism is based on the appearance of topological obstacles that block interactions between the enhancer and promoter. As a result of the formation of stable contacts between insulators, one of the interacting regulatory elements appears to be isolated in the independent chromatin loop. Such a mechanism of insulator action was found using artificial insulators that contained binding sites for proteins capable of effective interaction with each other and formation of stable chromatin loops [69, 70], and using transgenic lines of Drosophila [71]. This mechanism manifests itself effectively only in the case when insulators are immediately adjacent to the suppressed elements (enhancers and promoters). When the size of the chromatin loop formed by insulators is larger, such an enhancer blockage pathway is not utilized [72].The second, more common, mechanism is based on the establishment of direct contacts between the proteins associated with the insulator and enhancer-promoter complex. For example, it has been demonstrated in transgenic lines of Drosophila that insulators may directly interact with promoters and enhancers [71, 73]. In such a case, when the insulator is located between the enhancer and promoter, insulator proteins interfere with the establishment of proper contacts between the transcriptional complexes assembled at the enhancer and promoter, which leads to partial or complete inability of the enhancer to stimulate transcription from the promoter.

The mechanisms that determine the barrier function of insulators have been described in detail in Drosophila and mammals. In particular, it was found that IAP help to recruit the protein complexes responsible for nucleosome remodeling and modification to insulators [74-78], resulting in the formation of open chromatin zones. At the same time, some insulators can recruit the protein complexes directly involved in transcription stimulation [75]. Due to the formation of nucleosome-free DNA regions and recruitment of transcriptional complexes, insulators suppress the spread of repressive chromatin, which, nevertheless, does not exclude the possibility of direct interaction between insulators and silencers initiating heterochromatization.

To date, only a single DNA-binding insulator protein, CTCF, has been described in vertebrates [79, 80], which is probably due to the absence of convenient model systems for the study of insulators. CTCF is capable of supporting long-range interactions between distal areas of chromatin [60, 79–81]. Thus, CTCF is the first architectural protein characterized in a mammalian genome [32, 80].

Except for their key role in the formation of chromatin architecture, CTCF protein domains remain poorly studied and the mechanism of CTCF performance in maintaining long-range interactions has not been characterized yet. The main part of the protein consists of 11 C2H2-type zinc fingers (ZF), with only four of them (4th to 7th) being essential for the recognition of the core DNA motif [82]. The remaining zinc fingers seem to recognize the specific nucleotide sequences stabilizing CTCF association with DNA. The most logical suggestion is that a protein supporting long-range interactions is capable of effective di- and multimerization. Indeed, CTCF has been shown to be able to homodimerize; however, the domain responsible for this activity has not been identified yet [83]. Evidence has been obtained that the C-terminal domain of CTCF also interacts directly with its own zinc fingers [84]. However, such interaction cannot be highly specific, because CTCF zinc fingers bind many other transcription factors, as well: CHD8, Sin3A, and YB-1 [85-87].

The cohesin complex, which associates directly with CTCF [90], is suggested to play a significant role in the organization of long-range interactions [60, 80, 88, 89]. The cohesin complex is recruited to chromatin by CTCF and facilitates the formation of long-range interactions between CTCF genomic sites. This model is consistent with genome-wide studies demonstrating a high degree of colocalization of CTCF and cohesin subunits [91, 92]. However, a very slight decrease in binding of cohesins to chromatin has been shown in experiments on CTCF inactivation, suggesting the implication of other transcription factors in the recruitment of the cohesin complex at chromatin [92-94]. Moreover, inactivation of CTCF and cohesins leads to various disruptions of the chromatin architecture [95, 96], which can be attributed to independent functioning of these proteins.

The most well-studied vertebrate insulator, HS4, consisting of 1,200 bp and located at the 5'-end of the chick β-globin locus, is used in biotechnology (*Fig. 2*) [97, 98]. A core region of 250 bp has been found in this insulator, which exhibits the activity of the complete insulator and contains five fragments (FI, FII, FIII, FIV, FV), each of which has its own functional value. A site that binds CTCF, which is necessary and sufficient for the manifestation of the enhancer-blocking activity of HS4, has been identified in the FII region of the insulator [99]. Proteins USF1 and USF2, which bind as heterodimers to the FIV region, are responsible for boundary formation between active chromatin and heterochromatin [100]. USF has been shown to recruit the protein complexes responsible for modification of the histones associated with transcription stimulation [100, 101]. The protein BGP1/Vezf1, which possesses a DNA-binding domain consisting of zinc fingers, associates with other regions of the HS4 insulator (FI, FIII, FV) [102]. The protein BGP1/Vezf1 protects GC-rich regions of the insulator from methylation, which af-

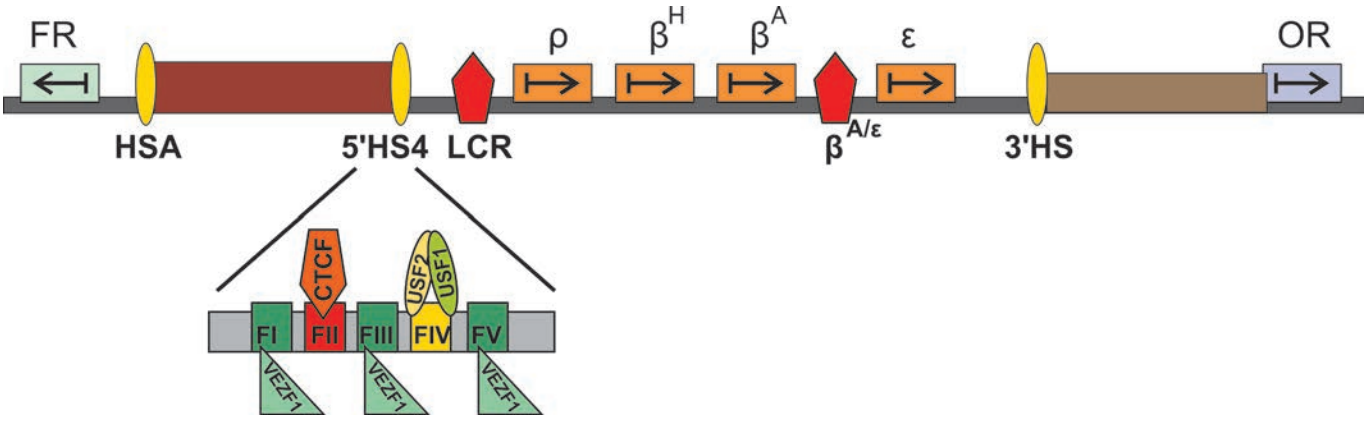

Fig.2. Schematic representation of β-globin locus and adjacent sequences. Designations ρ, β^H, β^A, ε correspond to the genes β-globin locus; FR – folate receptor gene; OR – olfactory receptor gene. Arrows indicate the direction of gene transcription. HSA, 5′HS4, 3′HS – insulators; LCR, $\beta^{A/\varepsilon}$ – enhancers of β-globin locus. Insulator HS4 is represented schematically in detail. FI, FIII, FV –binding sites for protein Vezf1/BGP1. FII and FIV – protein CTCF- and heterodimer USF1/2-binding sites, respectively

fects the recruitment of insulator proteins to DNA and, therefore, results in insulator inactivation. According to the existing model, BGP1/Vezf1 terminates weak transcription from the region of heterochromatin, which may play an important role in protection of the β-globin locus from the spread of inactive chromatin [103].

Since its discovery, insulator HS4 has been actively utilized for transgene expression in mammalian cell cultures [98]. Two complete copies of HS4 have been integrated into a vector for producing transgenic animals expressing a target protein in milk [104]. It was demonstrated that the insulator substantially enhances the expression of target proteins, but it has no significant affect on the specificity of transgene expression only in the mammary gland, and does not provide a direct correlation between the copy number of the construct and the level of target protein production [105].

Most effectively, HS4 insulator can be applied in vectors that for some reason have a limited size. Thus, a full-size 1.2 kbp insulator significantly reduces the efficiency of cellular transformation with lentiviral vectors (probably due to the limitations imposed on the size of the viral particle). Therefore, HS4-duplicated core element of 250 bp, which contains the binding sites of all the identified transcription factors required for the manifestation of insulator activity, is used in vectors of this class [98, 106]. Insulators are also successfully used for protecting reporter gene expression in vectors designed based on mobile elements [51] and retroviruses [107].

Despite the examples of successful use of a 1.2-kbp HS4 insulator or its core region [98, 108], abundant data have been obtained showing that HS4 does not have a positive effect on target gene expression. This can be explained by the fact that the cell cultures that were used in the experiments differed significantly in the set of transcription factors that bind with the HS4 insulator.

In conclusion, the following basic mechanisms for the protection of transgene expression using the HS4 insulator can be put forth: 1) formation of a nucleosome-free DNA region that can disrupt the linear spread of heterochromatin; and 2) recruitment of protein complexes that enhance nucleosome mobility, modify histones, stimulate transcription, protect CpG-sites from methylation, and terminate weak transcription. It has not been determined yet whether the HS4 insulator is capable of guiding construct integration into transcriptionally active chromatin zones and directly interacting with the target gene promoter for further transcription stimulation. Apparently, the main disadvantage of HS4 and other insulators is the dependence of their activity on the set of particular transcription factors expressed in the cell line.

ENHANCING TRANSGENE EXPRESSION USING A/T-RICH SEQUENCES ASSOCIATED WITH NUCLEAR MATRIX PROTEINS (S/MAR)

In order to enhance transformation efficiency and improve the stability of transgene expression, sequences of 300-5,000 bp, usually A/T-rich, which interact with a fraction of the nuclear matrix (S/MAR, scaffold matrix attachment region), as shown in experiments *in vitro*, have been widely used from the beginning of the 90s [108-110]. S/MAR regions possess a number of distinctive properties: they are A/T-rich regions, sensitive to DNase I, and potentially tend to form left-hand-

ed helix and triplex structures [111, 112]. It is assumed that it is the A/T-rich composition of these elements which leads to the destabilization of the double helix and ability of MAR to generate areas rich in various secondary structures [113, 114].

Based on the characteristics of the secondary structure, there is about an order of 50,000 elements predicted for the human genome that supposedly share the properties of S/MAR [115, 116]. A total of 1,500 regions that have the most relevant characteristics of S/MAR have been selected from this pool. Only several of them turned out to share a high level of homology with mouse orthologs, implying that the nucleotide sequence of S/MAR regions lacks distinctive, conserved elements.

The structure of S/MAR elements indicates that they might serve as recombination hotspots. Indeed, it was shown that disruption sites that occur due to inversions associated with human diseases are often localized in S/MAR-elements [117, 118], and integration of retroviruses into the genome occurs in close vicinity to S/MAR at a high frequency [119, 120]. According to some reports, S/MARs participate in the regulation of DNA replication [121-123]. It was found that S/MAR elements enhance transgene expression and reduce expression variability during the generation of stable cell lines [41, 124]. Expression of a gene surrounded by S/MAR elements has been experimentally established to be proportional to the gene copy number [125]. It is assumed that S/MAR elements can be functionally regarded as insulators that protect transgene expression from the positive/negative effects of the surrounding chromatin.

Initially, it was thought that lamina are a major component of nuclear matrix proteins [126]. Later, many other additional proteins, including transcription factors, were found in the nuclear matrix [127]. S/MAR often contain the binding sites of such transcription factors as SATB1, Fast1, CEBP, SAF-A, and SAF-B (proteins that preferentially bind to A/T-rich regions), NMP4 (matrix protein), CTCF and Hox family proteins [83, 116, 128-131]. Topoisomerase II also predominantly associates with A/T-rich regions within S/MAR [132-134]. Reduced density of nucleosome distribution in S/MAR elements and increased concentration of histone acetylation complexes is explained by the association of numerous transcription factors and ability of these elements to form secondary structures.

SATB1 is the most well-studied matrix protein involved in many biological processes, such as differentiation of T cells and epidermis [135–137]. SATB1 can be included in the class of architectural proteins capable of maintaining specific long-range interactions [135]. SATB1 forms homodimers and binds to A/T-rich sequences with two CUT domains and one C-terminal homeobox. Apart from participation in chromatin domain formation, SATB1 recruits ASF1 (ATP-dependent factor involved in chromatin organization) and the ISWI complex (enhances nucleosome mobility) [128, 138].

SAF-A, another matrix protein, includes a DNA-binding (SAF) and an RNA-binding (RGG) domain. It is interesting that Xist RNA, which regulates dosage compensation in mammals, also associates with the RGG domain. This interaction determines the localization of Xist RNA on the X chromosome [139]. According to the existing model [140], SAF-A recruits Xist RNA to a S/MAR element located in the region of initiation of heterochromatin formation on the X chromosome. Interaction between the proteins SAF-A and SATB1 further results in the formation of a loop between neighboring S/MAR complexes, which ultimately leads to the spread of Xist RNA on chromosome X and its subsequent inactivation.

According to the most commonly used model, S/MAR elements interact with the proteins of the nuclear skeleton (matrix proteins), resulting in the formation of chromatin loops where S/MAR serves as a core element [141]. Genes located within a chromatin loop formed by S/MAR are assumed to be protected from the negative influence of the surrounding chromatin [109]. Nevertheless, the structure of the nuclear matrix and role of S/MAR in the organization of the chromosome architecture still remain elusive. According to recent concepts, the matrix presents labile conglomerates of proteins, which transiently interact with S/MAR protein complexes comprising the chromosomes [141].

Despite the lack of understanding of the mechanisms underlying S/MAR action, abundant experimental data has been obtained demonstrating the effectiveness of using these elements for enhancing the expression of target proteins in mammalian cell cultures [142]. For example, S/MAR of the lysozyme gene from the chicken egg causes a 5- to 10-fold increase in the level of monoclonal antibody expression in CHO cells [109, 143]. Later, other, more effective mammalian S/MARs were characterized [144]. S/MARs have been successfully used to increase the expression level of erythropoietin, as well as human growth factor TGF-β receptor type II [108]. Furthermore, S/MAR appears to function both within viral vectors [145] and vectors designed based on transposable elements [146]. S/MAR effectively protects transgene expression from repression (barrier activity) and also supports a higher level of transcription from promoters within expression vectors (stimulatory activity) [144]. Several S/MARs are capable of increasing the efficacy of vector construct integration into chromosomes [147, 148]. Moreover, S/MAR proteins are able to provide integration of new additional

copies of the vector construct in a region already containing integrated construct copies. The best possible explanation for such a characteristic of S/MAR is that the interaction between architectural proteins (such as SAF-A and SATB1) provides a contact between S/MAR copies located in the genome and plasmid (analogue of the homing phenomenon in Drosophila mentioned above). Apparently, the increased recombination activity provided by S/MAR elements enhances the efficiency of transgene integration into specific regions of the genome. Thus, the positive impact of S/MAR on transgene expression might be largely determined by directed integration of a vector construct into normally transcriptionally active S/MAR-containing areas. This implication is consistent with the finding that many of the studied S/MARs have a positive influence on gene expression only when integrated into the genome [125, 144]. In order to increase the amplification rate of a construct in cell clones, S/MAR was combined with the mammalian replication initiation region [149, 150]. Treatment of primary transfectants with MTX enabled to achieve large-scale amplification of a construct in cell clones, which led to a stable multifold increase in the production of the target protein [150].

In conclusion, it can be stated that S/MAR present regulatory elements that are less studied than insulators. The most probable mechanisms of S/MAR action in enhancing transgene expression are 1) site-specific integration of S/MAR-bearing constructs into the regions of transcriptionally active chromatin and amplification of the copy number of the integrated construct, 2) association with S/MAR complex elements that guide transcriptionally active chromatin zones and thus suppress the spread of heterochromatin, and 3) immediate promoter activation by transcription factors that directly bind to S/MAR.

ENHANCING TRANSGENE EXPRESSION IN CELL CULTURES BY REGULATORY ELEMENTS BEARING A STRONG PROMOTER OF HOUSEKEEPING GENES

Between 2000 and 2002, a small company named CobraTherapeutics developed a technological platform based on regulatory elements isolated from housekeeping genes, which are actively transcribed at all stages of development and in all cells of an organism, for obtaining efficient cell lines producing recombinant proteins [45]. These regulatory elements were named ubiquitous chromatin opening elements (UCOE) since the promoter regions of the actively transcribed genes are characterized by a low density of nucleosomes, which is due to the presence of DNA-binding TF stimulating transcription. The best characterized UCOE are DNA regions that contain a pair of divergent gene promoters, *HNRPA2B1* and *CBX3* or *TBP* and *PSNB1*, which are actively transcribed in all cells of an organism [151]. The first experiments used large regulatory elements of 12-16 kbp, which significantly increased the percentage of transfected cells and provided high-level and stable transgene expression for a long cultivation period [151, 152]. Thus, UCOE causes a 16-fold increase in the efficiency of the CMV promoter, which is highly susceptible to inhibition by RNA interference and methylation of CpG regions [152, 153]. It was shown that UCOE can maintain a high expression level of a transgene integrated into pericentromeric heterochromatin. UCOE are also effective as part of lentiviral vectors [154-159]. It can be assumed that UCOE are bound by transcription factors that recruit the complexes preventing methylation of CpG repeats and forming chromatin areas with reduced nucleosome density in the promoter regions comprising lentiviral vectors [155, 160].

It should be noted that, unlike other regulatory elements such as LCR and enhancers, which exhibit pronounced cell specificity, promoters of housekeeping genes can function effectively in various cell lines. In experiments with various UCOE that were reduced in size in order to assess the possibility of using UCOE in expression vectors, more compact-size variants of UCOE (1.5 to 3 kbp) have been obtained. Such truncated elements completely retain their activity during the generation of high-producing cell lines [152].

UCOE actively participate in the process of transcriptional regulation, which implies the existence of direct interactions between the promoter regulatory elements responsible for the expression of the reporter gene located in the vector and the transcription factors associated with UCOE. Therefore, UCOE can effectively act only on certain promoters and the functional activity of these promoters does not manifest itself in cell lines [161]. Some studies have demonstrated that UCOE themselves can be used as promoters for providing stable expression of a reporter gene [162]. However, contribution in transgene expression of the transcription initiated from promoters comprising UCOE is ambiguous, and its role remains elusive. In particular, there are experimental data showing that UCOE do not always effectively enhance the expression of a target protein in CHO cells [162, 163]. Negative results obtained using UCOE can be explained by the fact that strong promoters comprising UCOE induce transcription that in some cases is capable of triggering RNA interference and/or recruiting repressive complexes to the promoter that transcribes the reporter gene.

It was also demonstrated that a combination of two strong promoters may in some cases facilitate the generation of stable cell lines and enhance transgene expression [164]. Analysis of various combinations of two of the promoters CMV, SV40, RPL32, EF1-α and

β-actin showed that only the *RPL32* promoter, integrated before any other of the studied promoters, can significantly increase the efficiency of stable cell clone selection. It is worth mentioning that the direction of the *RPL32* promoter should coincide with the direction of the promoter responsible for reporter gene expression, and core elements of the *RPL32* promoter in this case are essential components of the system for providing a stimulating effect.

In general, combining strong promoters is a promising way to improve the efficiency of generating cell clones producing a target protein. Strong promoters bearing a combination of enhancer and core promoter recruit protein complexes, which in turn support a transcriptionally active state of chromatin. According to the data of genome-wide studies, promoters act as effective boundaries that are able to protect genome areas against the spread of repressive chromatin regions [165, 166].Transcription factors that bind to properly matched promoter pairs can mutually reinforce each other's activities. Apparently, the use of some promoters can provide advantageous integration of a construct into certain chromosome areas with the highest levels of transcription. A more complete understanding of the mechanisms of transcription activation will further allow researchers to modify promoters in order to improve their performance when using them in expression systems.

ENHANCING THE TRANSGENE EXPRESSION LEVEL IN CELL CULTURES BY REGULATORY ELEMENTS PROTECTING FROM HP1-DEPENDENT REPRESSION

The Chromagenic company has developed a technological platform based on a test-system which effectively allows the identification of regulatory elements capable of suppressing the spread of heterochromatin areas [45]. The test-system is based on the recruitment of the HP1 protein, which is responsible for heterochromatin formation, to a plasmid using the DNA-binding domain of the Lex protein [167]. The chimeric protein HP1-Lex binds to Lex-specific sites on the plasmid and recruits other components of the heterochromatin complex, which launches the inactivation of the adjacent promoter. This results in repression of zeo^R, which is responsible for resistance to the antibiotic Zeocin, and the death of transfected cells when cultured in a selective medium with the addition of Zeocin. The screening aimed at detecting DNA fragments, integration of which between Lex binding sites and the zeo^R promoter protects the promoter from HP1-dependent repression, enabled to find a series of regulatory elements 500 to 2,000 bp in length called antirepressors (STAR). Other known regulatory elements such as the insulator HS4, MAR, and UCOE lack that ability. A comparative analysis of various regulatory elements [168] has shown that STAR elements are most effective when using them for generating high-producing CHO cell lines. However, the mechanism of STAR element action remains unexplored. There is still no evidence on what transcription factors bind with elements of this class and provide them with functional activity.

CONCLUSION

To date, no universal regulatory element with a clear mechanism of action has been found that can be effectively used in all types of vector constructs designed to generate cell lines producing various proteins at a high level. This is largely due to the complexity of the mechanisms that regulate promoter activity and also the absence of actual evidence on the original concepts of strict organization of genes with the same expression profile into transcriptional domains surrounded by special regulatory elements from a class of insulators or S/MAR. Clearly, some mechanisms must exist that suppress excessive transcription even for the strongest promoters. RNA interference is one of such mechanisms. It is possible that a detailed understanding of the mechanisms of transcription activation and suppression will lead to the development of artificial promoters that allow researchers to obtain stable high levels of target gene expression in transgenic systems. ●

The work was supported by the Russian Scientific Fund (grant № 14-24-00166).

REFERENCES

1. Demain A.L., Vaishnav P. // Biotech. Advances. 2009. V. 27. P. 297–306.
2. Durocher Y., Butler M. // Curr. Opin. Biotech. 2009. V. 20. P. 700–707.
3. Khan K.H. // Adv. Pharm. Bull. 2013. V. 3. P. 257–263.
4. Kim J.Y., Kim Y.G., Lee G.M. // Appl. Microbiol. Biotechnol. 2012. V. 93. P. 917–930.
5. Hacker D.L., De Jesus M., Wurm F.M. // Biotechnol. Adv. 2009. P. 1023–1027.
6. Tjio J.H., Puck T.T. // J. Exp. Med. 1958. V. 108. P. 259–271.
7. Kao F.T., Puck T.T. // Proc. Natl. Acad. Sci. USA. 1968. V. 60. P. 1275–1281.
8. Browne S.M., Al-Rubeai M. // Trends Biotech. 2007. V. 25. P. 425–432.
9. Folger K.R., Wong E.A., Wahl G., Capecchi M.R. // Mol. Cell. Biol. 1982. V. 2. P. 1372–1387.
10. Folger K.R., Thomas K., Capecchi M.R. // Mol. Cell Biol. 1985. V. 5. P. 59–69.
11. Robins D.M., Ripley S., Henderson A.S., Axel R. // Cell. 1981. V. 23. P. 29–39.
12. Thomas K.R., Folger K.R., Capecchi M.R. // Cell. 1986.

V. 44. P. 419–428.
13. Hayward B.E., Hussain A., Wilson R.H., Lyons A., Woodcock V., McIntosh B., Harris T.J. // Nucl. Acids Res. 1986. V. 14. P. 999–1008.
14. Wuest D.M., Harcum S.W., Lee K.H. // Biotechnol. Adv. 2012. V. 30. P. 629–638.
15. Urlaub G., Chasin L.A. // Proc. Natl. Acad. Sci. USA. 1980. V. 77. P. 4216–4220.
16. Urlaub G., Kas E., Carothers A.M., Chasin L.A. // Cell. 1983. V. 33. P. 405–412.
17. Inouye S., Tsuji F.I. // FEBS Lett. 1994. V. 341. P. 277–280.
18. Stepanenko O.V., Verkhusha V.V., Kuznetsova I.M., Uversky V.N., Turoverov K.K. // Curr. Protein Pept. Sci. 2008. V. 9. P. 338–369.
19. Niu J., Zhang B., Chen H. // Mol. Biotechnol. 2014. V. 56. P. 681–688.
20. Wijshake T., Baker D.J., van de Sluis B. // Biochim. Biophys. Acta. 2014. V. 1842. P. 1942–1950.
21. Castel S.E., Martienssen R.A. // Nat. Rev. Genet. 2013. V. 14. P. 100–112.
22. Fatica A., Bozzoni I. // Nat. Rev. Genet. 2014. V. 15. P. 7–21.
23. Morris K.V., Mattick J.S. // Nat. Rev. Genet. 2014. V. 15. P. 423–437.
24. Lai T., Yang Y., Ng S.K. // Pharmaceuticals (Basel). 2013. V. 6. P. 579–603.
25. Bradley A.J., Lurain N.S., Ghazal P., Trivedi U., Cunningham C., Baluchova K., et al. // J. Gen. Virol. 2009. V. 90. P. 2375–2380.
26. Goldberg M.L. Sequence Analysis of Drosophila Histone Genes: PhD thesis. Stanford University, 1979.
27. Corden J., Wasylyk B., Buchwalder A., Sassone-Corsi P., Kedinger C., Chambon P. // Science. 1980. V. 209. P. 1406–1414.
28. Burke T.W., Kadonaga J.T. // Genes Dev. 1996. V. 10. P. 711–724.
29. Lagrange T., Kapanidis A.N., Tang H., Reinberg D., Ebright R.H. // Genes Dev. 1998. V. 12. P. 34–44.
30. Lewis B.A., Kim T.K., Orkin S.H. // Proc. Natl. Acad. Sci. USA. 2000. V. 97. P. 7172–7177.
31. Lim C.Y., Santoso B., Boulay T., Dong E., Ohler U., Kadonaga J.T. // Genes Dev. 2004. V. 18. P. 1606–1617.
32. Maksimenko O., Georgiev P. // Front. Genet. 2014. V. 5. P. 28.
33. Xu X., Nagarajan H., Lewis N.E., Pan S., Cai Z., Liu X., Chen W., Xie M., Wang W., Hammond S., et al. // Nat. Biotechnol. 2011. V. 29. P. 735–741.
34. Becker J., Hackl M., Rupp O., Jakobi T., Schneider J., Szczepanowski R., Bekel T., Borth N., Goesmann A., Grillari J., et al. // J. Biotechnol. 2011. V. 156. P. 227–235.
35. Jakobi T., Brinkrolf K., Tauch A., Noll T., Stoye J., Pühler A., Goesmann A. // J. Biotechnol. 2014. V. 190. P. 64–75.
36. Running Deer J., Allison D.S. // Biotechnol. Prog. 2004. V. 20. P. 880–889.
37. Orlova N.A., Kovnir S.V., Hodak J.A., Vorobiev I.I., Gabibov A.G., Skryabin K.G. // BMC Biotechnol. 2014. V. 14. P. 56.
38. Mariati, Koh E.Y., Yeo J.H., Ho S.C., Yang Y. // Bioengineered. 2014. V. 5. P. 340–345.
39. Andersen C.R., Nielsen L.S., Baer A., Tolstrup A.B., Weilguny D. // Mol. Biotechnol. 2011. V. 48. P. 128–137.
40. de Groote M.L., Verschure P.J., Rots M.G. // Nucl. Acids Res. 2012. V. 40. P. 10596–10613.
41. Kwaks T.H., Otte A.P. // Trends Biotechnol. 2006. V. 24. P. 137–142.
42. Holmqvist P.H., Mannervik M. // Transcription. 2013. V. 4. P. 18–23.
43. Kwaks T.H., Sewalt R.G., van Blokland R., Siersma T.J., Kasiem M., Kelder A., Otte A.P. // J. Biotechnol. 2005. V. 115. P. 35–46.
44. Moltó E., Fernández A., Montoliu L. // Brief Funct. Genomic Proteomic. 2009. V. 8. P. 283–296.
45. Palazzoli F., Bire S., Bigot Y., Bonnin-Rouleux F. // Nat. Biotechnol. 2011. V. 29. P. 593–597.
46. Kim A., Dean A. // Mol. Cells. 2012. V. 34. P. 1–5.
47. Vishwanathan N., Le H., Le T., Hu W.S. // Curr. Opin. Biotechnol. 2014. V. 30. P. 113–119.
48. Recillas-Targa F., Valadez-Graham V., Farrell C.M. // BioEssays. 2004. V. 26. P. 796–807.
49. Emery D.W. // Hum. Gene Ther. 2011. V. 22. P. 761–774.
50. Furlan-Magaril M., Rebollar E., Guerrero G., Fernández A., Moltó E., González-Buendía E., Cantero M., Montoliu L., Recillas-Targa F. // Nucl. Acids Res. 2011. V. 39. P. 89–103.
51. Bire S., Ley D., Casteret S., Mermod N., Bigot Y., Rouleux-Bonnin F. // PLoS One. 2013. V. 8. e82559.
52. Chetverina D., Aoki T., Erokhin M., Georgiev P., Schedl P. // BioEssays. 2014. V. 36. P. 163–172.
53. Kyrchanova O., Georgiev P. // FEBS Lett. 2014. V. 588. P. 8–14.
54. Labrador M., Corces V.G. // Cell. 2002. V. 111. P. 151–154.
55. Bell A.C., West A.G., Felsenfeld G. // Science. 2001. V. 291. P. 447–450.
56. Handoko L., Xu H., Li G., Ngan C.Y., Chew E., Schnapp M., Lee C.W., Ye C., Ping J.L., Mulawadi F., et al. // Nat. Genet. 2011. V. 43. P. 630–638.
57. Dixon J.R., Selvaraj S., Yue F., Kim A., Li Y., Shen Y., Hu M., Liu J.S., Ren B. // Nature. 2012. V. 485. P. 376–380.
58. Sanyal A., Lajoie B.R., Jain G., Dekker J. // Nature. 2012. V. 489. P. 109–113.
59. Sexton T., Yaffe E., Kenigsberg E., Bantignies F., Leblanc B., Hoichman M., Parrinello H., Tanay A., Cavalli G., et al. // Cell. 2012. V. 148. P. 458–472.
60. Holwerda S., de Laat W. // Front. Genet. 2012. V. 3. P. 217.
61. Nora E.P., Dekker J., Heard E. // BioEssays. 2013. V. 35. P. 818–828.
62. Gibcus J.H., Dekker J. // Mol. Cell. 2013. V. 49. P. 773–782.
63. Kravchenko E., Savitskaya E., Kravchuk O., Parshikov A., Georgiev P., Savitsky M. // Mol. Cell Biol. 2005. V. 25. P. 9283–9291.
64. Li H.B., Müller M., Bahechar I.A., Kyrchanova O., Ohno K., Georgiev P., PirrottaV. // Mol. Cell Biol. 2011. V. 31. P. 616–625.
65. Venken K.J., Bellen H.J. // Meth. Mol. Biol. 2012. V. 859. P. 203–228.
66. Fujioka M., Wu X., Jaynes J.B. // Development. 2009. V. 136. P. 3077–3087.
67. Fujioka M., Sun G., Jaynes J.B. // PLoS Genet. 2013. V. 9. e1003883.
68. Tanay A., Cavalli G. // Curr. Opin. Genet. Dev. 2013. V. 23. P. 197–203.
69. Ameres S.L., Drueppel L., Pfleiderer K., Schmidt A., Hillen W., Berens C. // EMBO J. 2005. V. 24. P. 358–367.
70. Bondarenko V.A., Jiang Y.I., Studitsky V.M. // EMBO J. 2003. V. 22. P. 4728–4737.
71. Kyrchanova O., Maksimenko O., Stakhov V., Ivlieva T., Parshikov A., Studitsky V.M., Georgiev P. // PLoS Genet. 2013. V. 9. e1003606.
72. Savitskaya E., Melnikova L., Kostuchenko M., Kravchenko E., Pomerantseva E., Boikova T., Chetverina D., Parshikov A., Zobacheva P., Gracheva E., et al. // Mol. Cell Biol. 2006. V. 26. P. 754–761.
73. Erokhin M., Davydova A., Kyrchanova O., Parshikov A.,

Georgiev P., Chetverina D. // Development. 2011. V. 138. P. 4097–4106.
74. Nakayama T., Shimojima T., Hirose S. // Development. 2012. V. 139. P. 4582–4590.
75. Ghirlando R., Giles K., Gowher H., Xiao T., Xu Z., Yao H., Felsenfeld G. // Biochim. Biophys. Acta. 2012. V. 1819. P. 644–651.
76. Vorobyeva N.E., Mazina M.U., Golovnin A.K., Kopytova D.V., Gurskiy D.Y., Nabirochkina E.N., Georgieva S.G., Georgiev P.G., Krasnov A.N. // Nucl. Acids Res. 2013. V. 41. P. 5717–5730.
77. Yajima M., Fairbrother W.G., Wessel G.M. // Development. 2012. V. 139. P. 3613–3622.
78. Li M., Belozerov V.E., Cai H.N. // Mol. Cell Biol. 2010. V. 30. P. 1067–1076.
79. Herold M., Bartkuhn M., Renkawitz R. // Development. 2012. V. 139. P. 1045–1057.
80. Merkenschlager M., Odom D.T. // Cell. 2013. V. 152. P. 1285–1297.
81. Chaumeil J., Skok J.A. // Curr. Opin. Immunol. 2012. V. 24. P. 153–159.
82. Nakahashi H., Kwon K.R., Resch W., Vian L., Dose M., Stavreva D., Hakim O., Pruett N., Nelson S., Yamane A., et al. // Cell Rep. 2013. V. 3. P. 1678–1689.
83. Yusufzai T.M., Felsenfeld G. // Proc. Natl. Acad. Sci. USA. 2004. V. 101. P. 8620–8624.
84. Pant V., Kurukuti S., Pugacheva E., Shamsuddin S., Mariano P., Renkawitz R., Klenova E., Lobanenkov V., Ohlsson R. // Mol. Cell Biol. 2004. V. 24. P. 3497–3504.
85. Chernukhin I.V., Shamsuddin S., Robinson A.F., Carne A.F., Paul A., El-Kady A.I., Lobanenkov V.V., Klenova E.M. // J. Biol. Chem. 2000. V. 275. P. 29915–29921.
86. Lutz M., Burke L.J., Barreto G., Goeman F., Greb H., Arnold R., Schultheiss H., Brehm A., Kouzarides T., Lobanenkov V., et al. // Nucl. Acids Res. 2000. V. 28. P. 1707–1713.
87. Ishihara K., Oshimura M., Nakao M. // Mol. Cell. 2006. V. 23. P. 733–742.
88. Mehta G.D., Kumar R., Srivastava S., Ghosh S.K. // FEBS Lett. 2013. V. 587. P. 2299–2312.
89. Lee B.K., Iyer V.R. // J. Biol. Chem. 2012. V. 287. P. 30906–30913.
90. Xiao T., Wallace J., Felsenfeld G. // Mol. Cell Biol. 2011. V. 31. P. 2174–2183.
91. Parelho V., Hadjur S., Spivakov M., Leleu M., Sauer S., Gregson H.C., Jarmuz A., Canzonetta C., Webster Z., Nesterova T., et al. // Cell. 2008. V. 132. P. 422–433.
92. Wendt K.S., Yoshida K., Itoh T., Bando M., Koch B., Schirghuber E., Tsutsumi S., Nagae G., Ishihara K., Mishiro T., et al. // Nature. 2008. V. 451. P. 796–801.
93. Hadjur S., Williams L.M., Ryan N.K., Cobb B.S., Sexton T., Fraser P., Fisher A.G., Merkenschlager M. // Nature. 2009. V. 460. P. 410–413.
94. Nativio R., Wendt K.S., Ito Y., Huddleston J.E., Uribe-Lewis S., Woodfine K., Krueger C., Reik W., Peters J.M., Murrell A. // PLoS Genet. 2009. V. 5. e1000739.
95. Zuin J., Dixon J.R., van der Reijden M.I., Ye Z., Kolovos P., Brouwer R.W., van de Corput M.P., van de Werken H.J., Knoch T.A., van IJcken W.F., et al. // Proc. Natl. Acad. Sci. USA. 2014. V. 111. P. 996–1001.
96. Gosalia N., Neems D., Kerschner J.L., Kosak S.T., Harris A. // Nucl. Acids Res. 2014. V. 42. P. 9612–9622.
97. Chung J.H., Bell A.C., Felsenfeld G. // Proc. Natl. Acad. Sci. USA. 1997. V. 94. P. 575–580.
98. Emery D.W., Yannaki E., Tubb J., Stamatoyannopoulos G. // Proc. Natl. Acad. Sci. USA. 2000. V. 97. P. 9150–9155.
99. Bell A.C., West A.G., Felsenfeld G. // Cell. 1999. V. 98. P. 387–396.
100. West A.G., Huang S., Gaszner M., Litt M.D., Felsenfeld G. // Mol. Cell. 2004. V. 16. P. 453–463.
101. Huang S., Li X., Yusufzai T.M., Qiu Y., Felsenfeld G. // Mol. Cell Biol. 2007. V. 27. P. 7991–8002.
102. Dickson J., Gowher H., Strogantsev R., Gaszner M., Hair A., Felsenfeld G., West A.G. // PLoS Genet. 2010. V. 6. e1000804.
103. Giles K.E., Gowher H., Ghirlando R., Jin C., Felsenfeld G. // Cold Spring Harbor Symp. Quant. Biol. 2010. V. 75. P. 1–7.
104. Maksimenko O.G., Deikin A.V., Khodarovich Yu.M., and Georgiev P.G. // Acta Naturae. 2013. V. 5. № 1(16). P. 33–47.
105. Rival-Gervier S., Pantano T., Viglietta C., Maeder C., Prince S., Attal J., Jolivet G., Houdebine L.M. // Transgenic Res. 2003. V. 12. P. 723–730.
106. Hanawa H., Yamamoto M., Zhao H., Shimada T., Persons D.A. // Mol. Therapy. 2009. V. 17. P. 667–674.
107. Aker M., Tubb J., Groth A.C., Bukovsky A.A., Bell A.C., Felsenfeld G., Kiem H.P., Stamatoyannopoulos G., Emery D.W. // Hum. Gene Ther. 2007. V. 18. P. 333–343.
108. Kim J.M., Kim J.S., Park D.H., Kang H.S., Yoon J., Baek K., Yoon Y. // J. Biotech. 2004. V. 107. P. 95–105.
109. Girod P.A., Zahn-Zabal M., Mermod N. // Biotech. Bioeng. 2005. V. 91. P. 1–11.
110. Harraghy N., Gaussin A., Mermod N. // Curr. Gene Ther. 2008. V. 8. P. 353–366.
111. Wang T.Y., Han Z.M., Chai Y.R., Zhang J.H. // Mol. Biol. Rep. 2010. V. 37. P. 3553–2560.
112. Bode J., Schlake T., Rios-Ramirez M., Mielke C., Stengert M., Kay V., Klehr-Wirth D. // Int. Rev. Cytol. 1995. V. 162. P. 389–454.
113. Platts A.E., Quayle A.K., Krawetz S.A. // Cell Mol. Biol. Lett. 2006. V. 11. P. 191–213.
114. Evans K., Ott S., Hansen A., Koentges G., Wernisch L. // BMC Bioinformatics. 2007. V. 8. P. 71.
115. Liebich I., Bode J., Frisch M., Wingender E. // Nucl. Acids Res. 2002. V. 30. P. 372–374.
116. Girod P.-A., Nguyen D.-Q., Calabrese D., Puttini S., Grandjean M., Martinet D., Regamey A., Saugy D., Beckmann J.S., Bucher P., et al. // Nat. Methods. 2007. V. 4. P. 747–753.
117. Welcsh P.L., King M.C. // Hum. Mol. Genet. 2001. V. 10. P. 705–713.
118. Iarovaia O.V., Shkumatov P., Razin S.V. // J. Cell Sci. 2004. V. 117. P. 4583–4590.
119. Kulkarni A., Pavithra L., Rampalli S., Mogare D., Babu K., Shiekh G., Ghosh S., Chattopadhyay S. // Biochem. Biophys. Res. Commun. 2004. V. 322. P. 672–677.
120. Johnson C.N., Levy L.S. // Virol. J. 2005. V. 2. P. 68.
121. Koina E., Piper A. // J. Cell Biochem. 2005. V. 95. P. 391–402.
122. Mearini G., Chichiarelli S., Zampieri M., Masciarelli S., D'Erme M., Ferraro A., Mattia E. // FEBS Lett. 2003. V. 547. P. 119–124.
123. Piechaczek C., Fetzer C., Baiker A., Bode J., Lipps H.J. // Nucl. Acids Res. 1999. V. 27. P. 426–428.
124. Galbete J.L., Buceta M., Mermod N. // Mol. Biosyst. 2009. V. 5. P. 143–150.
125. Bode J., Benham C., Knopp A., Mielke C. // Crit. Rev. Eukaryot. Gene Expr. 2000. V. 10. P. 73–90.
126. Berezney R., Coffey D.S. // Biochem. Biophys. Res. Commun. 1974. V. 60. P. 1410–1417.
127. Albrethsen J., Knol J.C., Jimenez C.R. // J. Proteomics. 2009. V. 72. P. 71–81.

128. Cai S., Han H.J., Kohwi-Shigematsu T. // Nat. Genet. 2003. V. 34. P. 42–51.
129. Renz A., Fackelmayer F.O. // Nucl. Acids Res. 1996. V. 24. P. 843–849.
130. Agrelo R., Souabni A., Novatchkova M., Haslinger C., Leeb M., Komnenovic V., Kishimoto H., Gresh L., Kohwi-Shigematsu T., Kenner L., et al. // Dev. Cell. 2009. V. 16. P. 507–516.
131. Arope S., Harraghy N., Pjanic M., Mermod N. // PLoS One. 2013. V. 8. e79262.
132. Berrios M., Osheroff N., Fisher P.A. // Proc. Natl. Acad. Sci. USA. 1985. V. 82. P. 4142–4146.
133. Feister H.A., Onyia J.E., Miles R.R., Yang X., Galvin R., Hock J.M., Bidwell J.P. // Bone. 2000. V. 26. P. 227–234.
134. Adachi Y., Kas E., Laemmli U.K. // EMBO J. 1989. V. 8. P. 3997–4006.
135. Kohwi-Shigematsu T., Kohwi Y., Takahashi K., Richards H.W., Ayers S.D., Han H.J., Cai S. // Methods. 2012. V. 58. P. 243–254.
136. Burute M., Gottimukkala K., Galande S. // Immunol. Cell Biol. 2012. V. 90. P. 852–859.
137. Naito T., Tanaka H., Naoe Y., Taniuchi I. // Int. Immunol. 2011. V. 23. P. 661–668.
138. Yasui D., Miyano M., Cai S., Varga-Weisz P., Kohwi-Shigematsu T. // Nature. 2002. V. 419. P. 641–645.
139. Hasegawa Y., Brockdor V.N., Kawano S., Tsutsui K., Nakagawa S. // Dev. Cell. 2010. V. 19. P. 469–476.
140. Tattermusch A., Brockdorff N. // Hum. Genet. 2011. V. 130. P. 247–253.
141. Razin S.V., Iarovaia O.V., Vassetzky Y.S. // Chromosoma. 2014. V. 123. P. 217–224.
142. Harraghy N., Buceta M., Regamey A., Girod P.A., Mermod N. // Methods Mol. Biol. 2012. V. 801. P. 93–110.
143. Zahn-Zabal M., Kobr M., Girod P.A., Imhof M., Chatellard P., de Jesus M. // J. Biotech. 2001. V. 87. P. 29–42.
144. Harraghy N., Regamey A., Girod P.-A., Mermod N. // J. Biotechnol. 2011. V. 154. P. 11–20.
145. Buceta M., Galbete J.L., Kostic C., Arsenijevic Y., Mermod N. // Gene Therapy. 2011. V. 18. P. 7–13.
146. Ley D., Harraghy N., Le Fourn V., Bire S., Girod P.A., Regamey A., Rouleux-Bonnin F., Bigot Y., Mermod N. // PLoS One. 2013. V. 8. e62784.
147. Grandjean M., Girod P.A., Calabrese D., Kostyrko K., Wicht M., Yerly F., Mazza C., Beckmann J.S., Martinet D., Mermod N. // Nucl. Acids Res. 2011. V. 39. e104.
148. Puttini S., van Zwieten R.W., Saugy D., Lekka M., Hogger F., Ley D., Kulik A.J., Mermod N. // BMC Mol. Biol. 2013. V. 14. P. 26.
149. Shimizu N., Miura Y., Sakamoto Y., Tsutsui K. // Cancer Res. 2001. V. 61. P. 6987–6990.
150. Noguchi C., Araki Y., Miki D., Shimizu N. // PLoS One. 2012. V. 7. . e52990.
151. Antoniou M., Harland L., Mustoe T., Williams S., Holdstock J., Yague E., Mulcahy T., Griffiths M., Edwards S., Ioannou P.A., et al. // Genomics. 2003. V. 82. P. 269–279.
152. Williams S., Mustoe T., Mulcahy T., Griffiths M., Simpson D., Antoniou M., Irvine A., Mountain A., Crombie R. // BMC Biotech. 2005. V. 5. P. 17.
153. Benton T., Chen T., McEntee M., Fox B., King D., Crombie R., Thomas T.C., Bebbington C. // Cytotechnology. 2002. V. 38. P. 43–46.
154. Zhang F., Thornhill S.I., Howe S.J., Ulaganathan M., Schambach A., Sinclair J., Kinnon C., Gaspar H.B., Antoniou M., Thrasher A.J. // Blood. 2007. V. 110. P. 1448–1457.
155. Zhang F., Frost A.R., Blundell M.P., Bales O., Antoniou M.N., Thrasher A.J. // Mol. Ther. 2010. V. 18. P. 1640–1649.
156. Dighe N., Khoury M., Mattar C., Chong M., Choolani M., Chen J., Antoniou M.N., Chan J.K. // PLoS One. 2014. V. 9. e104805.
157. Pfaff N., Lachmann N., Ackermann M., Kohlscheen S., Brendel C., Maetzig T., Niemann H., Antoniou M.N., Grez M., Schambach A., et al. // Stem Cells. 2013. V. 31. P. 488–499.
158. Brendel C., Müller-Kuller U., Schultze-Strasser S., Stein S., Chen-Wichmann L., Krattenmacher A., Kunkel H., Dillmann A., Antoniou M.N., Grez M. // Gene Ther. 2012. V. 19. P. 1018–1029.
159. Boscolo S., Mion F., Licciulli M., Macor P., De Maso L., Brce M., Antoniou M.N., Marzari R., Santoro C., Sblattero D. // Nat. Biotechnol. 2012. V. 29. P. 477–484.
160. Lindahl A.M., Antoniou M. // Epigenetics. 2007. V. 2. P. 227–236.
161. Nair A.R., Jinger X., Hermiston T.W. // BMC Res. Notes. 2011. V. 4. P. 178.
162. Jonuschies J., Antoniou M., Waddington S., Boldrin L., Muntoni F., Thrasher A., Morgan J. // Curr. Gene Ther. 2014. V. 14. P. 276–288.
163. Otte A.P., Kwaks T.H., van Blokland R.J., Sewalt R.G., Verhees J., Klaren V.N., Siersma T.K., Korse H.W., Teunissen N.C., Botschuijver S., et al. // Biotechnol. Prog. 2007. V. 23. P. 801–807.
164. Hoeksema F., Hamer K., Siep M., Verhees J.A., Otte A.P. // Biotechnol. Res. Int. 2011. 492875.
165. Wang J., Lawry S.T., Cohen A.L., Jia S. // Cell Mol. Life Sci. 2014. V. 71. P. 4841–4852.
166. Kwaks T.H.J., Barnett P., Hemrika W., Siersma T., Sewalt R.G., Satijn D.P., Brons J.F., van Blokland R., Kwakman P., Kruckeberg A.L., et al. // Nat. Biotechnology. 2003. V. 21. P. 553–558.
167. Schwartz Y.B., Linder-Basso D., Kharchenko P.V., Tolstorukov M.Y., Kim M., Li H.B., Gorchakov A.A., Minoda A., Shanower G., Alekseyenko A.A., et al. // Genome Res. 2012. V. 22. P. 2188–2198.

PARP1 Inhibitors: Antitumor Drug Design

N. V. Malyuchenko[1*], E. Yu. Kotova[2], O. I. Kulaeva[1,2], M. P. Kirpichnikov[1], V. M. Studitskiy[1,2*]
[1]Lomonosov Moscow State University, Leninskie Gory, 1/12, Moscow, 119991, Russia
[2]Fox Chase Cancer Center, Philadelphia, PA, 19111-2497, USA
E-mail: mal_nat@mail.ru; Vasily.Studitsky@fccc.edu
Received 10.12.2014

ABSTRACT **The poly (ADP-ribose) polymerase 1 (PARP1) enzyme is one of the promising molecular targets for the discovery of antitumor drugs. PARP1 is a common nuclear protein (1–2 million molecules per cell) serving as a "sensor" for DNA strand breaks. Increased PARP1 expression is sometimes observed in melanomas, breast cancer, lung cancer, and other neoplastic diseases. The PARP1 expression level is a prognostic indicator and is associated with a poor survival prognosis. There is evidence that high PARP1 expression and treatment-resistance of tumors are correlated. PARP1 inhibitors are promising antitumor agents, since they act as chemo- and radiosensitizers in the conventional therapy of malignant tumors. Furthermore, PARP1 inhibitors can be used as independent, effective drugs against tumors with broken DNA repair mechanisms. Currently, third-generation PARP1 inhibitors are being developed, many of which are undergoing Phase II clinical trials. In this review, we focus on the properties and features of the PARP1 inhibitors identified in preclinical and clinical trials. We also describe some problems associated with the application of PARP1 inhibitors. The possibility of developing new PARP1 inhibitors aimed at DNA binding and transcriptional activity rather than the catalytic domain of the protein is discussed.**

KEYWORDS **PARP1 inhibitors, poly (ADP-ribose) polymerase 1, antitumor agents.**

ABBREVIATIONS **PARP1 – poly (ADP-ribose) polymerase 1; BER – base excision repair; NER – nucleotide excision repair; MMR – mismatch repair; HR –homologous recombination; NHEJ –non-homologous end joining; SSB – single-strand break; DSB – double-strand break; TMZ – temozolomide; Topo I – topoisomerase 1; CT – clinical trial; PLD – potentially lethal damage.**

INTRODUCTION

Modern drug discovery and design are based on molecular targeting. The poly (ADP-ribose) polymerase 1 (PARP1) enzyme is one of the targets used in anticancer drug design. It is involved in many cellular processes, from DNA repair to cell death [1]. Recently, recognition of DNA breaks by the PARP1 enzyme was demonstrated to be one of the earliest events that occur upon DNA damage. Once DNA strand breaks occur, in particular due to alkylating agents and radiation, PARP1 binds to the break sites using the so-called "zinc fingers" located in the DNA-binding domain of PARP1 and simultaneously synthesizes oligo-(ADP-ribose) or poly-(ADP-ribose) chains, which are covalently bound to various acceptor proteins or the PARP1 molecule, by transferring an ADP-ribose moiety from NAD+. This leads to chromatin decondensation at the break site, facilitating access for repair enzymes. Modified poly-(ADP-ribosyl)ated chromatin proteins attract chromatin remodeling factors. One of the key mechanisms of PARP1-dependent decondensation is based on the fact that an activated PARP1 facilitates the removal of the H1 linker histone from transcription initiation sites. Removal of H1 leads to chromatin decondensation, which allows repair enzymes to attack the damaged DNA sites. It should be noted that DNA repair with active involvement of PARP1 occurs only upon minimal genotoxic damage. Stronger damage triggers apoptosis, while more extensive DNA damage results in overactivation of PARP, leading to cell necrosis.

There is abundant data on the involvement of PARP1 in carcinogenesis. Loss of PARP1 leads to disturbances in the DNA repair process and inhibition of the transcription of several genes involved in DNA replication and cell cycle regulation. Underexpression of PARPI leads to genome shuffling and chromosomal abnormalities and may contribute to overall genome instability. At the same time, increased PARP1 expression is observed in melanomas and lung and breast tumors [2–7]. In this case, the increased expression is considered to be a prognostic feature associated with a poor survival prognosis [8]. A high level of PARP1 expression was shown to correlate with a more aggressive phenotype of breast cancers (BCs) (estrogen-negative BC) [9]. PARP1 expression may correlate with tumor resistance to therapy [10]. This higher "malignancy" is apparently due to the fact that the increased PARP1 expression facilitates damaged DNA repair and, there-

by, overcoming the genetic instability characteristic of transformed cells.

There are various mechanisms of the pro-tumor activity of PARP1. In some cases, they are mediated by various tumor-associated transcription factors. Carcinogenesis can be caused by PARP1-dependent deregulation of the factors involved in the cell cycle and mitosis, as well as the factors regulating the expression of the genes associated with the initiation and development of tumors [11]. The relationship between PARP1 and the NF-kB factor has been revealed. PARP1 was found to co-regulate the NF-kB activity and lead to increased secretion of pro-metastatic cytokines. The NF-kB signaling cascade is known to be essential for tumor growth [12]. Inhibition of PARP1 disables a pro-invasive phenotype [13, 14]. PARP1 is known to control the expression of heat shock protein 70 (HSP70) [15, 16], which significantly contributes to the survival of tumor cells and their resistance to antitumor agents [17]. PARP1 interacts with the p21 protein, which controls the cell cycle. This may also promote a tumor phenotype [18]. The p21 protein directly interacts with PARP1 during DNA repair, and p21 knockdown leads to an increased enzymatic activity of PARP1. Expression of p21 in tumors is often suppressed due to p53 regulation [19], which may explain the possible role of PARP1 in carcinogenesis. PARP1 was also found to be involved in the hormone-dependent regulation of carcinogenesis. In prostate cancer cells expressing the androgen receptor (AR), PARP1 is recruited to the sites of AR localization and stimulates AR activity [20]. Similar chromatin-dependent mechanisms with the participation of PARP1 are involved in the estrogen-dependent regulation of gene expression in breast cancer (BC).

Since PARP1 is a key enzyme regulating certain carcinogenic changes in the cell, it is regarded as an important molecular target for designed antitumor agents and PARP1 inhibitors are considered to be promising anticancer drugs.

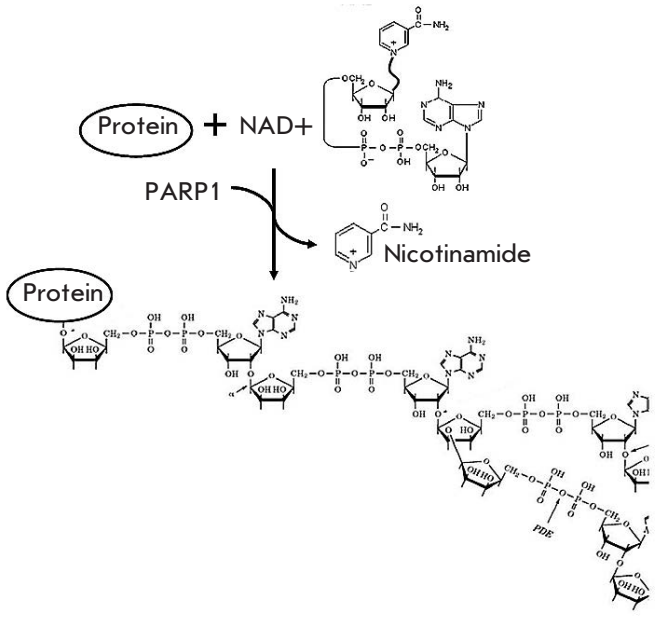

Fig. 1. Protein poly (ADP-ribosyl)ation reaction

THE HISTORY OF PARP1 INHIBITOR DESIGN

Since the effect of radiation therapy and many chemotherapeutic approaches to cancer is determined by DNA damage, PARP1 inhibitors can be used to enhance conventional methods and act as chemosensitizers and radiosensitizers. In cells treated with anticancer agents, PARP1 inhibition suppresses the repair of potentially lethal damage and may lead to the destruction of abnormal cells. Similarly, PARP1 inhibitors in some cases increase the efficacy of DNA-alkylating agents (e.g., Temozolomide) and topoisomerase I inhibitors (e.g., topotecan), as well as ionizing radiation. PARP1 inhibitors are also effective in radiosensitization of tumor cells. Along with the synergistic effect of PARP1 inhibitors and other DNA-damaging antineoplastic agents, a direct toxic effect of PAPR1 inhibitors is observed in some tumor cells.

The first generation of typical PARP1 inhibitors, nicotinamide analogues, was developed about 30 years ago based on observations that nicotinamide, a second product of the PARP1-catalyzed reaction, causes moderate inhibition of the reaction *(Fig. 1)*. In first-genera-

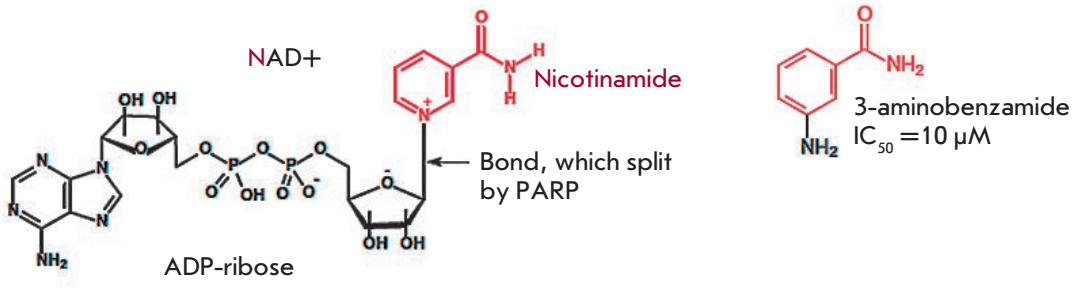

Fig. 2. First-generation PARP1 inhibitor, 3-aminobenzamide (3-AB). A nicotinamide pharmacophore group is shown in red

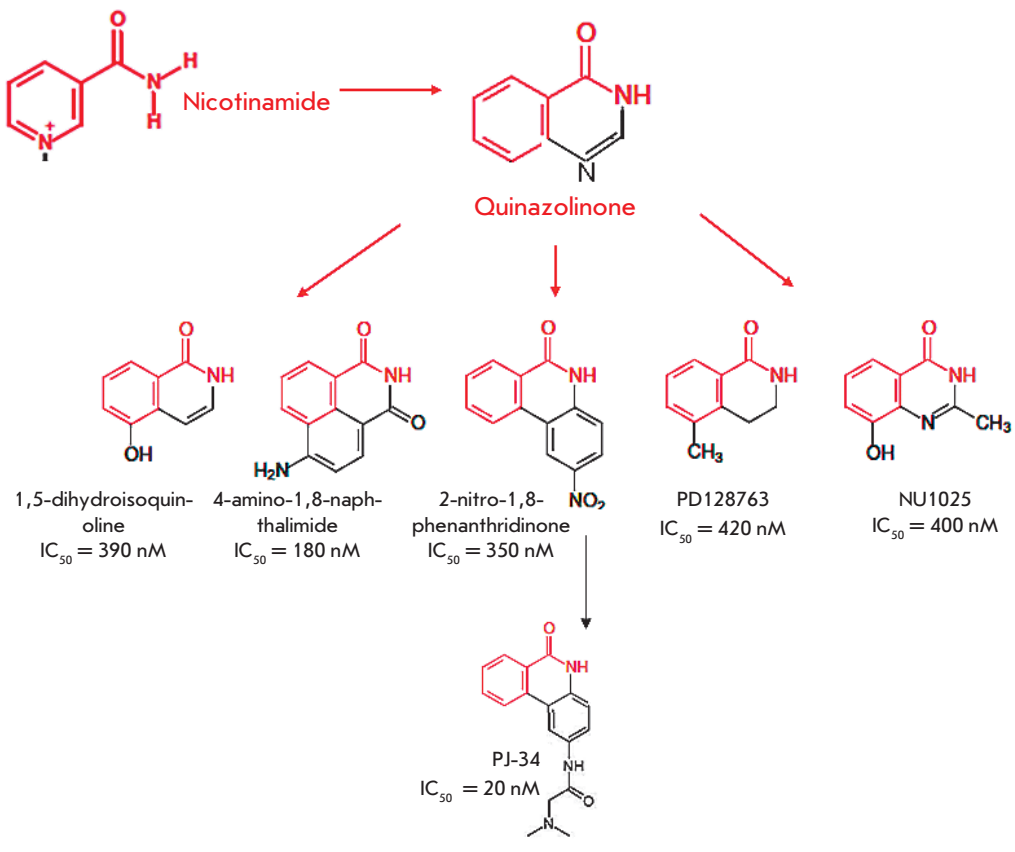

Fig. 3. Second-generation inhibitors. A nicotinamide pharmacophore group is shown in red

tion PARP1 inhibitors, the heterocyclic nitrogen atom at the third position was replaced by a carbon atom, which led to the development of a class of benzamide analogues [21]. Substitution at the third position led to improved drug solubility *(Fig. 2)*. Investigation of the activity of 3-substituted benzamides (e.g., 3-aminobenzamide, 3-AB) provided a better understanding of the PARP1 function. These drugs turned out to have a cytotoxic effect on tumor cells when used concomitantly with genotoxic stress agents [22]. Despite the encouraging results in the investigation of first-generation PARP1 inhibitors, benzamides proved ineffective in practice. In preclinical trials in cell cultures, they had to be used at millimolar concentrations, which made them inappropriate for trials in animals. Furthermore, benzamides inhibited other cellular pathways [23]. Nevertheless, they provided the basis for developing more effective drugs. Virtually all currently used PARP1 inhibitors comprise the nicotinamide/benzamide pharmacophore group.

In the 1990s, more effective second-generation PARP1 inhibitors were developed based on quinazoline analogues (in particular, 1,5-dihydroisoquinoline). This group of compounds includes isoquinolines, quinazolinediones, phthalazinones, and phenanthridinones. Second-generation PARP1 inhibitors were more effective and target-specific [24]. Some of these compounds became the basis for further development of various drug groups *(Fig. 3)*. In particular, the production of phenanthridinones led to the development of PJ-34, which was further used in clinical trials (CTs) [25]. An alternative approach (chemical synthesis based on the analysis of the structure and activity relationship, SAR) led to the identification of 3,4-dihydro-5-methyl-1-[2H]-isoquinolinone (PD128763) and 8-hydroxy-2-methylquinazolin-4-[3H]-one (NU1025). Both of these compounds are ~50 times more effective PARP1 inhibitors than 3-AB.

Later on, more potent inhibitors were developed on the analogy with existing ones. All of them contained a carboxamide group of the benzamide pharmacophore in the second aromatic ring. This was the modification that proved crucial for increasing the activity of inhibitors. The reasons explaining the relationship between these structural features and the increased activity became apparent after structural studies. Crystallization of PARP1 inhibitors showed that the carboxamide group forms several important hydrogen bonds with Ser904-OG and Gly863-N in the catalytic domain of PARP1, which improves the interaction between the heterocycle of these inhibitors and the protein [26]. In this case, the amide group of more effective inhibitors (PD128763, 4ANI, and NU1025) is restricted in the het-

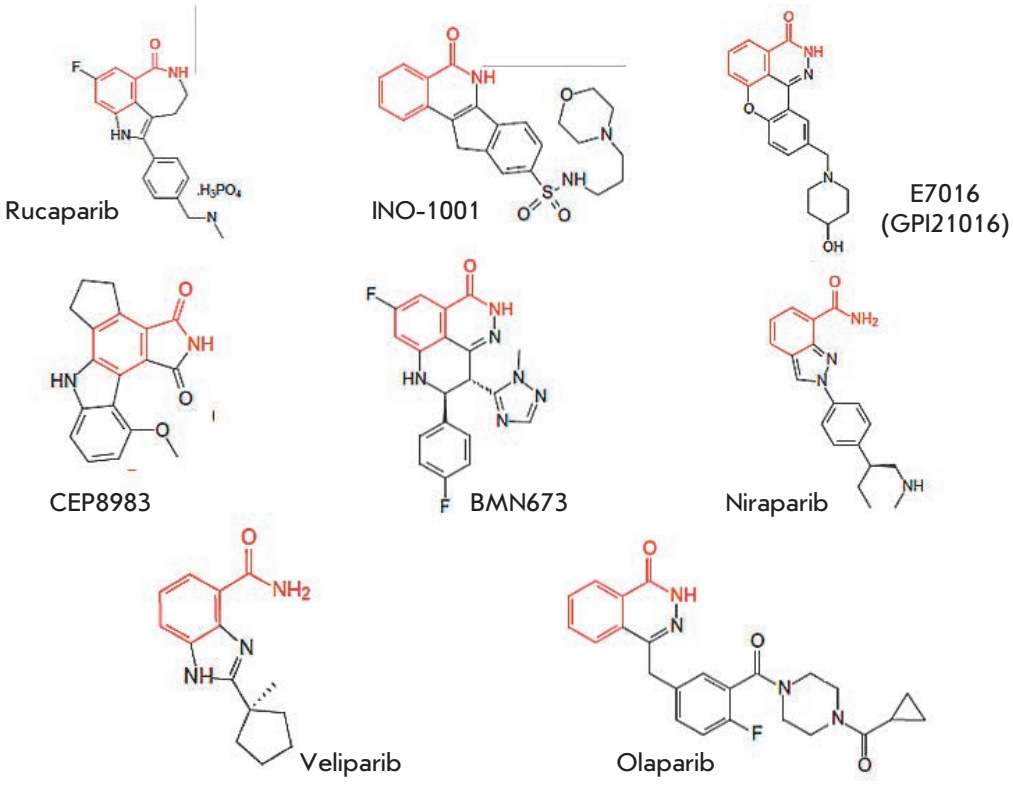

Fig. 4. Structures of third-generation PARP1 inhibitors. A nicotinamide pharmacophore group is shown in red

erocyclic ring. The significance of aromatic (ϖ-ϖ) interactions between a phenolic group of PARP1 inhibitors and a phenolic group of Tyr907 of the PARP1 protein was also revealed. On the basis of the structural analysis of NU1085 binding, several tricyclic lactam indoles and benzimidazoles were developed in which a carboxamide group was introduced in a favorable orientation by its inclusion into a 7-membered ring [27–30]. These compounds (for example, AG14361) are capable of forming crucial hydrogen bonds with Gly863, Ser904, and Glu988 of the PARP1 protein [31].

Further search led to the development of more potent third-generation PARP inhibitors, the first characterized representative of which was rucaparib (K_i = 1.4 nM) [32]. At present, a number of benzimidazole-based PAPP1 inhibitors of the third generation have been synthesized. Many of them (e.g., rucaparib, iniparib, olaparib, veliparib, niraparib, talazoparib, CEP-9722, and E7016) are currently undergoing clinical trials (see reviews [33–38], *Fig. 4*, *table*).

MECHANISMS OF ACTION OF PARP1 INHIBITORS: DIRECT ANTITUMOR ACTION

PARP1 inhibition leads to failure of DNA repair. PARP1 is known to bind to single-strand and double-strand DNA breaks in response to DNA damage [39]. In the absence of damage, the PARP1 activity is minimal. However, the appearance of damages causes its immediate and significant (up to 500 times) activation. PARP1 finds DNA breaks, acting as a sensor and providing a rapid recruitment of repair proteins to the break site. PARP1 controls several DNA repair pathways, including base excision repair (BER), nucleotide excision repair (NER), mismatch repair (MMR), and repair of double-strand breaks through homologous recombination (HR) and non-homologous end-joining (NHEJ) [39].

Inhibition of PARP leads to inactivation of the repair system and retention of spontaneous single-strand breaks (SSBs) *(Fig. 5A)*, which may induce the subsequent formation of double-strand DNA breaks (DSBs). DSBs can be repaired in two ways, either by "error-free DNA repair" using HR, or by repair with possible replacement of the nucleotides in a sequence by NHEJ [40, 41]. In some tumor cells with disruption in the homologous recombination system (e.g., BRCA-mutated cells), the NHEJ system can be turned on. However, the use of NHEJ in these tumors leads to destabilization of the genome and, eventually, cell death due to rapid accumulation of genetic errors [42–44].

In 2005, there was a breakthrough in the research of PARR1 inhibitors. Two independent groups of researchers demonstrated that BRCA1- and BRCA2-deficient cell lines are sensitive to the direct action of PARP inhibitors. It was the first evidence that PARP1

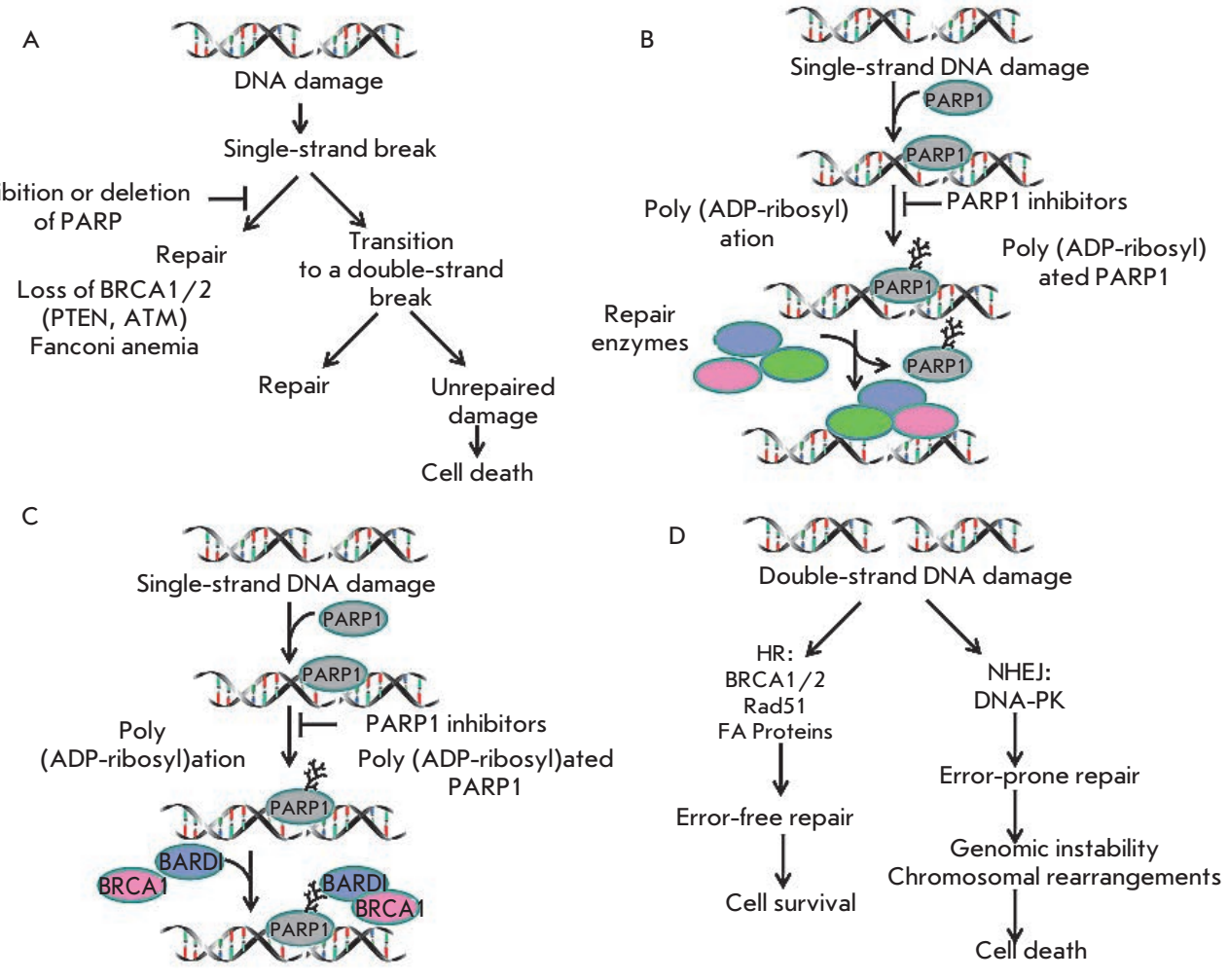

Fig. 5. Direct cytotoxic effect of PARP1 inhibitors. *A* — inhibition of PARP1 leads to inactivation of a repair system and preservation of spontaneously occurring single-strand breaks (SSBs), which causes formation of double-strand breaks. *B* — because of the action of PARP1 inhibitors, PARP1 remains bound to damaged DNA and, thus, cannot dissociate from it and clear the area for PARP1-dependent repair enzymes. *C* — in the presence of PARP inhibitors, mutant BRCA1 is less accumulated at the DNA damage site, *D* — when double-strand breaks occur in HR-deficient cells, another NHEJ system is activated. As a result, repair errors occur that can lead to genomic instability and cell death

inhibitors can act as independent remedies in the case of tumors in which certain DNA repair pathways are disrupted [45, 46]. The tumor-associated *BRCA1* gene is known to play an important role in the repair of double-strand breaks through the HR mechanism. BRCA1-deficient cells are characterized by less effective HR, and DNA repair in these cells mainly occurs via the BER system. BRCA2 interacts with the RAD51 protein and also plays a significant role in HR. Cells with mutations in the BRCA2 region responsible for binding to RAD51 exhibit hypersensitivity to DNA damage and chromosomal instability [47]. For example, 10–15% of serious ovarian cancers are hereditary and caused by a mutation in the *BRCA1* or *BRCA2* gene. HR repair defects arising from mutations in *RAD51*, *DSS1*, *RPA1*, or *CHK1* were shown to cause increased sensitivity of cells to PARP1 inhibition [48]. In the case of homologous recombination deficiency, inhibition of DNA damage repair leads to cell death due to the inability to fix all DNA damage.

The direct action of PARP1 inhibitors on tumor cells may also be explained by another mechanism. Because of inhibitor action, PARP1 is believed to remain bound to damaged DNA, and, therefore, it cannot dissociate from the DNA and "clear" the area for PARP1-dependent repair enzymes *(Fig. 5B)*.

The third model of the direct action of PARP1 inhibitors is based on the observations of Li and Yu [49], who showed that mutant BRCA1 is less accumulated at the DNA damage site in the presence of PARP1 inhibitors *(Fig. 5C)*.

A fourth model of the direct action of PARP1 inhibitors *(Fig. 5D)* was also proposed. According to this model, double-strand breaks in HR-deficient cells result in activation of another NHEJ system [44]. As previously shown, key proteins in this system (Ku70, Ku80, and DNA-PKcs) have PARP1-binding motifs and can be controlled via ADP-ribosylation [50, 51].

In clinical studies, olaparib monotherapy resulted in inhibition of tumors with mutations in *BRCA1* or *BRCA2* (breast cancer and ovarian cancer) [52, 53]. In this case, BRCA1- or BRCA2-deficient cells were 57 or 133 times more sensitive to PARP1 inhibition, respectively [46]. However, the efficacy of this therapy was low; a positive response was observed in less than 50% of patients [54]. Therefore, it is very important to correctly identify the prognostic markers of PARP1 inhibitor therapy. Mutations in the *RAD51, NBS1, ATM, ATR, Chk1, Chk2, Rad54, FANCD2, FANCA, 53BP1, PALB2, FANCC,* and *PTEN* genes may serve these markers [39, 55–59].

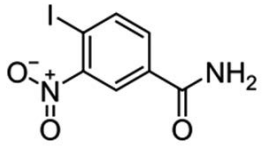

Iniparib

Fig. 6. The structure of iniparib

Terminal mutations of the *BRCA1* or *BRCA2* gene in tumor cells lead to defects in the homologous DNA recombination system whose normal activity involves both BRCA proteins. In this case, tumor cells become extremely dependent on one of the five other repair systems, with PARP1 being involved in each of them. In the case of homologous recombination deficiency, PARP1 inhibition leads to cell apoptosis because of the impossibility to repair all DNA damage. This process is called "synthetic lethality." Several studies have shown

Table. Clinical trials of PARP1 inhibitors. Data were borrowed from reviews [42, 43]

Name	Therapy	Tumors	CT phase
Rucaparib AG014699	Monotherapy	BRCA mutant lung cancer, ovarian cancer	2
Rucaparib	+temozolomide	Solid tumors, melanoma	2
Rucaparib	+carboplatin	Solid tumors	1
Olaparib	Monotherapy	Solid tumors, BRCA, TNBC/HGSOC carriers	2
Olaparib	+topotecan	Solid tumors	1
Olaparib	+dacarbazine	Solid tumors	1
Olaparib	+bevacizumab	Solid tumors	1
Olaparib	+paclitaxel	Ovarian Cancer	2
Olaparib	+paclitaxel	Stomach cancer	2
Olaparib	+cisplatin	Solid tumors	1
Veliparib ABT-888	Monotherapy	Solid tumors	1
Veliparib	+topotecan	Solid tumors	1
Veliparib	+carboplatin	Solid tumors	1
Veliparib	+temozolomide	Solid tumors, liver tumors, prostate cancer	2
Veliparib	+cyclophosphamide	Solid tumors and lymphomas	2
INO-1001	+temozolomide	Melanoma	1
MK4827	Monotherapy	Solid tumors and lymphoma	2
MK4827	+temozolomide	Ovarian cancer/glioblastoma	1
MK4827	+doxorubicin	Ovarian cancer/glioblastoma	1
CEP-9722	Monotherapy	Solid tumors	1
CEP-9722	+temozolomide	Lymphomas	1
BMN-673	Monotherapy	Solid tumors	1
Iniparib (BSI-201)	+gemcitabine +carboplatin	mTNBC	2
Iniparib	+gemcitabine +cisplatin	Lung cancer	2
Iniparib	+gemcitabine +carboplatin	mTNBC	3

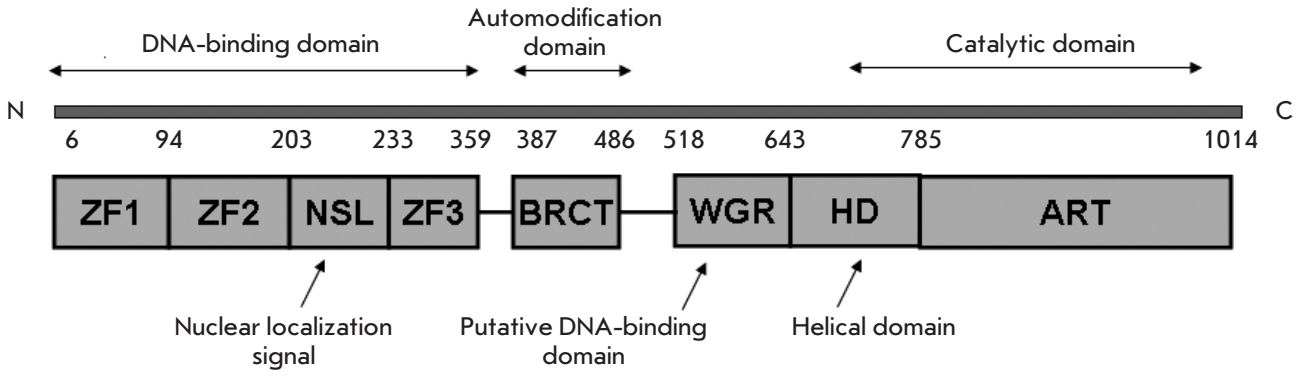

Fig. 7. Structural and functional organization of PARP1. The PARP1 structure is composed of three main functional domains: N-terminal DNA-binding domain, internal automodification domain, and C-terminal catalytic domain [108, 109], as well as additional functional sites

that administration of PARP1 inhibitors is a promising treatment in patients with tumors arising from defects in the *BRCA* genes.

MECHANISMS OF ACTION OF PARP1 INHIBITORS: SYNERGISTIC ACTION

PARP1 inhibitors do not always have a direct cytotoxic effect on tumor cells. In these cases, the desired effect can be achieved by concomitant administration of PARP1 inhibitors and other DNA-damaging drugs.

SYNERGISTIC ACTION OF PARP1 INHIBITORS AND DNA METHYLATING AGENTS

As early as in the 1980s, it was shown by the example of 3-AB that PARP inhibitors enhance the action of DNA-methylating agents [22]. DNA-methylating agents, such as dacarbazine (DTIC) and temozolomide (TMZ), are currently widely used in the treatment of brain tumors and melanomas. These drugs are capable of methylating DNA at the O^6 and N^7 positions of guanine and the N^3position of adenine. Removal of N-methylpurines (N^7-MEG and N^3-MEA) leads to the emergence of SSBs, while inhibition of PARP1 inactivates repair of this damage [60]. Early studies demonstrated that PD128763 and NU1025 enhance TMZ-induced DNA damage and increase TMZ cytotoxicity 4–7 times when used at lower TMZ concentrations (50–100 times) [61]. Improved efficacy of TMZ (up to 6 times) in the presence of NU1085 was observed in 12 different human tumor lines, independent of their tissue origin and p53 status [62]. A series of benzimidazoles and tricyclic lactam indoles, including AG14361 at a concentration as low as 0.4 μM, enhances TMZ-induced inhibition of LoVo (human colon cancer) cell growth by a factor of 5.3 [30]. This synergistic action of inhibitors of PARP and Topo I was observed in numerous studies *in vitro*. It should be emphasized that PARP1 inhibitors were found to increase the cytotoxicity of TMZ primarily in the S-phase, which is indicative of the synergistic action mechanism. The inhibitors are most likely to cause accumulation of DSBs during replication [63, 64]. An enhanced antitumor activity of TMZ in the presence of various PARP inhibitors *in vivo* was demonstrated in many experiments. Here are some examples. Combined treatment with NU1025 and TMZ increases the survival rate of mice with brain lymphomas [65]. The GPI 15427 inhibitor enhances the TMZ-induced inhibition of tumor growth and the antimetastatic activity in a B16 melanoma model [66]. Veliparib enhances the activity of TMZ in subcutaneous, orthotropous, and metastatic models of human xenografts, including lymphomas and ovarian, lung, pancreatic, breast, and prostate cancers [67]. Interestingly, both GPI 15427 and veliparib pass through the blood-brain barrier and enhance the antitumor activity of TMZ in mice with intracranial melanomas, gliomas, and lymphomas [68]. In children tumor models, rucaparib enhances the antitumor activity of TMZ in neuroblastoma and medulloblastoma xenografts [69]. Complete tumor regression caused by treatment with TMZ and CEP-6800 was observed in mice bearing xenografts U251MG (human glioblastoma) [70] and SW620 (human colon cancer) [32, 71]. These and other data obtained in experiments *in vivo* gave rise to clinical trials of PARP inhibitors together with DNA methylating agents *(see table)*.

SYNERGISTIC ACTION OF INHIBITORS OF PARP1 AND TOPOISOMERASE I (TOPO I)

Topo I activity is known to be enhanced in some tumors [72]. Topo I inhibitors are used against various forms of tumors. For example, topotecan is used in the treatment of

small-cell lung cancer, ovarian cancer, and cervical cancer. Irinotecan is used in the treatment of colon cancer. Topo I introduces temporary damage to DNA to remove the stress accumulated in the DNA during transcription and replication. Topo I inhibitors, e.g., camptothecins, stabilize the Topo I-DNA cleavage complex at a stage where DNA breaks occur. Repair of Topo I-induced damage involves BER/SSB. In this case, cells lacking the key BER protein, XRCC1, are hypersensitive to camptothecin. PARP enzymes are believed to be involved in this process, recruiting XRCC1 to Topo I-dependent DNA breaks [73], which, in turn, recruit tyrosyl-DNA-phosphodiesterase (TDP 1), which removes Topo I from DNA [74]. Furthermore, PARP1 is capable of interacting with Topo I and repairing Topo I-dependent SSBs [75]. Several studies have demonstrated the potentiation of topoisomerase I inhibitors in the presence of PARP inhibitors [30, 32, 71]. Here are some examples. In 1987, Mattern M.R. *et al.* were the first to use PARP inhibitors as potential enhancers of Topo I inhibitors. They showed that 3-AB increases the cytotoxicity of Camptothecin in L1210 cells [76]. Later on, the synergistic action of Topo I and PARP1 inhibitors was extensively studied. It was shown in 12 human tumor cell lines that NU1025 and NU1085 enhance the cytotoxicity of topotecan, regardless of the tissue origin of these lines and p53 status [62]. CEP-6800 and GPI 15427 enhance the chemosensitivity of colon cancer cell lines to Topo I inhibitors [70, 77]. Encouraging results were also obtained in *in vivo* experiments studying the combined effect of PARP and Topo I inhibitors. CEP-6800 increased the irinotecan-dependent inhibition of tumors in mice bearing HT29 xenografts by 60% [70], while olaparib increased the toxicity of topotecan, so that its dose could be reduced by a factor of 8 [78]. These and other results of *in vivo* experiments gave rise to clinical trials of a combined application of PARP inhibitors and Topo I inhibitors *(table)*.

SYNERGISTIC ACTION OF PARP1 INHIBITORS AND RADIOTHERAPY

Ionizing radiation causes various damage to DNA, modification of bases, SSBs, and DSBs; the latter are believed to be the most cytotoxic ones. Sensitization of cells which have been treated with PARP inhibitors to ionizing radiation is less significant than their sensitization to chemical compounds and typically increases the cytotoxicity by less than two times. However, given the large number of patients subjected to radiation therapy, this combination may be reasonable. Early studies demonstrated that inhibition of PARP leads to radiosensitization of mammalian cells [79]. Later on, it was shown that various PARP inhibitors (ANI, NU1025, olaparib, and E7016) enhance the radiosensitization efficacy in various cell lines by a factor of 1.3–1.7 [80]. In some studies, PARP inhibitors selectively induced radiosensitization of actively replicating cells in the S-phase [24]. This suggested a mechanism by which PARP inhibition increases the sensitivity to ionizing radiation. The inhibition prevents the repair of SSBs, converting them into DSBs during the movement of the replication fork in the S-phase [81]. This hypothesis is supported by the observation that PARP inhibition leads to the formation of additional γH2AX and RAD51 foci (which is indicative of an increased frequency of homologous recombination repair (HRR) at the stalled replication fork). The ability of cells to recover after potentially lethal damage (PLD) is a predisposing factor for radiation resistance *in vivo*. However, there is a chance for preservation of radioresistant tumor cells that can reproduce the tumor after radiation therapy [82]. PARP1 inhibitors (e.g., PD128763, NU1025, and AG14361) were shown to prevent recovery of tumor cells after PLD [63]. A number of studies have revealed the effectiveness of radiosensitization by PARP1 inhibitors *in vivo*. The PD128763 inhibitor induced a threefold increase in the therapeutic activity of X-rays in mice bearing SCC7, RIF-1, and KHT sarcomas [83]. Preclinical studies demonstrated that veliparib significantly enhances the antitumor activity of ionizing radiation in xenograft models of human colon, lung, and prostate cancers [68, 84, 85].

PARP1 INHIBITOR EFFECT IN COMBINATION WITH OTHER CYTOTOXIC DRUGS

There is some evidence of the ability of PARP inhibitors to enhance the effect of other antitumor cytotoxins. For example, 6(5H)-phenanthridinone enhances the cytotoxicity of carmustine in mice lymphoma [86]. PJ34 increases the cytotoxicity of doxorubicin in HeLa cells, presumably due to an increased level of topoisomerase II [87]. A similar compound, INO-1001, enhances the antitumor activity of doxorubicin in xenografts of MDA-MB-231 and MCA-K lung cancer cells [88]. Reports of the synergistic action of PARP inhibitors and platinum compounds, such as cisplatin and carboplatin, are contradictory. Nevertheless, some studies demonstrated that PARP1 is activated by cisplatin-induced DNA damage [89], which gave rise to clinical trials of PARP inhibitors combined with cisplatin derivatives *(table)*.

APPLICATION ISSUES OF EXISTING PARP1 INHIBITORS AND PROSPECTS FOR NEW INHIBITOR DISCOVERY

Almost all existing PARP1 inhibitors are nicotinamide mimetics, i.e. aimed at binding to the catalytic domain of PARP1 and competition with NAD+. In experiments *in vitro*, as well as in a variety of preclinical and some clinical trials, PARP1 inhibitors showed quite good results as antitumor agents. However, a number of prob-

lems were uncovered in more systematic, controlled, extensive clinical trials of PARP1 inhibitors. First, compounds inhibiting NAD+ binding have a rather low specificity for PARP1 and also block other enzymatic pathways involving NAD+. It should be noted that NAD+ is a cofactor that interacts with many enzymes involved in a number of cellular processes, and, therefore, competition with NAD+ leads to high toxicity. Second, enzymatic PARP1 inhibitors activate viral replication and are contraindicated for patients infected with viruses such as the human T-cell lymphotropic virus (HTLV) or Kaposi's sarcoma-associated herpes virus (KSHV) [90–92]. Third, the safety issue in long-term administration of existing PARP1 inhibitors still remains open. Tumor cells are known to be able to rapidly acquire resistance to drugs used as a long-term monotherapy [93]. For these reasons, many PARP1 inhibitors did not pass long-term systematic clinical trials. Trials of some PARP1 inhibitors were discontinued as early as at stages I and II due to high toxicity and some side effects. The history of iniparib (BSI-201) is illustrative in this respect. This drug was the most developed compared to the other PARP1 inhibitors and entered a phase III randomized clinical trial.

Phase III clinical trials of BSI-201 (iniparib) began in July 2009 to assess the efficacy of this drug in combination with chemotherapy in female patients with metastatic triple-negative breast cancer (mTNBC). The study involved 519 females with mTNBC from 109 centers in the USA. And as early as in 2013, Sanofi-aventis announced the termination of clinical trials as no improvement in patients' condition and overall survival of patients treated with iniparib and chemotherapy was observed compared to the control group (chemotherapy alone). A number of circumstances led to the failure of clinical trials of iniparib. The main cause for the failure was that preclinical experiments were not complete by the time of group recruitment for clinical trials; very little information on the iniparib action mechanism was gained. Iniparib had been admitted to phase I CTs before the results of preclinical studies were obtained [94, 95]. In this regard, one more fact is interesting: Bipar company, which designed iniparib and the project for Sanofi, did not disclose the compound structure for patent reasons. Later on, it occurred that, unlike all the other PARP1 inhibitors having a similar structure, only iniparib had a flexible carboxyl group capable of rotating around the amide bond, which significantly weakened binding of the inhibitor to PARP1 *(Fig. 6)*. One of Sanofi's experts confided that "If Bipar had provided us with the iniparib structure; we would probably have been able to assume that it would not be a good PARP1 inhibitor." However, despite an insufficient description of the drug (known structure and pharmacodynamic data), the company included it in clinical trials, which cost Sanofi-aventis 285 million dollars.

The quite high toxicity and some side effects caused by enzymatic PARP1 inhibitors in CTs necessitate alternation in the strategy for new PARP1 inhibitor development. Since PARR1 consists of several functional domains and exhibits accessory, along with enzymatic, activities, in particular DNA-binding and transcriptional ones *(Fig.7)*, PARP1 activity can be regulated by inhibiting these functional domains. In particular, drugs aimed at inhibiting PARP1 binding to DNA are being developed [96]. According to these authors, discovery of compounds capable of preventing PARP1 involvement in the transcription process may lead to the development of a new class of drugs with higher specificity and less severe side effects. More information about the role of PARP1 in transcriptional regulation can be found in [97–101]. The use of a transcriptional system, which was previously obtained by these authors, in mononucleosome and polynucleosome systems enables the discovery and verification of transcriptional inhibitors of PARP1.

In conclusion, it should be noted that PARP1 inhibitors are of great interest and practical value not only in oncology, but also in the treatment of various inflammatory processes, cardiovascular and neurological diseases, as well as age-related diseases. The therapeutic effect of PARP inhibitors in these processes was beyond the scope of this review (see reviews [102–107] for details). ●

This work was supported by the Federal Target Program "Research and developments in the priority directions of the scientific-technological complex of the Russian Federation for 2014–2020" (Agreement of the Ministry of Education of the Russian Federation No 14.604.21.0063, RFMEFI60414X0063).

REFERENCES

1. Kraus W.L., Hottiger M.O. // Mol. Aspects Med. 2013. V. 34. № 6. P. 1109–1123.
2. Rodríguez M.I., Peralta-Leal A., O'Valle F., Rodriguez-Vargas J.M., Gonzalez-Flores A., Majuelos-Melguizo J., López L., Serrano S., de Herreros A.G., Rodríguez-Manzaneque J.C., et al. // PLoS Genet. 2013. V. 9. № 6. P. e1003531.
3. Nowsheen S., Cooper T., Stanley J.A., Yang E.S. // PLoS One. 2012. V. 7. № 10. P. e46614.
4. Galia A., Calogero A.E., Condorelli R., Fraggetta F., La Corte A., Ridolfo F., Bosco P., Castiglione R., Salemi M. // Eur. J. Histochem. 2012. V. 56. № 1. P. e9.
5. Csete B., Lengyel Z., Kádár Z., Battyáni Z. // Pathol. Oncol. Res. 2009. V. 15. № 1. P. 47–53.

6. Telli M.L., Ford J.M. // Clin. Breast Cancer. 2010. V. 10. Suppl 1. P. E16–22.
7. Shimizu S., Nomura F., Tomonaga T., Sunaga M., Noda M., Ebara M., Saisho H. // Oncol. Rep. 2004. V. 12. № 4. P. 821–825
8. Rojo F., García-Parra J., Zazo S., Tusquets I., Ferrer-Lozano J., Menendez S., Eroles P., Chamizo C., Servitja S., Ramírez-Merino N., et al. // Ann. Oncol. 2012. V. 23. № 5 P. 1156–1164.
9. Domagala P., Huzarski T., Lubinski J., Gugala K., Domagala W. // Breast Cancer Res. Treat. 2011. V. 127. № 3. P. 861–869.
10. Michels J., Vitale I., Galluzzi L., Adam J., Olaussen K.A., Kepp O., Senovilla L., Talhaoui I., Guegan J., Enot D.P., et al. // Cancer Res. 2013. V. 73. № 7. P. 2271–2280.
11. Simbulan-Rosenthal C.M., Ly D.H., Rosenthal D.S., Konopka G., Luo R., Wang Z.Q., Schultz P.G., Smulson M.E. // Proc. Natl. Acad. Sci. USA. 2000. V. 97. № 21. P. 11274–11279.
12. Dajee M. Lazarov M., Zhang J.Y., Cai T., Green C.L., Russell A.J., Marinkovich M.P., Tao S., Lin Q., Kubo Y., Khavari P.A..// Nature. 2003. V. 421.№ 6923. P. 639–643.
13. Martín-Oliva D., O'Valle F., Muñoz-Gámez J.A., Valenzuela M.T., Nuñez M.I., Aguilar M., Ruiz de Almodóvar J.M., Garcia del Moral R., Oliver F.J. // Oncogene. 2004. V. 23. № 31. P. 5275–5283.
14. Ohanna M., Giuliano S., Bonet C., Imbert V., Hofman V., Zangari J., Bille K., Robert C., Bressac-de Paillerets B., Hofman P., et al. // Genes Dev. 2011. V. 25. № 12. P. 1245–1261.
15. Tulin A., Spradling A. // Science. 2003. V. 299. № 5606. P. 560–562.
16. Petesch S.J., Lis J.T. // Cell. 2008. V. 134. № 1. P. 74–84.
17. Leu J.I., Pimkina J., Frank A., Murphy M.E., George D.L. // Mol. Cell. 2009. V. 36. № 1. P. 15–27.
18. Cazzalini O., Donà F., Savio M., Tillhon M., Maccario C., Perucca P., Stivala L.A., Scovassi A.I., Prosperi E. // DNA Repair. 2010. V. 9. № 6. P. 627–635.
19. Abbas T., Dutta A. // Nat. Rev. Cancer. 2009. V. 9. № 6. P. 400–414.
20. Schiewer M.J., Goodwin J.F., Han S., Brenner J.C., Augello M.A., Dean J.L., Liu F., Planck J.L., Ravindranathan P., Chinnaiyan A.M., et al. // Cancer Discov. 2012. V. 2. № 12. P. 1134–1149.
21. Purnell M.R., Whish W.J. // Biochem. J. 1980. V. 185. № 3. P. 775–777.
22. Durkacz B.W., Omidiji O., Gray D.A., Shall S. // Nature. 1980. V. 283. № 5747. P. 593–596.
23 Milam K.M., Cleaver J.E. // Science. 1984. V. 223. № 4636. P. 589–591.
24. Banasik M., Komura H., Shimoyama M., Ueda K. // J. Biol. Chem. 1992. V. 267. № 3. P. 1569–1575.
25. Jagtap P., Szabó C. // Nat. Rev. Drug Discov. 2005. V. 4. № 5. P. 421–440.
26. Ruf A., de Murcia G., Schulz G.E. // Biochemistry. 1998. V. 37. № 11. P. 3893–3900.
27. Canan Koch S.S., Thoresen L.H., Tikhe J.G., Maegley K.A., Almassy R.J., Li J., Yu X.H., Zook S.E., Kumpf R.A., Zhang C., et al. // J. Med. Chem. 2002. V. 45. № 23. P. 4961–4974.
28. Skalitzky D.J., Marakovits J.T., Maegley K.A., Ekker A., Yu X.H., Hostomsky Z., Webber S.E., Eastman B.W., Almassy R., Li J., et al. // J. Med. Chem. 2003. V. 46. № 2. P. 210–213.
29. Tikhe J.G., Webber S.E., Hostomsky Z., Maegley K.A., Ekkers A., Li J., Yu X.H., Almassy R.J., Kumpf R.A., Boritzki T.J., et al. // J. Med. Chem. 2004. V. 47. № 22. P. 5467–5481.
30. Calabrese C.R., Batey M.A., Thomas H.D., Durkacz B.W., Wang L.Z., Kyle S., Skalitzky D., Li J., Zhang C., Boritzki T., et al. // Clin. Cancer Res. 2003. V. 9. № 7. P. 2711–2718.
31. Marsischky G.T., Wilson B.A., Collier R.J. // J. Biol. Chem. 1995. V. 270. № 7. P. 3247–3254.
32. Thomas H.D., Calabrese C.R., Batey M.A., Canan S., Hostomsky Z., Kyle S., Maegley K.A., Newell D.R., Skalitzky D., et al. // Mol. Cancer Ther. 2007. V. 6. № 3. P. 945–956.
33. Mason K.A., Buchholz T.A., Wang L., Milas Z.L., Milas L. // Am. J. Clin. Oncol. 2014. V. 37. № 1. P. 90–100.
34. Ekblad T., Schüler H., Macchiarulo A. // FEBS J. 2013. V. 280. № 15. P. 3563–3575.
35. Hilton J.F., Tran M.T., Shapiro G.I. // Front. Biosci. (Landmark Ed). 2013. V. 18. P. 1392–1406.
36. Papeo G., Montagnoli A., Cirla A. // Expert. Opin. Ther. Pat. 2013. V. 23. № 4. P. 503–514.
37. Sonnenblick A., Azim H.A. Jr., Piccart M. // Nat. Rev. Clin. Oncol. 2015. V. 12. № 1. P. 27–41.
38. Curtin N.J., Szabo C. // Mol. Aspects Med. 2013. V. 34. № 6. P. 1217–1256.
39. De Lorenzo S.B., Hurley R.M., Kaufmann S.H. // Front Oncol. 2013. V. 11. № 3. P. 228.
40. Kuzminov A. // Proc. Natl. Acad. Sci. USA. 2001. V. 98. № 15. P. 8241–8246.
41. Chapman J.R., Boulton S.J. // Mol. Cell Biol. 2012. V. 47. № 4. P. 497–510.
42. Deindl S., Hota S.K., Blosser T.R., Prasad P., Bartholomew B., Zhuang X. // Cell. 2013. V. 152. № 3. P. 442–452.
43. Min I.M., Core L.J., Munroe R.J., Schimenti J., Lis J.T. // Genes Dev. 2011. V. 25. № 7. P. 742–754.
44. Patel A.G., Sarkaria J.N., Kaufmann S.H. // Proc. Natl. Acad. Sci. USA. 2011. V. 108. № 8. P. 3406–3411.
45. Bryant H.E., Thomas H.D., Parker K.M., Flower D., Lopez E., Kyle S., Meuth M., Curtin N.J., Helleday T. // Nature. 2005. V. 434. № 7035. P. 913–917.
46. Farmer H., Lord C.J., Tutt A.N., Johnson D.A., Richardson T.B., Santarosa M., Dillon K.J., Hickson I., Knights C., Martin N.M., et al. // Nature. 2005. V. 14. № 434. P. 917–921.
47. Donoho G., Brenneman M.A., Cui T.X., Donoviel D., Vogel H., Goodwin E.H., Chen D.J., Hasty P. // Genes, Chromosomes Cancer. 2003. V. 36. № 4. P. 317–331.
48. McCabe N., Turner N.C., Lord C.J., Kluzek K., Bialkowska A., Swift S., Giavara S., O'Connor M.J., Tutt A.N., et al. // Cancer Res. 2006. V. 66. № 16. P. 8109–8115.
49. Li M., Yu X. // Cancer Cell. 2013. V. 23. № 5. P. 693–704.
50. Miwa M., Masutani M. // Cancer Sci. 2007. V. 98. № 10. P. 1528–1535.
51. Paddock M.N., Higdon R., Kolker E., Takeda S., Scharenberg A.M. // DNA Repair. 2011. V. 10. № 3. P. 338–343.
52. Fong P.C., Yap T.A., Tutt A., Wu P., Mergui-Roelvink M., Mortimer P., Swaisland H., Lau A., O'Connor M.J., Ashworth A., et al. // N. Engl. J. Med. 2009. V. 361. № 2. P. 123–134.
53. Hutchinson L. // Nat. Rev. Clin. Oncol. 2010. V. 7. №10. P. 549.
54. Chan S.L. // Lancet. 2010. V. 376. № 9737. P. 211–213.
55. Bunting S.F., Callen E., Wong N., Chen H.-T., Polato F., Gunn A., Bothmer A., Feldhahn N., Fernandez-Capetillo O., Cao L., et al. // Cell. 2010. V. 141. № 2. P. 243–254.
56. Mukhopadhyay A., Elattar A., Cerbinskaite A., Wilkinson S.J., Drew Y., Kyle S., Los G., Hostomsky Z., Edmondson R.J., Curtin N.J. // Clin. Cancer Res. 2006. V. 16. № 8. P. 2344–2351.
57. Mendes-Pereira A.M., Brough R., McCarthy A., Taylor J.R., Kim J.S., Waldman T., Lord C.J., Ashworth A. // EMBO Mol. Med. 2009. V. 1. № 6. P. 315–322.

58. Buisson R., Coulombe Y., Launay H., Cai H., Stasiak A.Z., Stasiak A., Xia B., Masson J.Y. // Nat. Struct. Mol. Biol. 2010. V. 17. № 10. P. 1247–1254.
59. Williamson C.T., Turhan A.G., Zamò A., O'Connor M.J., Bebb D.G., Lees-Miller S.P. // Mol. Cancer Ther. 2010. V. 9. № 2. P. 347–357.
60. Villano J.L., Seery T.E., Bressler L.R. // Cancer Chemother. Pharmacol. 2009. V. 64. № 4. P. 647–655.
61. Boulton S., Pemberton L.C., Porteous J.K., Curtin N.J., Griffin R.J., Golding B.T., Durkacz B.W. // Br. J. Cancer. 1995. V. 72. № 4. P. 849–856.
62. Delaney C.A., Wang L.Z., Kyle S., Srinivasan S., White A.W., Calvert A.H., Curtin N.J., Durkacz B.W., Hostomsky Z., Maegley K., et al. // Clin. Cancer Res. 2000. V. 6. № 7. P. 2860–2867.
63. Liu S.K., Coackley C., Krause M., Jalali F., Chan N., Bristow R.G. // Radiother. Oncol. 2008. V. 88. № 2. P. 258–268.
64. Liu X., Shi Y., Guan R., Donawho C., Luo Y., Palma J., Zhu G.D., Johnson E.F., Rodriguez L.E., Ghoreishi-Haack N., et al. // Mol. Cancer Res. 2008. V. 6. № 10. P. 1621–1629.
65. Tentori L., Leonetti C., Scarsella M., d'Amati G., Portarena I., Zupi G., Bonmassar E., Graziaia G. // Blood. 2002. V. 99. № 6. P. 2241–2244.
66. Tentori L., Leonetti C., Scarsella M., D'Amati G., Vergati M., Portarena I., Xu W., Kalish V., Zupi G., Zhang J., Graziani G. // Clin. Cancer Res. 2003. V. 9. № 14.P. 5370–5379.
67. Palma J.P., Rodriguez L.E., Montgomery D., Ellis P.A., Bukofzer G., Niquette A., Liu X., Shi Y., Lasko L., Zhu G.D., et al. // Clin. Cancer Res. 2009. V. 15. № 13. P. 7277–7290.
68. Donawho C.K., Luo Y., Penning T.D., Bauch J.L., Bouska J.J., Bontcheva-Diaz V.D., Cox B.F., DeWeese T.L., Dillehay L.E., Ferguson D.C., et al. // Clin. Cancer Res. 2007. V. 13. № 9. P. 2728–2737.
69. Daniel R.A., Rozanska A.L., Mulligan E.A., Drew Y., Thomas H.D., Castelbuono D.J., Hostomsky Z., Plummer E.R., Tweddle D.A., Clifford S.C., et al. // Br. J. Cancer. 2010. V. 103. № 10. P. 1588–1596.
70. Miknyoczki S.J., Jones-Bolin S., Prichard S. // Mol. Cancer Ther. 2003. V. 2. № 4. P. 371–382.
71. Calabrese C.R., Almassy R., Barton S., Batey M.A., Calvert A.H., Canan-Koch S., Durkacz B.W., Hostomsky Z., Kumpf R.A., Kyle S., et al. // J. Natl. Cancer Inst. 2004. V. 96. № 1.P. 56–67.
72. Kaufmann S.H., Charron M., Burke P.J., Karp J.E. // Cancer Res. 1995. V. 55. № 6. P. 1255–1260.
73. El-Khamisy S.F., Masutani M., Suzuki H., Caldecott K.W. // Nucl. Acids Res. 2003. V. 31. № 19. P. 5526–5533.
74. Plo I., Liao Z.Y., Barceló J.M., Kohlhagen G., Caldecott K.W., Weinfeld M., Pommier Y. // DNA Repair. 2003. V. 2. № 10. P. 1087–1100.
75. Malanga M., Althaus F.R. // Biochem. Cell Biol. 2005. V. 83. № 3. P. 354–364.
76. Mattern M.R., Mong S.M., Bartus H.F., Mirabelli C.K., Crooke S.T., Johnson R.K. // Cancer Res. 1987. V. 47. № 7. P. 1793–1798.
77. Tentori L., Leonetti C., Scarsella M., Muzi A., Mazzon E., Vergati M., Forini O., Lapidus R., Xu W., Dorio A.S., et al. // FASEB J. 2006. V. 20. № 10. P. 1709–1711.
78. Zander S.A., Kersbergen A., van der Burg E., de Water N., van Tellingen O., Gunnarsdottir S., Jaspers J.E., Pajic M., Nygren A.O., Jonkers J., et al. // Cancer Res. 2010. V. 70. № 4. P. 1700–1710.
79. Ben-Hur E., Chen C.C., Elkind M.M. // Cancer Res. 1985. V. 45. № 5. P. 2123–2127.
80. Russo A.L., Kwon H.C., Burgan W.E., Carter D., Beam K., Weizheng X., Zhang J., Slusher B.S., Chakravarti A., Tofilon P.J., Camphausen K. // Clin. Cancer Res. 2009. V. 15. № 2. P. 607–612.
81. Saleh-Gohari N., Bryant H.E., Schultz N., Parker K.M., Cassel T.N., Helleday T. // Mol. Cell. Biol. 2005. V. 25. № 16. P. 7158–7169.
82. Barendsen G.W., van Bree C., Franken N.A.P. // Int. J. Oncol. 2001. V. 19. № 2. P. 247–256.
83. Leopold W.R., Sebolt-Leopold J.S. Chemical approaches to improved radiotherapy. Boston: Kluwer, 1992. P. 179–196.
84. Albert J.M., Cao C., Kim K.W., Willey C.D., Geng L., Xiao D., Wang,H., Sandler A., Johnson D.H., Colevas A.D., et al. // Clin. Cancer Res. 2007. V. 13. № 10. P. 3033–3042.
85. Barreto-Andrade J.C., Efimova E.V., Mauceri H.J., Beckett M.A., Sutton H.G., Darga T.E., Vokes E.E., Posner M.C., Kron S.J., Weichselbaum R.R. // Mol. Cancer Ther. 2011. V. 10. № 7. P. 1185–1193.
86. Holl V., Coelho D., Weltin D., Hyun J.W., Dufour P., Bischoff P. // Anticancer Res. 2000. V. 20. № 5A. P. 3233–3241.
87. Magan N., Isaacs R.J., Stowell K.M. // Anticancer Drugs. 2012. V. 3. № 6. P. 627–637.
88. Mason K.A., Valdecanas D., Hunter N.R., Milas L. // Invest. New Drugs. 2008. V. 26. № 1. P. 1–5.
89. Guggenheim E.R., Ondrus A.E., Movassaghi M., Lippard S.J. // Bioorg. Med. Chem. 2008. V. 16. № 23. P. 10121–10128.
90. Ohsaki K., Sakakibara S., Do E., Yada K., Yamanishi K. // J. Virol. 2004. V. 78. № 18. P. 9936–9946.
91. Wang H., Tang Q., Maul G.G., Yuan Y. // J. Virol. 2008. V. 82. № 6. P. 2867–2882.
92. Nakajima H., Ohkuma K., Ishikawa M., Hasegawa T. // J. Pharmacol. Exp. Ther. 2005. V. 312. № 2. P. 472–481.
93. Mandery K., Fromm M.F. // Br. J. Pharmacol. 2012. V. 165. № 2. P. 345–362.
94. Kopetz S. // J. Clin. Oncol. 2008. V. 26 (Suppl.). P. a3577.
95. Mahany J.J. // J. Clin. Oncol. 2008. V. 26 (Suppl.). P. a3579.
96. Kotova E., Tulin A.V. // Meth. Mol. Biol. 2011. V. 780. P. 491–516.
97. Maluchenko N.V., Kotova E., Chupyrkina A.A., Nikitin D.V., Kirpichnikov M.P., Studitsky V.M. // Mol. Biol. (Mosc.). 2015. V. 49. № 1. P. 1–15.
98. Kotova E., Tulin A.V. // Proc. Natl. Acad. Sci. USA. 2010. V. 107. № 14. P. 6406–6411.
99. Dantzer F // FEBS J. 2013. V. 280. № 15. P. 3508–3518.
100. O'Donnell A., Yang S.H., Sharrocks A.D. // EMBO Rep. 2013. V. 12. № 12. P. 1084–1091.
101. Thomas C. // Mol. Aspects Med. 2013. V. 34. P. 1124–1137.
102. Mouchiroud L., Auwerx J. // Crit. Rev. Biochem. Mol. Biol. 2013. V. 48. № 4. P. 397–408.
103. Bürkle A. // Mol. Aspects Med. 2013. V. 34. P. 1046–1065.
104. Ma Y., He X., Nie H., Hong Y., Sheng C., Wang Q., Xia W., Ying W. // Curr. Drug Targets. 2012. V. 13. № 2. P. 222–229.
105. Ying W. // Scientifica (Cairo). 2013. V. 2013. Article ID: 691251.
106. Baxter P., Xu Y., Swanson R.A. // Transl. Stroke Res. 2014. V. 5. № 1. P. 136–144.
107. Rosado M.M., Novelli F., Pioli C. // Immunology. 2013. V. 139. № 4. P. 428–437.
108 Nishikimi M., Kameshita I., Taniguchi T., Shizuta Y. // J. Biol. Chem. 1982. V. 257. № 11. P. 6102–6105.
109. Kameshita I., Taniguchi T., Shizuta Y. // J. Biol. Chem. 1984. V. 259. № 8. P. 4770–4776.

Injured Nerve Regeneration using Cell-Based Therapies: Current Challenges

E. S. Petrova
Federal State Budgetary Scientific Institution «Institute of Experimental Medicine»,
St. Petersburg, Akad. Pavlov str.,12, 197376, Russia
E-mail: lemmorphol@yandex.ru
Received: 11.03.2015

ABSTRACT **This paper reviews the recent research progress in the past several years on promoting peripheral nerve recovery using stem and progenitory cells. The emphasis is placed on studies aimed at assessing various stem cells capable of expressing neurotrophic and growth factors and surviving after implantation in the nerve or a conduit. Approaches to improving nerve conduit design are summarized. The contribution of stem cells to axonal regeneration and neural repair is discussed. The side effects associated with cell-based treatment are highlighted. From the studies reviewed, it is concluded that the fate of transplanted stem cells needs further elucidation in a microenvironment-dependent manner.**
KEYWORDS **nerve regeneration, nerve, cell therapy, stem cells.**
ABBREVIATIONS **PNS - peripheral nervous system; SC - stem cells; NGF - nerve growth factor; VEGF- vascular endothelial growth factor; BDNF – brain-derived neurotrophic factor; bFGF - basic fibroblast growth factor; HGF - hepatocyte growth factor; NF-3 - neurotrophin-3; MRI - Magnetic Resonance Imaging; GFP- green fluorescent protein; MSC - mesenchymal stem cells.**

INTRODUCTION

Re-growth of peripheral nerve fibers could be induced using different approaches. Historically, enhanced nerve regeneration has been promoted by the administration of drugs [1], physical factors (magnetic field) [2, 3], and electrical stimulation [4–6]. Nerve surgery [7] and the microsurgical suture technique [8] have witnessed impressive development in recent years. Another option is bioartificial structures (conduits) that could serve as an alternative to autologous nerve grafts aimed at bridging the defects in nerve continuity. However, these approaches have failed to produce an efficient tool for nerve repair. A possible explanation is that, despite extensive studies by A.Waller, S.Ramon y Cajal, and Doynikov B.S. in the field of nerve regeneration [9–11], the molecular mechanisms underlying posttraumatic processes in nerve fibers remain poorly understood and require further investigation.

Following crushing or transaction injuries, degeneration takes place at a distance from the site of the injury, including axon degeneration, myelin breakdown and removal, and macrophage infiltration. All these events are collectively known as Wallerian degeneration. Within hours of nerve injury, axonal regeneration occurs: re-growth of nerve fibers proceeds from the proximal nerve segment. Scar tissue forms at the site of the lesion, obstructing axonal guidance, which results in traumatic neuroma formation. In addition, the degenerative processes lead to poor re-innervation of the target tissue or organ. These challenges emphasize the need for the development of new therapeutic strategies for stimulating nerve regeneration.

An important role in axonal re-growth is played by the humoral factors that provide a microenvironment for the guidance of axonal sprouts. This list includes growth and neurotrophic molecules, cytokines, and extracellular matrix proteins [12–14]. To study their effect on nerve repair, several models have been proposed: targeted delivery of growth factors into the injured nerve or conduit using microcapsules or osmotic minipumps (infusion pumps for continuous administration of test agents); application of nerve grafts or plasmids expressing neurotrophic and angiogenic factors [15–18].

A promising approach to fostering nerve regeneration is cell therapy, whereby trophic and growth factors are provided by engrafted cells such as syngeneic Schwann cells (neurolemmocytes) [12, 13, 15]. Following a traumatic injury, it is the Schwann cells that form the myelin sheath and produce such factors as NGF,VEGF,BDNF and other molecules that promote nerve repair. However, the production of viable donor Schwann cells in a desired concentration sometimes fails.

In the past decade, cell therapy for nerve defects has progressed to the use of embryonic stem cells, MSC, olfactory cells, stem cells of hair follicles, and other stem cells alongside donor Schwann cells. The findings of these studies are reviewed in [19–25]. However, the growing body of studies carried out in Russia and abroad raises new questions that have to be addressed. The objective of this study was to review papers on nerve repair published over the last three years.

It is important to highlight the current challenges in this field: (i) selection of cells capable of production of neurotrophic and growth factors and long-term survival when engrafted at the lesion site or conduit, (ii) investigation of the mechanisms behind the growth and regeneration of nerve fibers, (iii) improvement of conduits and their luminal fillers, (iv)development of efficient therapeutic strategies using stem cells, and (v) evaluation of nerve regeneration following injury and cell therapy. Few studies ask questions with regard to the potential side effects brought about by treatment.

The effect of cell therapy on nerve reconstruction could be evaluated using different models. Cells are administered into the injured nerve or conduit bridging the proximal and distal stumps intravenously or intramuscularly [26]. Nerve defect models have been developed and successfully used: nerve crush with forceps [27–31], nerve ligation injury [32], and nerve transection followed by approximation [33]. Of particular interest are studies involving synthetic conduits for the repair of nerve gaps. Over the past several years, bioabsorbable materials for fabricating conduits and luminal fillers have become the focus of much research. Such materials will offer optimal microenvironments for graft survival [20, 34–36].

CELL TYPES USED IN CELL THERAPY FOR NERVE REGENERATION

Current research on nerve regeneration is generally performed on mesenchymal stem cells (MSC) derived from bone marrow [37], adipose tissue [24, 25, 38–42], umbilical cord stroma [43], and amniotic fluid [44]. The choice of bone marrow or fat tissue is guided by the fact that they provide an easy access and autologous source to stem cells for transplantation therapies. In addition, MSC have the capacity to modulate immune responses. Recently, MSC were shown to display immunosuppressive activity [40, 45]. The analysis of the molecular mechanisms underlying the interaction between MSC and immune cells demonstrated that MSC suppress T and B lymphocytes and inhibit dendric cell maturation [46]. However, this is not in agreement with the findings of McGrath *et al.* [37], who found that, in a rat sciatic nerve injury model, MSC combined with a fibrin glue conduit promote axon regeneration only when exposed to immunosupressive treatment with cyclosporine A. Three weeks postoperatively, macrophage and lymphocyte infiltration was decreased following cyclosporine A administration, which promoted axonal re-growth. Conflicting findings regarding the effects of MSC on immune responses can be explained by the origin of stem cells and the route of delivery. *In vitro* studies demonstrated that MSC derived from bone marrow, fat tissue, and umbilical cord have various effects on antibody production by B-cells [47]. It is also shown that MSC from different sources differ in plasticity, neuronal differentiation potential, and paracrine activity [48, 49].

Another study has noted the migratory capacity of MSC [50]. MSC enhance axon regeneration not only when delivered to the injured nerve or conduit bridging the nerve gap [26, 39, 51], but also when administered intravenously [27, 30, 52]. The MSC migration potential makes possible their detection at the site of sciatic nerve injury on day 7 post intravenous injection to mice and enhance functional recovery of the sciatic nerve [27].

Along with MSC, neuronal stem cells (NSC) are also used in cell therapy. Lin *et al.* [53] harvested spinal cord-derived NSC from 14- to 15-day rat embryos and cultured them for 7 days in a differentiation medium. When differentiated into cells with neuronal and glial phenotypes (the onset of βIII-tubulin or GFAP production, respectively), they were implanted into sectioned distal tibial nerves. The engraftment restored function in the denervated rat gastrocnemius muscle. Similar experiments were performed in the past [54]; however, the novelty of the work by Lin *et al.* [53] lies in the time point at 7 d post transection they discovered optimal for cell transplantation. After several days post nerve injury, the acute phase of inflammation is over, pro-inflammatory cytokines are fewer, and Schwann cells start to proliferate and produce trophic factors [53]. This milieu is attractive to implanted NSC rather than the nerve milieu immediately after a trauma.

In several studies, axon regeneration in mice was evaluated using NSC derived from the subventricular zone of adult mice [55]. This approach makes possible the survival of motor neurons in the spinal cord of the host undergoing retrograde degeneration after a sciatic nerve injury. In addition, it results in a 3-fold increase in the number of regenerating myelinated axon fibers distal to the site of nerve defect. It is suggested that NSC, as well as MSC, have immunomodulatory properties [55].

Researchers from the USA [56] and Japan [57] working independently carried out experiments with induced pluripotent stem cells (iPSCs) for neural tissue engineering. For a brief time, iPSCs derived from somatic cells of an adult organism (in particular, skin fibroblasts) through gene activation were widely used

for cell therapy studies. This is because of the high proliferative potential of these cells and their easy accessibility. Bioabsorbable conduits seeded with these cells improve axon regeneration several fold versus controls [57]. This effect is much more pronounced when using bioabsorbale conduits seeded with iPSCs and bFGF-loaded microspheres [58]. The use of NSC derived from human iPSCs showed that engrafted cells contribute in the distal segment of the injured nerve among nerve fibers [56]. The human nuclear antigen (NuMA) was utilized to detect the engrafted cells in histological examinations [56]. Concurrent identification of NuMA and the Schwann cell specific marker S100β allowed researchers to conclude that transplanted cells differentiate into neurolemmocytes. More importantly, the mechanism by which axon growth is accelerated is linked to the contribution of the engrafted NSC cells to myelin sheath formation. There is evidence that in various nerve injury models iPSCs have the capacity to differentiate into different cell types: for example, neurons positive for βIII-tubuline [59] or vascular smooth muscle cells [60]. Finally, allowing for the findings of these pioneering studies, it is concluded that the fate of iPSCs in the engrafted microenvironment is complicated and requires further investigation.

Raheja *et al*. [33] attempted bone-marrow-derived mononuclear cells (BM-MNC) in a rat sciatic nerve injury model. A month post inoculation, the outcome of nerve regeneration was found to be cell dose-dependent. Unfortunately, the authors did not speculate on the possible reasons for this observation. Likely, this is the result of BM-MNC paracrine activity reported previously [61]. It cannot be ruled out that transplanted MNC are engaged in rapid clearance of myelin debris, thus enhancing regenerative outgrowth.

The search for more effective regenerative options led to the discovery of a new cell type derived from skeletal muscle – muscle-derived stem/progenitor cells [31, 62, 63]. Tamaki *et al.* [63] demonstrated that after implantation into the nerve stump these precursor cells are capable of differentiating into Schwann cells, endoneurial and perineurial cells, as well as blood vessel cells (endotheliocyte, perycites, smoth muscle cells). Their availability and easy accessibility favor their use for autologous grafting, but there are findings reporting side effects associated with the use of these cells [62].

STUDYING THE MECHANISMS BEHIND THE EFFECT OF REGENERATIVE THERAPIES ON PERIPHERAL NERVE REPAIR

The factors influencing the successful outcome of cell therapy on nerve repair are poorly understood and could be classified into the following: (i) differentiation toward the Schwann cell lineage, (ii) contribution to myelination of regenerating axons, (iii) production of trophic factors and extracellular matrix proteins that provide a milieu for axonal outgrowth, (iv) stimulation of proliferation and differentiation of endogenous cells, (v) stimulation of angiogenesis, and (vi) immunosupression in the injured nerve.

Differentiation of stem cells toward the Schwann cell phenotype

It remains debatable whether Schwann-like cells derived from implanted stem cells can be successfully used. There is a hypothesis positing that transplanted stem cells can directly differentiate into Schwann cells and facilitate axonal myelination. By contrast, an alternative hypothesis states that this cannot take place without prior *in vitro* transdifferentiation or predifferentiation of stem cells. The term predifferentiation refers to the use of NSC or ENC. The term transdifferentiation applies to the use of MSC. Although a more appropriate word would be transdetermination, proposed by V.E Okhotin *et al*. [64]. It is known that *in situ* MSC have the potential to differentiate along mesodermal lineages: bone, muscle, adipose tissue, etc; they are determined to differentiate into their particular cell types. Culturing of MSC in chemically defined media induces a switch in lineage commitment, known as transdetermination, toward neurolemmocytes, neurons, astrocytes, and other cell types.

Tomita *et al.* [28] performed *in vitro* and *in vivo* studies of glial differentiation of MSC derived from human adipose tissue. It was established that following exposure to glial growth factors MSC transdifferentiate into a Schwann cell phenotype. Lineage-committed MSC demonstrated a 7-fold higher survival rate after implantation than multipotent MSC in a rat tibial nerve injury study. In addition, transdifferentiated MSC (labeled with GFP) contribute to axon myelination: approximately 30% of engrafted cells were integrated in the myelin sheath of the regenerating axons. They were positive for GFP and P0, the marker of neurolemmocytes. The ability of MSC to differentiate toward a Schwann cell phenotype has been observed by others [65, 66].

Another hypothesis suggests that transdetermination of MSC into Schwann cells does not take place, and that rather they remain in their uncommitted state [67]. In contrast, therapy-associated axon growth is enforced by MSC production of trophic factors rather than their transdifferentiation [26, 67, 68].

Stem cell production of trophic factors and extracellular matrix molecules

In the past three years, many studies pertaining to nerve repair have been conducted with stem cells of

different origins: bone marrow, adipose tissue, umbilical cord blood, etc. Stem cells have gained research interest as a promising source of biochemical mediators [69]. The capacity for producing a broad spectrum of trophic factors, growth factors, and cytokines has been well established [27, 38, 70, 71]; however, in an age-dependent manner in humans and animals [72, 73].

The most potent trophic factors secreted by MSC and used in regenerative therapies are NGF, BDNF, NF-3, and insulin-like growth factor-1 (IGF-I) [24, 27, 29, 38, 51]. Furthermore, MSC produce angiogenic factors such as VEGF and platelet-derived growth factor (PDGF) [27, 38].

There is convincing evidence that adipose-derived stem cells release the brain-derived neurotrophic factor (BDNF) and promote axonal regeneration. It was found that antibody-based neutralization of BDNF has an inhibitory effect on axonal recovery [29]. Using an antibody assay, it was demonstrated that MSC introduced into the conduit, which bridges the nerve defect, express bFGF [71].

Unfortunately, the mechanisms and cellular events governed by stem-cell-secreted factors are not fully elucidated. Fairbairn *et al*. suggest that these neurotrophic molecules target sensory and motor neurons [26]. Transplanted stem cells at the injury site mediate a retrograde neuroprotective effect on adjacent motor and sensory neurons, thereby increasing axon numbers. MSC delivered to the injured nerve prevent neuronal loss in the dorsal root ganglia by producing BDNF, endothelial growth factor, hepatocyte growth factor, and the insulin-like growth factor [70].

A positive outcome in stem-cell-based therapy is observed 1 week following surgery [29]. It is know that peripheral nerve injury induces axonal degeneration and demyelination in the distal stump [9, 74, 75]: nerve transection leads to complete degeneration of the nerve fibers of the distal segment of the injured nerve, whereas crush injury allows to preserve some axons. In this regard, it is tempting to speculate that the presence of implanted stem cells with paracrine activity at the site of the injury in the very early days promotes axonal survival rather than re-growth.

Stimulation of endogenous host cells

Endogenous Schwann cells create a growth-permissive environment for nerve reconstruction. These are cells capable of producing trophic factors, cytokines and extracellular matrix proteins required for axonal maintenance and regeneration [12–14]. Cell therapy is thought to activate endogenous Schwann cells. Incorporation of stem cells into the injured nerve or a bridging conduit upregulates the proliferation of local Schwann cells and secretion of bioactive molecules [51, 71, 76, 77]. The administration of NSC enhances NGFandHGF expression in these Schwann cells [77]. Marconi *et al*. [27] investigated the effect of a conditioned medium on cultured MSC and found that under *in vitro* conditions MSC produce a range of neuroprotective factors, except for the glial-derived neurotrophic factor(GDNF). Interestingly, GDNF levels were detected in the injured nerve of mice treated with MSC. A possible explanation could be that endogenous Schwann cells are stimulated by engrafted MSC to express GDNF in the local milieu.

Improved axonal recovery in response to cell therapy is associated with elevated angiogenesis. A recent study reported that the outcome of axonal regeneration depends on the vascular supply and perfusion [78]. Genetic studies showed that angiogenic factors enhance nerve reconstruction [16, 17]. Improved blood supply to the nerve with a lesion is due to the fibroblast growth factor, endothelial growth factor, placenta growth factor, and other angiogenic molecules released by MSC [38]. Adipose-derived stem cells seeded into a fibrin nerve conduit improve capillary formation in the tube and facilitate nerve regeneration by expressing VEGF-A and angiopoietin-1 [79].

Inhibition of connective tissue and scar formation

The inflammatory responses and fibrosis processes induced thereof impede axonal invasion. It is considered that regenerative strategies ameliorate these consequences. Marconi *et al*. [27] used a rat model of sciatic nerve crush injury to assess axonal degeneration in the distal segment after administration of MSC. The expression of the T-lymphocyte marker CD3 and the monocyte/macrophage marker $CD11b^{+}$was down-regulated at the injured nerve on the 7, 14, and 21 days post administration of MSC. The engrafted stem cells modulate the immune response and modify the microenvironment [46]. Hsu *et al.* [80] used a chitosan-laminin scaffold filled in a silicone conduit and tested in a rat sciatic nerve injury model. In addition, this conduit was seeded with endogenous bone marrow-derived MSC. A histological analysis indicated that the area around the tube wall was characterized by prominent eosinophil and macrophage infiltration, whereas treatment with MSC reduced the extent of the inflammation within the injured region. The axon growth-enhancing effect of MSC seems to be due to anti-inflammatory cytokines. The range of cytokines-produced MSC is reviewed in [81].

There is evidence that neural stem-cell-based therapy is an option for mitigating the inflammatory response in an injured nerve after surgery. It was shown that the levels of inflammatory cytokines (interleukin 1 and 6) are decreased following NSC treatment [52].

Unfortunately, understanding of the role of cytokines in axonal degeneration and recovery remains frustratingly poor: therefore, the use of stem cells requires fundamental research.

TISSUE-ENGINEERED CONDUITS FOR PERIPHERAL NERVE REGENERATION

In clinical practice, axonal regeneration across >3 cm gaps is achieved by autologous nerve grafting. Treatment-associated adverse effects (neuromas) and limited accessibility of donor grafts prompted a search for conduits to replace autologous tissues (reviewed in [20, 35, 80, 82, 83]). The classification of conduits to bridge nerve defects is well presented in the recent review paper [35].

Current research is focused on resorbable constructs and luminal fillers for axonal guidance [84]. Candidate constructs should meet the following criteria: biocompatibile, porous, and biodegradable with nontoxic degradation products.

Experimental conduits can be filled with collagen, fibrin, laminin, hydrogel, and keratin. There are strategies to promote a favorable microenvironment in the conduit for axonal growth by localized release of growth factors (fibroblast growth factor, VEGF, neurotrophins (NF-3, NGF), neuropoietic cytokines) and stem cell delivery. Growth factors guide axonal growth into implanted tubes and promote Schwann cell proliferation, which creates a permissive microenvironment for nerve reconstitution.

Another important criterion for conduits is to support the differentiation and survival of supportive cells seeded within the lumen [59, 85].

Although conduits can be biocompatible, nontoxic and resorbable, however, they fail to promote stem cell survival. For example, polycaprolactone conduits are hydrophobic and prevent cell adhesion, whereas poly-(lactic-co-glycolic acid) conduits release inhibitory byproducts for cell proliferation upon degradation [80]. Besides being a permissive conduit for survival of bone-marrow-derived MSC, the chitosan-laminin scaffold has drawbacks. It was found that chitosan breakdown products cause chronic inflammatory damage [80].

Alongside the development of synthetic tubes to bridge nerve gaps, a search is currently underway for novel nerve guidance conduits. Blood vessels have been widely used as biologic tubes [52, 86]. Importantly, even in the past [74], successful outcomes were achieved with blood vessels as artificial nerve guides. A recent study evaluated the potential of using xenographic conduits to promote axonal re-growth [87]. As nerve guidance conduits, acellular nerve, artery, and dermis were assessed in a rodent model. The nerve, artery, and dermal tissue were decellularized, leaving extracellular matrix proteins. Histological evaluation of the extracellular matrix content showed that all decellularized conduits were positive for collagen types I, III, and IV, fibronectin and laminin in various combinations. The artery conduit rich in collagen types I and IV and laminin but negative for collagen type III and fibronectin outperformed the other two types of conduits and permitted axonal re-growth and myelination.

There are works with the use of acellular nerve conduits and stem cells. These conduits carry basal membranes and collagen fibers and enhance cell proliferation, migration, and adhesion. Furthermore, they facilitate the survival of transplanted stem cells [22, 67, 88, 89]. To ensure cell viability within an acellular conduit, it is important to consider the procedure used for decellularization. A variety of decellularization approaches for nerve gap repair are summarized in [22], where cold temperature preservation, chemical detergent decellularization, and irradiation are discussed.

It has been demonstrated that acellular nerve xenografts combined with bone marrow stromal cells cause neither rejection nor inflammation and have axonal growth-promoting properties in a rat model [88]. After implantation, conduit-seeded cells differentiate into Schwann-like cells. Expression of NGF, BDNF, and other factors by these cells creates a microenvironment similar to endoneurium. Electrophysiological evaluation of nerve conductivity and morphological examination of regenerated nerves demonstrated that nerve regeneration and functional recovery was equal between xenogeneic and autologous acellular nerve graft transplants (the autologous nerve grafting technique is the gold standard for peripheral nerve reconstruction) [88].

In summary, a wide spectrum of conduits has become available. The outcome of engrafted stem cells is determined by conduit materials and scaffolds. Moreover, the survival and differentiation of cells seeded within a nerve conduit require further study. There is an opinion that the majority of transplanted cells fail to survive, which has prompted efforts to elevate cell viability.

STRATEGIES TO IMPROVE THE EFFICACY OF REGENERATION THERAPY FOR NERVE DAMAGE

In the past several years, new approaches have been introduced to enhance cell therapies for nerve reconstitution. For example, concomitant transplantation of MSC and adjacent cells has been reported [90]. Co-cultivation of MSC and lemmocytes directs the differentiation of MSC towards a Schwann cell lineage, with lemmocytes producing much higher levels of neurotrophic factors as compared with neurolemmocytes. The use of MSC in combination with Schwann cells for

conduit seeding proved to be more efficient for axonal regeneration than conduits seeded with either single cell suspension [90].

Laser irradiation has been a useful tool in axon repair using a biodegradable conduit [91, 92]. The positive effect is likely due to inhibition of inflammatory responses in the injured nerve.

Using various models, the combination of biochemical mediators seeded on a nerve conduit has proved instrumental in promoting transplanted cell viability, thereby stimulating axonal growth. Luo *et al.* reported the use of MSC in combination with TGF-β1 to ameliorate the apoptotic cell death of transplanted cells [93]. As a consequence, enhanced angiogenesis and decreased immune response contribute to successful nerve repair [93]. A poly-lactic-co-glycolic-acid nerve conduit loaded with NSC and neurotrophin-3 (NF-3) improves engrafted cell survival. NF-3 provides a permissive microenviroment for NSC to survive and differentiate mainly towards neurons [35]. Another study demonstrated the potential for combining stem cells with substance P for enhancing nerve recovery in the skin [94].

The combined use of bone-marrow-derived stromal cells and chondroitinase ABC (a bacterial enzyme used to treat herniated discs) was found superior to stem cell monotherapy in terms of augmenting nerve regeneration and preventing implanted cell death [95]. A possible mechanism is that chondroitinase ABC digests the chondroitin sulfate which is involved in connective tissue scar formation at the injured site.

EVALUATION OF THE DEGREE OF NERVE REGENERATION AFTER TREATMENT

All experimental studies are concerned with the appropriate evaluation of the extent of axonal outgrowth. In our opinion, morphometric parameters such as semithin transverse sections of nerves or conduits have emerged as a reliable diagnostic indicator of nerve regeneration. This method has been widely applied in regenerative studies [4, 32, 36, 51, 91, 94].

Immunostaining can also be carried out to quantify nerve fibers using antibodies to axonal markers such as βIII-tubulin [37, 79] or neurofilaments (NF) [36, 51, 57], the P0 protein [75] or the Schwann cell marker myelin [28]. A modern method based on calculating the area covered by structures containing Schwann cell or axonal markers has been reported [51, 57].

Immunohistochemical techniques allow one to evaluate the degree of nerve regeneration by transverse sections of the nerve. Longitudinal sections of the nerve can also be used for quantification. The length of regenerating axons is calculated using the neuronal growth cone protein GAP-43 [27], PGP 9.5, a broad neural marker expressed in nerve fibers and the neurons of the peripheral nervous system [68] and the axonal marker βIII-tubulin [79].

Alongside a morphometric evaluation, physiological tests have been used for the assessment of regenerative success [28, 30, 42, 54, 67] and nerve conductivity [39, 53, 60, 75, 96].

Another approach to assessing nerve recovery is to look at the retrograde degeneration of the motor neurons and sensory neurons of spinal ganglia following the nerve injury [40, 52, 79, 97]. Using a sciatic nerve injury rat model, a laminin-coated chitosan conduit seeded with MSC was shown to suppress cell death of motor neurons in the lumbar spinal cord and improved axonal outgrowth several fold with regard to the non-seeded conduit [80]. It is also true that cell seeded polycaprolactone scaffolds attenuate retrograde degeneration of the neurons of spinal ganglia in rats with a sciatic nerve injury [70]. Of note, the neuroprotective effect is associated with conduits primed with stem cells pre-differentiated towards a Schwann cell phenotype [70]. There is evidence to suggest that embryonic neural tissue allografted into the injured site supports the survival of sensory neurons [98].

Nerve regeneration could be evaluated by measuring the weight and the area of the innervated muscle and its structural characteristics. Complete functional nerve regeneration is impeded by structural changes in the target tissues after denervation. For example, sciatic nerve transaction leads to gastrocnemius atrophy. The extent of nerve repair was evaluated by weighing the innervated muscle, a histological analysis of muscle fibers, and immunohistochemical staining of pre-and postsynaptic terminals at nerve muscle synapses [34, 54, 65, 86, 96, 99].

In 2012, a few papers were published concerning the use of *in vivo* MRI monitoring for assessing nerve regeneration after injury and MSC transplantation [100, 101]. An advantage of MRI is the capacity for tracking the fate of transplanted cells labeled with a superparamagnetic iron oxide nanoparticle [41, 102].

ADVERSE EFFECTS ASSOCIATED WITH CELL THERAPY

The possible adverse effects of cell therapy have been widely discussed [103–108]. Negative consequences include host immune response to non-self stem cells, tumor development, inflammation and connective tissue scar formation, disturbance of gut microflora, etc. This issue of side effects following embryonic and adult stem cell delivery to the injured nerve has also been raised in [62, 85, 109].

A careful review of the literature published in the past several years suggests a paucity of studies addressing the issue of stem-cell-related tumorogenesis,

because embryonic stem cells were discarded for their highest tumorogenic capacity compared to all other stem cells. NSC can only be used after pre-differentiation, for example, into neural and glial cells, which reduces tumor initiation.

The search for suitable stem cells could yield unexpected findings. Lavasani *et al*. [62] reported the use of murine muscle-derived stem/progenitor cells (MDSPC) for repairing nerve defects. It was shown that these cells are able to generate neurospheres and undergomyogenic, neuronal, and glial differentiation, expressing lineage-specific markers. After differentiation, MDSPC generate large neoplastic growths 11 weeks post-implantation.

Simultaneously, MDSPC were implanted into gastrocnemius muscles, where they underwent normal myogenic differentiation into myocytes. This finding highlights the importance of microenvironment-specific transformation.

Successful outcomes seem to be restricted to the use of pre-differentiated stem cells, whereas uncommitted MSC can lead to detrimental consequences [85, 110]. The risk of tumor development should be assessed in long-term studies. Unfortunately, in the field of regenerative therapy such observations are scarcely found. Some follow-up studies have reported no side effects at 12 months post transplantation [56, 111].

Importantly, much attention has been focused on clarifying the relationship between MSC and derived tumor cells, because there are plenty of pathways implicated in stem-cell-dependent tumor progression. There is evidence suggesting a role for the angiogenic, growth promoting, and immunosupressive effects of MSC in maintaining neoplastic growth [112, 113]. However, MSC are capable of tumor suppression [69, 114]. Long-term co-culturing of murine embryonic MSC derived from bone marrow with U251MGglioma cells changes the effect of MSC on tumor cells in a time-dependent fashion: at the early stage of culturing MSC promote tumor cell division, followed by tumor cell division suppression [115]. The relationship between MSC and tumor cells is being investigated; however, current knowledge is limited. Further work is needed to reach an unambiguous conclusion.

Along with papers providing experiential evidence of the negative outcomes of cell therapy, there is a study that reports an insignificant or even unobservable effect after cell therapy [116]. It is likely that the effect is short-term as previously described for stem cells evaluated in other experimental models [108,117]. These issues need to be explored in future.

CONCLUSION

Numerous studies pertaining to the development of new regenerative therapies for nerve reconstitution show the effectiveness of stem cell treatment for axonal outgrowth and conductivity recovery. Unfortunately, the mechanism by which endogenous and exogenous stem cells contribute to regenerative success or failure remains poorly understood. Further studies are also required to identify the factors mediating the interaction between implanted stem cells and host cells, such as Schwann cell, macrophages, vessel cells, loose connective tissue cells, and epi- and perineurial cells.

The most recent studies were based on MSC derived from different sources: bone marrow, adipose tissue, cord blood, etc. The intrinsic property of these cells to produce biochemical mediators could promote the regenerative process after a traumatic injury. In addition, these cells permit autologous transplantation.

The findings obtained with experimental animals in the last decade have been extended to clinical trials [118–121]. Importantly, in 2012, positive effects of cell-based therapy were first reported using an animal model of diabetic polyneuropathy [60,93].

Despite numerous published studies, the fate of transplanted stem cells and precursor cells remains an issue of limited knowledge [39, 85, 122]. This is particularly important given the application of the novel materials used as conduits to bridge a gap between proximal and distal nerve stumps. The conduit provides a permissive microenvironment for cell survival and differentiation of transplanted cells. Conduits alone fail to promote transplanted cell survival and engraftment without additional therapeutic approaches.

The search is still on for means of providing directional guidance to regenerating axons. The cell-based approaches recently reported raise a wide array of questions that need to be addressed. To ensure safe medical techniques, it is important to accumulate data on the pre-differentiation and trans-determination of engrafted cells, which would clarify the mechanisms whereby engrafted stem cells facilitate regeneration. To reduce the side effects associated with cell therapies, the fate of implanted stem cells and precursor cells should be clearly defined for a period comparable with the lifespan of laboratory animals. The design of conduits and luminal fillers should be refined in terms of the microenvironment they provide for survival, differentiation, and functioning of implanted cells. ●

REFERENCES

1. Mohammadi R., Azad-Tigran M., Amini K. // Injury. 2013. V. 44. № 4. P. 565–569.
2. Ninel V.G., Norkin I.A., Puchinyan D.M. Bogomolova N.V., Korshunova G.A.1, Matveeva O.V., Aytemirov S.M. // Fundamental research.2012. № 12. P. 336–340.
3. Beck-Broichsitter B.E., Lamia A., Geuna S., Fregnan F., Smeets R., Becker S.T., Sinis N. // Biomed.Res.Int. 2014. V. 2014. P. 401760.
4. Shchudlo N.A., Borisova I.V., Shchudlo M.M. // Morfologiia. 2012. V. 142. № 6. P. 30–35.
5. Maciel F.O., Viterdo F., Chinaque L.F.C., Souza B.M. // Acta Cir. Bras. 2013. V. 28. № 1. P. 39–47.
6. de Assis D.C.M., Lima K.M., Goes B.T., Cavalcanti J.Z., Paixão A.B., Vannier-Santos M.A., Martinez A.M., Baptista A.F. // Biomed Res Int. 2014. V. 2014. P. 572949.
7. MerkulovM.V., GolubevI.O., KrupatkinA.I., Kuz'michyov V.A., Bushuev O.M., ShiryaevaG.N., KutepovI.A. // Bulletin of Traumatology and Orthopedics Im. N.N. Priorov. 2012. № 3. P. 53–58.
8. Bersnev V.P., Khamzaev R.I., Boroda Iu.I. // Vestn. Khir. Im. I. I. Grekov. 2009. V. 168. № 1. P. 61–63.
9. Waller A. Lond. J. Med. 1852. V. 4. № 43. P. 609–625.
10. Ramon y Cajal S. Degeneration and regeneration of the nervous system. V. 1-2. L.: Oxf. H.Milford. 1928. 50 p.
11. Doynikov B.S. The selected works on Neuromorphology and neuropathology. M.: Medgiz. 1955. 468 p.
12. Gordon T. // Neurosurgical Focus. 2009. V. 26. № 2. P. E3.
13. Lutz A.B., Barres B.A. // Developmental Cell. 2014. V. 28. № 1. P. 7–17.
14. Gu Y., Zhu J., Xue C., Li Z., Ding F., Yang Y., Gu X. // Biomaterials. 2014. V. 35. № 7. P. 2253–2263.
15. Pfister L.A., Papalonzos M., Merkle H.R., Gander B. // J. Peripher. Nerv. Syst. 2007. V. 12. № 2. P. 65–82.
16. Masgutov R.F., Salafutdinov I.I., Bogov A.A., Trofimova A.A., Khannanova I.G., Mullin R.I., Islamov R.R., Chelyshev Yu.A., Rizvanov A.A. // Genes and Cells. 2011. V. 6. № 3. P. 67–70.
17. Chelyshev Y.A., Mukhamedshina Y.O., Shaimardanova G.F., Nickolaev S. I. // Neurological Vestnik Im. V.M. Bekhterev. 2012. V. 44. № 1. P. 76–83.
18. Masgutov R.F., Rizvanov A.A., Bogov A.A. (jr.), Gallyamov A.R., Kiyasov A.P., Bogov A.A. // Prakticheskaya meditsina. 2013. V. 69. № 1–2. P. 99–103.
19. Walsh S, Midha R. // Neurosurgery. 2009.V.65. № 4. P. 80–86.
20. Chimutengwende-Gordon M., Khan W. // Open Orthop J. 2012. V.6. № 1. P. 103-107.
21. Petrova E.S. // Tsitologiia. 2012. V. 54. № 7. P. 525–540.
22. Szynkaruk M., Kemp S.W.P., Wood M.D., Gordon T., Borschel G.H. //Tissue Eng. Part B. Rev. 2013. V. 19. № 1. P. 83–96.
23. Zack-Williams S.D., Butler P.E.., Kalaskar D.M. // World J. Stem Cells. 2015. V. 7. № 1. P. 51–64.
24. Widgerow A.D., Salibian A.A., Kohan E., Sartiniferreira T., Afzel H., Tham T., Evans G.R. // Microsurgery. 2014. V. 34. № 4. P. 324–330.
25. Martinez A.M., Goulart C.O., Bruna dos Santos Ramalho, Oliveira J.T., Almeida F.M. // World. J. Stem. Cells. 2014. V. 6. № 2. P.179–194.
26. Fairbairn N.G., Meppelink A.M., Ng-Glazier J., Randolph M.A., Winograd J.M. // World J. Stem Cells. 2015. V. 7. № 1. P. 11–26.
27. Marconi S., Castiglione G., Turano E., Bissolotti G., Angiari S., Farinazzo A., Constantin G., Bedogni G., Bedogni A., Bonetti B. // Tissue engineering. 2012. V. 18. № 11-12. P. 1264–1272.
28. Tomita K., Madura T., Mantovani C., Terenghi G. // J. Neurosci. Res. 2012. V. 90. № 7. P. 1392–1402.
29. Karagyaur M.N. Effect of mesenchymal stem cells on the peripheral nerve recovery after injury. Moscow: FSBI: «RCRPC» Ministry of Health of the RF, 2013.
30. Matthes S.M., Reimers K., Janssen I., Liebsch C., Kocsis J.D., Vogt P.M., Radtke C. // Biomed Res Int. 2013. V. 2013. P. 573169.
31. Zeng X, Zhang L., Sun L., Zhang D., Zhao H., Jia J., Wang W. // Exp Ther. Med. 2013. V. 5. № 1. P. 193–196.
32. Petrova E.S., Isaeva E.N.// Biology Bulletin. 2014. № 6. P. 549–556.
33. Raheja A., Suri V., Suri A., Sarkar C., Srivastava A., Mohanty S., Jain K.G., Sharma M.C., Mallick H.N., Yadav P.K. et al. // J. Neurosurg. 2012. V. 117. № 6. P. 1170–1181.
34. Xiong Y., Zhu J., Fang Z.U.,Zeng C.G.,Qi G.L., Li M.H.,Zhang W.,Quan D.P., Wan J. // Inter. J. Nanomedicine. 2012. V. 7. P. 1977–1989.
35. Daly W., Yao L., Zeugolis D., Windebank A., Pandit A. // J. R. Intarface. 2012. V. 9. № 67. P. 202–221.
36. Georgiou M., Golding J.P., Loughlin A.J., Kingham P.J., Phillips J.B. // Biomaterials. 2015. V. 37. P. 242–251.
37. McGrath A.M., Brochlin M., Kingham P.J., Novikov L.N., Wiberg M., Novikova L.N. // Neurosci Letters. 2012. V. 516. № 2. P. 171–176.
38. Lopatina T., Kalinina N., Karagyaur M., Stambolsky D., Rubina K., Revischin A., Pavlova G., Parfyonova Y., Tkachuk V. //PLoS One. 2011. V.14. № 6. P. e17899.
39. Kim D.Y., Choi Y.S., Kim S.E., Lee J.H., Kim S.M., Kim Y.J., Rhie J.W., Jun Y.J.// J. Korean. Med. Sci. 2014. № 3. P. 183–192.
40. Hsueh Y.-Y., Chang Y.J., Huang T.C., Fan S.C., Wang D.H., Chen J.J., Wu C.C., Lin S.C. // Biomaterials. 2014. V. 35. № 7. P. 2234–2244.
41. Tseng T.C., Hsu S.H. // Biomaterials. 2014. V. 35. № 9. P. 2630–2641.
42. Marinescu S.A., Zărnescu O., Mihai I.R., Giuglea C., Sinescu R.D. // Rom. J. Morphol. Embryol. 2014. V. 55. № 3. P. 891–903.
43. Pereira T., Gartner A., Amorim I., Almeida A,. Caseiro A.R., Armada-da-Silva P.A., Amado S., Fregnan F., Varejão A.S., Santos J.D. et al. // Biomed Res Int. 2014. 2014: 302659.
44. Li Y., Guo L., Ahn H.S., Kim M.H., Kim S.W. // J. Cell. Mol. Med. 2014. V. 18. № 6. P. 1028–1034.
45. Stagg J., Galipeau J. // Curr. Mol. Med. 2013. V. 13. № 5. P. 856–867.
46. Rubtsov Y.P., Suzdaltseva Y.G., Goryunov K.V., Kalinina N.I., Sysoeva V.Y., Tkachuk V.A. // Acta Naturae. 2012. V. 4. № 1(12). P. 23–31.
47. Aĭzenshtadt A.A., Ivanova N.A., Bagaeva V.V., Smolianinov A.B., Pinevich A.A., Samoĭlovich M.P., Klimovich V.B. //Cell and Tissue Biology. 2014. V. 8. № 3. P. 193–198.
48. Zemel'ko V.I., Kozhukharova I.B., Alekseenko L.L., Domnina A.P., Reshetnikova G.F., Puzanov M.V., Dmitrieva R.I., Grinchuk T.M., Nikol'skiĭ N.N., Anisimov S.V.//Tsitologiia. 2013. V. 55. № 2. P. 101–110.
49. Han C., Zhang L., Song L., Liu Y., Zou W., Piao H., Liu J. // Chin. Med. J. (Engl). 2014. V. 127. № 2. P. 329–337.
50. Tiurin-Kuz'min P.A., Vorotnikov A.V., Tkachuk V.A. // Ross. Fiziol. Zh. Im. I.M.Sechenova. 2013. V. 99. № 3. P. 294–312.

51. Cartarozzia L.P., Spejoa A.B., Ferreira R.S., Barravierab B., Duekc E., Carvalhod G.L., Goesd A.M., Oliveiraa A.L.R. // Brain Res. Bull. 2015. V. 112. P. 14–24.
52. Lerner M.Z., Matsushita T., Lankford K.L., Radtke C., Kocsis J.D., Young N.O. // Laryngoscope. 2014. V. 124. № 11. P. 2555–2560.
53. Lin S., Xu L., Hu S.,Zhang C., Wang Y., Xu J. // Muscle a. Nerve. 2013. V. 47. № 2. P. 194–201.
54. Thomas C.K., Erb D.E., Grumbles R.M., Bunge R.P. // J. Neurophysiol. 2000. V. 84. № 1. P. 591–595.
55. Franchi S., Valsecchi A.E., Borsani E., Procacci P., Zaffa C., Sartori P., Rodella L.F., Vescovi A., Maione S., Rossi F.et al. // Pain. 2012. V. 153. № 4. P. 850–861.
56. Wang A., Tang Z., Park I.H., Zhu Y., Patel S., Daley G.Q., Li S. // Biomaterials. 2011. V. 32. № 22. P. 5023–5932.
57. Uemura T., Takamatsu K., Ikeda M., Okada M., Kazuki K., Ikada Y., Nakamura H. //Biochem. Biophys. Res. Commun. 2012. V. 419. № 1. P. 130–135.
58. Ikeda M., Uemura T., Takamatsu K., Okada M., Kazuki K., Tabata Y., Ikada Y., Nakamura H. // J. Biomed. Mater. Res. A. 2014. V. 102. № 5. P. 1370–1378.
59. Kuo Y.C., Lin C.C. // Colloids. Surf. B. Biointerfaces. 2013. V. 1. № 103. P. 595–600.
60. Okawa T., Kamiya H., Himeno T., Kato J., Sieno Y., Fujiya A., Kondo M., Tsunekawa S., Naruse K., Hamada Y. et al. // Cell Transplant. 2013. V. 22. № 10. P. 1767–1783.
61.Baikova J.P., FatkhudinovT.K., BolshakovaG.B., BuharovaT.B.,KakturskyL.V., GoldshteinD.V. , Dubovaya T.K. // Bulletin of Experimental Biology and Medicine. 2011. V. 152. №1. P. 128–132.
62. Lavasani M., Pollett J.B., Usas A., Thompson S.D., Pollett A.F., Huard J. // PLoS One. 2013 V. 8. № 12. P. e82173.
63. Tamaki T., Hirata M., Soeda S., Nakajima N., Saito K., Nakazato K., Okada Y., Hashimoto H., Uchiyama Y., Mochida J. // PLoS One. 2014. V. 9. № 3. P. e91257.
64. Okhotin V.E., Revischin A.V., Pavlova G.V. // Pacific Medical Journal. 2012. № 2, P. 60–65.
65. Frattini F, Lopes F.R., Almeida F.M., Rodrigues R.F., Boldrini L.C., Tomaz M.A., Baptista A.F., Melo P.A., Martinez A.M. // Tissue Eng Part A. 2012. V. 18. № 19-20. P. 2030–2039.
66. Orbay H., Uysal A.C., Hyakusoku H., Mizuno H. // J. Plastic. Reconst. Aesthet. Surg. 2012. V. 65. № 5. P. 657–664.
67. Wang Y., Zhao Z., Ren Z., Zhao B., Zhang L., Chen J., Xu W., Lu S., Zhao Q., Peng J. // Neurosci Lett. 2012. V. 514. № 1. P. 96–101.
68. Suganuma S., Tada K., Hayashi K., Takeuchi A., Sugimoto N., Ikeda K., Tsuchiya H. // J. Orthop. Sci. 2013. V. 18. № 1. P. 145–151.
69. Kalinina N.I.,Sysoeva V.Yu., Rubina K.A., Parfenova Ye.V., Tkachuk V.A. // Acta Naturae. 2011. V. 3. № 4 (11). P. 30–37.
70. Reid A.J., Sun M., Wiberg M., Downes S., Terenghi G., Kingham P.J. // Neuroscience. 2011. V. 199. P. 515–522.
71. Ribeiro-Resende V.T., Carrier-Ruiz A., Lemes R.M.R., Reis R.A.M., Mendez-Otero R. // Mol. Neurodegeneration. 2012. V. 7. P. 34.
72.Efimenko A., Dzhoyashvili N., Kalinina N., Kochegura T., Akchurin R., Tkachuk V., Parfyonova Y. // Genes and Cells. 2012. V. 7. № 4. P. 73–82.
73. Mantovani C., Terenghi G., Magnaghi V. // Neural Regen Res. 2014. V. 9. № 1. P. 10–15.
74. Nozdrachev A.D., Chumasov E.I. The peripheral nervous system. St.Petersburg: Science, 1999. 281 p.
75. Sta M., Cappaert N.L., Ramekers D., Baas F., Wadman W.J. // J. Neurosci. Methods. 2014. V. 222. P. 189–198.
76. Wang J., Ding F., Gu Y., Liu J., Gu X. // Brain Res. 2009. V. 1262. P.7–15.
77. Xu L., Zhou S., Feng G.Y., Zhang L.P., Zhao D.M., Liu Q., Huang F. // Mol. Neurobiol. 2012. V. 46. P. 265–274.
78. Bersnev V.P., Yakovenko I.V., Semenyutin V.B., Kokin G.S. Surgical treatment of damaged nerves in view of their blood flow and intraoperative diagnosis. L.: Ros. Scientific Inst. Neurosurgeon. Institute. A.L.Polenova. 1991. 30p.
79. Kingham P.J., Kolar M.K., Novikova L.N., Novikov L.N., Wiberg M. // Stem Cells Dev. 2014. V. 23. № 7. P. 741–754.
80. Hsu S.H., Kuo W.C., Chen Y.T., Yen C.T., Chen Y.F., Chen K.S., Huang W.C., Cheng H. // Acta Biomater. 2013. V. 9. № 5. P. 6606–6615.
81. Salgado A.J., Reis R.L., Sousa N.J., Gimble J.M. // Curr. Stem. Cell. Res.Ther. 2010. V. 5. № 2. P. 103–110.
82. Kuffler D.P. // Prog. Neurobiol. 2014. V. 116. P. 1–12.
83. Ramburrun P., Kumar P., Choonara Y.E., Bijukumar D., Lisa C. du Toit, Pillay V. // Biomed. Res. Int. 2014. V. 2014. P. 132350.
84. Nectow A.R., Marra K.G., Kaplan D.L. // Tissue Eng Part B Rev. 2012. V. 18. № 1. P. 40–50.
85. Ladak A., Olson J., Tredget E.E., Gordon T. // Exp. Neurology. 2011. V. 228. № 2. P. 242–252.
86. Cunha A.S., Costa M.P., Silva C.F. // Acta Cir. Bras. 2013. V. 28. № 2. P. 94–101.
87. Liao I.C., Wan H., Qi S., Cui C., Patel P., Sun W., Xu H. // J. Tissue Eng. 2013. 4: 2041731413481036.
88. Jia H., Wang Y., Tong X.J., Liu G.-B., Li Q., Zhang L.X., Sun X.H. // Synapse. 2012. V. 66. № 3. P. 256–269
89. Khuong H.T., Kumar R., Senjaya F., Grochmal J., Ivanovic A., Shakhbazau A., Forden J., Webb A., Biernaskie J., Midha R. // Exp Neurol. 2014. V. 254. P. 168–179.
90.Dai L.G., Huang G.S., Hsu S.H. // Cell Transplantation. 2012. V.22. № 11. P. 2029–2039.
91. Shen C.C., Yang Y.C., Liu B.S. // J. biomed. Materials Res. 2013. V. 101. № 1. P. 239–252.
92. Yang C.C., Wang J., Chen S.C., Hsieh Y.L. // J. Tissue Eng. Regen. Med. 2013. doi: 10.1002/term.1714.
93. Luo H., Zhang Y., Zhang Z., Jin Y. // Biomaterials. 2012. V. 33. № 17. P. 4277–4287.
94. Zhu F.B., Liu D.W., Zhang H.Y., Xu J.C., Peng Y., Zhong Q.L., Li Y.T. // Zhonghua. Shao. Shang. Za. Zhi. 2012. V. 28. № 1. P. 25–31.
95. Wang Y., Jai H., Li W.Y., Tong X.J., Liu G.B., Kang S.W. // Cell. Mol. Neurobiol. 2012. V. 32. № 3. P. 361–371.
96. Marinescu S.A., Zărnescu O., Mihai I.R., Giuglea C., Sinescu R.D. // Rom. J. Morphol. Embryol. 2014. V. 55. № 3. P. 891–903.
97. Jonsson S., Wiberg R., McGrath A.M., Novikov L.N., Wiberg M., Novikova L.N., Kingham P.J. // PLoS One. 2013. V. 8. № 2. P. e56484.
98. Masgutov R.F., Masgutova G.A., Raginov I.S., Malomuzh A.I., Nigmetzyanova M.V., Chelyshev Yu.A. // Bulletin of Experimental Biology and Medicine. 2009. V. 147. № 4. P. 537–538.
99. Liu Y., Nie L., Zhao H., Zhang W., Zhang Y.Q., Wang S.S, Cheng L.// PLoS One. 2014. V. 9. № 10. P. e110993.
100. Duan X.H., Cheng L.N., Zhang F., Liu J., Guo R.M., Zhong X.M., Wen X.H., Shen J. //Eur. J.Radiol. 2012. V. 81. № 9. P. 2154–2160.
101. Liao C.D., Zhang F., Guo R.M., Zhong X.M., Zhu J., Wen X.H., Shen J. // Radiology. 2012. V. 262. № 1. P. 161–171.
102. Li K., Qin J., Wang X., Xu Y., Shen Z., Lu X., Zhang G.// Cytotherapy. 2013. V. 15. № 10. P. 1275–1285.

103. Ugryumov M.V., Konovalov A.N., Gusev E.I. // Bulletin of the Russian Academy of Medical Sciences 2004. № 11. P. 8–17.
104. Stadnikov A.A., Shevliuk N.N. // Morfologiia. 2006. V. 130. № 6. P.84–88.
105. Barmadé-Heider F., Frisén J. // Cell Stem Cell. 2008. V. 3. № 1. P. 16–24.
106. Anisimov S.V. Cell therapy for Parkinson's disease // Adv. Gerontol. 2009. V. 22. № 3. P. 418–439.
107. Loseva E.V. // Neurocomputers: development, application. 2014. №7. P. 32–44.
108. Popov B.V. Cellular mechanisms of regenerative capacity of mesenchymal stem cells, the role of the gene product of the retinoblastoma family. St Petersburg: INC RAS, 2014.
109. Keilhoff G., Fansa H. // Exp. Neurology. 2011. V. 232. № 3. P. 110–113.
110. Pan Y., Cai S. // Mol. Cell Biochem. 2012. V. 368. № 1–2. P. 127–135.
111. Hu N., Wu H., Xue C., Gong Y., Wu J., Xiao Z., Yang Y., Ding F., Gu X. // Biomaterials. 2013. V. 34. № 1. P. 100–111.
112. Klopp A.H., Gupta A., Spaeth E., Andreeff M., Marini F. // Stem Cells. 2011. V. 29. № 1. P. 11–19.
113. Castellone M.D., Laatikainen L.E, Laurila J.P., Langella A., Hematti P., Soricelli A., Salvatore M., Laukkanen M.O. // Stem Cells. 2013. V. 31. № 6. P. 1218–1223.
114. Tian L.L., Yue W., Zhu F., Li S., Li W. // J. Cell. Physiol. 2011. V. 226. № 7. P. 1860–1867.
115. Chistyakova I.A., Poljanskaya G.G. // Tsitologiia. 2014. V. 56. № 11. P. 801–808.
116. Shi W., Yao J., Chen X., Lin W., Gu X., Wang X. //Artif. Cells Blood. Substit. Immobil. Biotechnol. 2010. V. 38. № 1. P. 29–37.
117. Loseva E.V., Podgornyĭ O.V., Poltavtseva R.A. Mareĭ M.V., Loginova N.A., Kurskaia O.V., Cukhikh G.T., Chaĭlakhian R.K., Aleksandrova M.A. // Ross. Fiziol. Zh. Im. I.M. Sechenova. 2011. V. 97. № 2. P. 155–168.
118. Braga-SilvaJ., GehlenD., PadoinA.V., MachadoD.C., GaricocheaB., CostadaCostaJ. // J. Hand. Surg. Eur . 2008. V. 33. № 4. P. 488–493.
119. Salafutdinov I.I., Masgutov R.F., Bogov A.A., Rizvanov A.A., Hannanova I.G., Mullin R.I., Bogov A.A. The therapeutic potential of cell-stromal vascular fraction of adipose tissue in the regeneration of peripheral nerve defects // In: Stem cells and regenerative medicine / edited V.A.Tkachuka. Moscow: Max-press. 2012. P. 70–71.
120. Li Z., Qin H., Feng Z., Liu W., Zhou Y., Yang L., Zhao W., LiY. // Neural Regen. Res. 2013. V. 8. № 36. P. 3441–3448.
121. Boiko E.V., Bisaga G.N., Kovalenko A.V., Isaeva G.E., Kovalenko I.Yu., Novitsky A.V., Bukin S.V. // Vestnik Russian Military Medical Academy. 2014. №3. P. 12–18.
122. Widgerow A.D., Salibian A.A., Lalezari S., Evans G.R. // J. Neurosci. Res. 2013. V. 19. № 12. P. 1517–1524.

Extracellular Nucleic Acids in Urine: Sources, Structure, Diagnostic Potential

O. E. Bryzgunova[1*], P. P. Laktionov[1,2]
[1]Institute of Chemical Biology and Fundamental Medicine, Siberian Branch of the Russian Academy of Sciences, 8 Lavrentiev Avenue, 630090, Novosibirsk, Russia
[2]E.N. Meshalkin Novosibirsk Research Institute of Circulation Pathology, st. Rechkunovskaya 15, 630055, Novosibirsk, Russia
*E-mail: olga.bryzgunova@niboch.nsc.ru
Received: 29.10.2014
Revision received: 19.05.2015

ABSTRACT **Cell-free nucleic acids (cfNA) may reach the urine through cell necrosis or apoptosis, active secretion of nucleic acids by healthy and tumor cells of the urinary tract, and transport of circulating nucleic acids (cirNA) from the blood into primary urine. Even though urinary DNA and RNA are fragmented, they can be used to detect marker sequences. MicroRNAs are also of interest as diagnostic probes. The stability of cfNA in the urine is determined by their structure and packaging into supramolecular complexes and by nuclease activity in the urine. This review summarizes current data on the sources of urinary cfNA, their structural features, diagnostic potential and factors affecting their stability.**
KEYWORDS **urinary cell-free DNA and RNA, apoptosis, necrosis, active secretion, urine nucleases, cell-free NA based non-invasive diagnostics.**
ABBREVIATIONS **cfDNA, cell-free DNA; cfNA, cell-free nucleic acids; cfRNA, cell-free RNA; NA, nucleic acids; cirNA, circulating nucleic acids.**

SOURCES OF URINARY CELL-FREE NUCLEIC ACIDS *(FIGURE)*

Cell-free nucleic acids (cfNA) may get urine as a result of renal cfNA transport from the blood or directly from the cells that came into contact with this biological fluid. The reviews [1, 2] summarize the mechanisms of generation and general properties of cell-free and circulating NA in the blood. Apoptosis is considered to be the main source of cfNA. NAs circulate in the blood as a part of complexes with biopolymers and may be packaged in membrane structures [1, 3]. Circulating DNA is highly fragmented, and the fragments' size is proportional to a nucleosome [1]. The blood contains mRNA and ribosomal RNA, as well as non-coding RNA and miRNA, which can circulate both as part of nucleoprotein complexes and as part of membrane-coated microparticles, including exosomes [4–6]. Transport of nucleic acids from the blood into the primary urine implies the transport of the components from the afferent artery into the renal corpuscle. Glomerular filtration of plasma, which is responsible for this process, is limited by the permeability of the basal membrane and slit membranes between podocytes pedicles. For example, only complexes smaller than 6.4 nm in diameter [7] and with a molecular weight no greater than 70 kDa [8] can enter the nephron lumen; it corresponds to DNA of about 100 bp in size. The size of the pores in the glomerular barrier is about 30 Å; even though shut-like pores with a 110–115 Å radius have been detected, they are very rare [9]. Negatively charged molecules, such as polyanions in the basal membrane and sialoglycoproteins in the lining on podocytes surface and between their pedicles [7], play an important role in the passage of substances through the juxtaglomerular apparatus. It is known that DNA [10–12] and RNA [13–15] are primarily present in the blood as part of supramolecular complexes, such as nucleosomes [1], RNA complexes with blood lipoproteins [16, 17], or larger membrane-protected microparticles and exosomes [4] or apoptotic bodies. However, the size of a mononucleosome exceeds the size of even the largest pores of the kidney barrier and, therefore, mononucleosomes in their classical configuration are unable to pass through the barrier.

The overall health of a patient can also affect the transport of nucleic acids from the blood. An increase in the amount of DNA in the urine of patients with acute pancreatitis [18] was reported as early as in 1967, and in 2012 the urine of smokers was shown to contain more DNA than that of non-smokers (9.46 and 9.04 ng/mL for women, respectively; 4.96 and 2.93 ng/mL for men,

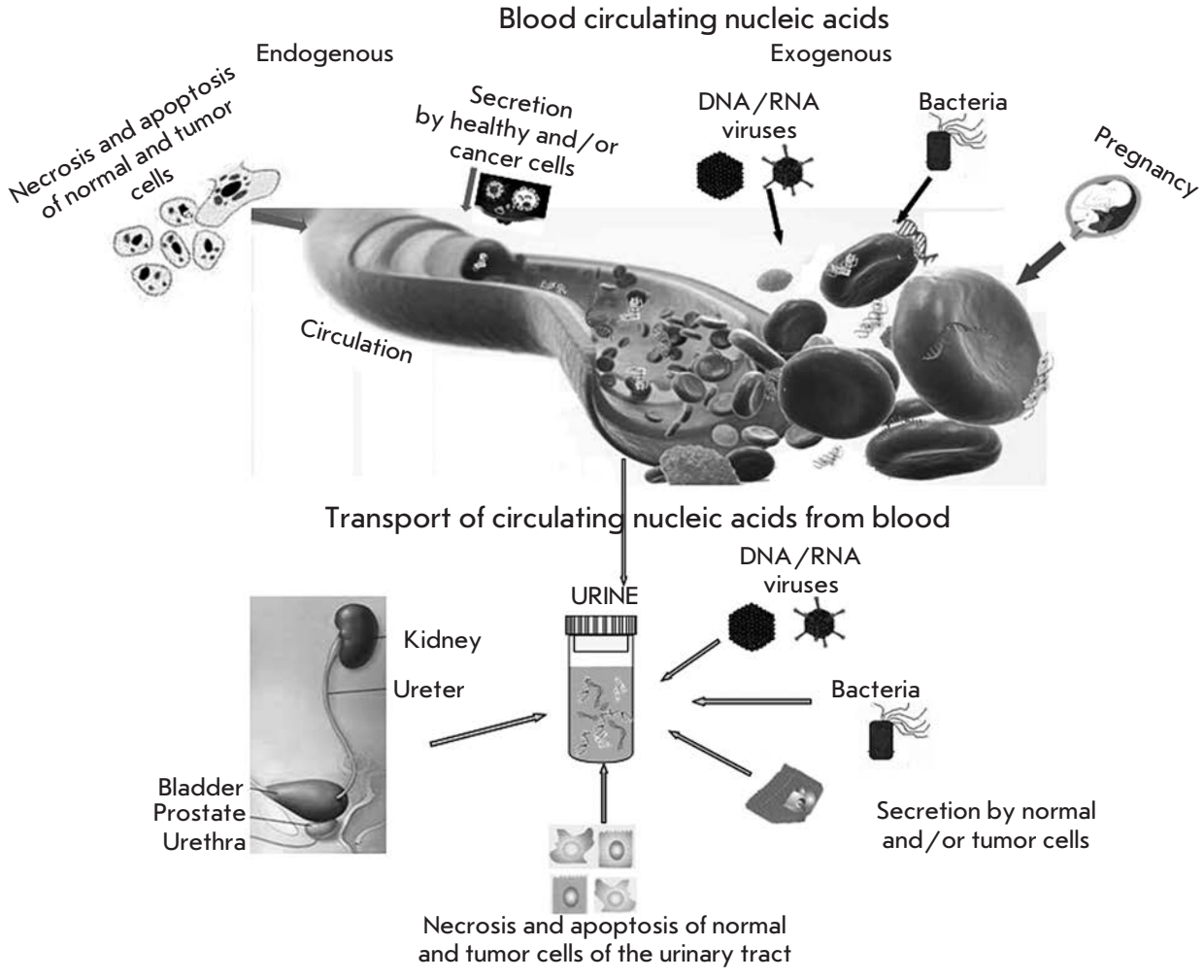

Sources of cell-free nucleic acids in the urine and blood

respectively) [19]. Murine experiments have demonstrated that upon intraperitoneal administration of dying cells a portion of DNA avoids intracellular degradation and phagocytosis, circulates in the blood as a polymer, and is partially excreted with urine in acid-insoluble form [20].

A study of the degradation products of [^{32}P]-labeled DNA of phage λ introduced into the peritoneal cavity of mice showed that the majority of these products were re-used by the cells or were hydrolyzed into acid-soluble fragments, and only ~3.2% were excreted in the urine over 3 days. A small portion of the introduced DNA (0.06%) was detected in the acid-insoluble fraction of urinary nucleic acid (length ≥15–20 bp).

It should also be stressed, however, that the excretion of "unprotected" purified DNA/RNA may be different from that of DNA/RNA from dying cells. Necrotic and especially apoptotic DNA is bound to proteins and is much better protected from nucleases than the purified DNA used in the model system. At the same time, DNA/RNA-binding proteins may have both positive and negative effects on the transportation of DNA/RNA through the kidney barrier. These assumptions are supported by the introduction of human Raji lymphoma cells whose apoptosis has been induced by γ-radiation into the abdominal cavity of mice; the urine of the experimental animals contained human Alu-sequences that were absent in the urine of the control animals (which did not receive injections of Raji cells) [20].

Another proof of circulating DNA transport from the blood into the urine is the specific Y-chromosomal DNA detected in the urine of women who have received blood from male donors [20]. Furthermore, the urine of women carrying a male fetus also contains specific Y-chromosomal DNA [20, 21]. The fetal DNA in the maternal urine was found to be considerably shorter than that in her plasma [21]. Another confirmation

of polymeric DNA transport from the blood into the urine was obtained by analysis of cell-free DNA of cancer patients. It is known that 80–90% of pancreatic and intestine tumors carry mutant forms of the *K-ras* gene, which were found by Botezatu *et al.* [20] in cell-free DNA in the urine of patients with pancreatic (stage IV) and colorectal (stage III–IV) cancer. The concentration of tumor DNA in the urine was quite high; the mutant *K-ras* gene was detected in urinary cfDNA in five of the eight patients with pancreatic cancer and in four out of five patients with colorectal adenocarcinomas [20]. The feasibility of DNA transport from the blood into the urine was demonstrated in experiments which detected the presence of *Mycobacterium tuberculosis* DNA in the urine of patients with tuberculosis [22, 23].

Therefore, DNA fragments, 50–100 bp in size, which are detected in the blood are, apparently, partially protected by histones, but can, nevertheless, reach the urine. In addition, it has been suggested that the binding of DNA to histones, e.g. to H3K27me2, may contribute to the export of cell-free DNA [24].

Another obvious and, apparently, primary source of cfDNA and cfRNA in the urine is apoptosis/necrosis of urinary tract cells. Indeed, under normal circumstances up to 3×10^6 of the bladder and urinary tract epithelium cells can be excreted into the urine within 24 hours (calculations based on the Kakhovsky–Addis method) [25].These cells and endothelial cells may partially enter apoptosis, and fragmented apoptotic DNA/RNA from the cells will inevitably reach the urine [20]: e.g., after transplantation of kidneys from male donors, the concentration of Y-chromosomal DNA in women's urine increases in the case of rejection and returns to normal levels after the inhibition of the immune response against the transplant [26–28]. MALDI-TOF-mass spectrometry revealed the presence of SNP-alleles of the donor kidney in the urinary cell-free DNA [29]. Mutations and microsatellite disorders specific to malignant renal [30] and bladder [31–33] tumors and aberrantly methylated DNA specific to prostate [34, 35] and bladder tumors [33, 36–40] were detected in cell-free DNA in the urine of patients with urogenital cancers. The urine of patients with gynecological and urological diseases or HIV contains HPV DNA that affects deep layers of the skin and the mucous membranes of the internal organs [41]. In the case of bladder cancer, the urinary cell-free DNA contains not only genomic, but also mitochondrial DNA sequences [42].

The concentration of RNA in human urine is 20–140 ng/mL [43, 44]. Another confirmation that cfRNA appear in the urine as a result of apoptosis/necrosis of urogenital tract cells is the detection of survirin, cytokeratin 20, mucin 7, and Ki-67mRNAs in the urine of patients with bladder cancer and urinary tract infections [45, 46]. We were unable to find any data on RNA transport from the circulating blood into the urine.

Strictly speaking, the data on the presence of onco-/fetus-specific NA in the urine do not provide a direct answer to the question of what portion of cfNA originate from the apoptosis/necrosis of the cells that line the urinary tract (it should be noted that cells of prostatic origin constitute no more than 10% of the total urine cell pool [47]). The available data on the concentration of tumor-specific NA in the urine and blood of patients with urogenital system cancers indicate that the transport of tumor-specific cfNA from the blood does not define the concentration of these cfNA in the urine. For example, methylated forms of *GSTP1* and *RASSF1A* genes are detected in 15 and 65% of the urine samples of patients with renal cancer, but only in 6 and 11% of the serum samples of the patients, respectively [48]; i.e., these marker DNAs cannot come from the blood and most likely are transported directly into the urine. These and other [49, 50] data confidently demonstrate that the major portion of cancer-specific cell-free NA in the urine of patients with urogenital tract cancers does not come from the blood and, is, apparently, the result of direct transport of tumor cells or their breakdown products into the urinary tract of diffusion through kidney tissues.

PARTICULAR FEATURES OF URINARY NUCLEIC ACIDS STRUCTURE AND COMPOSITION

Cell-free DNA fragments in the urine can be divided into two groups based on their size: heterogeneous high-molecular-weight DNA (1 kbp or higher) and relatively homogeneous low-molecular-weight DNA (150–250 bp) [20, 43, 51, 52]. Low-molecular-weight DNAs of 10–150 and 150–200 bp were also found in the urine [53].

Only few papers are devoted to the study of DNA and RNA in the cell-free fraction of the urine, whereas the bulk of research involves the search for cancer-specific markers in total urine or in urine cells only. Tumor-specific changes in DNA identified in DNA circulating in the blood are present in urinary cfDNA as well: e.g., point mutations, microsatellite composition disorders, characteristic methylation profile of oncogenes, presence of viral DNA [30, 33, 36, 41].

DNA markers were mainly analyzed by PCR. Microsatellite adjustments (in one or more of the 28 markers (D1S251, HTPO, D3S1317, D3S587, D3S1560, D3S1289, D3S1286, D3S1038, D4S243, FGA, CSF, ACTBP2, D8S348, D8S307, D9S747, D9S242, IFNa, D9S162, D11S488, THO, vWA, D13S802, MJD, D17S695, D17S654, D18S51, MBP, D21S1245) were found in the urine of 76% of patients with kidney tumors [30]. 27% of patients with bladder tumors [31] had at least one dis-

order of microsatellite DNA (D4S243, D9S747, D9S171, D17S695, D17S654).

Cell-free DNA with mutations in the *FGFR3* gene were found in the urine of 34.5% of patients with bladder cancer [33]; *P53*, in 52.9% of patients with liver cancer [54]; *K-ras*, in 95% of patients with colon cancer [55].

Aberrantly methylated DNA typical for prostate tumor cells (*GSTP1*gene) were found in the urine of 36% of prostate cancer patients [34, 56] and 3.2% of those with benign prostatic hyperplasia [35]. Changes in methylation were observed in a number of genes of the urinary cell-free DNA of bladder cancer patients: *CDKN2A* (46.7%), *ARF* (26.7%), *GSTP1* (46.7%), *MGMT* (26.7%), *RARβ2* (60%), *TIMP3* (46.7%), *CDH1* (66.7%), *RASSF1A* (53%) and *APC* (53%) [37]. Moreover, simultaneous determination of the methylation status of four genes, *MYO3A*, *CA10*, *NKX6*, *SOX11* or *MYO3A*, *CA10*, *NKX6*, *DBC1,* in urinary cfDNA allows one to detect bladder cancer with a high sensitivity (81.3%) and specificity (97.3%), whereas simultaneous determination of the methylation status of five genes, *MYO3A*, *CA10*, *NKX6*, *DBC1*, *SOX11* or *MYO3A,CA10*, *NKX6*, *DBC1*, *PENK,* enables the detection of bladder cancer with a sensitivity of 85.2% and a specificity of 94.5% [40].

HPV type 16 DNA was detected in the urine of women with cervical abnormalities, including 88.8% of cancer patients, 76.5% of patients with high-grade lesions, and 45.5% of patients with low-grade lesions [57]. The urine of patients with prostate cancer who underwent surgical treatment contained HPV DNA in 50% of cases [58].

In respect to marker cfRNA, quantitative RT-PCR detected specific Ki-67 mRNA, which was absent from the urine of five healthy donors, in two out of the four patients with bladder cancer and two out of the four patients with urinary tract infections [46]. Furthermore, RT-PCR detected mRNA of survirin (sensitivity 90.4%, specificity 94.7%), cytokeratin 20 (sensitivity 82.6%, specificity 97.4%), and mucin 7 (sensitivity 62.6%, specificity 94.7%) ($P<0.001$) in the urine of bladder cancer patients. The combination of these three markers enables the detection of bladder cancer with a sensitivity of 100% at a specificity of 89.5% [45].

Determination of the concentration of CD147, BIGH3, and STMN1 mRNA in cell-free urine supernatant (after centrifugation of the total urine at 10,000 rpm) revealed that the concentration of mRNA is 2–67 times higher in patients with urothelial bladder cancer than in healthy donors [59].

AMACR (α-methylacyl coenzyme A racemase) mRNA is a promising prostate cancer-specific marker specific. The detection of AMACR mRNA in the urine sediment of 92 men, 43 of whom were diagnosed with prostate cancer, enables the identification of patients with a sensitivity of 70% and specificity of 71%, whereas the determination of PCA3 mRNA enables 72% sensitivity and 59% specificity [60]. Simultaneous determination of AMACR and PCA3 mRNA increases the sensitivity and specificity of the test to 81 and 84%, respectively.

Analysis of the ratios of ETS2 (v-ets erythroblastosis virus E26 oncogene homolog 2) mRNA and uPA (urokinase plasminogen activator) mRNA in cell-free RNA in total urine (without centrifugation/precipitation of the cells) make it possible to diagnose bladder cancer with 100% specificity and 75.4% sensitivity [61].

However, the use of urinary mRNA for the development of diagnostic systems for various diseases remains quite a challenge, since the urine contains a lot of nucleases, including RNases (their diversity is described in the next chapter). High concentration of enzymes that hydrolyze RNA complicates the processing of cell-free RNA, including the isolation stage. Unlike long mRNAs, miRNAs are more resistant to nucleases due to their small size (20–25 nucleotides), and the ability to form stable complexes with biopolymers or to be packed into different microparticles, e.g., exosomes [4]. The urine indeed contains m-, sca-, sno-, sn-, pi-, and miRNAs, including those in exosomes [4, 62]. Based on these data, more and more researchers are trying to develop test systems for the diagnosis of various cancers by analyzing miRNA in urine.

For example, it has been shown that the ratio of miRNA-126 and miRNA-152 concentrations in the urine enables detection of bladder cancer at 82% specificity and 72% sensitivity [63]. Determination of microRNA-210, -10b, and 183 concentrations increases the specificity of the detection of bladder cancer to 91% with a sensitivity of at least 71% [64].

More than 204 group-specific miRNA were found in the urine of healthy donors, cancer patients, and pregnant women; some of them may be potential markers (e.g., miR-515-3p, 335, 892a, 509-5p, 223*, 873, 302d, 616*, 134) [44].

The level of microRNA 483-5p expression in the cell-free fraction of the urine was found to be significantly higher (Mann-Whitney, $P = 0.013$) in prostate cancer patients [65].

The study of miRNA of the epithelial-mesenchymal transition (EMT) [66] in urine sediment and supernatant from 51 bladder cancer patients and 24 healthy volunteers revealed a decrease in the amount of miRNA-200, miRNA-192, and -155 families in the sediment, as well as decreased expression of miRNA-192 and increased expression of miRNA-155 in the urine supernatant of the patients. In addition, the level of expression of miRNA-200, miRNA-205, and miRNA-192 families in the urine sediment of the patients was

significantly correlated with the expression of EMT markers in the urine, including mRNA of zinc finger E-box-binding homeobox 1, vimentin, transforming growth factor-1, and the homolog gene of Ras family (member A). The levels of miRNA-200c and miRNA-141 in the urine sediment of the patients returned to normal after the removal of the bladder tumor.

DNA- AND RNA-HYDROLYZING ENZYMES IN THE URINE

Human urine is a suitable environment for the functioning of NA-hydrolyzing enzymes: adult daily urine contains 2.0–4.0 g of potassium, 100–400 mg of calcium, 50–150 mg of magnesium, 3.6 g of sodium, 270–850 μg of zinc [25] and the pH value of urine normally ranges from 5.0 to 7.0.

DNase I is the major DNA-hydrolyzing enzyme in the urine [67-70], as well as in the blood [1], and its activity in the urine is more than 100-fold higher than its activity in serum [71] and amounts to 400÷1200 act. U/L (specific activity of DNase I is 2000 act. U/mg, in blood 4.4 ± 1.8 act. U/L). Cell-free DNA in the urine can be hydrolyzed by all DNase I isoforms, which are known to differ in pI value, primary structure, and/or content of sialic acid [72]. In addition, genetic polymorphism of DNase I in urine was reported in [69]. A murine model experiment demonstrated that the concentration of DNase I in the urine can significantly increase with the onset of systemic lupus erythematosus (from 24 to 521 ng/mL), thereby indirectly reflecting the disorders occurring in the body [73]. The activity of DNase I in the blood is inhibited by actin [68, 74, 75]: however, actin concentration in the urine is, apparently, significantly lower than that in the blood (the concentration of actin is determined based on the concentration of 3-methylhistidine, a specific metabolite of actin and myosin) [76].

The urine also contains DNase II [70, 71, 77]. The activity of DNase II in human urine is *ca.* 30 -times lower than that of DNase I [77]. At the same time, it is 1.5–5 times higher than in the blood [78] and amounts to *ca.* 13–40 act. U/L of the urine.

In addition to DNases, the urine also contains phosphodiesterase I, which has a pH-optimum of 9.0 (the enzyme is stable at pH 3.0 to 11.0) [71, 79].

As for RNA-hydrolyzing enzymes of the urine, unfortunately, their studies were conducted primarily in the 20th century (1970s–90s.). RNase 2 is the most abundant RNA-hydrolyzing enzyme in human urine, where its concentration is *ca.* 20 times higher than that of RNase I. The molecular weight of RNase 2 as determined by electrophoresis in SDS-PAGE and gel filtration is 32 kDa and 38, respectively: the pH-optimum is in the range of 7.2–7.6 [80].

Ribonuclease I (RNase I) is the second most abundant RNA-hydrolyzing enzyme in the urine [81]. The molecular weight of this enzyme is ~16 kDa, the enzyme is active at pH 7.0, and is inhibited by Cu^{2+}, Hg^{2+} and Zn^{2+}ions. RNase I is a pyrimidine-specific enzyme, and it hydrolyzes poly(C) and poly(U) more effectively than poly(A) and poly(G). RNase I is also able to hydrolyze RNA:DNA heteroduplexes [82].

In addition to RNases 2 and 1, human urine also contains RNase C and U with pH optimum of 8.5 and 7.0, respectively [83], as well as RNase 7, UL, US, UpI-1, and UpI-2. RNase C (33 kD) is a glycoprotein, which preferably hydrolyzes synthetic poly(C) homopolymer, and is similar to mammalian pancreatic RNases. RNase U (18 kDa) is also a glycoprotein and uses RNA as a substrate, but it is almost inactive against poly(C) and has a lower homology with pancreatic RNases. In terms of amino acid composition, this enzyme is similar to human spleen RNase. Other researchers also found RNAases with a molecular mass of 33 [84] and 21.5 kDa [85], a pH optimum of 6.5, and a more efficient hydrolysis of poly(C) in human urine. RNase 7 (14.5 kDa) is present in the urine in concentrations of 235–3467.2 mg/L [86]. RNase 7 exhibits antibacterial activity at alkaline pH values.

Pyrimidine-specific RNase UL (38 kDa) and US (13 kDa), with pH optima of 8.0 and 6.75, respectively, were found in the urine of adult individuals [87]. The urine of pregnant women contained RNase UpI-1 (34 kDa) and UpI-2 (38 kDa) with pH-optima of 7.7 and 6.6, respectively [88].

Therefore, cell-free DNA and RNA are heterogeneous with respect to their size and composition. They may appear in the urine both from the blood and from the cells of the urogenital system, mainly through apoptosis, necrosis, oncosis, and active secretion (as a part of exosomes). The biological function of urinary cell-free nucleic acids has not been investigated, but DNA, RNA, and small RNA are of interest for early noninvasive diagnostics of oncological diseases of various etiologies. ●

REFERENCES

1. Bryzgunova O., Laktionov P. // Biochemistry (Moscow). Supplement Series B: Biomed. Chem. 2014. V. 8. P. 203–219.
2. Fleischhacker M., Schmidt B. // Biochim. Biophys. Acta. 2007. V. 1775. P. 181–232.
3. van der Vaart M., Pretorius P. // Ann. N.Y. Acad. Sci. 2008. V. 1137. P. 18–26.
4. Li M., Zeringer E., Barta T., Schageman J., Cheng A., Vlassov A. // Phil. Trans. R. Soc. B. 2014. V. 369. P. 20130502.
5. Sita-Lumsden A., Fletcher C., Dart D., Brooke G., Waxman

J., Bevan C. // Biomark. Med. 2013. V. 7. P. 867–877.
6. Rykova E., Morozkin E., Ponomaryova A., Loseva E., Zaporozhchenko I., Cherdyntseva N., Vlassov V., Laktionov P. // Expert Opin. Biol. Ther. 2012. V. 12. Suppl 1. P. S141–S153.
7. Pokrovsky V., Korot'ko G. Human Physiology. M.: Medicine, 1997. P. 277-280.
8. Lote C. Principles of Renal Physiology. London: Chapman & Hall, 1994. P. 33–44.
9. Tencer J., Frick I., Oquist B., Alm P., Rippe B. // Kidney Int. 1998. V. 53. P. 709–715.
10. Holdenrieder S., Stieber P., Bodenmüller H., Busch M., von Pawel J., Schalhorn A., Nagel D., Seidel D. // Ann. N.Y. Acad. Sci. 2001. V. 945. P. 93–102.
11. Kiroi K., Tanaka C., Toi M. // Breast Cancer. 1999. V. 6. P. 361–364.
12. Lin J., Fan R., Zhao Z., Cummings O., Chen S. // Am. J. Surg. Pathol. 2013. V. 37. P. 539–547.
13. Ng E., Tsui N., Lam N., Chiu R., Yu S., Wong S., Lo E., Rainer T., Johnson P., Lo Y. // Clin. Chem. 2002. V. 48. P. 1212–1217.
14. Halicka H., Bedner E., Darzynkiewicz Z. // Exp. Cell Res. 2000. V. 260. P. 248–256.
15. Hasselmann D., Rappl G., Tilgen W., Reinhold U. // Clin. Chem. 2001. V. 47. P. 1488–1489.
16. Gahan P., Stroun M. // Cell Biochem. Funct. 2010. V. 28. P. 529–538.
17. Vickers K., Palmisano B., Shoucri B., Shamburek R., Remaley A. // Nat. Cell Biol. 2011. V. 13. P. 423–433.
18. Sorenson G. // Clin. Cancer Res. 2000. V. 6. P. 2129–2137.
19. Simkin M., Abdalla M., El-Mogy M., Haj-Ahmad Y. // Epigenomics. 2012. V. 4. P. 343–352.
20. Botezatu I., Serdyuk O., Potapova G., Shelerov V., Alechina R., Molyaka Y., Anan'ev V., Bazin I., Garin A., Narimanov M., et al. // Clin. Chem. 2000. V. 46. P. 1078–1084.
21. Koide K., Sekizawa A., Iwasaki M., Matsuoka R., Honma S., Farina A., Saito H., Okai T. // Prenatal Diagnosis. 2005. V. 25. P. 604–607.
22. Tuuminen T. // Front. Immunol. 2012. V. 3. P. 1–6.
23. Peter J., Green C., Hoelscher M., Mwaba P., Zumla A., Dheda K. // Curr. Opin. Pulm. Med. 2010. V. 16. P. 262–270.
24. Peters D., Pretorius P. // Clin. Chim. Acta. 2011. V. 412. P. 806–811.
25. Chirkin A., Okorokov A., Goncharik I. Diagnostic guide to physician. Minsk: Belarus, 1993. 688 p.
26. Zhang J., Tong K., Li P., Chan A., Yeung C., Pang C., Wong T., Lee K., Lo D. // Clin. Chem. 1999. V. 45. P. 1741–1746.
27. Zhong X., Hahn D., Troeger C., Klemm A., Stein G., Thomson P., Holzgreve W., Hahn S. // Ann. N.Y. Acad. Sci. 2001. V. 945. P. 250–257.
28. Zhang Z., Ohkohchi N., Sakurada M., Mizuno Y., Miyagi T., Satomi S., Okazaki H. // Transplantation Proc. 2001. V. 33. P. 380–381.
29. Li Y., Hanh D., Wenzel W., Hanh S., Holzgreve F. // Ann. N.Y. Acad. Sci. 2006. V. 1075. P. 144–147.
30. Eisenberger C., Schoenberg M., Enger C., Hortopan S., Shah S., Chow N., Marshall F., Sidransky D. // J. Natl. Cancer Inst. 1999. V. 91. P. 2028–2032.
31. Utting M., Werner W., Dahse R., Schubert J., Junker K. // Clin. Cancer Res. 2002. V. 8. P. 35–40.
32. Mao L., Lee D., Tockman M., Erozan Y., Askin F., Sidransky D. // Proc. Natl. Acad. Sci. USA. 1994. V. 91. P. 9871–9875.
33. Karnes R., Fernandez C., Shuber A. // Mayo. Clin. Proc. 2012. V. 87. P. 835–839.
34. Goessl C., Krause H., Muller M., Heicappell R., Schrader M., Sachsinger J., Miller K. // Cancer Res. 2000. V. 60. P. 5941-5945.
35. Jeronimo C., Usadel H., Henrique R., Silva C., Oliveira J., Lopes C., Sidransky D. // Urology. 2002. V. 60. P. 1131–1135.
36. Goessl C., Muller M., Straub B., Miller K. // Eur. Urology. 2002. V. 41. P. 668–676.
37. Hoque M., Begum S., Topaloglu O., Chatterjee A., Rosenbaum E., Criekinge W., Westra W., Schoenberg M., Zahurak M., Goodman S., Sidransky D. // J. Nat. Cancer Inst. 2006. V. 98. P. 996–1004.
38. Reinert T., Modin C., Castano F., Lamy P., Wojdacz T., Hansen L., Wiuf C., Borre M., Dyrskjot L., Orntoft T. // Clin. Cancer Res. 2011. V. 17. P. 5582–5592.
39. Reinert T. // Adv. Urol. 2012. V. 2012. P. 503271.
40. Chung W., Bondaruk J., Jelinek J., Lotan Y., Liang S., Czerniak B., Issa J. // Cancer Epidemiol. Biomarkers Prev. 2011. V. 20. P. 1483–1491.
41. Vorsters A., Micalessi I., Bilcke J., Ieven M., Bogers J., van Damme P. // Eur. J. Clin. Microbiol. Infect. Dis. 2012. V. 31. P. 627–640.
42. Ziegler A., Zangemeister-Wittke U., Stahel R. // Cancer Treatment Rev. 2002. V. 28. P. 255–271.
43. Bryzgunova O., Skvortsova T., Kolesnikova E., Starikov A., Rykova E., Vlassov V., Laktionov P. // Ann. N.Y. Acad. Sci. 2006. V. 1075. P. 334–340.
44. Weber J., Baxter D., Zhang S., Huang D., Huang K., Lee M., Galas D., Wang K. // Clin. Chem. 2010. V. 56. P. 1733–1741.
45. Pu X., Wang Z., Chen Y., Wang X., Wu Y., Wang H. // J. Cancer Res. Clin. Oncol. 2008. V. 134. P. 659–665.
46. Menke T., Warnecke J. // Ann. N.Y. Acad. Sci. 2004. V. 1022. P. 185–189.
47. Truong M., Yang B., Jarrard D. // J. Urology. 2013. V. 189. P. 422–429.
48. Hoque M., Begum S., Topaloglu O., Jeronimo C., Mambo E., Westra W., Califano J., Sidransky D. // Cancer Res. 2004. V. 64. P. 5511–5517.
49. Payne S., Serth J., Schostak M., Kamradt J., Strauss A., Thelen P., Model F., Day J., Liebenberg V., Morotti A., et al. // Prostate. 2009. V. 69. P. 1257–1269.
50. Goessl C., Muller M., Heicappell R., Krause H., Miller K. // Ann. N.Y. Acad. Sci. 2001. V. 945. P. 51–58.
51. Su Y., Wang M., Brenner D., Ng A., Melkonyan H., Umansky S., Syngal S., Block T. // J. Mol. Diagn. 2004. V. 6. P. 101–107.
52. Su Y., Wang M., Aiamkitsumrit B., Brenner D., Block T. // Cancer Biomarkers. 2005. V. 1. P. 177–182.
53. Melkonyan H., Feaver W., Meyer E., Scheinker V., Shekhtman E., Xin Z., Umansky S. // Ann. N.Y. Acad. Sci. 2008. V. 1137. P. 73–81.
54. Lin S., Dhillon V., Jain S., Chang T., Hu C., Lin Y., Chen S., Chang K., Song W., Yu L., et al. // J. Mol. Diagn. 2011. V. 13. P. 474–484.
55. Su Y., Wang M., Brenner D., Norton P., Block T. // Ann. N.Y. Acad. Sci. 2008. V. 1137. P. 197–206.
56. Bryzgunova O., Morozkin E., Yarmoschuk S., Vlassov V., Laktionov P. // Ann. N.Y. Acad. Sci. 2008. V. 1137. P. 222–225.
57. Daponte A., Pournaras S., Mademtzis I., Hadjichristodoulou C., Kostopoulou E., Maniatis A., Messinis I. // J. Clin. Virol. 2006. V. 36. P. 189–193.
58. Zambrano A., Kalantari M., Simoneau A., Jensen J., Villarreal L. // Prostate. 2002. V. 53. P. 263–276.
59. Bhagirath D., Abrol N., Khan R., Sharma M., Seth A.,

Sharma A. // Clin. Chim. Acta. 2012. V. 413. P. 1641–1646.
60. Ouyang B., Bracken B., Burke B., Chung E., Liang J., Ho S. // J. Urol. 2009. V. 181. P. 2508–2513.
61. Hanke M., Kausch I., Dahmen G., Jocham D., Warnecke J. // Clin. Chem. 2007. V. 53. P. 2070–2077.
62. Miranda K., Bond D., McKee M., Skog J., Paunescu T., Silva N., Brown D., Russo L. // Kidney Int. 2010. V. 78. P. 191–199.
63. Hanke M., Hoefig K., Merz H., Feller A., Kausch I., Jocham D., Warnecke J., Sczakiel G. // Urol. Oncology. 2009. V. 28. P. 665–661.
64. Eissa S., Matboli M., Hegazy M., Kotb Y., Essawy N. // Transl Res. 2015. pii. S1931-5244(15)00003-1.
65. Korzeniewski N., Tosev G., Pahernik S., Hadaschik B., Hohenfellner M., Duensing S. // Urol. Oncol. 2015. V. 33. P. 16.e17–22.
66. Wang G., Chan E., Kwan B., Li P., Yip S., SzetoC., Ng C. // Clin. Genitourin. Cancer. 2012. V. 10. P. 106–113.
67. Dittmar M., Bischofs C., Matheis N., Poppe R., Kahaly G. // J. Autoimmun. 2009. V. 32. P. 7–13.
68. Eulitz D., Mannherz H. // Apoptosis. 2007. V. 12. P. 1511–1521.
69. Kishi K., Yasuda T., Ikehara Y., Sawazaki K., Sato W., Iida R. // Am. J. Hum. Genet. 1990. V. 47. P. 121–126.
70. Ito K., Minamiura N., Yamamoto T. // J. Biochem. 1984. V. 95. P. 1399–1406.
71. Nadano D., Yasuda T., Kishi K. // Clin. Chem. 1993. V. 39. P. 448–452.
72. Yasuda T., Awazu S., Sato W., Iida R., Tanaka Y., Kishi K. // J. Biochem. 1990. V. 108. P. 393–398.
73. Macanovic M., Lachmann P. // Clin. Exp. Immunol. 1997. V. 108. P. 220–226.
74. Mannherz H. // J. Biol. Chem. 1992. V. 267. P. 11661–11664.
75. Hitchock S. // J. Biol. Chem. 1980. V. 255. P. 5668–5673.
76. Calles-Escandon J., Cunningham J., Snyder P., Jacob R., Huszar G., Loke J., Felig P. // Am. J. Physiol. 1984. V. 246. P. e334–338.
77. Murai K., Yamanaka M., Akagi K., Anai M. // J. Biochem. 1980. V. 87. P. 1097–1103.
78. Yasuda T., Takeshita H., Nakazato E., Nakajima T., Hosomi O., Nakashima Y., Kishi K. // Anal. Biochem. 1998. V. 255. P. 274–276.
79. Ito K., Yamamoto T., Minamiura N. // J. Biochem. 1987. V. 102. P. 359–367.
80. Mizuta K., Yasuda T., Ikehara Y., Sato W., Kishi K. // Z. Rechtsmed. 1990. V. 103. P. 315–322.
81. Yasuda T., Sato W., Kishi K. // Biochim. Biophys. Acta. 1988. V. 965. P. 185–194.
82. Potenza N., Salvatore V., Migliozzi A., Martone V., Nobile V., Russo A. // Nucl. Acids Res. 2006. V. 34. P. 2906–2913.
83. Cranston J., Perini F., Crisp E., Hixson C. // Biochim. Biophys. Acta. 1980. V. 616. P. 239–258.
84. Rabin E., Weinberger V. // Biochem. Med. 1975. V. 14. P. 1–11.
85. Reddi K. // Prep. Biochem. 1977. V. 7. P. 283–299.
86. Spencer J., Schwaderer A., Dirosario J., McHugh K., McGillivary G., Justice S., Carpenter A., Baker P., Harder J., Hains D. // Kidney Int. 2011. V. 80. P. 174–180.
87. Iwama M., Kunihiro M., Ohgi K., Irie M. // J. Biochem. 1981. V. 89. P. 1005–1016.
88. Sakakibara R., Hashida K., Kitahara T., Ishiguro M. // J. Biochem. 1992. V. 111. P. 325–330.

Additivity of the Stabilization Effect of Single Amino Acid Substitutions in Triple Mutants of Recombinant Formate Dehydrogenase from the Soybean *Glycine max*

A. A. Alekseeva[1,2], I. S. Kargov[2,3], S. Yu. Kleimenov[1,4], S. S. Savin[2,3], V. I. Tishkov[1,2,3*]
[1]A.N.Bach Institute of Biochemistry, Federal Research Center "Fundamentals of Biotechnology" of the Russian Academy of Sciences, Leninskiy Prospect, 33/2, Moscow,119071, Russia
[2]Innovations and High Technologies MSU Ltd, Tsimlyanskaya St., 16, Moscow, 109559, Russia
[3]Department of Chemistry, M.V. Lomonosov Moscow State University, Leninskie Gory, 1/3, Moscow, 119991, Russia
[4]N.K. Koltsov Institute of Developmental Biology of the Russian Academy of Sciences, Vavilova St., 26, Moscow, 119334, Russia
*E-mail: vitishkov@gmail.com
Received: 03.07.2015

ABSTRACT **Recently, we demonstrated that the amino acid substitutions Ala267Met and Ala267Met/Ile272Val (Alekseeva *et al.*, Biochemistry, 2012), Phe290Asp, Phe290Asn and Phe290Ser (Alekseeva *et al.*, Prot. Eng. Des. Select, 2012) in recombinant formate dehydrogenase from soya *Glycine max* (SoyFDH) lead to a significant (up to 30–100 times) increase in the thermal stability of the enzyme. The substitutions Phe290Asp, Phe290Asn and Phe290Ser were introduced into double mutant SoyFDH Ala267Met/Ile272Val by site-directed mutagenesis. Combinations of three substitutions did not lead to a noticeable change in the catalytic properties of the mutant enzymes. The stability of the resultant triple mutants was studied through thermal inactivation kinetics and differential scanning calorimetry. The thermal stability of the new mutant SoyFDHs was shown to be much higher than that of their precursors. The stability of the best mutant SoyFDH Ala267Met/Ile272Val/Phe290Asp turned out to be comparable to that of the most stable wild-type formate dehydrogenases from other sources. The results obtained with both methods indicate a great synergistic contribution of individual amino acid substitutions to the common stabilization effect.**
KEYWORDS **protein engineering, multi-point mutants, rational design, stabilization, stability, synergistic effect, formate dehydrogenase, *Glycine max*.**

INTRODUCTION

$NAD(P)^+$-dependent formate dehydrogenases ([1.2.1.2], FDHs) have been found in bacteria, yeast, fungi, and plants [1–3]; however, plant FDHs have been far less studied than enzymes from microorganisms. Our laboratory has actively studied plant recombinant formate dehydrogenases, including FDH from the soybean *Glycine max* (SoyFDH) [3–7]. A plasmid vector was constructed that enabled expression of the soluble and active SoyFDH in *Escherichia coli* cells [8]. Increased interest in this enzyme stems from the fact that the Michaelis constant values of SoyFDH both for NAD^+ and formate are lower than those of formate dehydrogenases from other sources (*Table 1*). Systematic studies of various formate dehydrogenases [2] and analysis of the structure-function relationship have revealed a number of amino acid residues that affect the stability and catalytic properties of soybean formate dehydrogenase [3–7]. More than 20 mutant SoyFDHs were prepared using site-directed mutagenesis. More than half of them had a higher thermal stability compared to the one for the wild-type enzyme, while the Michaelis constants practically didn't change. The most interesting results were obtained using enzyme stabilization approaches such as filling the cavity inside the protein globule [4] and substitution of a hydrophobic residue by hydrophilic ones on the protein globule surface [5, 6]. SoyFDHs with a substitution of one or two amino acid residues, Ala267Met and Ala267Met/Ile272Val, respectively, were produced using the first approach.

In this case, the thermal stability of a double mutant was significantly higher compared to that of its precursor [4]. In the case of the second approach, a hydrophobic residue, Phe290, located in the coenzyme-binding domain on the surface of the protein globule was replaced by eight other amino acid residues [5, 6]. In this work, three triple mutants were produced by introducing the point substitutions Phe290Asp, Phe290Asn, and Phe290Ser into double mutant Ala267Met/Ile272ValSoyFDH. The Phe290Asp substitution providing the strongest stabilization effect was assumed to produce a triple mutant with the highest stability. The other two triple mutants were obtained to elucidate how the differences in the stabilization effect at the 290th position will affect the overall stability and catalytic properties of SoyFDH with three amino acid substitutions.

MATERIALS AND METHODS

Molecular-biology-grade reagents were used for genetic engineering experiments. Bactotryptone, yeast extract, and agar (Difco, USA), glycerol (99.9%) and calcium chloride (ultra pure), dipotassium hydrogen phosphate, sodium dihydrogen phosphate (pure for analysis), lysozyme (Fluka/BioChemika, Switzerland), lactose (analytical grade), ampicillin and chloramphenicol (Sigma, USA), and glucose and sodium chloride (analytical grade (Helicon, Russia) were used in microbiological experiments. Restriction endonucleases, phage T4 DNA ligase, and Pfu DNA polymerase (Fermentas, Lithuania) were used for cloning DNA fragments and site-directed mutagenesis. Reagent kits (Fermentas, Lithuania) were used to isolate DNA from agarose gel and plasmids from *E. coli* cells. Oligonucleotides for PCR and sequencing were synthesized by the Syntol company (Russia). Water purified by a MilliQ device (Millipore, USA) was used in these experiments.

All reagents used in protein electrophoresis were manufactured by Bio-Rad (USA). NAD^+ with a purity ≥ 98% (AppliChem, Germany), sodium formate and EDTA (Merck, Germany), sodium azide (Sigma, Germany), ammonium sulfate (chemically pure grade, DiaM, Russia), sodium dihydrogen phosphate, disodium phosphate, and urea (analytical grade, Reakhim, Russia) were used to isolate an enzyme and examine its properties.

Site-directed mutagenesis reaction

Site-directed mutagenesis enabling Phe290Asp, Phe290Asn, and Phe290Ser substitutions in the SoyFDH amino acid sequence were introduced as previously described [5]; however, instead of the pSoyFDH2 plasmid with the wild-type SoyFDH gene, the pSoyFDH2_M1M2 plasmid was used as an initial template. This plasmid contains a gene encoding SoyFDH with Ala267Met and Ile272Val substitutions.

For each mutant plasmids were isolated from three colonies. The correctness of mutation introduction was proved by sequencing of the plasmid DNA at the Genome Center for Collective Use (Engelhardt Institute of Molecular Biology, Moscow).

Expression of mutant SoyFDHs in *E. coli* cells

Wild-type SoyFDH and its mutant forms were expressed in *E.coli* BL21(DE3) Codon Plus/pLysS cells. To generate a producer strain, the cells were transformed with an appropriate plasmid and plated on Petri dishes with an agar medium containing ampicillin (150 μg/mL) and chloramphenicol (25 μg/mL). To prepare the inoculum, a single colony was taken from a plate and cultured at 30 ˚C overnight in 4 mL of a modified 2YT medium (10 g/L yeast extract, 16 g/L bactotryptone, 1.5 g/L sodium dihydrogen phosphate, 1 g/L dipotassium hydrogen phosphate, pH 7.5) in the presence of 150 μg/mL ampicillin and 25 μg/mL chloramphenicol. Then, the cells were subcultured into a fresh medium (1 : 100 dilution) and cultured at 37 ˚C to $A_{600} \approx 0.6–0.8$. The inoculum (10% of the total medium volume) was added into conical 1L baffled flasks. The cells were cultured at 30 ˚C and 80–90 rpm until an absorbance of $A_{600}=0.6–0.8$. Then, the cells were induced by adding a solution of lactose (300 g/L) to a final concentration of 20 g/L. After induction, the cells were cultured for 17 h and then pelleted using an Eppendorf 5403 centrifuge (20 min, 5,000 rpm, 4 ˚C). The resulting biomass was re-suspended in a 0.1 M sodium phosphate buffer pH 8.0 at a 1 : 4 (weight-volume) ratio. The resulting suspension was frozen and stored at −20 ˚C.

Isolation and purification of mutant enzymes

To isolate mutant SoyFDHs, a 20% cell suspension in a 0.1 M sodium phosphate buffer, pH 8.0, was subjected to two cycles of freezing-thawing; then, the cells were disrupted using a Branson Sonifier 250 ultrasonic cell disruptor (Germany) under continuous cooling. The precipitate was removed by centrifugation on an Eppendorf 5804R centrifuge (11,000 rpm, 30 min).

The enzyme purification procedure included precipitation of ballast proteins with ammonium sulfate (saturation of 40%), precipitation of the target protein (with ammonium sulfate saturation of 85%) and its subsequent reconstitution in a solution containing 45% ammonium sulfate, hydrophobic chromatography on Phenyl Sepharose, and desalting on a Sephadex G-25 column [4, 5]. The sample purity was monitored by analytical electrophoresis in a 12% polyacrylamide gel in the presence of 0.1% sodium dodecyl sulfate (Bio-Rad electrophoresis apparatus).

Formate dehydrogenase activity measurement

The enzymatic activity was determined spectrophotometrically by the absorbance of NADH at 340 nm (ε_{340}=6,220 $M^{-1}cm^{-1}$) on a Schimadzu UV1800PC spectrophotometer at 30 ˚C in 0.1 M sodium phosphate buffer, pH 7.0, containing 0.3 M sodium formate and 0.4 mg/mL NAD^+.

Determination of the Michaelis constant

Michaelis constants for NAD^+ and formate were determined spectrophotometrically by measuring the dependence of enzymatic activity on the concentration of one of the substrates in a range from 0.3 up to 6–7 K_M at saturating concentrations of the second substrate (> 20 K_M). The exact concentration of initial NAD^+ solutions was measured at 260 nm (ε_{260} = 17,800 $M^{-1}cm^{-1}$). The exact concentration of sodium formate was determined enzymatically using formate dehydrogenase, based on the formation of NADH caused by oxidation of the formate ion to CO_2. 50 μL of a NAD^+ solution (20 mg/mL in 0.1 M phosphate buffer, pH 8.0), 20 μL of a formate dehydrogenase solution (50 U/mL), and 0.1 M phosphate buffer, pH 8.0, were added to a quartz spectrophotometric cuvette (total and reaction volumes were 4 and 2 mL, respectively) to a total volume of 1.96 mL. The cell was incubated at 37 ˚C for 15 min, and then the absorbance at 340 nm was determined. 0.1 mL of a 3 M sodium formate solution in 0.1 M phosphate buffer, pH 7.0, prepared by weight in a volumetric flask was added to a 100 mL volumetric flask with 0.1 M phosphate buffer, pH 8.0, using a 0.1 mL glass pipette and adjusted to a volume of 100 mL with the same buffer. The resulting solution was stirred, and a 40 μL sample of the solution was added to the cell with the reaction mixture. Upon completion of the reaction (15–20 min), the solution absorbance was measured. The absorbance was subtracted with an initial absorbance value, and the resultant difference was used to calculate the exact concentration of sodium formate. K_M values were determined by nonlinear regression using the Origin Pro 8.5 software.

Determination of catalytic constants

The catalytic constant values were calculated from the dependence of the activity of several enzyme samples on the active site concentrations of the samples by linear regression using the Origin Pro 8.5 software. The concentrations of active sites were determined by measuring quenching of enzyme fluorescence by NAD^+ and the azide ion [7]. Measurements were performed in 0.1 M sodium phosphate buffer, pH 7.0, on a Cary Eclipse fluorimeter (Varian, USA).

Thermal stability analysis based on the thermal inactivation kinetics

The enzyme thermal stability was studied in 0.1 M sodium phosphate buffer, pH 7.0, containing 0.01 M EDTA. Series of 1.5 mL plastic test tubes with 50 μL of an enzyme solution (0.2 mg/mL) in each were prepared for each experiment. The tubes were placed in a water thermostat pre-heated to a required temperature (46–66 ˚C, temperature accuracy of ± 0.1 ˚C). At a certain time point, one tube was taken out and transferred into ice for 5 min, after which the tube was centrifuged at 12,000 rpm on an Eppendorf 5415D centrifuge for 3 min. The residual formate dehydrogenase activity was measured as described above. The thermal inactivation rate constant k_{in} was determined as the slope of the natural logarithm of residual activity vs time (semilogarithmic coordinates, $\ln(A/A_0)$ $-t$)) by linear regression using the Origin Pro 8.5 software.

Analysis of the enzyme thermal stability using differential scanning calorimetry

Differential scanning calorimetry experiments were performed using a DASM-4 adiabatic differential scanning microcalorimeter (Biopribor, Bach Institute of Biochemistry, Federal Research Center "Fundamentals of Biotechnology", Russia). The reaction volume of platinum capillary calorimetric cells was 0.48 mL. To prevent the formation of air bubbles and evaporation of solutions at elevated temperatures, 2.2 atm extra pressure was maintained in the calorimetric cells. The instrument calibration was carried out by feeding one cell to a fixed power (ΔW = 25 μW).

Before a calorimetric experiment, the temperature drift of instrument readings was determined. During measurement, the blank cell contained 0.1 M sodium phosphate buffer, pH 7.0, and the sample cell contained SoyFDH dissolved in the same buffer. The enzyme concentration was 2.0 mg/mL, and the heating rate was 1 ˚C/min.

The thermal denaturation reversibility was analyzed by re-scanning of a sample after its cooling to 10–12 ˚C directly in a calorimeter. The absence of a denaturation peak upon repeated measurements confirmed irreversible denaturation.

Processing and analysis of denaturation curves were performed according to a standard procedure by means of special macroses using the Matlab 8.0 software. The calorimeter drift and a step change in the heat capacity associated with the denaturation completeness were subtracted from the measured data before calculating the denaturation parameters. The calorimetric specific heat capacity (ΔC_p) was calculated based on the area under the curve of the protein excess heat capacity vs temperature; the denaturation (melting) temperature

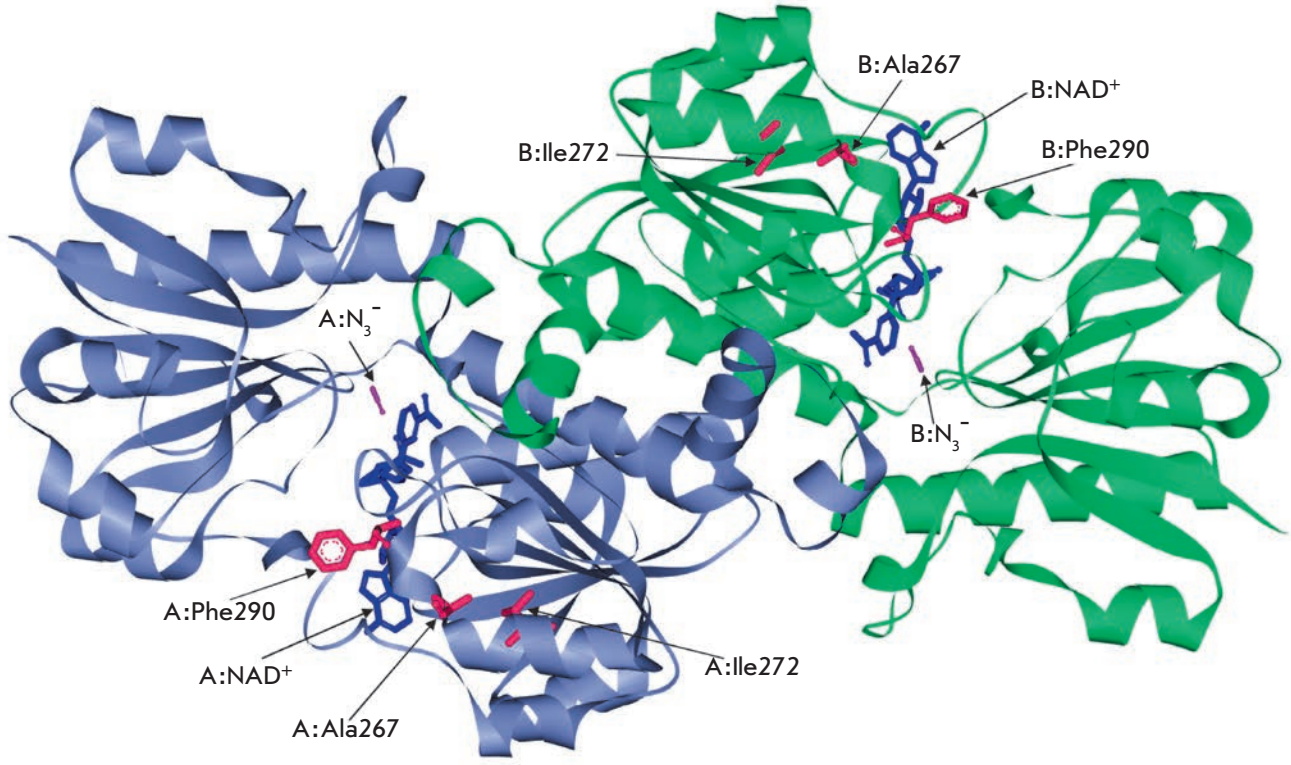

Fig. 1. 3D-structure of a ternary complex of SoyFDH with coenzyme NAD^+ and strong inhibitor N_3^-

T_m was determined as the temperature at the maximum on the same curve. The error of ΔC_p calculation was 5–8%. The experimental error of the T_m measurement did not exceed 0.2 °C.

Computer simulation

The SoyFDH structure was analyzed using the Accelrys Discovery Studio 2.1 software package. The same package was used to prepare images of the protein globule.

RESULTS AND DISCUSSION

As already noted, triple mutant SoyFDHs were produced by introduction of three amino acid residues (Asp, Asn, and Ser) into the 290th position of a double mutant with Ala267Met/Ile272Val substitutions. *Figure 1* presents the structure of the [SoyFDH-NAD^+-N_3^-] ternary complex indicating the positions of the Ala267, Ile272, and Phe290 residues selected for site-directed mutagenesis in the protein globule. As seen from the figure, all three residues are located in the coenzyme-binding domain; however, the first two residues are more distant from the NAD^+ molecule than the Phe290 residue. The substitutions at the 290th position had a much more noticeable effect on both the catalytic properties and the thermal stability compared to the replacements at positions 267 and 272 [4–6]. We assumed that a combination of the three amino acid substitutions would provide a more stable mutant SoyFDH. For convenience purposes, the Ala267Met, Ile272Val, Phe290Asn, Phe290Asp, and Phe290Ser substitutions are thereafter designated as M1, M2, M3, M4, and M5, respectively.

Production of mutant SoyFDHs

Substitutions of the nucleotides responsible for the desired mutations were performed by a polymerase chain reaction. Three plasmids for each of the three mutants were isolated. According to sequencing, the *soyfdh* gene in all plasmids contained the desired mutations only. Plasmids encoding the *soyfdh* gene with mutations leading to amino acid substitutions (A267M/I272V/F290N), (A267M/I272V/F290D), and (A267M/I272V/F290S) were used to transform the *E. coli* BL21(DE3)CodonPlus/pLysS strain. All three mutant SoyFDHs were demonstrated to be expressed in the active and soluble forms in recombinant strains. According to analytical polyacrylamide gel electrophoresis in the presence of sodium dodecyl sulfate, the purity of the isolated SoyFDH samples was not less than 95%.

The kinetic properties of the mutant enzymes

Table 1 shows the values of the catalytic constant and Michaelis constants for NAD^+ and formate for the three

Table 1. Kinetic parameters of wild-type and mutant SoyFDHs compared to those of formate dehydrogenases from other sources

Enzyme	k_{cat}, s^{-1}	$K_M^{formate}$, mM	$K_M^{NAD^+}$, μM	$k_{cat}/K_M^{NAD^+}$, $(\mu M*s)^{-1}$	$k_{cat}/K_M^{formate}$, $(mM*s)^{-1}$	Reference
wt-SoyFDH	2.9	1.5	13.3	0.22	1.93	[4-6]
SoyFDHM1 (A267M)	5.0	2.1	9.9	0.51	2.38	[4]
SoyFDH M1+M2 (A267M/I272V)	2.2	2.4	13.3	0.17	0.92	[5]
SoyFDH M3 (F290N)	2.8	4.5	14.0	0.40	1.02	[5]
SoyFDH M4 (F290D)	5.1	5.0	12.8	0.20	0.62	[5]
SoyFDH M5 (F290S)	4.1	4.1	9.1	0.45	1.00	[5]
SoyFDH M1+M2+M3 (A267M/I272V/F290N)	3.2±0.2	2.2±0.3	14.1±0.7	0.23	1.45	Present study
SoyFDH M1+M2+M4 (A267M/I272V/F290D)	2.9±0.2	2.8±0.4	20.3±1.3	0.14	1.04	Present study
SoyFDH M1+M2+M5 (A267M/I272V/F290S)	3.7±0.1	2.3±0.3	16.1±0.4	0.23	1.61	Present study
wt-AthFDH	3.8	2.8	50	0.08	1.36	[8]
wt-LjaFDH	1.2	6.1	25.9	0.05	0.20	[9]
wt-CboFDH	3.7	5.9	45	0.08	0.63	[10,11]
wt-MorFDH	7.3	7.5	80	0.09	0.97	[2]
wt-PseFDH	7.3	6.5	65	0.11	1.12	[2]
PseFDHGAV	7.3	6	35	0.21	1.22	[2,3]
PseFDHSM4	7.3	3.2	41	0.18	2.28	Own data

PseFDH, MorFDH, CboFDH, AraFDH, and LjaFDH are formate dehydrogenases from bacteria *Pseudomonas* sp.101 and *Moraxella* sp. C1, yeast *Candida boidinii*, and plants *Arabidopsis thaliana* and *Lotus japonicus*, respectively.

new multi-point mutant SoyFDHs, as well as similar values for mutant precursors and some other bacterial, yeast, and plant formate dehydrogenases. As seen from *Table 1*, the introduction of an additional substitution into the 290th position of a double mutant has no effect on the Michaelis constant for formate, whereas the K_M value for NAD^+ is either comparable to or higher than that of a double mutant precursor. These data are well correlated with the fact that all mutable residues are located in the coenzyme-binding domain. The catalytic constant of a double mutant is less than that of point mutants with substitution at the 290th position. Combination of the three amino acid replacements leads to the k_{cat} value of triple mutants being either comparable or higher than that of the double mutant but less than that of point mutants with the substitutions Phe290Asp and Phe290Asn. Also, the lack of correlation between the catalytic properties of double, triple, and point mutants should be noted. For example, mutant SoyFDH Phe290Asp has the highest k_{cat} value among point mutants with a substitution at the 290th position, while the triple mutant containing this substitution has the lowest catalytic constant among multi-point mutants.

In summary, it can be concluded that the kinetic parameters and catalytic properties of SoyFDHs with the substitutions Ala267Met/Ile272Val/Phe290Asn and Ala267Met/Ile272Val/Phe290Ser remained at the level of the wild-type enzyme and mutant formate dehydrogenases from *Pseudomonas* sp. 101, PseFDH GAV and PseFDH SM4 (*Table 1*); in mutant SoyFDH A267M/I272V/F290D, these parameters slightly deteriorated but still remained better than in CboFDH, which is widely used at present.

Analysis of the thermal stability of mutant SoyFDHs through thermal inactivation kinetics

The thermal inactivation kinetics of mutant SoyFDHs with the substitutions Ala267Met/Ile272Val/

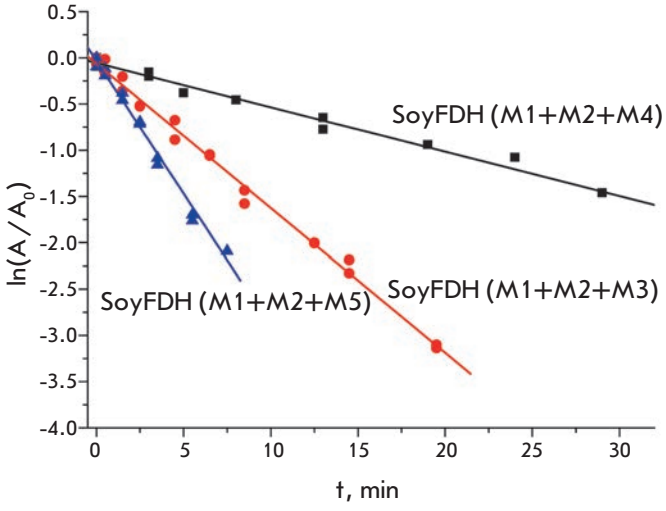

Fig. 2. Dependence of the natural logarithm of the residual activity on time for triple mutant SoyFDHs at 64 °C, 0.1 M sodium phosphate buffer, pH 7.0. M1 – Ala267Met, M2 – Ile272Val, M3 – Phe290Asn, M4 – Phe290Asp, M5 – Phe290Ser

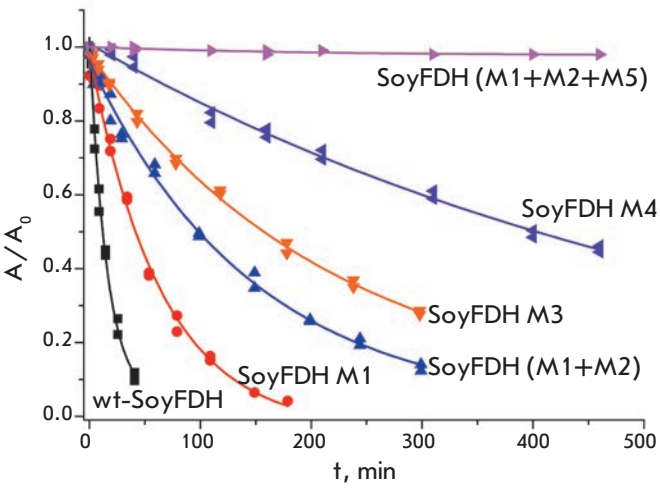

Fig.3. Dependence of the residual activity on time for wild-type (wt-SoyFDH) and several mutant SoyFDHs at 54 °C. 0.1 M sodium phosphate buffer, pH 7.0. M1 – Ala267Met, M2 – Ile272Val, M3 – Phe290Asn, M4 – Phe290Asp, M5 – Phe290Ser

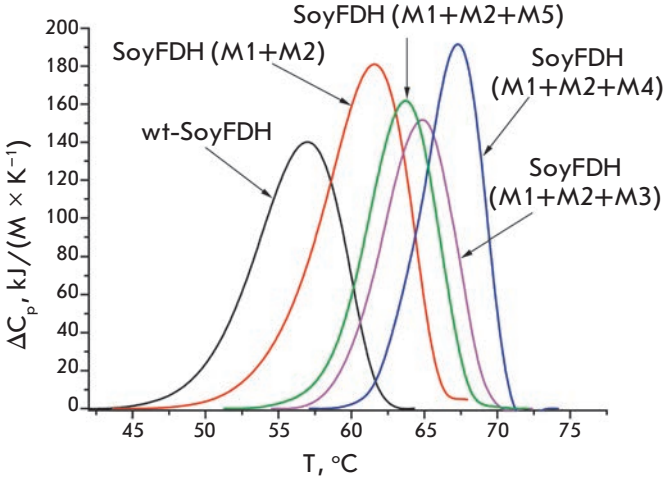

Fig.5. Differential scanning calorimetry melting curves for wild-type and multi-point mutant SoyFDHs. 0.1 M sodium phosphate buffer, pH 7.0. Enzyme concentration is 2 mg/mL, heating rate is 1 C/min. M1 – Ala267Met, M2 – Ile272Val, M3 – Phe290Asn, M4 – Phe290Asp, M5 – Phe290Ser

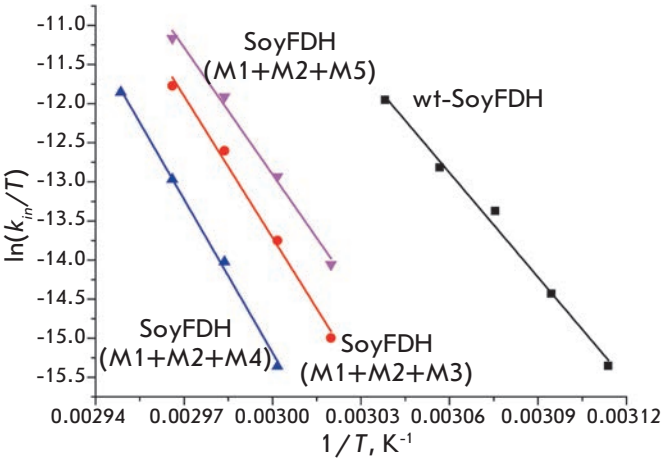

Fig. 4. Dependence of the inactivation rate constants on temperature in coordinates $\ln(k_{in}/T) - 1/T$ for wild-type and mutant SoyFDHs. 0.1 M sodium phosphate buffer, pH 7.0. M1 – Ala267Met, M2 – Ile272Val, M3 – Phe290Asn, M4 – Phe290Asp, M5 – Phe290Ser

Phe290Asn and Ala267Met/Ile272Val/Phe290Ser was studied in a temperature range of 58–64 °C, while SoyFDH Ala267Met/Ile272Val/Phe290Asp was analyzed in a range of 60–66 °C. Selection of the temperature range was based on the higher stability of the last mutant; therefore, higher temperatures had to be used for achieving the time intervals required for a decrease in activity similar to that observed in other mutants. The inactivation kinetics in the entire temperature range followed the first-order kinetics. The thermal inactivation rate constants were calculated from the slopes of these straight lines. The thermal inactivation rate constant value did not depend on the enzyme concentration in the entire temperature range, indicating the true monomolecular mechanism of the thermal inactivation process. *Figure 2* presents the dependence of the natural logarithm of the residual activity of the three new mutant enzymes on time at 64 °C. It is seen that mutant SoyFDH with the Ala267Met/Ile272Val/Phe290Asp substitutions has a higher stability than the other two

Table 2. Activation parameters $\Delta H^{\neq}$ and $\Delta S^{\neq}$ for thermal inactivation of wild-type and mutant SoyFDHs and wild-type formate dehydrogenases from various sources (0.1 M sodium phosphate buffer, pH7.0)

Enzyme	$\Delta H^{\neq}$, kJ/M	$\Delta S^{\neq}$, J/(M*K)	Reference
wt-SoyFDH	370 ± 20	830 ± 60	[4]
SoyFDHM1(A267M)	400	900	[4]
SoyFDH M1+M2 (A267M/I272V)	450±30	1,040±80	[4]
SoyFDHM5 (F290D)	520±30	1,240±70	[5]
SoyFDHM3 (F290N)	450±20	1,050±60	[5]
SoyFDHM5 (F290S)	440±20	1,020±70	[5]
SoyFDH M1+M2+M3 (A267M/I272V/F290N)	500±30	1,190±90	Present study
SoyFDH M1+M2+M4 (A267M/I272V/F290D)	540±20	1,310±50	Present study
SoyFDH M1+M2+M5 (A267M/I272V/F290S)	450±30	1,050±80	Present study
wt-AthFDH*	490	1,200	[2]
wt-PseFDH*	570	1,390	[2]
wt-CboFDH*	500	1360	[13]
wt-SceFDH*	420	n.d.**	[14]

* AthFDH, PseFDH, CboFDH, and SceFDH are formate dehydrogenases from plant *A. thaliana*, bacterium *Pseudomonas*sp.101,and yeast *C. boidinii* and *Saccharomices cerevisiae*, respectively.
**n.d. – no data

triple mutants. Unfortunately, the inactivation curves of the precursor mutants could not be obtained at this temperature, since they were almost completely inactivated in less than 5 min under these conditions. To illustrate the stabilization effect, *Fig. 3* shows the dependencies of the residual activity of several mutant SoyFDHs on time at 54 °C. It is seen that Ala267Met/Ile272Val/Phe290Asp SoyFDH is almost inactivated for about 8 h, while the half-inactivation period of the wild-type enzyme and mutant SoyFDHs with the Ala267Met, Ala267Met/Ile272Val, and Phe290Asp substitutions is 19, 56, 153, and 460 min, respectively. Thus, we can draw a conclusion about the large additive effect of the substitution introduced into the 290th position in Ala267Met/Ile272Val double mutant SoyFDH on an increased enzyme thermal stability.

Figure 4 shows the temperature dependence of the thermal inactivation rate constants for mutant SoyFDHs with triple substitutions and the wild-type enzyme in the coordinates $\ln(k_{in}/T)$ vs $1/T$, where T is the temperature in Kelvin. These coordinates are a linear anamorphosis for the equation of the temperature dependence of the rate constant for the transition state theory [12]:

$$\ln\left(\frac{k_{in}}{T}\right) = \ln\left(\frac{k_B}{h}\right) + \frac{\Delta S^{\neq}}{R} - \frac{\Delta H^{\neq}}{RT} = const - \frac{\Delta H^{\neq}}{R}\frac{1}{T},$$

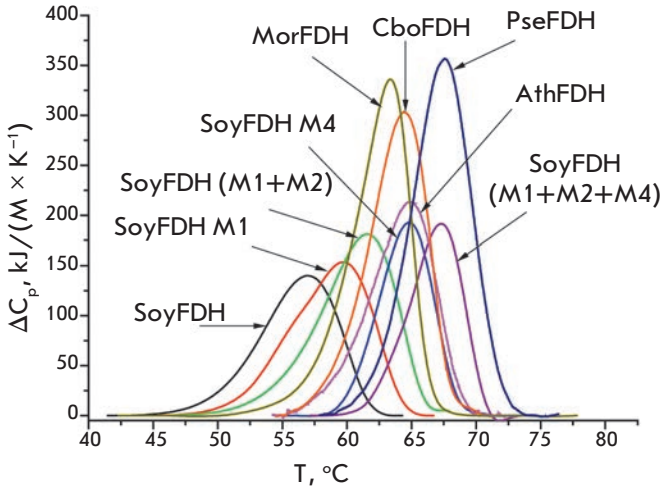

Fig. 6. Differential scanning calorimetry melting curves for multi-point mutant SoyFDHs and wild-type formate dehydrogenases from various sources. 0.1 M sodium phosphate buffer, pH 7.0. Enzyme concentration is 2 mg/mL; heating rate is 1 C/min. M1–Ala267Met, M2 – Ile272Val, M3–Phe290Asn, M4–Phe290Asp, M5 – Phe290Ser. PseFDH, MorFDH, CboFDH, SoyFDH, and AthFDH are recombinant wild-type formate dehydrogenases from bacteria *Pseudomonas* sp.101 and *Moraxella* sp.C1, yeast *C. boidinii*, soybean *G. max*, and plant *A. thaliana*, respectively

Table 3. Stabilization effect* for mutant SoyFDHs compared to the wild-type enzyme at various temperatures (0.1 M sodium phosphate buffer, pH7.0)

T, °C	Stabilization effect											
	1	2	3	4	5	6	7**	8	9**	10	11**	12
	wt-SoyFDH	SoyFDH M1 (A267M) [1]	SoyFDH M1+M2 (A267M/I272V) [1]	SoyFDH M3 (F290N) [2]	SoyFDH M4 (F290D) [2]	SoyFDH M5 (F290S) [2]	Stab.eff. (M1+M2)*Stab. eff. M3	SoyFDH M1+M2+M3	Stab.eff. (M1+M2)*Stab. eff. M4	SoyFDH M1+M2+M4	Stab.eff. (M1+M2)*Stab. eff. M5	SoyFDH M1+M2+M5
25	1	9	130	200	11,000	52	26,000	9,200	1,430,000	233,200	6,760	450
30	1	7	81	120	4,100	33	9,720	3,820	332,100	73,540	2,673	265
46	1	4.3	18	25	230	8.8	450	280	4,140	2,330	158	54
48	1	4	15	20	160	7.5	300	188	2,400	1,440	114	41
50	1	3.8	13	17	120	6.5	221	148	1,560	1,030	85	37
52	1	3.6	11	15	85	5.5	165	135	935	856	61	38
54	1	3.4	8.9	12	61	4.8	107	76	5,439	436	43	24
56	1	3.2	7.5	10	44	4.1	75	58	330	308	30.8	21
58	1	3	6.4	8.6	32	3.5	55	50	205	218	22	19
60	1	2.8	5.4	7.3	23	3.1	39	32	124	160	17	14
62	1	2.7	4.6	6.1	17	2.7	28	23	78	93	12	11
64	1	2.5	3.9	5.2	12	2.3	20	22	47	71	9	12
66	1							15		51		9

*Stabilization effect was calculated as the $(k_{in})^{wt}/(k_{in})^{mut}$ ratio at the same temperature. Values shown in bold were calculated using experimental constants. The other values of the stabilization effect were calculated using the transition state theory equation and appropriate activation parameters $\Delta H^{\neq}$ and $\Delta S^{\neq}$ from Table 2.
**Columns 7, 9 and 11 show the theoretical stabilization effect in the case of 100% additivity. These values were calculated as multiplication of the stabilization effect for double mutant Soy FDH (M1+M2) and the stabilization effect for a mutation at the 290th position.

where k_B and h are the Planck and Boltzmann constants, respectively; R is the universal gas constant; and $\Delta H^{\neq}$ and $\Delta S^{\neq}$ are activation parameters.

The linear form of the resulting dependences suggests that the dependence of the thermal inactivation rate constants of native SoyFDH and the mutant forms is actually described by the transition state theory equation.

Table 2 provides the values of the $\Delta H^{\neq}$ and $\Delta S^{\neq}$ activation parameters for the thermal inactivation process that are derived from the temperature dependences of the thermal inactivation rate constants using the equation from the transition state theory. It can be seen that the activation enthalpy $\Delta H^{\neq}$ and entropy $\Delta S^{\neq}$ values for the enzyme with an Ala267Met/Ile272Val/Phe290Asp triple substitution are the highest ones among all tested FDH mutants and are almost the same as those of one of the most thermostable FDH from *Pseudomonas* sp. 101 (PseFDH). It should be noted that the $\Delta H^{\neq}$ and $\Delta S^{\neq}$ values of the mutant with the Ala267Met/Ile272Val/Phe290Asp substitutions are higher than those of formate dehydrogenase from yeast *Candida boidinii* and plant *Arabidopsis thaliana*.

As seen from *Table 2*, the activation enthalpy of wild-type SoyFDH is lower than that of its mutants. This means that the thermal inactivation rate constant of all mutant SoyFDHs will decrease faster than that of wild-type SoyFDH as the temperature decreases: i.e. the stabilization effect should increase with decreasing temperature. The thermal inactivation rate constant and stabilization effect values were calculated in

Table 4. Data of differential scanning calorimetry for wild-type and mutant formate dehydrogenases from various sources (0.1 M sodium phosphate buffer, pH 7.0)

Enzyme	Melting temperature, T_m, °C	$T_m - T_m^{wt\text{-}SoyFDH}$, °C	Cooperativity value, $T_{1/2}$, °C	Reference
wt-PseFDH*	67.6	10.6	5.4	[17]
PseFDH GAV*	68.8	11.8	5.4	[17]
wt-MorFDH**	63.4	6.4	4.9	[17]
wt-AthFDH**	64.9	7.9	5.9	[17]
wt-CboFDH**	64.4	7.4	5.3	[17]
wt-SoyFDH**	57.0	0.0	7.1	[5]
SoyFDH M1 (A267M)	59.7	2.7	7.5	[4]
SoyFDHM1+M2 A267M/I272V	61.6	4.6	6.8	[4]
SoyFDHF290D	64.8	7.8	5.0	[5]
SoyFDHF290N	61.3	4.3	6.6	[5]
SoyFDH F290S	59.9	2.9	6.4	[5]
SoyFDH M1+M2+M3 (A267M/I272V/F290N)	64.9	7.9	5.8	Present study
SoyFDH M1+M2+M4 (A267M/I272V/F290D)	67.3	10.3	4.8	Present study
SoyFDHM1+M2+M5 (A267M/I272V/F290S)	63.7	6.7	5.6	Present study

* wt-PseFDH and PseFDH GAV are wild-type and mutant formate dehydrogenases from bacterium *Pseudomonas* sp.101,, respectively [2].
** wt-MorFDH, wt-CboFDH, and wt-AthFDH are wild-type recombinant formate dehydrogenases from bacterium *Moraxella* sp. C1, yeast *C.boidinii*, and plant *A. thaliana*, respectively.

a wide temperature range using the transition state-theory equation and $\Delta H^{\neq}$ and $\Delta S^{\neq}$ values obtained for wild-type SoyFDH and mutant enzymes. *Table 3* shows the stabilization effect values of mutant SoyFDHs compared to the wild-type enzyme. It is seen that the stabilization effect in the most stable mutant enzyme with the Ala267Met/Ile272Val/Phe290Asp substitutions ranges from 2,330 to 51 times at elevated temperatures (46–66 °C). It is much more than in the most successful point mutant Phe290Asp. Therefore, the Ala267Met/Ile272Val/Phe290Asp mutant is the most thermostable mutant among the mutant SoyFDHs described in this paper. Its thermal stability is higher than that of the formate dehydrogenases from *A. thaliana* and *C. boidinii*.

Since all the mutable residues are located in the coenzyme-binding domain, it was interesting to estimate the contribution of substitution at the 290th position to the overall stabilization effect of a triple mutant. The additivity concept is used to assess such a contribution. For this purpose, an experimental value of the stabilization effect is compared to a theoretically possible value. If the stabilization effects in the original mutants are independent of each other, the theoretical effect of the stabilization of a mutant that combines the analyzed substitutions will be equal to the product of the stabilization effects of the original mutants. Coincidence of the theoretical and experimental values means 100% additivity. If this value is less than 100%, then the additivity is not complete, and if it is more than 100%, then there is positive cooperativity or synergism of the stabilization effect. Columns 7, 9, and 11 of *Table 3* show values of the theoretical stabilization effect calculated as a multiplication of the stabilization effect value of the initial mutant SoyFDH with an Ala267Met/Ile272Val double substitution on the stabilization effect value of a mutant with an appropriate substitution at the 290th position. As seen from columns 6 and 7, in the case of mutant SoyFDH Ala267Met/Ile272Val/Phe290Asn, a 100% additivity is observed at 64 °C, while lowering the temperature leads to a slow decrease in this parameter. A similar pattern is observed for mutant SoyFDH Ala267Met/Ile272Val/Phe290Ser (*Table 3*; columns 11 and 12) at 62 °C and below; while at 64 °C, the stabilization additivity is greater

than 100%. A very interesting situation is observed for the most stable mutant SoyFDH Ala267Met/Ile272Val/Phe290Asp (*Table 3*; columns 9 and 10). The stabilization additivity exceeds 100% at all tested temperatures; however, this parameter is reduced with a decrease in temperature, like in the two previous cases. High additivity of the stabilization effect (up to 100%) upon combination of several amino acid substitutions was also observed for FDH from bacterium *Pseudomonas* sp. 101 a [15, 16], but the magnitudes of the stabilization effects are not comparable (1.1–2.5 times) with the effects observed in this work.

The cause for increasing theoretical stabilization effect (and, consequently, reducing effect of additivity) with lowering temperature is not yet clear, but it should be noted that the thermal inactivation rate constant of various SoyFDH mutants is differently dependent on the temperature, and a total change in the protein structure caused by the combination of amino acid substitutions may be different at different temperatures. Further experiments, which were beyond the goals and objectives of our work, will provide a more precise understanding of the causes of the observed effect.

Analysis of the thermal stability of mutant SoyFDHs by differential scanning calorimetry

The results of the study of multi-point mutant SoyFDHs by differential scanning calorimetry are presented in *Fig. 5*. For comparison, the melting curve of double-mutant SoyFDH Ala267Met/Ile272Val is also shown. *Figure 5* demonstrates that an increase in the heat transition temperature in triple mutants compared to a double mutant has the same tendency as for determining the thermal stability through thermal inactivation kinetics: the higher the stabilization effect of a substitution at the 290thposition is, the higher the phase transition temperature of a triple mutant is. As expected, mutant SoyFDH Ala267Met/Ile272Val/Phe290Asp proved to be the most stable one.

Figure 6 shows melting curves for the most stable mutant SoyFDHs and enzymes from other sources that provide an assessment of the magnitude of a thermal stability increase in the mutants. It is evident that SoyFDH Ala267Met/Ile272Val/Phe290Asp is more stable than FDH from *A. thaliana*, *C. boidinii*, and *Moraxella* sp. C1 and is very close to the enzyme from *Pseudomonas* sp. 101 (PseFDH), which is one of the most stable described formate dehydrogenases [2, 15].

Table 4 shows the values of the thermal transition parameters. It is seen that SoyFDH Ala267Met/Ile272Val/Phe290Asp has the highest phase transition temperature among all multi-point soybean FDH mutants, which agrees well with the data on the thermal inactivation kinetics. Comparison of this mutant form with formate dehydrogenases from other sources demonstrated that this enzyme ranks second after PseFDH for thermal stability.

Thus, we have produced three soybean mutant formate dehydrogenases that have a much higher thermal stability than the wild-type enzyme, as well as double- and point-mutant precursors. The distinctive feature is that the effect is achieved without a significant change in the catalytic parameters compared to the original SoyFDH. ●

This work was supported by the Russian Foundation for Basic Research (grants № 14-04-01625-a and 14-04-01665-a).

REFERENCES

1. Tishkov V.I., Popov V.O. // Biochemistry(Moscow). 2004. V. 69. N 11. P.1252–1267.
2. Tishkov V.I., Popov V.O. // Biomol. Eng. 2006. V. 23. № 1. P. 89–110.
3. Alekseeva A.A., Savin S.S., Tishkov V.I. // Acta Naturae. 2011. V. 3. № 4(11). P. 38–54.
4. Alekseeva A.A., Savin S.S., Kleimenov S.Yu., Uporov I.V., Pometun E.V., Tishkov V.I. // Biochemistry(Moscow) 2012. V. 77. № 10. P. 1199–1209.
5. Alekseeva A.A., Serenko A.A., Kargov I.S., Kleimenov S.Y., Savin S.S., Tishkov V.I. // Protein Eng. Des. Sel. 2012. V. 25. № 11. P. 781–788.
6. Kargov I.S., Kleimenov S.Y., Savin S.S., Tishkov V.I., Alekseeva A.A. // Protein Eng. Des. Sel. 2015. V. 28. № 6. P. 171–178.
7. Romanova E.G., Alekseeva A.A., Pometun E.V., Tishkov V.I. // Moscow Univ. Chem. Bull. 2010. V. 65. №. 3. P. 127–130.
8. Sadykhov, E.G., Serov, A.E., Yasnyi, I.E., Voinova, N.S, Alekseeva, A.A., Petrov, A.S., Tishkov, V.I. // Moscow Univ. Chem. Bull. 2006. V. 47. №. 1. P. 20-24.
9. Andreadeli A., Flemetakis E., Axarli I., Dimou M., Udvardi M. K., Katinakis P., Labrou N.E. // Biochim. Biophys. Acta. 2009. V. 1794. P. 976–984.
10. Slusarczyk H., Felber S., Kula M.R., Pohl M. // Eur. J. Biochem. 2000. V. 267. P. 1280–1289.
11. Felber S. Optimierung der NAD$^+$-abhängigen Formiatdehydrogenase aus Candida boidinii für den Einsatz in der Biokatalyse. Ph.D. Thesis. Heinrich-Heine University of Duesseldorf, 2001. URL: http://diss.ub.uni-duesseldorf.de/ebib/diss/file?dissid=78.
12. Cornish-Bowden A. Fundamentals of Enzyme Kinetics. 4th Ed. Wiley-Blackwell, 2012. 510 p.
13. Tishkov V.I., Uglanova S.V., Fedorchuk V.V., Savin S.S. // Acta Naturae. 2010. V. 2. №. 2(5). P. 82–87.
14. Serov A.E., Tishkov V.I. // Moscow Univ. Chem. Bull. 2006. V. 47. № 2. P. 1–5.
15. Rojkova A.M., Galkin A.G., Kulakova L.B., Serov A.E., Savitsky P.A., Fedorchuk V.V., Tishkov V.I. // FEBS Lett. 1999. V. 445. № 1. P. 183–188.
16. Serov A.E., Odintseva E.R., Uporov I.V., Tishkov V.I. // Biochemistry (Moscow). 2005. V. 70. №4. P. 804–808.
17. Sadykhov E.G., Serov A.E., Voynova N.S., Uglanova S.V., Petrov A.S., Alekseeva A.A., Kleimenov S.Yu., Popov V.O., Tishkov V.I. // Appl. Biochem. Microbiol. 2006. V. 42. № 3. P. 236–240.

Structural and Functional Characterization of Recombinant Isoforms of the Lentil Lipid Transfer Protein

I. V. Bogdanov, E. I. Finkina, S. V. Balandin, D. N. Melnikova, E. A. Stukacheva, T. V. Ovchinnikova*

Shemyakin and Ovchinnikov Institute of Bioorganic Chemistry, Russian Academy of Sciences, Miklukho-Maklaya str., 16/10, 117997 Moscow, Russia

*E-mail: ovch@ibch.ru

Received: 06.02.2015

ABSTRACT **The recombinant isoforms Lc-LTP1 and Lc-LTP3 of the lentil lipid transfer protein were overexpressed in *E. coli* cells. It was confirmed that both proteins are stabilized by four disulfide bonds and characterized by a high proportion of the α-helical structure. It was found that Lc-LTP1 and Lc-LTP3 possess antimicrobial activity and can bind fatty acids. Both isoforms have the ability to bind specific IgE from sera of patients with food allergies, which recognize similar epitopes of the major peach allergen Pru p 3. Both isoforms were shown to have immunological properties similar to those of other plant allergenic LTPs, but Lc-LTP3 displayed a less pronounced immunoreactivity.**

KEYWORDS **lipid transfer protein, isoform, lentil, allergen, cross-reactivity, heterologous expression, antimicrobial activity, lipid binding.**

ABBREVIATIONS **ASIT – allergen-specific immunotherapy; TNS – 2-(*p*-toluidino)-6-naphthalenesulfonic acid; BSA – bovine serum albumin; ELISA – enzyme-linked immunosorbent assay; GSH and GSSG – reduced and oxidized glutathione; LTP – lipid transfer protein; MES – 2-(N-morpholino)ethanesulfonic acid; PBS – phosphate-buffered saline; PBST – phosphate-buffered saline containing Tween-20; TBS – Tris-buffered saline; TBST – Tris-buffered saline containing Tween-20; TMB – 3,3',5,5'-tetramethylbenzidine.**

INTRODUCTION

Plant lipid transfer proteins (LTPs) are a class of small cationic proteins with spatial structures comprising three or four α-helices and stabilized by four disulfide bonds. Hydrophobic cavities in plant LTPs enable them to reversibly bind and transport various lipid molecules [1]. Many proteins of this class possess antimicrobial activity and inhibit the growth of pathogenic bacteria and fungi. LTP synthesis in plants is induced by various stress factors, including attacks by pathogenic microorganisms, draught, excessive soil salinity, etc. [2]. Plant LTPs are believed to be involved in the protection of plants against biotic and abiotic environmental stress factors, in cell wall synthesis, cuticular wax deposition, plant growth modulation, and many other processes [3].

The structure of plant LTPs is highly resistant to thermal denaturation and chemical degradation, as well as to enzymatic cleavage. It is believed that many LTPs, which are highly resistant to degradation by digestive enzymes, are potent allergens responsible for the development of allergic reactions to plant food products [4]. Many LTPs cause latex and pollen allergies. The major peach allergen Pru p 3 is the dominant LTP allergen with a high allergenic capacity. It is involved in the development of allergic cross-reactions to plant foods and pollen [5].

Natural and recombinant allergens, including those belonging to the LTP class, are currently widely used in the development of modern test systems for component-resolved diagnostics. Studies aimed at creating vaccines for preventive allergen-specific immunotherapy (ASIT) on the basis of natural and recombinant allergens are underway [6]. Different isoforms of allergens typically have different immunoreactivities. Therefore, it seems prudent to search for and study isoforms with reduced immunoreactivity, which can be used to develop hypoallergenic variants of major allergens with high clinical effectiveness and low risk of adverse reactions during ASIT [7].

Earlier, we discovered a subfamily of eight lipid transfer proteins (Lc-LTP1-8) in lentil *Lens culinaris* seeds. One of these proteins, namely, Lc-LTP2, was isolated and characterized as a protein possessing antimicrobial activity [8]. It has been demonstrated that

Lc-LTP2, like several other plant LTPs, is a food allergen. We have registered it in the IUIS database as Len c 3 [9]. This work focuses on the recombinant production and comparative study of the structural-functional and immunological properties of the two isoforms of lentil LTP: Lc-LTP1 and Lc-LTP3.

EXPERIMENTAL

Heterologous expression of LTPs in *Escherichia coli* cells

cDNA of lentil *L. culinaris* or peach *Prunus persica* and the following pairs of gene-specific primers were used for PCR amplification of nucleotide sequences encoding the proteins studied:

Lc-LTP1

5'-GCGAGATCTATTGATGGAAGAATGGCAATCT-CATGCGGAACA-3' (forward)

5'-GCGAATTCGCGGATCCTTAGAACCTGATG-GTG-3' (reverse);

Lc-LTP3

5'-GCGAGATCTGATCCGATGGCAGTCTCATGTG-GAACT-3' (forward)

5'-GCGAATTCGCGGATCCCTTCAAAACT-TAATG-3' (reverse);

Pru p 3

5'-GCGGGATCCATGATAACATGTGGCCAAG-3' (forward)

5'-GCGGAATTCTCACTTCACGGTGGCGCAGTT-3' (reverse).

The expression cassettes carrying a T7 promoter, the ribosomal binding site, a start codon (ATG), sequences encoding histidine octamer and modified thioredoxin A (M37L), cleavage sites (Ile-Asp-Gly-Arg-Met, Asp-Pro-Met or Met) and mature proteins Lc-LTP1 (GenBank AY793553), Lc-LTP3 (GenBank AY793555) and Pru p 3 (GenBank AY792996) were collected after several successive PCR stages and ligated with the BglII/XhoI fragment of a low-copy-number pET-31b(-) plasmid vector (Novagen) 5.25 kbp in size. Expression plasmids pET-His8-TrxL-Lc-LTP1, pET-His8-TrxL-Lc-LTP3, and pET-His8-TrxL-Pru p 3 (lengths of 6047, 6043, and 6021 bp, respectively) were obtained (*Fig. 1*). These plasmid vectors were used to transform *E. coli* strain BL-21 (DE3) cells carrying the T7 RNA polymerase gene.

The cells of producing strains were grown in a LB medium containing 50 μg/mL of ampicillin and 20 mM of glucose up to A_{600}~0.7. Synthesis of LTP was induced by adding isopropylthio-β-*D*-galactopyranoside to the medium to a final concentration of 0.2 mM. The cells were then grown in 2L flasks with 0.5 L of the nutrient medium for 4–5 h at 25°C (Lc-LTP3 and Pru p 3) or 37°C (Lc-LTP1), using a thermostatic orbital shaker at a stirring rate of 220 rpm.

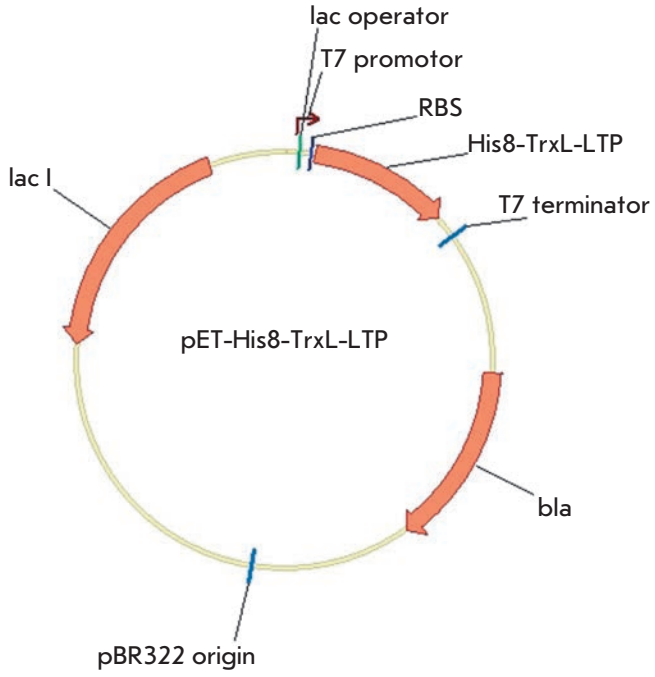

Fig. 1. Genetic map of the expression plasmid pET-His8-TrxL-LTP. The plasmid carries a bacteriophage T7 promoter with a *lac* operator, a ribosomal binding site (RBS), the fusion protein coding the sequence His8-TrxL-LTP, where LTP is Lc-LTP1, Lc-LTP3 or Pru p 3, and a T7 terminator; *bla* is the β-lactamase gene; and *lacI* is the lac repressor gene

Isolation and purification of recombinant LTPs

Cell pellets obtained by centrifugation were resuspended in buffer A (50 mM Tris-HCl, 0.5 M NaCl, 20 mM imidazole, pH 7.8) containing 1 mM phenylmethylsulfonyl fluoride at a ratio of 1:5 (v/v). The cells were destroyed on ice in an ultrasonic homogenizer using eight cycles of 45 s. The clarified cell lysate obtained by centrifugation was used for Lc-LTP3 and Pru p 3 purification. Metal chelate chromatography was performed on a Ni^{2+}sepharose column at a flow rate of 0.7 mL/min. The fusion proteins were eluted with buffer A containing 0.5 M imidazole. Lc-LTP1 was isolated from inclusion bodies, which were washed twice with buffer A containing 1% Triton-X100 and then solubilized in buffer A containing 6 M guanidine hydrochloride. Metal chelate chromatography was performed in the same buffer system containing 6 M guanidine hydrochloride. All eluates were dialyzed against 3 L of acidified water (pH 3.0) at 4°C overnight. The resulting dialysates were freeze-dried. The fusion proteins were cleaved with cyanogen bromide. For this, the fusion proteins were first dissolved in 80% TFA in a concentration of 10–20 mg/mL. A 100-fold molar excess of cyanogen

bromide was then added, and the mixture was incubated in the dark at room temperature for 16–20 h. The reaction was stopped by adding a threefold volume of water. The samples were then evaporated in a vacuum concentrator. The target proteins were purified by repeated metal chelate chromatography on the same column in the same buffer system containing 6 M guanidine hydrochloride. The final purification of the recombinant proteins was performed on a Reprosil-Pur C18-AQ column (Dr. Maisch GmbH) in the presence of 0.1% TFA at a flow rate of 2 mL/min in a gradient of acetonitrile concentration from 5 to 80% over 60 min. Refolding of the purified Lc-LTP1 was performed in a buffer (50 mM Tris-HCl, pH 8.0, 20 mM NaCl, 0.8 mM KCl, 1 mM EDTA) containing 1 M urea, 0.8 M L-arginine, and 2 mM GSH/0.2 mM GSSG [10]. For the refolding, the recombinant protein was dissolved in this buffer to a concentration of 0.1 mg/mL, incubated at 4°C overnight and purified by RP-HPLC on a Luna C18 column (Phenomenex) in the presence of 0.1% TFA using a gradient of acetonitrile concentration from 5 to 80% over 60 min. The fractions obtained at different isolation stages were analyzed by SDS-PAGE (15% gel) in the Tris-glycine system according to Laemmli [11].

Mass spectrometry, Edman microsequencing and CD spectroscopy

The molecular weights of the recombinant LTPs were determined using a Reflect III MALDI-TOF mass spectrometer (Bruker) equipped with a UV laser (336 nm). The amino acid sequence was determined using the Procise cLC 491 protein sequencing system (Applied Biosystems). Circular dichroism spectra were recorded at room temperature using a J-810 spectropolarimeter (Jasco) in a cell with an optical path of 0.01 cm in a wavelength range of 180–250 nm (scan rate 1 nm) using aqueous solutions of the recombinant proteins at a concentration of 1 mg/mL.

Sera and antibodies

Sera from allergic patients (n = 20) were collected at the Center of Molecular Diagnostics at the Central Research Institute of Epidemiology. Out of them, we selected the sera from nine patients allergic to plant products, which contained IgE specific to recombinant Pru p 3. Sera samples from nonallergic individuals were used as a negative control. Total IgE levels in the sera of allergic patients were determined using a Total IgE HRP EIA kit (Dr. Fooke) according to the manufacturer's instructions.

Polyclonal anti-Lc-LTP2-antibodies were prepared by immunization of rabbits. At the first stage of preparing a hyperimmune serum, the rabbits were subcutaneously administered recombinant Lc-LTP2 (150 μg/rabbit) with complete Freund's adjuvant, then a half dose of the antigen with incomplete Freund's adjuvant, and finally the recombinant protein in PBS. Polyclonal anti-Lc-LTP2-antibodies were purified by fractional precipitation of proteins with ammonium sulfate. Sera samples obtained from the same rabbits prior to immunization were used as a negative control.

Immunoblotting

A lentil seed extract was prepared as described in [8]. Following SDS-PAGE (15% gel), the proteins were electrotransferred to a nitrocellulose membrane in a buffer containing 20% of methanol and 0.1% of SDS. At the first stage, the membrane was incubated in a 1% solution of nonfat dry milk in TBS. The membrane was washed with TBST and incubated in a solution of polyclonal rabbit anti-Lc-LTP2-antibodies in a 1% milk solution in TBS (dilution 1:200) for 2 h at room temperature. After washing, the membrane was incubated in a solution of goat anti-rabbit IgG-horseradish peroxidase conjugated antibodies (Sigma) in a 1% milk solution in TBS for 1 h at room temperature. The membrane washed with TBST was then treated with a TMB solution for membranes (Sigma). The enzymatic reaction was terminated by washing the membrane with water to remove residual substrate.

Enzyme-linked immunosorbent assay (ELISA)

The recombinant LTPs (0.5 μg) were added to the wells of a 96-well plate (Costar) in 50 μL of TBS and incubated for 1 h at 37°C. After washing with the same TBST buffer solution, the plate was incubated at 37°C for 2 h with a 1% solution of BSA in TBS. The plate was then incubated at 37°C for 2 h with sera from allergic patients prepared by serial dilutions (1:2–1:16) in TBS. After washing with TBST, a solution of goat anti-human IgE-horseradish peroxidase conjugated antibodies (Sigma) was added to the wells and the plate was incubated at 37°C for 1 h. Bound antibodies were detected after washing the wells with TBST using TMB for ELISA (Sigma). The enzymatic reaction was stopped by adding 4N H_2SO_4. The resulting data were analyzed by measuring the absorbance in the wells at 450 nm.

For ELISA with polyclonal rabbit anti-Lc-LTP2 antibodies, free binding sites were blocked under the same conditions and the plate was incubated with a solution of polyclonal rabbit anti-Lc-LTP2 antibodies in TBS (1:500—1:64,000 dilutions) at 37°C for 1 h. After washing with TBST, a solution of goat anti-rabbit IgG-horseradish peroxidase conjugated antibodies in TBS was added to the wells and the plate was incubated at 37°C for 1 h. Detection was also performed using TMB.

In ELISA inhibition assays, smaller amounts of the recombinant proteins (0.2 μg) were used for coating and

the patients' sera were pre-incubated with serial dilutions of the recombinant Pru p 3 at a concentration of 0.02–200 μg/mL at 37°C for 3 h.

Antimicrobial activity

The bacteria *Agrobacterium tumefaciens* A281, *Clavibacter michiganensis* Ac-1144, and *Pseudomonas syringae* B-1546 were inoculated into a liquid LB medium and incubated at 30°C under constant stirring until A_{600} = 1.0–1.5. The test fungi *Aspergillus niger* F-2259, *Fusarium solani* F-142, *Alternaria alternata* F-3047, *Botrytis cinerea* F-3700, and *Neurospora crassa* F-184 were grown on potato sucrose agar at room temperature until active sporulation. Aliquots (110 μL) of the bacterial cultures (4×10^4 CFU/mL) or spore suspension (10^4 spores/mL) in the culture medium and 10 μL of sterile protein solutions of different concentrations in 0.1% TFA were added to the wells of a 96-well plate. Each version of the test was performed in triplicate. The plate was incubated in a thermostatic shaker at 30°C. Culture growth was assessed by measuring the absorbance in the wells at 620 nm. 0.1% TFA was used as a negative control. The protein concentrations ensuring 50% inhibition of culture growth (IC_{50}) were determined after 24 or 48 h bacterial or fungal culture incubation, respectively. Spore germination and hyphal morphology were evaluated using a CKX41 light inverted microscope (Olympus) after 12 and 24 h spore incubation in a liquid culture medium with the protein solutions.

Fatty acid binding

Fluorescence spectra were recorded using an F-4000 spectrofluorimeter (Hitachi) at 25°C. The spectral width of the slit of the monochromator excitation and emission was 5 nm. TNS fluorescence was excited at 320 nm and recorded in the 330–450 nm range. The maximum fluorescence intensity was detected at 437 nm. A TNS solution in a concentration of 3 μM in a buffer solution (175 mM *D*-mannitol, 0.5 mM K_2SO_4, 0.5 mM $CaCl_2$, 5 mM MES, pH 7.0) with or without stearic acid (to a concentration of 65 μM) was incubated in a cuvette for 1 min under constant stirring. Fluorescence spectra were subsequently recorded. Recombinant LTPs were then added to a concentration of 2.5 μM, incubated for 2 min, and fluorescence spectra were recorded [12]. The results are expressed as a percentage of the fluorescence intensity of the protein-TNS complex according to the formula $((F - F_0)/F_C) \times 100\%$, where F_0 is the fluorescence intensity of TNS in the solution; F and F_C are the fluorescence intensities of the protein-TNS complex either with or without the lipid added, respectively.

RESULTS AND DISCUSSION

Lipid transfer proteins in plant genomes are represented by gene families encoding different LTP isoforms. Multiple isoforms of the lipid transfer protein have been detected in a single plant, thus giving grounds for more in-depth research of the biological role of each of them. It was suggested that the expression of certain LTP isoforms is primarily regulated by the environment and that the synthesis of multiple LTP isoforms is an element of the plant defense system against a variety of abiotic and biotic stresses [13]. This assumption was confirmed in studies of the differential gene expression of LTP isoforms in various organs and tissues of plants under abiotic and biotic stress conditions using sesame [14], arabidopsis [15], pepper [16], the castor oil plant [17], grapes [18], and tomato [19]. It was shown that biosynthesis of certain LTP isoforms in plants is tissue-specific and that the genes of certain isoforms are expressed at different stages of plant ontogeny.

Recently we found eight LTPs in germinated lentil seeds, named Lc-LTP1–8 [8]. It was shown that biosynthesis of the isolated isoforms of the lentil lipid transfer protein Lc-LTP2,4,7,8 occurs during early development of seedlings and may take place due to the involvement of these proteins in plants protection against pathogens or in lipid transport during the active metabolism phase during germination. The biological role of the isoforms Lc-LTP1,3,5,6 remains unclear.

The structural and functional properties of one of the lentil LTPs, namely, Lc-LTP2, were studied in detail. The spatial structure of this protein is typical of

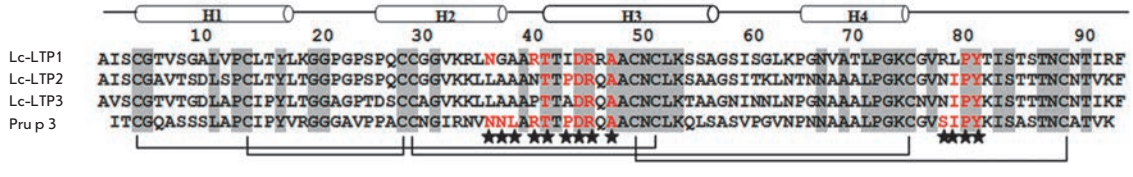

Fig. 2. Comparison of the amino acid sequences of lentil LTP isoforms and the major peach allergen Pru p 3. Conservative amino acid residues are shown in gray. The disulfide bonds are shown as brackets. α-Helical regions of Lc-LTP2 are shown above [20]. The amino acid residues included in the conformational epitopes of Pru p 3 are shown in red with stars [21]

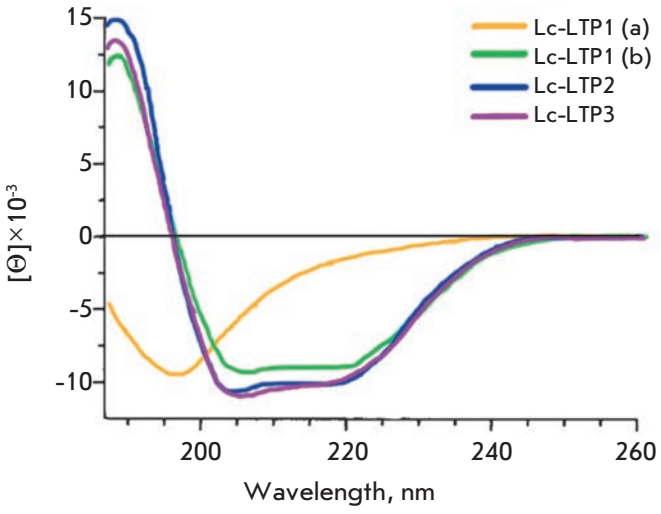

Fig. 3. CD spectra of lentil LTPs. (a), (b) – CD spectra of the recombinant Lc-LTP1 before and after refolding, respectively

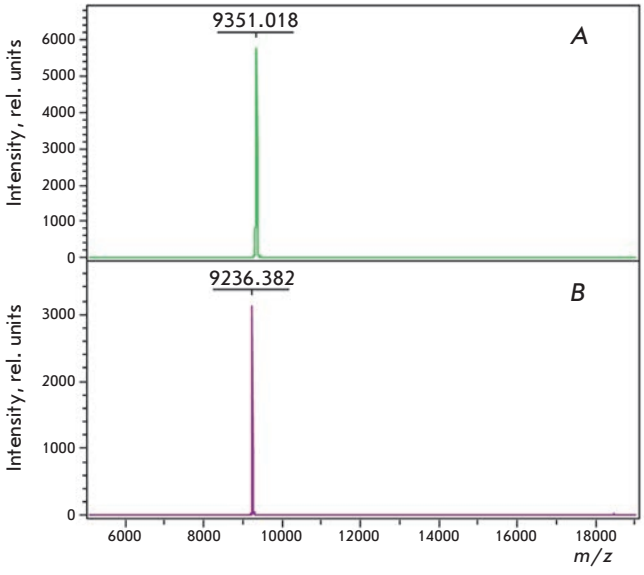

Fig. 4. MALDI-TOF mass spectra of the recombinant Lc-LTP1 (a) and Lc-LTP3 (b)

that of a representative of the LTP class comprising four α-helixes [20]. Hydrophobic amino acid residues in the protein are pointed inwards and form a hydrophobic cavity capable of hosting lipid ligands. Lc-LTP2 binds lipids, exhibits antimicrobial activity, and is a major lentil allergen registered as Len c 3 [9].

This work focuses on the isolation and comparative study of the structural-functional and immunological properties of two other lentil LTP isoforms. The isoforms Lc-LTP1 and Lc-LTP3 chosen for a comparative study differ most significantly from Lc-LTP2 in terms of their amino acid sequence (72 and 77% homology, respectively) (*Fig. 2*). These proteins consist of 93 amino acid residues, including eight conservatively located cysteine residues. Their isoelectric points lie in the alkaline pH range (9.53 and 8.32 for Lc-LTP1 and Lc-LTP3, respectively). These proteins contain amino acid residues comprising conformational epitopes of the dominant LTP class allergen, peach Pru p 3, which suggests that the two lentil LTP isoforms possess allergenic properties.

Isolation and characterization of recombinant lentil LTP isoforms

The recombinants Lc-LTP1 and Lc-LTP3 were prepared in a manner similar to that described for Lc-LTP2 [9]. Isolation and purification of the recombinant proteins were performed using soluble (Lc-LTP3) and insoluble (Lc-LTP1) cellular fractions and involved several steps. During the expression, the fusion protein His8-TrxL-Lc-LTP3 was predominantly accumulated in its soluble form in the cytoplasm. His8-TrxL-Lc-LTP1, which has an isoelectric point lying at a higher pH, was accumulated in both soluble and insoluble forms. However, the solution primarily contained the His8-TrxL-Lc-LTP1 forms with a truncated C-terminal region, which may have been formed by proteolytic cleavage of Lc-LTP1. Therefore, expression of the fusion protein was carried out at a higher temperature and it was isolated from the insoluble cell fraction. The fusion proteins were purified by metal chelate chromatography in either nondenaturing or denaturing conditions using step gradient elution with imidazole. The fusion proteins were cleaved with cyanogen bromide in an acidic medium, and the reaction products were separated by repeated metal chelate chromatography. The final purification of the recombinant proteins was performed by RP-HPLC.

The secondary structure of the recombinant proteins was studied by CD spectroscopy. The CD spectrum of Lc-LTP3 was similar to that of Lc-LTP2 and featured a curve typical of proteins with a high content of α-helical structures. The CD spectrum of recombinant Lc-LTP1 had a different shape and suggested that the protein is not structured (*Fig. 3*). Therefore, purified Lc-LTP1 was refolded at low temperature under mild denaturing conditions in the presence of 1 M urea, L-arginine, which prevents protein aggregation, and a pair of oxidized and reduced glutathiones. The reaction products were separated by RP-HPLC. An analysis of the Lc-LTP1 CD spectrum after refolding showed that the protein assumed the conformation typical of plant LTPs.

The recombinant protein samples were analyzed by SDS-PAGE. It was shown that in the absence of β-mer-

Table 1. Antimicrobial activity of the recombinant lentil LTPs

Microorganism	IC_{50}, μM		
	Lc-LTP1	Lc-LTP2	Lc-LTP3
Bacteria			
Agrobacterium tumefaciens	40	20–40	40
Clavibacter michiganensis	40	> 40	> 40
Pseudomonas syringae	> 40	> 40	> 40
Fungi			
Alternaria alternata	40	> 40	40
Aspergillus niger	5–10	10	10
Botrytis cinerea	20–40	10–20	> 40
Fusarium solani	20–40	> 40	40
Neurospora crassa	40	20–40	20–40

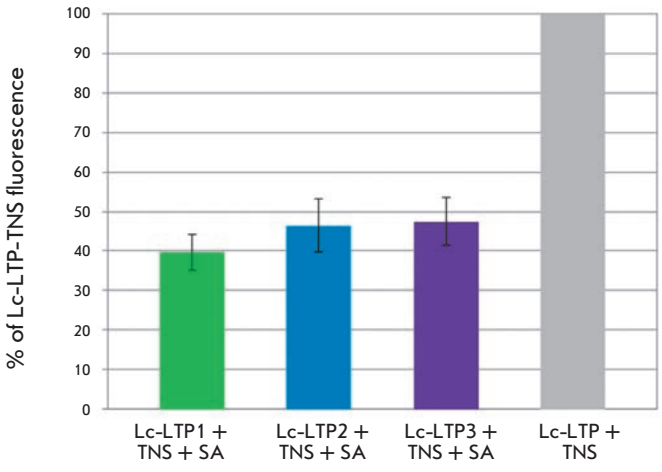

Fig. 5. Effect of stearic acid (SA) on the fluorescence level of the LTP-TNS complexes

captoethanol, Lc-LTP1 and Lc-LTP3 exist both in dimeric and monomeric forms, which is typical of LTPs [9]. Addition of a reducing agent leads to cleavage of disulfide bonds and dimer dissolution. Homogeneity and the identity of the recombinant LTPs and natural proteins were confirmed by MALDI-TOF mass spectrometry and automated Edman microsequencing. A mass spectrometric analysis showed that the molecular weights of the recombinant Lc-LTP1 (m/z of 9351.02) and Lc-LTP3 (m/z of 9236.38) correspond to the calculated weights of LTPs whose structures are stabilized by four disulfide bonds (9350.93 and 9235.65 Da, respectively) (*Fig. 4*). The measured m/z values correspond to the masses of protonated molecular ions $[M+H]^+$. The yields of the recombinant proteins were no lower than 3 and 5 mg/L of the culture, based on pure Lc-LTP1 and Lc-LTP3, respectively. Recombinant Pru p 3 was prepared in the same manner as Lc-LTP3, and its yield was 4 mg/L of the culture.

Functional activity of the recombinant lentil LTP isoforms

It is well known that many members of LTPs possess antimicrobial activity and the cytoplasmic membrane is the intended target of their antimicrobial action [22]. It is believed that cationic plant LTPs interact with the anionic components of the cytoplasmic membrane, which leads to its destabilization and disruption of permeability [20].

The comparative study of the antimicrobial activity of the three lentil LTP isoforms was conducted using the Gram-negative bacteria *A. tumefaciens* and *P. syringae* and Gram-positive bacterium *C. michiganensis*, as well as the fungi *A. alternata*, *A. niger*, *B. cinerea*, *F. solani*, and *N. crassa*. It was demonstrated that the recombinant Lc-LTP1 and Lc-LTP3, as well as Lc-LTP2, also exhibit antifungal and mild antibacterial activity and their antimicrobial action is nonspecific (*Table 1*). *A. niger* culture, the black rot plant pathogen, was the one most susceptible to all three proteins. It was shown that recombinant Lc-LTP1 and Lc-LTP3, as well as Lc-LTP2, inhibit spore germination of phytopathogenic fungi, mycelium growth and development, but do not affect the hyphal morphology. No significant difference in the strength of antimicrobial activity was observed for the three lentil LTP isoforms, despite the marked differences in the primary structures and acid-base properties of these proteins. Based on this, it was suggested that it is not solely the nonspecific electrostatic interaction between LTP and the membrane that is responsible for the antimicrobial effect.

In addition to antimicrobial activity, virtually all known plant LTPs have the ability to bind and transport a variety of lipids. The LTP structure has a hydrophobic cavity capable of binding hydrophobic molecules. Plant LTPs bind a wide range of ligands, including fatty acids with a C10–C18 chain length, acyl derivatives of coenzyme A, phospho- and galactolipids, prostaglandin B2, molecules of organic solvents, and certain drugs [23]. The effectiveness of the binding of various lipid ligands depends on the size of the hydrophobic cavity in the protein. It is believed that LTPs participate in many processes in plants via their ability to bind and carry various lipids.

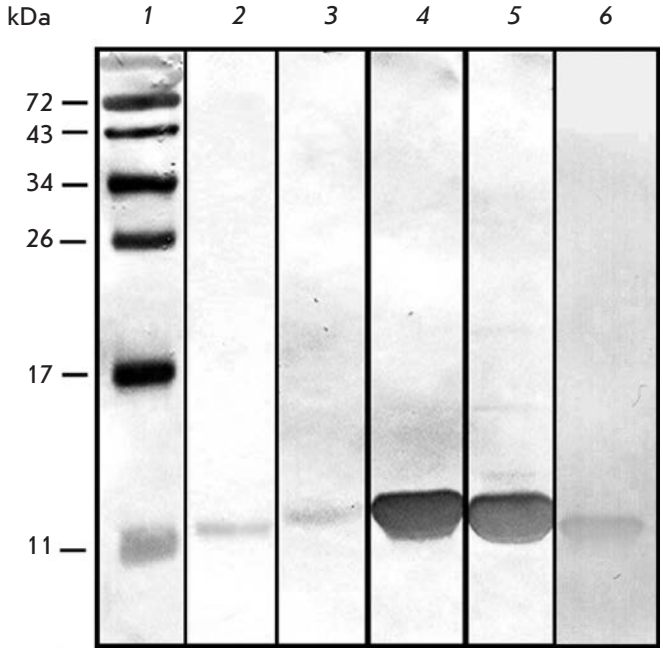

Fig. 6. Immunoblotting with rabbit polyclonal anti-Lc-LTP2 antibodies: 1 – molecular mass standards; 2 – the lentil seed extract; 3–5 – the recombinant Lc-LTP1,2,3, respectively; 6 – the recombinant Pru p 3

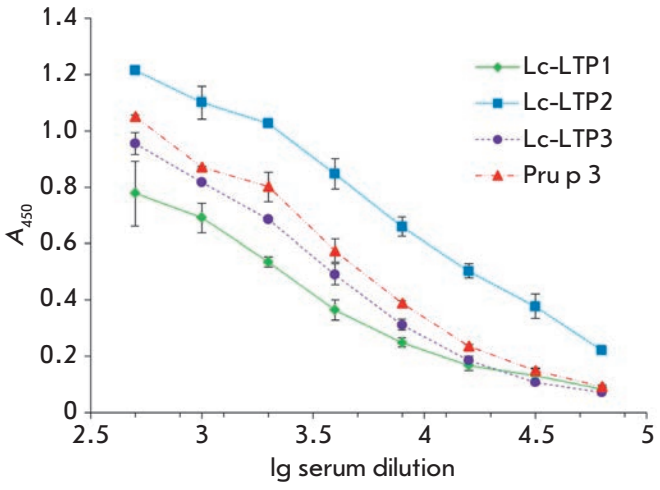

Fig. 7. ELISA with rabbit polyclonal anti-Lc-LTP2 antibodies

NMR spectroscopy has previously been used to show that the recombinant Lc-LTP2 has a hydrophobic cavity allowing it to interact with dimyristoylphosphatidylglycerol [20]. In this work, we studied the interaction of the three recombinant lentil LTPs with stearic acid using a fluorescent TNS probe, whose fluorescence increases in a hydrophobic environment. It was shown that addition of misfolded Lc-LTP1 (without prior refolding) to a TNS solution does not affect the intensity of its fluorescence. The fluorescence intensity of TNS, however, significantly increases after the addition of recombinant Lc-LTP2 and Lc-LTP3, as well as Lc-LTP1 after the refolding. This implies that protein-TNS complexes are formed, and a hydrophobic cavity capable of binding hydrophobic molecules is present in the structures of all three LTPs. The addition of each of the three recombinant lentil LTPs to a TNS–stearic acid mixture resulted in a less significant increase in the fluorescence intensity and was indicative of the competition between fatty acid molecules and TNS for binding sites in the proteins (*Fig. 5*). Thus, it was demonstrated that all three isoforms possess the ability to bind fatty acids. No significant difference in the effectiveness of fatty acid binding by the three proteins was observed, which can be attributed to the similar sizes of the hydrophobic cavities in the structures of the three lentil LTPs.

Immunological properties of the recombinant lentil LTP isoforms

LTPs from various plants have been characterized as allergens. Quite often, allergic reactions are caused by cross-reactivity between the major LTP allergen, peach Pru p 3, and homologous allergenic proteins from different plant foods and pollens. We have previously shown that lentil Lc-LTP2, registered in the IUIS database as Len c 3, is a food allergen. This allergen binds to specific IgE in sera of patients with food allergies, which recognize epitopes similar to those of the major peach allergen Pru p 3 so that it may cause allergic cross-reactions [9]. In this work, we have conducted a comparative study of the immunological properties and cross-reactivity of the two other lentil LTP isoforms. Polyclonal rabbit anti-Lc-LTP2 antibodies and sera of patients with food allergies containing specific IgE to the recombinant Pru p 3 were used in the study.

The interaction of rabbit polyclonal anti-Lc-LTP2 IgG with three lentil LTP isoforms and peach Pru p 3 was investigated by immunoblotting (*Fig. 6*) and ELISA (*Fig. 7*). The results of immunoblotting with pre-reduced recombinant LTPs demonstrated that polyclonal rabbit anti-Lc-LTP2 antibodies bind to all three lentil LTP isoforms and peach Pru p 3. As one would expect, the highest level of binding of anti-Lc-LTP2 antibodies was observed in the case of Lc-LTP2. The lowest one was observed in the case of Lc-LTP1, although, peach

Table 2. Characterization of sera from patients with food allergies

No.	Sex (M/F)	Total IgE, IU/mL	Specific IgE* (ELISA), A_{450}				Allergenic products
			Lc-LTP1	Lc-LTP2	Lc-LTP3	Pru p 3	
1	M	794	1.4 ± 0.09	1.26 ± 0.19	1.28 ± 0.1	1.35 ± 0.14	Nuts
2	F	556	0.7 ± 0.12	0.77 ± 0.11	0.84 ± 0.07	0.85 ± 0.05	Nuts
3	M	525	1.08± 0.04	1.08 ± 0.11	1.07 ± 0.02	1.09 ± 0.03	Nuts
4	F	479	0.53± 0.05	0.57 ± 0.03	0.37 ±.03	0.82 ± 0.05	Sesame, soy beans
5	M	417	0.28± 0.01	0.4 ± 0.02	0.32 ± 0.06	0.27 ± 0.01	Nuts, fruits
6	F	407	0.77± 0.07	0.93 ± 0.02	0.29 ± 0.08	1.01 ± 0.07	Nuts, tomatoes
7	F	302	0.33± 0.03	0.37 ±0.05	0.31 ± 0.1	0.33 ± 0.02	Nuts
8	M	71	0.6 ± 0.02	0.62 ± 0.02	0.4 ± 0.01	0.81 ± 0.02	Pea
9	F	25	0.46± 0.05	0.53 ± 0.14	0.45 ± 0.04	0.64 ± 0.02	Nuts

*Note. Data were obtained using 1:2 serum dilutions.

Pru p 3 is the least structurally similar to Lc-LTP2 (55% homology). The ELISA results were fundamentally the same as the results of immunoblotting, even though we used native proteins in this test. The maximum efficiency of binding to anti-Lc-LTP2 antibodies was observed for Lc-LTP2; while the lowest, for Lc-LTP1. The results of immunoblotting and ELISA reveal a similar structural organization of all LTPs and at least a partial similarity of their linear and conformational antigenic determinants.

The ability of recombinant proteins to bind to specific IgE in sera of patients allergic to fruits, nuts, and beans was demonstrated by ELISA (*Table 2*). All three lentil LTP isoforms bind to specific IgE, but the analysis of the majority of sera from the patients showed that their immunoreactivity was lower than that of Pru p 3. IgE-immunoreactivity of the recombinant Lc-LTP3 was lower than that of the two other isoforms. This indicates that all three isoforms of lentil LTPs have allergenic properties and according to the preliminary data, Lc-LTP3 is the least allergenic lentil LTP isoform. The less pronounced immunoreactivity of Lc-LTP3 may be attributed to the fact that it contains fewer amino acid residues constituting conformational epitopes of peach Pru p 3 (*Fig. 2*) compared to other lentil LTPs (7 of 13).

Cross-reactivity of the recombinant lentil LTP isoforms was investigated by ELISA using the recombinant Pru p 3 as an inhibitor of IgE-binding (*Fig. 8*). Inhibition of IgE-binding was observed for all three lentil LTPs. The results indicate that the isoforms Lc-LTP1, Lc-LTP3, and Lc-LTP2 contain epitopes that are similar to the major peach allergen Pru p 3.

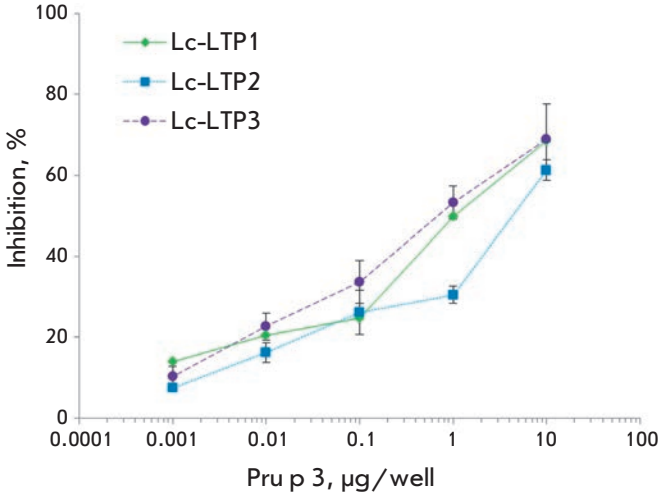

Fig. 8. Effect of the recombinant Pru p 3 on lentil LTP binding to specific IgE from the serum of patient no.3 with food allergy

CONCLUSIONS

In this study, we have obtained the recombinant isoforms of the lentil lipid transfer proteins Lc-LTP1 and Lc-LTP3 and conducted a comparative study of the structural-functional and immunological properties of the four lipid transfer proteins. Despite significant differences in the amino acid sequences of the three isoforms of lentil LTPs, their functional properties were quite similar. It was shown that all three proteins contain α-helical regions and are characterized by the presence of a hydrophobic cavity that ensures their

ability to bind fatty acids. All isoforms of lentil LTPs possess antimicrobial activity characterized by low specificity. The search for natural ligands of different lentil LTP isoforms, as well as identification of the factors affecting the induction of their biosynthesis, will pave the way for a deeper understanding of the functional role of the multiplicity of LTP isoforms.

At the same time, the study revealed certain differences in the immunoreactivity of the three lentil LTP isoforms. It was shown that Lc-LTP1 and Lc-LTP3, as well as Len c 3 deposited in the IUIS allergen database, are able of binding specific IgE from sera of patients with food allergies, recognizing epitopes similar to those of the major peach allergen Pru p 3. However, the immunoreactivity of Lc-LTP3 was less pronounced than that of the other isoforms. Further research into the structural organization and allergenic properties of Lc-LTP3 will reveal the key amino acid residues whose replacement leads to a decreased immunoreactivity of plant LTPs. It will also create conditions for the development of hypoallergenic variants of lipid transfer proteins and their use for allergen vaccination. ●

The authors would like to thank G.A.Shipulin and the employees of the Center of Molecular Diagnostics at the Central Research Institute of Epidemiology for providing the sera of patients with food allergies. This work was supported by the Russian Foundation for Basic Research (grant № 13-08-00956).

REFERENCES

1. Kader J.C. // Annu. Rev. Plant Physiol. Plant Mol. Biol. 1996. V. 47. P. 627–654.
2. Sun J.-Y., Gaudet D., Lu Z.-X., Frick M., Puchalski B., Laroche A. // Mol. Plant Microbe Interact. 2008. V. 21. № 3. P. 346–360.
3. Salcedo G., Sanchez-Monge R., Barber D., Diaz-Perales A. // Biochim. Biophys. Acta. 2007. V. 1771. P. 781–791.
4. .Pastorello E.A., Pompei C., Pravettoni V., Farioli L., Calamari A.M., Scibilia J., Robino A.M., Conti A., Iametti S., Fortunato D., et al. // J. Allergy Clin. Immunol. 2003. V. 112. P. 775–783.
5. Tordesillas L., Cuesta-Herranz J., Gonzalez-Muñoz M., Pacios L.F., Compés E., Garcia-Carrasco B., Sanchez-Monge R., Salcedo G., Diaz-Perales A. // Mol. Immunol. 2009. V. 46. № 4. P. 722–728.
6. Ferreira F., Briza P., Infuhr D., Schmidt G., Wallner M., Wopfner N., Thalhamer J., Achatz G. // Inflamm. Allergy Drug Targets. 2006. V. 5. № 1. P. 5–14.
7. Ferreira F., Hirtenlehner K., Jilek A., Godnik-Cvar J., Breiteneder H., Grimm R., Hoffmann-Sommergruber K., Scheiner O., Kraft D., Breitenbach M., et al. // J. Exp. Med. 1996. V. 183. № 2. P. 599–609.
8. Finkina E.I., Balandin S.V., Serebryakova M.V., Potapenko N.A., Tagaev A.A., and Ovchinnikova T.V. // Biochemistry (Moscow). 2007. V.72. № 4. P. 430–438.
9. Finkina E.I., Akkerdaas J., Balandin S.V., Santos Magadán S., Knulst A., Fernandez-Rivas M., Asero R., van Ree R., Ovchinnikova T.V. // Int. Arch. Allergy Immunol. 2012. V. 157. P. 51–57.
10. Wan L., Zeng L., Chen L., Huang Q., Li S., Lu Y., Li Y., Cheng J., Lu X. // Protein Expr. Purif. 2006. V. 48. № 2. P. 307–313.
11. Laemmli U.R. // Nature. 1970. V. 227. P. 680.
12. Buhot N., Gomes E., Milat M.L., Ponchet M., Marion D., Lequeu J., Delrot S., Coutos-Thevenot P., Blein J.P. // Mol. Biol. Cell. 2004. V. 15. № 11. P. 5047–5052.
13. Garcia-Olmedo F., Molina A., Segura A., Moreno M. // Trends Microbiol. 1995. V. 3. № 2. P. 72–74.
14. Choi A.M., Lee S.B., Cho S.H., Hwang I., Hur C.-G., Suh M.C. // Plant Physiol. Biochem. 2008. V. 46. P. 127–139.
15. Thoma S., Hecht U., Kippers A., Botella J., De Vries S., Somerville C. // Plant Physiol. 1994. V. 105. P. 35–45.
16. Jung H.W., Kim W., Hwang B.K. // Plant Cell Environ. 2003. V. 26. № 6. P. 915–928.
17. Tsuboi S., Osafune T., Tsugeki R., Nishimura M., Yamada M. // Biochem. 1992. V. 3. P. 500–508.
18. Gomès E., Sagot E., Gaillard C., Laquitaine L., Poinssot B., Sanejouand Y.H., Delrot S., Coutos-Thévenot P. // Mol. Plant Microbe Interact. 2003. V. 16. № 5. P. 456–464.
19. Trevino M.B., O'Conell M.A. // Plant Physiol. 1998. V. 116. P. 1461–1468.
20. Gizatullina A.K., Finkina E.I., Mineev K.S., Melnikova D.N., Bogdanov I.V., Telezhinskaya I.N., Balandin S.V., Shenkarev Z.O., Arseniev A.S., Ovchinnikova T.V. // Biochim. Biophys. Res. Commun. 2013. V. 439. № 4. P. 427–432.
21. Pacios L.F., Tordesillas L., Cuesta-Herranz J., Compes E., Sánchez-Monge R., Palacín A., Salcedo G., Díaz-Perales A. // Mol. Immunol. 2008. V. 45. № 8. P. 2269–2276.
22. Regente M.C., Giudici A.M., Villalaín J., De la Canal L. // Lett. Appl. Mic. 2005. V. 40. P. 183–189.
23. Carvalho A.O., Gomes V.M. // Peptides. 2007. V. 28. № 5. P. 1144-1153.

The Use of Transcription Terminators to Generate Transgenic Lines of Chinese Hamster Ovary Cells (CHO) with Stable and High Level of Reporter Gene Expression

N. B. Gasanov, S. V. Toshchakov, P. G. Georgiev, O. G. Maksimenko*
Institute of Gene Biology, Russian Academy of Sciences, Vavilova Str., 34/5, Moscow, 119334, Russia
E-mail: mog@genebiology.ru
Received: 25.03.2015

ABSTRACT **Mammalian cell lines are widely used to produce recombinant proteins. Stable transgenic cell lines usually contain many insertions of the expression vector in one genomic region. Transcription through transgene can be one of the reasons for target gene repression after prolonged cultivation of cell lines. In the present work, we used the known transcription terminators from the SV40 virus, as well as the human β- and γ-globin genes, to prevent transcription through transgene. The transcription terminators were shown to increase and stabilize the expression of the *EGFP* reporter gene in transgenic lines of Chinese hamster ovary (CHO) cells. Hence, transcription terminators can be used to create stable mammalian cells with a high and stable level of recombinant protein production.**

KEYWORDS **Recombinant proteins, production of proteins in cell lines, transcription termination, insulators, CHO.**

ABBREVIATIONS **RB – recombinant protein; CHO – Chinese hamster ovary cells; UTR – untranslated region of the gene; kbp – thousands of nucleotide base pairs; S/MAR – DNA regions associated with nuclear matrix proteins; insulators – regulatory elements that block the interaction between the enhancer and the promoter; UCOE – regulatory elements containing strong promoters of the housekeeping genes; STAR – regulatory elements protecting against HP1-dependent repression; EGFP – enhanced green fluorescent protein; CMV – cytomegalovirus; SV40 – simian virus 40; HSV – herpes simplex virus.**

INTRODUCTION

An increasing number of drugs are currently produced in cell culture bioreactors (first and foremost, those based on Chinese hamster ovary (CHO) cells) [1, 2]. However, the extremely high cost of the product is the main problem in manufacturing recombinant proteins in cell cultures. One of the ways to optimize the manufacturing process is to improve vectors for transgene generation, which allows one to significantly reduce the cost of manufacturing and maintenance of effective producer cell lines.

Transfection of linearized plasmid DNA has become the most common method used in bioengineering to generate cell lines for producing target proteins [3, 4]. This method can be employed to generate cell lines containing multiple copies of the expression vector that are usually inserted into one or, less frequently, several genomic sites. The cytomegalovirus (CMV) promoter, the SV40 early promoter, and strong housekeeping gene promoters, are typically used for transgene expression [5].

DNA sequences (usually the AT-rich ones) have been widely used since the early 1990s to enhance transfection efficiency and the stability of transgene expression; *in vitro* experiments demonstrated that these sequences interact with the matrix attachment region (MAR) [6–8]. The existing model assumes that the MAR elements interact with nuclear matrix proteins, thus reducing the dependence of the expression level of MAR-flanked genes on the negative effect of a chromatin environment.

Furthermore, known insulators are widely used to protect transgene transcription against repression and the negative effect of the surrounding genome [9–11].

The HS4 insulator (1.2 kbp) found at the border of the chicken β-globin locus is most typically used in bioengineering. Two copies of the HS4 insulator are usually inserted in the construct immediately downstream of the target gene. In some cases, either combinations of the known MAR and HS4 insulator are used or the HS4 core (500 bp) is multimerized [9]. These constructs enhance both the efficiency of transgene generation and the expression level of the transgene. However, the HS4 insulator is not equally efficient in all cell cultures and organisms.

Extended DNA fragments including housekeeping gene promoters (UCOE) [12, 13] and regulatory elements capable of blocking heterochromatin propagation [12, 14] are also used in bioengineering.

In general, it is fair to say that no universal regulatory elements with a comprehensible mechanism of action that could be efficiently used across all types of vector constructs intended for generating high-yield cell lines producing various proteins have been found yet. Even the strongest promoters are obviously expected to have mechanisms for suppressing excessive transcription. RNA interference is one of these mechanisms of transcription suppression [15, 16]. The suppression effects during transgene insertion are often associated with transcription through the transgene (e.g., transcription through enhancers inactivates their activity [17]). Long noncoding RNAs can also recruit repressive complexes to regulatory elements [18]. Based on the facts indicating that transcription occurring through regulatory elements plays a negative role in transgene expression, one can expect that transcription termination at transgene borders has a positive effect on the stabilization of transgene expression. Meanwhile, transcription is efficiently terminated only by some of the insulators under study [19].

Sequences of the well-studied transcription terminators from β- (βt) and ^{G}γ- (γt) globin genes were used in this work to test the role of transcription termination in the protection of transgene expression [20, 21]. Two copies of the best-characterized HS4 (2×Ins) insulator from chicken β-globin locus were used as controls [22]. The transcription terminators were shown to be able to significantly increase the stability of reporter gene expression in cellular pools. When generating isolated stable cell lines, the constructs containing terminator regions were characterized by a higher level of reporter gene translation product.

EXPERIMENTAL

Creation of constructs

In order to create a series of constructs, different sequences were inserted into the pEGFPN1 vector at the PciI restriction site located downstream of *EGFP* and upstream of cytomegalovirus promoter 640 bp away from the transcriptional start point: two tandem copies of the HS4 core insulator sequence from chicken β-globin locus (2×Ins) (476 bp), SV40 transcription terminator (SV40pA) (868 bp), transcription terminator from the human β-globin locus (βt) (1130 bp), and a combined element consisting of both βt and 2×Ins. A 1336-bp-long terminator from the human ^{G}γ-globin gene (γt) was inserted into the construct βt_EGFP at the restriction site AflII to obtain the construct βt_EGFP_γt.

Creation of transfected cell lines

Reporter gene expression was analyzed using Chinese hamster ovary (CHO-K1) cells, the cell culture most widely used in bioengineering to produce target proteins.

CHO-K1 cells were cultured on DMEM medium containing 10% of inactivated fetal bovine serum, 2mM *L*-glutamine, 35 mg/L *L*-proline, and commercially available antibiotic Mycokill-AB (PAA Laboratories) at a working concentration. The cells were re-inoculated every 5 days at a concentration of 10^5 cells/cm^2 and a 1:20 dilution ratio. The cells were cultured at 37°C in an atmosphere of 5% CO_2 and high moisture content. The cell culture was transfected with recombinant plasmids. Plasmids were linearized with the ApaLI restriction enzyme to ensure more efficient integration of the transgenic construct. The transfection protocol was as follows: The cells that reached 70–80% of the monolayer (8×10^4 cells/cm^2) were washed with a serum-free cell culture medium. The transfection mixture was prepared: 3–4 μg of linearized plasmid DNA was mixed with 375 μL of the serum-free cell culture medium. The commercially available transfection reagent Lipofectamine 2000 (with its amount calculated based on a ratio 3 μL of the reagent per 1 μg of plasmid DNA) was mixed with the same amount of the serum-free cell culture medium in a separate test tube. The solutions were combined and incubated at room temperature for 30–40 min. The washed cells were coated with the transfection mixture. The transfection mixture was replaced with a serum-containing DMEM culture medium 4–6 h after the transfection had been initiated.

The level of reporter gene expression was assessed according to the fluorescence intensity on day 2 after transfection (36–48 h) by flow cytometry on a MACSQuant Analyzer VYB (MiltenyiBiotec). Nontransfected CHO-K1 cells were used as negative control.

Cytofluorometric analysis

Prior to the cytofluorometric analysis, the cells were washed with phosphate buffered saline (PBS), treated

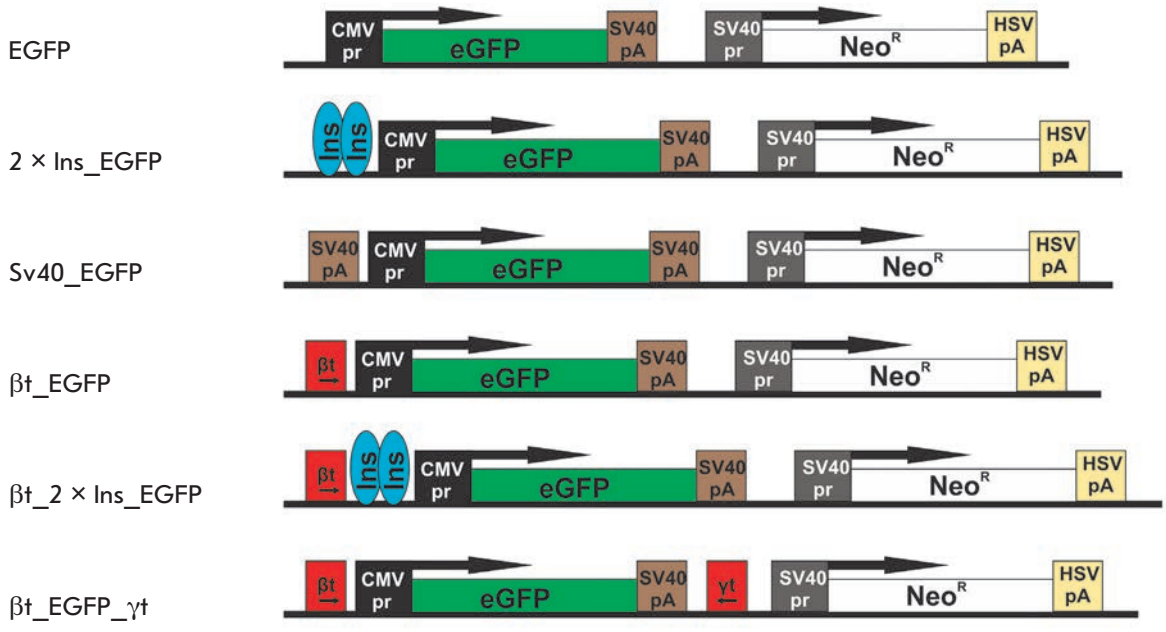

Fig. 1. Schemes of the constructs used to test DNA elements in the CHO-K1 cell culture. EGFP is the control plasmid pEGFPN1 containing no DNA elements. 2×Ins_EGFP is the control construct with two copies of the insulator from chicken β-globin locus inserted upstream of the cytomegalovirus promoter. SV40_EGFP, βt_EGFP, and βt_2×Ins_EGFP are the constructs with transcription terminators inserted upstream of the cytomegalovirus promoter. βt_EGFP_γt is the construct with transcription terminators surrounding the *EGFP* reporter gene. Cytomegalovirus and virus SV40 promoters are shown as black and gray squares, respectively; transcription terminators are shown as brown (SV40), yellow (HVS thymidine kinases), and red (*β*- and *γ*-globin genes) squares. The *EGFP* and neomycin resistance genes are shown as green and white rectangles, respectively; arrows indicate transcription direction. Insulators are shown as light blue ovals

with trypsin, and removed from the Petri dishes. They were subsequently washed twice to remove trypsin and thoroughly re-suspended in phosphate buffered saline. The resulting suspension (10^6 cells per mL of PBS) was transferred into 5-mL round-bottom test tubes.

The voltage in the flow cytofluorometer channels was selected so as not to take into account the autofluorescence of nontransfected cells. After calibration, all the samples were measured at a constant voltage. Thus, if EGFP fluorescence was detected, we counted the cells that emerged in the range of values above 10 on the logarithmic scale for a proper channel and measured all the quantitative values of the gene expression level.

Maintenance of the transfected cell pools

After the transfection, cell pools were cultured according to the above protocol. Transgene-free cells were removed by selecting the transfected cell pools using the commercially available antibiotic Geneticin (Invitrogen) at a concentration of 800 μg/mL. Since suppression of the transcriptional activity of the transgene reduces production of the antibiotic-resistance gene with time, the antibiotic concentration needs to be gradually reduced to 200 μg/mL after the cells have been cultured for 77 days.

Creation of individual clones

Pools of cultured cells were removed from the plates and diluted in 10 mL of the culture medium. Cell concentration was then determined using a Scepter automated cell counter (Millipore); the cells were diluted so that 1 mL of the medium contained 2–3 cells. The resulting suspension was transferred into 24-well plates (1 mL per well).

After cultivation in a DMEM medium containing antibiotic Geneticin at a concentration of 800 μg/μL for two weeks, we performed a cytofluorometric analysis of the clones that survived. The resulting cell lines were further maintained, and the expression level of EGFP was determined according to the procedure for transfected cell pools. EGFP fluorescence intensity was measured every 15 days.

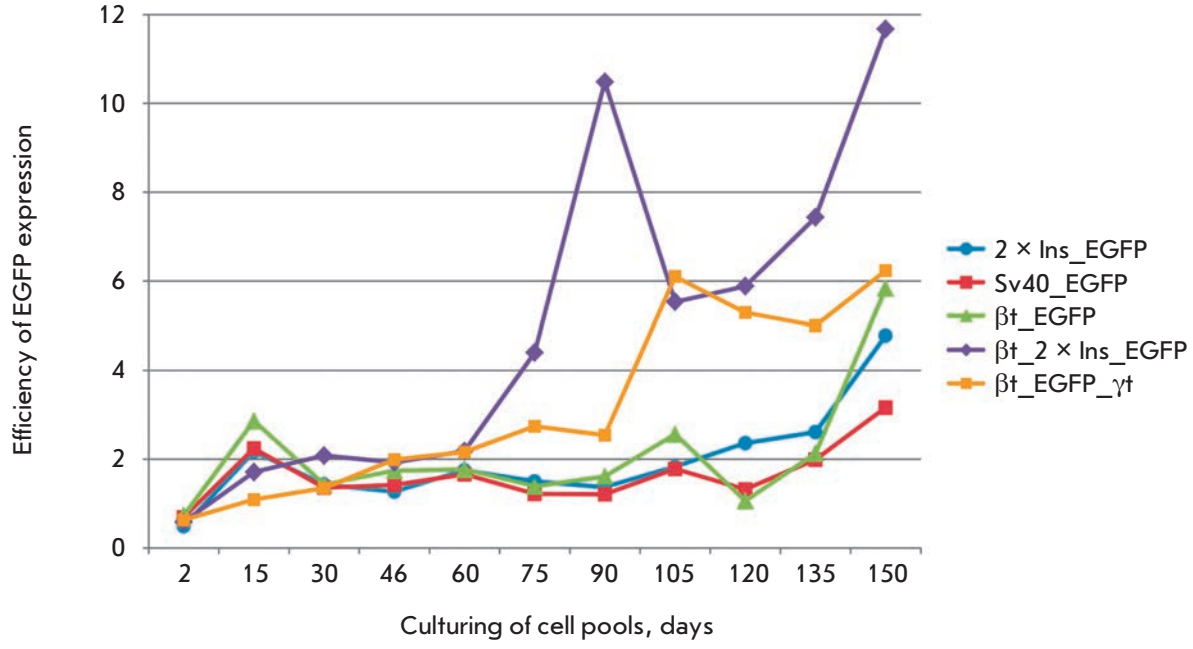

Fig. 2. Analysis of the expression level of the *EGFP* reporter gene in cellular pools transfected with constructs. The histogram shows the results of measuring the fluorescence of stable cellular pools using flow cytofluorometry every 15 days. The Y axis shows the efficiency of *EGFP* expression determined as the ratio between the percentage of *EGFP*-expressing cells in the pool of cells carrying the construct with this element (2×Ins_EGFP, SV40_EGFP, βt_EGFP, βt_2×Ins_EGFP, βt_EGFP_γt) and the percentage of *EGFP*-expressing cells with the control plasmid (EGFP). The mean expression level of *EGFP* in the pool of cells at a certain moment was assessed using the percentage of cells with a fluorescence intensity above 10 on a logarithmic scale in the corresponding channel. Each curve in the histogram represents an individual construct

RESULTS AND DISCUSSION

The enhanced green fluorescent protein (EGFP) gene under control of the CMV promoter was used as a reporter gene when studying the potential role of transcription terminators in stabilizing the transgene expression level in CHO cells. All the experimental constructs were compared to the control, the plasmid pEGFPN1 (Clontech) that contained the *EGFP* gene under the control of the CMV promoter (CMVpr) and SV40 transcriptional terminator (SV40pA) (EGFP construct in *Fig. 1*). In addition to the reporter gene, this plasmid contained the Neomycin resistance gene (Neo^R) under the control of the SV40 promoter (SV40pr) and transcription terminator of the herpes simplex virus thymidine kinase gene (HSVpA). In this case, the Neomycin resistance gene is needed for selecting transfected cells.

The well-studied transcription terminators of the β-globin gene (βt) and SV40pA were used to assess the effect of termination of transcription initiated downstream of the inserted transgene on reporter gene expression. In the constructs (SV40_EGFP and βt_EGFP), these terminators were inserted in forward orientation immediately upstream of the CMV promoter (*Fig. 1*). In order to completely isolate the reporter gene from transcription initiated in the surrounding chromatin, we created a derivative construct βt_EGFP (*Fig. 1*), which contained, in addition to the β-globin terminator, the transcription terminator from the ^{G}γ-globin gene (βt_EGFP_γt) inserted in reverse orientation at the 3'-end of the reporter gene. In this construct, the reporter gene is protected on both sides against transcription initiated from the surrounding chromatin.

In order to compare the efficiency of transcription terminators with the currently known regulatory elements stabilizing transgene expression in CHO cells, we used an element consisting of two copies of the HS4 core insulator sequence inserted immediately downstream of the CMV promoter (2×Ins_EGFP, *Fig. 1*). Finally, a βt_2×Ins_EGFP construct with the globin terminator inserted downstream of the two copies of the insulator was generated to study the cooperative effect of two regulatory elements with different functions: the insulator and transcription terminator (*Fig.* 1).

The levels of reporter gene expression during transfection of different construct variants were measured

Results of analysis of the temporal expression profile of the *EGFP* gene in individual cell clones

Clone	Fluorescence intensity (the median distribution), 30 days	Fluorescence intensity (the median distribution), 90 days	Decrease in expression activity	Mean value
EGFP #1	23.71	2.35	0.1	0.1
EGFP #2	16.11	1.7	0.11	
2xIns_EGFP #1	69.78	9.73	0.14	0.13
2xIns_EGFP #2	116.52	3.59	0.03	
2xIns_EGFP #3	103.66	16.6	0.16	
2xIns_EGFP #4	33.08	5.99	0.18	
2xIns_EGFP #5	77.74	10.55	0.14	
SV40_EGFP #1	67.93	13.1	0.19	0.76
SV40_EGFP #2	339.82	82.79	0.24	
SV40_EGFP #3	50.25	134.45	2.68	
SV40_EGFP #4	7.04	2.37	0.34	
SV40_EGFP #5	3.31	1.24	0.37	
βt_EGFP #1	78.44	15.54	0.2	2.07
βt _EGFP #2	79.86	19.63	0.25	
βt _EGFP #3	76.35	14.46	0.19	
βt_EGFP #4	2.19	13.34	6.09	
βt _EGFP #5	15.75	56.74	3.6	

using a CHO-K1 cell culture, which is most widely used in bioengineering to produce target proteins. Transfection was performed using the conventional procedure employing liposomes.

The levels of reporter gene expression were estimated every 15 days using flow cytofluorometry to determine the degree of transgene suppression in the cell pools transfected with the control (pEGFP_N1 and 2×Ins_EGFP) and experimental (SV40_EGFP, βt_pEGFP, βt_2×Ins_EGFP, and βt_EGFP_γt) constructs (*Fig. 2*). The mean expression level of the *EGFP* gene in the cell pool at a certain moment was determined according to the percentage of cells with a fluorescence intensity higher than 10 on the logarithmic scale (i.e., cells generating a significant amount of this protein). The ratio between the percentage of *EGFP*-expressing cells in the pool of cells carrying the construct with this element and the percentage of *EGFP*-expressing cells with the control plasmid (EGFP) was an indicator of the efficiency of a particular regulatory element in achieving a high and stable level of protein production.

The results of determining the *EGFP* expression level during culturing of the total population of transfected cells for 150 days (which corresponds to ~ 30 passages) indicate that the use of a transcription terminator downstream of the target gene promoter significantly enhances the efficiency of protein production during prolonged cultivation: over threefold for terminator SV40 and fivefold for terminator βt by the end of the experiments (*Fig.* 2). The regulatory element consisting of two copies of the insulator also had a similar effect.

The increase in the level of EGFP expression was higher in the pool of cells transfected with βt_EGFP_γt plasmid, where the reporter gene is surrounded by transcription terminators (*Fig. 2*). Thus, protection of the reporter gene (on both sides) against transcription initiated outside the transgene enhances stability and expression efficiency. Finally, the best results (a 12-fold increase) were achieved when the transcription terminator and two copies of the insulator were combined in the plasmid βt_2×Ins_EGFP (*Fig. 2*). A conclusion can be drawn that two regulatory elements with different mechanisms of action exhibit an additive effect on the stability and efficiency of regulatory gene expression.

Recombinant proteins are produced in actual practice by selecting stable cell lines generated from a single transfected cell and, therefore, having a heterogeneous genotype, which allows one to eliminate the effect of various negative factors and isolate the most efficient clone with the optimal site of construct integration in the genome.

Individual cellular clones were obtained using the limiting dilution technique after culturing total cell populations for 30 days. The median cell distribution over the fluorescence intensity was the main qualitative indicator of expression activity of the reporter gene.

The following individual clones were initially obtained: 10 clones containing the EGFP construct, 17 clones containing the 2×Ins_EGFP construct, 10 clones containing the SV40_EGFP construct, and 10 clones

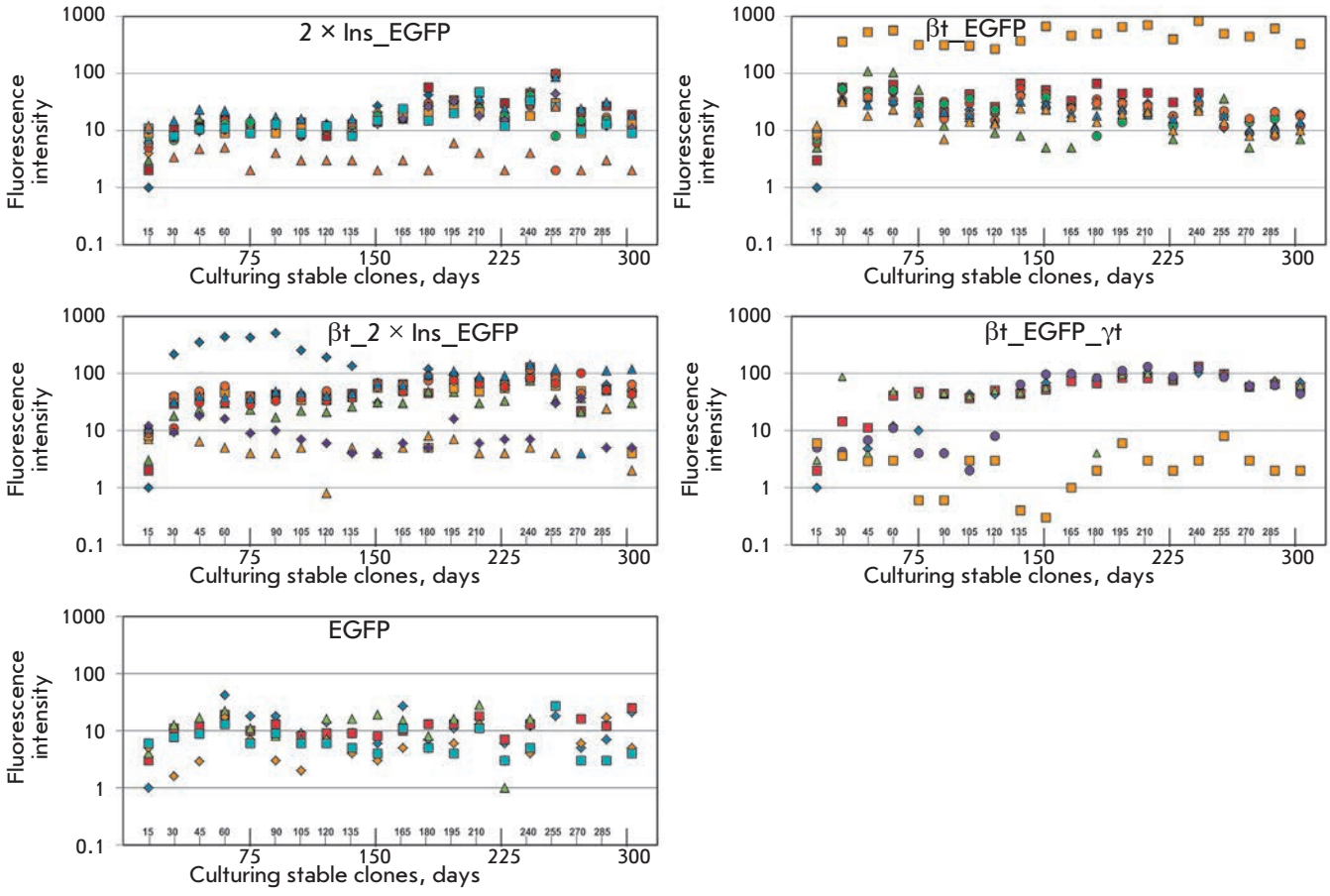

Fig. 3. Analysis of *EGFP* reporter gene expression in stable cell clones generated using the transfected cell pools. The histograms show the changes in the fluorescence intensity of stable cell clones recorded every 15 min by flow cytofluorometry. The X axis shows the measurement intervals. The Y axis shows the logarithmic scale of EGFP fluorescence intensity, which was determined as the distribution median. The mean expression level of *EGFP* in the cellular pool at a certain moment was assessed as a value being directly proportional to EGFP fluorescence intensity. Each point in the histogram represents an individual cell clone

containing the βt_EGFP construct. Among those, two clones with the EGFP construct, five clones with the 2×Ins_EGFP, five clones with the SV40_EGFP construct, and six clones containing the βt_EGFP construct were characterized by a sufficiently high level of *EGFP* expression.

It should be mentioned that clones containing the control construct initially showed a much lower level of *EGFP* expression compared to those containing the 2×Ins_EGFP, SV40_EGFP, and βt_EGFP constructs (*Table*).

The level of *EGFP* expression in stable cell clones containing the EGFP and 2×Ins_EGFP constructs decreased approximately tenfold after cultivation for 2.5 months. The average expression activity of the clones containing the SV40_pEGFP and βt_pEGFP constructs was ~ 75% of the initial value.

The results of measuring stable cell pools demonstrated that the most efficient cells characterized by a stable expression of the reporter gene were obtained after culturing for ~ 90 days. Hence, in order to study the clones generated from a stabilized cell population in more detail, we repeated the procedure of generating individual cell clones from total populations using the limiting dilution procedure after culturing stable pools for 90 days.

Identically to the previous experiment, the median cell distribution over the fluorescence intensity was the main quantitative indicator of the activity of reporter gene expression. Twelve individual clones with the EGFP, 2×Ins_EGFP, βt_EGFP, βt_2×Ins_EGFP, and βt_EGFP_γt constructs were initially obtained. Some clones died by the end of the experiment (culturing the cell clone for 300 days); hence, we report the data for

five clones containing the EGFP construct, 12 clones containing the 2×Ins_EGFP construct, nine clones containing the βt_EGFP construct, nine clones containing the βt_2×Ins_EGFP construct, and five clones containing the βt_EGFP_γt construct (*Fig. 3*). The measurements demonstrate that the resulting EGFP clones are characterized by a stable, but extremely low, level of fluorescence (the average values fluctuate around 10). The levels of fluorescence are slightly higher for 2×Ins_EGFP clones: only one clone has low activity, while the activities of the remaining ones lie in a range between 10 and 100. βt_EGFP clones are characterized by even higher average fluorescence values compared to 2×Ins_EGFP clones. Furthermore, one of the βt_EGFP clones exhibited ultra-high levels of fluorescence (between 10 and 1000). The βt_2×Ins_EGFP clones unexpectedly divide into two groups: one group (two clones) was characterized by low levels of fluorescence comparable to those of the clones containing the EGFP construct, while the second group was characterized by much higher values (about 100), which were on average higher than those for the 2×Ins_EGFP and βt_EGFP clones. This discrepancy in results probably arises from the fact that we used a more complex combination of regulatory elements (instable in certain genomic regions). Similar activity was observed for βt_EGFP_γt clones. Among them, one clone was characterized by an extremely low level of fluorescence, while the other ones exhibited a high level of fluorescence (about 100). The results of this experimental series can be used to draw a conclusion that transcription terminators are very efficient in establishment and maintenance of a high level of target protein production. The combined element (terminator attached to the insulator) and the variant containing the reporter gene surrounded by terminators are characterized by a higher efficiency of target protein production. However, these constructs require a more careful selection of clones, since some clones turned out to be ineffective due to some unknown reasons.

CONCLUSIONS

It has been demonstrated that transcription terminators, which can potentially isolate the transgene from transcriptional signals, are capable of maintaining the transgene transcription level stably high for an appreciably long period of time when culturing CHO-K1 cell lines. The terminator was found to maintain a stable level of transgene expression more effectively compared to the insulator. Furthermore, a combination of the transcription terminator and the insulator exhibits an additive effect, which enhances and stabilizes transgene expression. ●

This work was supported by the Russian Science Foundation (project № 14-24-00166).

REFERENCES

1. Kim J.Y., Kim Y.G., Lee G.M. // Appl. Microbiol. Biotechnol. 2012. V. 93. P. 917–930.
2. Hacker D.L., De Jesus M., Wurm F.M. // Biotech. Advances. 2009. P. 1023–1027.
3. Khan K.H. // Adv. Pharm. Bull. 2013. V. 3. P. 257–263.
4. Browne S.M., Al-Rubeai M. // Trends Biotech. 2007. V. 25. P. 425–432.
5. Lai T., Yang Y., Ng S.K. // Pharmaceuticals (Basel). 2013. V. 6. P. 579–603.
6. Kim J.M., Kim J.S., Park D.H., Kang H.S., Yoon J., Baek K., Yoon Y. // J. Biotech. 2004. V. 107. P. 95–105.
7. Girod P.A., Zahn-Zabal M., Mermod N. // Biotech. Bioeng. 2005. V. 91. P. 1–11.
8. Harraghy N., Gaussin A., Mermod N. // Curr. Gene Ther. 2008. V. 8. P. 353–366.
9. Recillas-Targa F., Valadez-Graham V., Farrell C.M. // BioEssays. 2004. V. 26. P. 796–807.
10. Kwaks T.H., Otte A.P. // Trends Biotechnol. 2006. V. 24. P. 137–142.
11. Maksimenko O.G., Deykin A.V., Khodarovich Y.M., Georgiev P.G. // Acta Naturae. 2013. V. 5. № 1(16). P. 33–46.
12. Palazzoli F., Bire S., Bigot Y., Bonnin-Rouleux F. // Nat. Biotechnol. 2011. V. 29. P. 593–597.
13. Antoniou M., Harland L., Mustoe T., Williams S., Holdstock J., Yague E., Mulcahy T., Griffiths M., Edwards S., Ioannou P.A., et al. // Genomics. 2003. V. 82. P. 269–279.
14. Kwaks T.H.J., Barnett P., Hemrika W., Siersma T., Sewalt R.G., Satijn D.P., Brons J.F., van Blokland R., Kwakman P., Kruckeberg A.L., et al. // Nat. Biotechnol. 2003. V. 21. P. 553–558.
15. Saxena A., Carninci P. // BioEssays. 2011. V. 33. P. 830–839.
16. Martianov I., Ramadass A., Barros A.S., Chow N., Akoulitchev A. // Nature. 2007. V. 445. P. 666–670.
17. Erokhin M., Davydova A., Parshikov A., Studitsky V.M., Georgiev P., Chetverina D. // Epigenetics Chromatin. 2013. V. 6. P. 31.
18. Khalil A.M., Guttman M., Huarte M., Garber M., Raj A., Rivea M.D., Thomas K., Presser A., Bernstein B.E., van Oudenaarden A., et al. // Proc. Natl. Acad. Sci. USA. 2009. V. 106. P. 11667–11672.
19. Silicheva M., Golovnin A., Pomerantseva E., Parshikov A., Georgiev P., Maksimenko O. // Nucleic Acids Res. 2010. V. 38. P. 39–47.
20. Nojima T., Dienstbier M., Murphy S., Proudfoot N.J., Dye M.J. // Cell Rep. 2013. V. 25. P. 1080–1092.
21. Plant K.E., Dye M.J., Lafaille C., Proudfoot N.J. // Mol. Cell. Biol. 2005. V. 25. P. 3276–3285.
22. Hanawa H., Yamamoto M., Zhao H., Shimada T., Persons D.A. // Mol. Therapy. 2009. V. 17. P. 667–674.

The Same Synaptic Vesicles Originate Synchronous and Asynchronous Transmitter Release

P. N. Grigoryev and A. L. Zefirov
Kazan State Medical University, Ministry of Health of the Russian Federation, Butlerov Str., 49, Kazan, 420012, Russia
*E-mail: zefiroval@rambler.ru
Received 16.02.2015

ABSTRACT **Transmitter release and synaptic vesicle exo- and endocytosis during high-frequency stimulation (20 pulses/s) in the extracellular presence of different bivalent cations (Ca^{2+}, Sr^{2+} or Ba^{2+}) were studied in frog cutaneous pectoris nerve-muscle preparations. It was shown in electrophysiological experiments that almost only synchronous transmitter release was registered in a Ca^{2+}-containing solution; a high intensity of both synchronous and asynchronous transmitter release was registered in a Sr^{2+}-containing solution, and asynchronous transmitter release almost only was observed in a Ba^{2+}-containing solution. It was shown in experiments with a FM 1-43 fluorescent dye that the synaptic vesicles that undergo exocytosis-endocytosis during synchronous transmitter release (Ca-solutions) are able to participate in asynchronous exocytosis in Ba-solutions. The vesicles that had participated in the asynchronous transmitter release (Ba-solutions) could subsequently participate in a synchronous release (Ca-solutions). It was shown in experiments with isolated staining of recycling and reserve synaptic vesicle pools that both types of evoked transmitter release originate from the same synaptic vesicle pool.**
KEYWORDS **motor nerve ending; evoked synchronous and asynchronous transmitter release; Ca^{2+}, Sr^{2+}, Ba^{2+} ions; synaptic vesicle exocytosis and endocytosis; synaptic vesicle pools.**
ABBREVIATIONS **EPP – end-plate potential.**

INTRODUCTION

Transmitter release in chemical synapses involves the release of discrete packages of transmitter (quanta) through fusion of a vesicle with the presynaptic membrane. The fusion process may occur either at rest (spontaneous transmitter release) or after the action potential reaches the presynaptic terminal and voltage-gated calcium channels-mediated influx of Ca^{2+} into nerve endings occurs (evoked release). The evoked transmitter release is caused by two components: synchronous, where transmitter quanta are released within several milliseconds after an action potential; and asynchronous release, persisting for tens or hundreds of milliseconds [1–3]. Synchronous transmitter release is the main component in most synapses, whereby more than 90% of quanta can be released at low-frequency stimulation [4, 5]. However, the share of asynchronous transmitter release rises at higher stimulation frequencies [6]. The use of solutions containing various alkaline earth metal ions is an experimental approach in changing the share of synchronous and asynchronous transmitter release. The share of asynchronous release rises when Ca^{2+} ions are replaced with $Sr^{2+}$and Ba^{2+} [2, 7, 8]. Synchronization of the transmitter quantum release is believed to be caused by several presynaptic mechanisms, such as rapid short-term opening of calcium channels during membrane depolarization, the properties of the protein "machine" of transmitter release triggering quantal transmitter release only at high intracellular calcium concentrations, and also the short distance between the calcium channels and the calcium sensor of exocytosis [9]. Mechanisms of asynchronous neurotransmitter release remain poorly understood. The Ca^{2+} sensor of asynchronous release is thought to be located at a larger distance from the calcium channel and is characterized by different Ca^{2+}binding dynamics [10–13].

Meanwhile, it can be assumed that the vesicles involved in the synchronous and asynchronous transmitter release differ from each other and can reside in independent populations. This idea is not unreasonable. First, the study of synaptic vesicle exo- and

endocytosis in motor nerve endings has made it possible to identify two functionally distinct pools (recycling and reserve synaptic vesicle pools). The recycling pool is characterized by docked vesicles at active zones. This pool is quickly depleted at high-frequency activity, and its recovery is provided by vesicle mobilization and fast endocytosis. The reserve pool of synaptic vesicles is larger and participates in the replenishment of the recycling vesicle pool under high-frequency stimulation; it is involved in the release process later and is replenished by slow endocytosis [14, 15]. Second, there is evidence to suggest the existence of separate populations of vesicles ensuring spontaneous [16, 17] and asynchronous transmitter release [18, 19], which are, however, not involved in the evoked synchronous transmitter release. In this paper, we made an attempt to evaluate the identity of the vesicle pools involved in the synchronous and asynchronous transmitter release in motor nerve endings using electrophysiological approaches and confocal fluorescence microscopy.

MATERIALS AND METHODS

Object of study, solutions

The experiments were performed using isolated frog cutaneous pectoris nerve-muscle preparations (*Rana temporaria*) in winter (December through February). This study was carried out in compliance with the International Guidelines for Proper Conduct of Animal Experiments. The standard Ringer's solution was used: 115.0 mM NaCl, 2.5 mM KCl, 1.8 mM $CaCl_2$, and 2.4 mM $NaHCO_3$; pH 7.2–7.4 and temperature of 20°C were maintained. All the experiments were conducted only for the nerve terminals on the surface. Along with the standard solution (Ca-solution), we used solutions in which $CaCl_2$ was replaced with either $SrCl_2$ or $BaCl_2$ at a concentration of 1.8 mM (Sr- and Ba-solutions). The evoked transmitter release and vesicle exocytosis were induced by prolonged high-frequency stimulation (20 pulses/s) of the motor nerve with square-wave electrical pulses of 0.1–0.2 ms duration at suprathreshold amplitude delivered by a DS3 stimulator (Digitimer Ltd., UK). Muscle fiber contractions were blocked by transverse muscle cutting. All the reagents were purchased from Sigma (USA).

Electrophysiology

Multiquantal end-plate potentials (EPPs) and monoquantal asynchronous signals were registered using glass microelectrodes (tip diameter less than 1 μm; resistance, 2–10 MΩ) filled with a 3 M KCl solution. A microelectrode was inserted into the muscle fiber at nerve endings under visual control. The resting membrane potential was monitored with a milli-voltmeter. The experiments in which the resting membrane potential decreased were discarded. The signals were converted into digital signals using ADC La-2USB. An original software Elph (developed by A.V. Zakharov) was used for signal accumulation and analysis.

Quantitative assessment of synchronous transmitter release

We used the modified method of variation of parameters, which was described in detail previously, for quantitative assessment of the quantal contents of EPPs [20]. The area of each EPP in the series were calculated. Thereafter, the region where the mean EPP area remained virtually unchanged was searched for on the plots showing the dynamics of EPP area decrease under high-frequency stimulation (usually stimulation for 10–30 s). EPP area variations were used to calculate the quantal value; i.e., the mean EPP area induced by one quantum of transmitter (q):

$$q = \sigma^2/<V>, \quad (1)$$

where σ is the dispersion of the EPP area and <V> is the mean EPP area in this region.

The quantal content of each EPP in the series can then be determined:

$$mi = V_i/q, \quad (2)$$

where m_i is the quantal content of the i^{th}EPP and V_i is the area of the i^{th}EPP.

Quantitative assessment of asynchronous transmitter release in Ca- and Sr-containing solutions

Asynchronous transmitter release was assessed by quantifying the number of monoquantal signals appearing after EPP between stimulations (50 ms) and counting their frequencies (the number of quanta per second). Monoquantal signals were determined both automatically and visually.

Quantitative assessment of asynchronous transmitter release in Ba-containing solutions

Stimulation in Ba-containing solutions causes a large amount of transmitter quanta release, thus leading to stable end-plate depolarization, which is confirmed by biochemical methods [21]. High-frequency stimulation in Ba-solutions leads to an enormous amount of asynchronously occurring monoquantal signals, which overlap and cannot be determined [7, 22]. Therefore, transmitter release (frequency of monoquantal asynchronous potentials) was assessed from the depolarization change in the membrane potential mediated by

asynchronous signals; correction for nonlinear summation was applied using the formula [22]:

$$n = \frac{V}{1 - V/(E - \varepsilon)} \cdot \frac{1}{a \cdot \tau}, \quad (3)$$

where V is depolarization of the postsynaptic membrane, mV; E is the resting membrane potential, mV; a is the mean amplitude of asynchronous monoquantal signals, mV;τ is the time constant of asynchronous monoquantal signals, ms; and ε is the acetylcholine equilibrium potential (≈ −15 mV).

Fluorescence microscopy

Synaptic vesicle exo- and endocytosis were examined using a FM 1-43 fluorescent dye (SynaptoGreen C4, Sigma, USA) at a concentration of 6 μM. The dye was reversibly bound to the presynaptic membrane and became trapped inside the newly formed synaptic vesicles (loading of the nerve endings) during endocytosis (after stimulation of exocytosis) [23]. Since endocytosis continues for some time after exocytosis, the dye was present in the solution both during stimulation (20 pulses/s) and within five minutes after stimulation termination. The preparation was then washed in a dye-free solution for 20 min to remove the dye bound to superficial membranes. In this case, bright fluorescent spots were observed in the nerve endings showing the accumulation of FM1-43-labeled vesicles at the active zones. Stimulation of exocytosis of the preliminarily loaded vesicles causes the release (unloading) of the dye from nerve endings [23]. Fluorescence was observed using a BX51W1 motorized microscope (Olympus, Germany) equipped with a DSU confocal scanning disk and a OrcaR2 CCD camera (Hamamatsu, Japan) connected to a PC through an Olympus CellˆP software. The optics for analyzing FM 1-43 fluorescence included Olympus U-MNB2 filters and Olympus LUMPLFL 60xw (1.0 NA) water immersion lens. Fluorescence intensity was analyzed in the 20-μm long central portion of the nerve ending. ImagePro software was used to assess the fluorescence intensity as relative fluorescence units of a pixel minus the background fluorescence. The background fluorescence was determined as the mean fluorescence intensity in a 50 × 50 pixel square in an image area showing no nerve terminals [12, 24, 25]. The profile of fluorescence in the nerve endings was calculated as the averaged fluorescence intensity of pixel rows arranged perpendicular to the longitudinal axis of the nerve ending with 1 pixel increments.

Statistical analysis was performed using the Origin Pro program. The quantitative results of the study are presented as a mean ± standard error, where *n* is the number of independent experiments. Statistical significance was assessed using Student's t-test and ANOVA.

RESULTS

Transmitter release under high-frequency stimulation in Ca-, Sr-, and Ba-containing solutions

Multiquantal EPPs (synchronous transmitter release) accompanied by occasional monoquantal asynchronous signals were registered under high-frequency stimulation in a Ca-containing solution (*Fig. 1A*). The quantal content of the first multiquantal EPP in the series was 321 ± 120 quanta ($n = 6$),while a reduction in the quantal content was observed under high-frequency stimulation, comprising 44.3 ± 9.0% ($n = 6$) of the baseline level by the end of the third minute of stimulation (*Fig. 1B*). Asynchronous release during the first second of high-frequency stimulation was low (5.9 ± 1.4 quanta s^{-1}, $n = 7$), but it rose to 40.0 ± 9.7 s^{-1} ($n = 7$) by the end of the third minute of stimulation (*Fig. 1B*). Monoquantal asynchronous signals disappeared within one second after the end of stimulation. Calculations showed that 880,251 ± 275,892 quanta ($n = 6$) were released over three minutes of stimulation in a Ca-solution through synchronous secretion, and 6751 ± 1476 quanta (n = 7) were induced by asynchronous release.

Multiquantal EPPs followed by monoquantal asynchronous signals were also recorded in Sr-solutions under high-frequency stimulation (*Fig. 1A*). The initial quantal content was significantly lower than that in a Ca-solution: i.e., 4.7 ± 0.8 ($n = 4$). By the end of the first minute of stimulation the quantal content of EPP increased to 34.3 ± 9.1 (n = 4) and remained at a relatively stable level until the end of the stimulation (*Fig. 1B*). The asynchronous release was found to be more significant in a Sr-solution than in a Ca-solution. The frequency of monoquantal signals during the first second of stimulation was 32.6 ± 5.8 quanta/s, while being 185.2 ± 10.7 quanta/s ($n = 5$) at the end of the third minute *(Fig. 1B*). After the end of stimulation, monoquantal asynchronous signals disappeared within one second. It was found that for 3 min of stimulation in a Sr-solution the amount of transmitter quanta released by the synchronous and asynchronous release was 126,359 ± 29,687 ($n = 4$) and 31,633 ± 1912 ($n = 5$), respectively. The asynchronous transmitter release appearing in Ca- and Sr-solutions did not change the resting membrane potential.

High-frequency stimulation of the motor nerve in a Ba-solution caused the emergence of one-to-three-quantal EPPs and a large number of monoquantal asynchronous signals. The quantal content of EPPs grew quickly by 2–3 s and gradually decreased to 1.85 ± 0.47 ($n = 7$) by the end of stimulation (*Fig. 1B*). Pro-

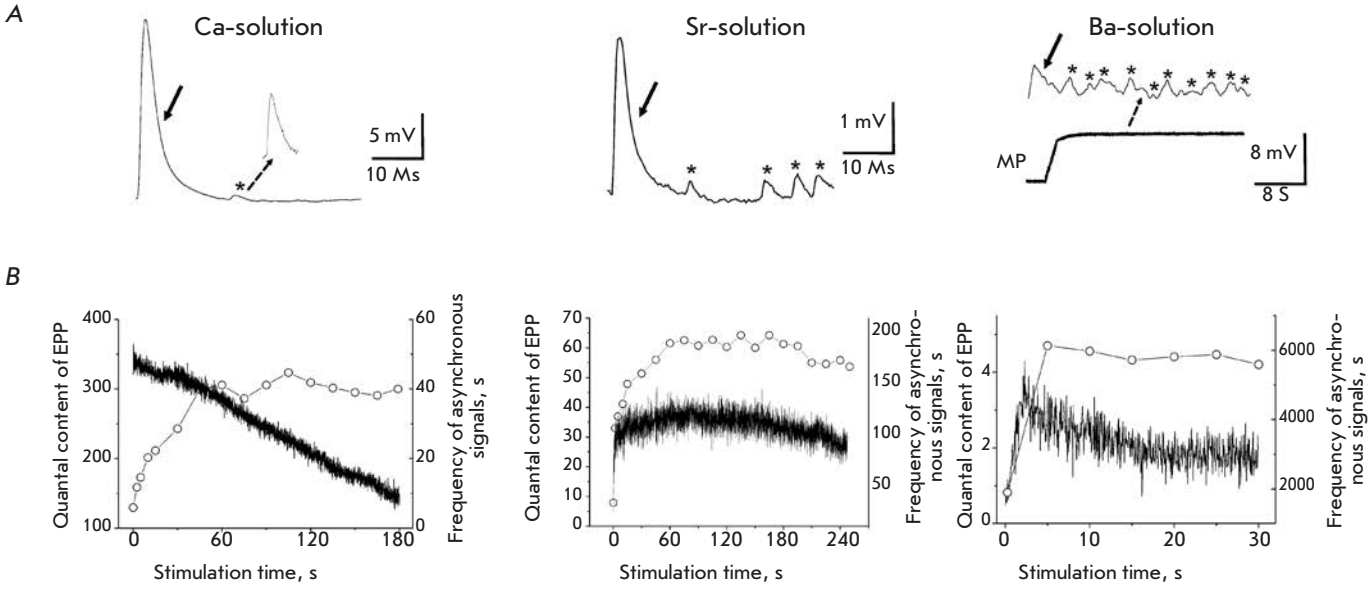

Fig. 1. Synchronous and asynchronous transmitter release in Ca-, Sr-, and Ba- solutions under high-frequency stimulation. Examples of registered end-plate potentials (EPP) and asynchronous monoquantal signals during high-frequency stimulation (20 pulses/s) in Ca-, Sr-, and Ba-solutions (1.8 mM). The arrows indicate EPPs, and the asterisks show asynchronous monoquantal signals. It is noticeable that muscle fiber depolarization develops in Ba-solutions (*A*). Dynamics of the averaged (over all experiments) quantal content of EPP (dark lines, Y axis is shown to the left) and the averaged frequency of asynchronous monoquantal signals (white circles, Y axis is shown to the right) under high-frequency stimulation (*B*)

longed stimulation during the first few seconds resulted in depolarization of muscle fibers from the resting level of −45 ± 2.9 mV to −37 ± 3.1 mV (n = 7) that was retained during the entire stimulation period. After the end of stimulation, the membrane potential returned to its original level within 3–7 s. Calculation using equation 3 (see the Materials and Methods section) led to a conclusion that this depolarization can be caused by asynchronous monoquantal signals with a frequency of 6131 ± 455 s^{-1} (n = 7). Further calculations showed that stimulation in a Ba-solution for 30 s leads to synchronous release of 1224 ± 180 quanta (n = 7) and an asynchronous release of 189,648 ± 41,712 quanta (n= 7).

These data suggest that almost all transmitter quanta are released synchronously (about 99.2%) in Ca-solutions under high-frequency stimulation, while asynchronous release is negligible. Application of a Sr-solution reduced the share of synchronously released quanta to 80% and that of asynchronously released quanta rose to 20%. Almost only asynchronous transmitter release (approximately 99.4%) was observed in Ba-solutions. We later used Ca- and Ba-solutions to study the exo- and endocytosis of the synaptic vesicles involved in the synchronous and asynchronous transmitter release.

Exocytosis and endocytosis of synaptic vesicles involved in synchronous and asynchronous transmitter release

The efficiency of synaptic vesicle endocytosis was evaluated by loading with a FM 1-43 dye under prolonged high-frequency stimulation in Ba- and Ca-solutions. It is known that the efficiency of capturing the FM 1-43 dye depends on the intensity of synaptic vesicle exocytosis and transmitter release. Therefore, the same number of transmitter quanta released during the stimulation time is needed to ensure loading with the FM 1-43 dye in Ba- and Ca-solutions. An analysis of the cumulative curves (the total number of synchronously and asynchronously released quanta, *Fig. 2A*) showed that 180,000 transmitter quanta in Ca-and Ba-solutions were released during stimulation for approximately 30 s. That is the duration of the stimulation we used to load the dye in our experiments. Under these conditions, we observed bright fluorescent spots in the Ca- and Ba-solutions (the fluorescence intensity of nerve endings was 0.114 ± 0.008 (n = 23) and 0.119 ± 0.011 relative units (n = 20), respectively) (*Figs. 2B, 3C*). These data indicate that during both synchronous and asynchronous vesicle exocytosis, effective recycling processes to form new synaptic vesicles occur.

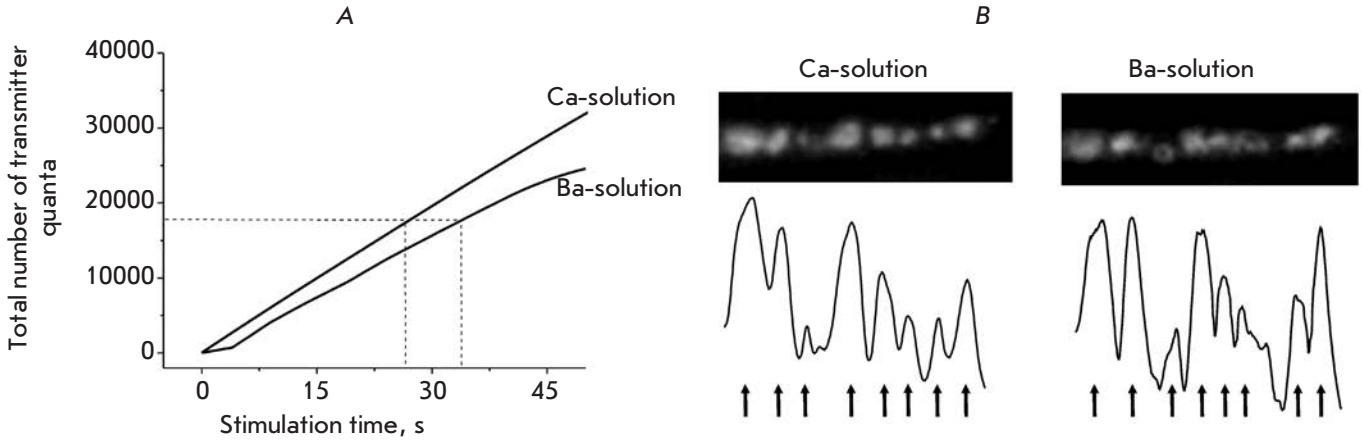

Fig. 2. Synaptic vesicle endocytosis in Ca- and Ba- solutions. Cumulative curves of synchronously and asynchronously released quanta of neurotransmitter in Ca- and Ba-solutions during high-frequency stimulation (based on the data in *Fig. 1B*). It is noticeable that 180,000 neurotransmitter quanta (the dashed line) are released during stimulation for 30 s (A). Images of FM 1-43 fluorescence at the same nerve terminal area after loading with FM 1-43 under stimulation for 30 s in Ca- and Ba-solutions (see details in the text). The profile of nerve terminal fluorescence is shown at the bottom. It is noticeable that the topographies of the spots are analogous (indicated by arrows) (B)

The following experiments were aimed at assessing the ability of the vesicles involved in asynchronous transmitter release to undergo synchronous exocytosis.

For that purpose, nerve endings were preliminarily loaded with FM 1-43 in a Ba- or Ca-solution (stimulation of asynchronous or synchronous exocytosis, respectively) and the dynamics of dye-unloading under high frequency stimulation in a Ca-solution (synchronous exocytosis stimulation) was compared. It was shown that the dynamics of dye-unloading was the same (*Fig. 3B*) under these conditions. After 1 min of stimulation of the preliminarily loaded nerve endings in the Ba- and Ca-solutions, the fluorescence intensity decayed to 80.1 ± 1.2 (n = 7) and 76.0 ± 1.2% (n = 7), respectively; after 15 minutes, it decayed to 55.9 ± 2.2 (n = 7) and 55.3 ± 5.4% (n = 7), respectively, and fluorescent spots disappeared (*Fig. 3B*). Hence, the synaptic vesicles participating in asynchronous exocytosis and transmitter release were able to undergo synchronous exocytosis.

In several experiments we performed an in-depth analysis of the fluorescence spots in the nerve endings of the same sample preparation that occur during stimulation of synchronous and asynchronous release. First, the spots arising after dye-loading in a Ca-solution were analyzed. The dye was then unloaded (stimulation for 15 min); the nerve endings were re-loaded with the dye in the Ba-solution, and fluorescent spots were analyzed. A spatial analysis of the fluorescence spots of the same nerve endings in Ca- and Ba-solutions revealed their identity (*Fig. 2B*). These findings suggest that recycling processes occur in the same regions of the nerve endings adjacent to the active zones during both the synchronous and asynchronous vesicle exocytosis.

Evaluation of participation of the recycling and reserve vesicle pools in asynchronous transmitter release

In this part of the study, isolated loading of either recycling or reserve vesicle pools with a FM 1-43 dye in a Ca-solution was conducted, followed by an evaluation of their ability to participate in asynchronous transmitter release. Short-term (12 s) high-frequency (20 pulses/s) stimulation was used for loading the recycling vesicle pool [26]. Weak fluorescent spots appeared in the nerve endings showing the accumulation of the recycling vesicle pool at active zones. Subsequently, we analyzed the dynamics of dye-unloading under stimulation of synchronous (Ca-solution) and asynchronous (Ba-solution) transmitter release. No differences in the fluorescence decay dynamics were revealed. After 1 min of stimulation in the Ca-and Ba-solutions, the fluorescence intensity of nerve terminals dropped to 74.2 ± 4.3 (n = 4) and 72.2 ± 3.4% (n = 5), respectively; after 5 min, to 60.8 ± 4.3 (n = 4) and 61.4 ± 4.3% (n = 5), respectively (*Figs. 4B, 4C*).

The modified protocol was used for reserve vesicle pool loading [26]. Initially, the preparation was subjected to high-frequency stimulation for 3 min in a Ca-solution with FM 1-43. This protocol leads to staining of the recycling and reserve vesicle pools. After washing, the preparation was subjected to high-frequency stimulation again, but for 25 s, thus causing dye release by the recycling vesicle pool. As a result, the remaining

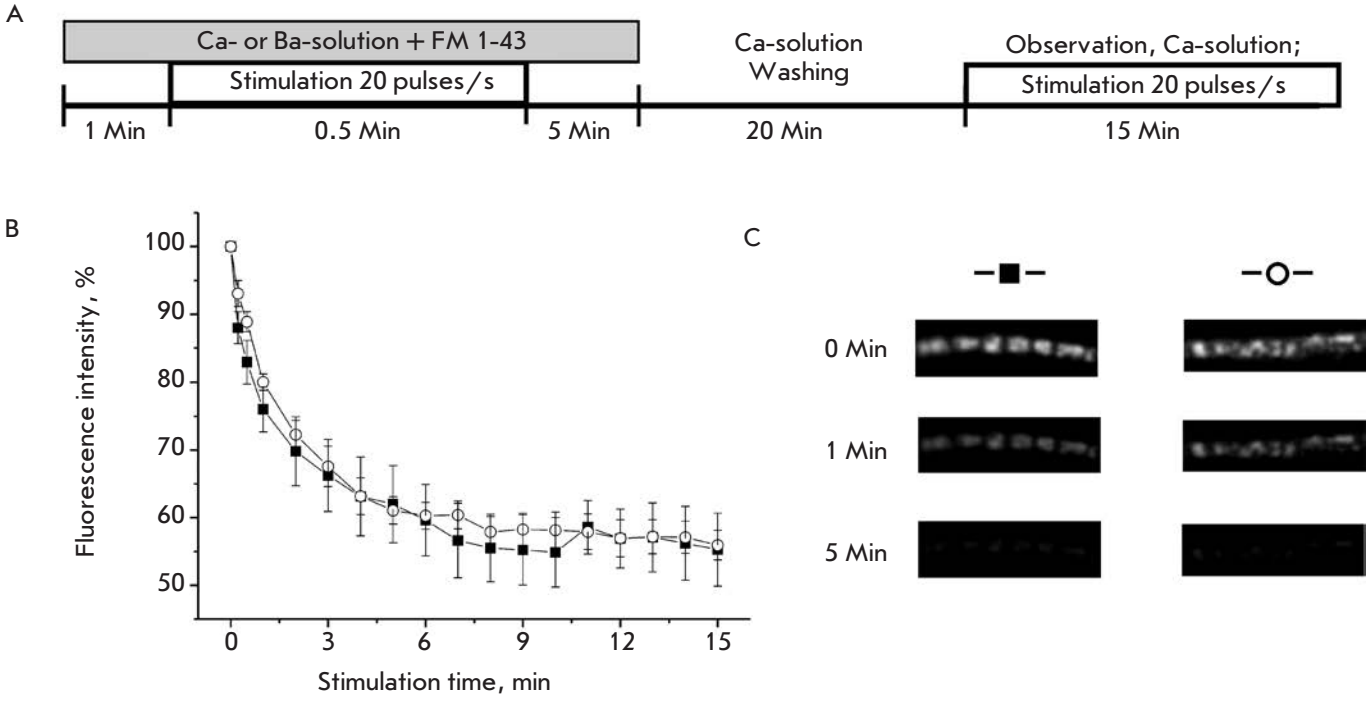

Fig. 3. Exocytosis of synaptic vesicles loaded with the FM 1-43 dye in Ca- and Ba- solutions. Experimental scheme. Nerve terminals were loaded with the dye in Ca- and Ba- solutions and then unloaded in a Ca-solution (A). The dynamics of fluorescence intensity decay (dye unloading) of the nerve terminals preliminarily stained in Ca- (black squares) and Ba- (white circles) solutions, % of the initial value (B). Examples of fluorescent images from B (C)

stained synaptic vesicles in a nerve ending belonged mostly to the reserve pool [26]. The subsequent high-frequency stimulation of stained preparations in the Ca- (synchronous transmitter release stimulation) and Ba-solutions (asynchronous transmitter release stimulation) led to the same fluorescence decay in nerve endings (*Fig. 4E*). After stimulation in the Ca-and Ba-solutions for 1 min, the fluorescence intensity of nerve endings decayed to 83.1 ± 2.2 (n = 7) and 76.9 ± 4.1% (n = 6), respectively; after stimulation for 15 min, to 44.3 ± 2.9 (n = 7) and 42.3 ± 2.7% (n = 6), respectively (*Figs. 4E, F*). These data suggest that both the recycling and reserve vesicle pools are capable of asynchronous transmitter release, along with synchronous release.

DISCUSSION

Experimental data showing differences in the mechanisms of synchronous and asynchronous transmitter release have been recently obtained. An assumption was made that both types of evoked transmitter release can be initiated in the region where various presynaptic calcium channels are located [9, 19, 27] using a multitude of protein molecules that provide the docking processes and synaptic vesicle fusion. Calcium-binding proteins synaptotagmins 1,2,9 are the main candidates for the role of a Ca-sensor of synchronous release; synaptotagmin 7 and Doc2 are the ones in asynchronous release [9]. The complexins and synaptobrevin 2 proteins are involved in the regulation of synchronous transmitter release; VAMP4 and synapsin 2 participate in the regulation of asynchronous transmitter release [28–30]. These findings raise the question of the identity of the vesicle pools involved in the synchronous and asynchronous transmitter release.

Our data show that the same synaptic vesicles are able to originate synchronous and asynchronous transmitter release with the same recycling processes. This is supported by the ability of the vesicles which have undergone the endocytosis-exocytosis cycle during synchronous transmitter release (Ca-solutions) to become involved in asynchronous exocytosis in Ba-solutions (*Fig. 4*). Conversely, the vesicles that are initially involved in asynchronous release (Ba-solutions) can be subsequently involved in synchronous release (Ca-solutions) (*Figs. 3B, 3C*). Efficient dye entrapment under release stimulation in Ba-solutions (*Figs. 2B, 3C*) indicates that both the asynchronous and synchronous transmitter release occur via full exocytosis

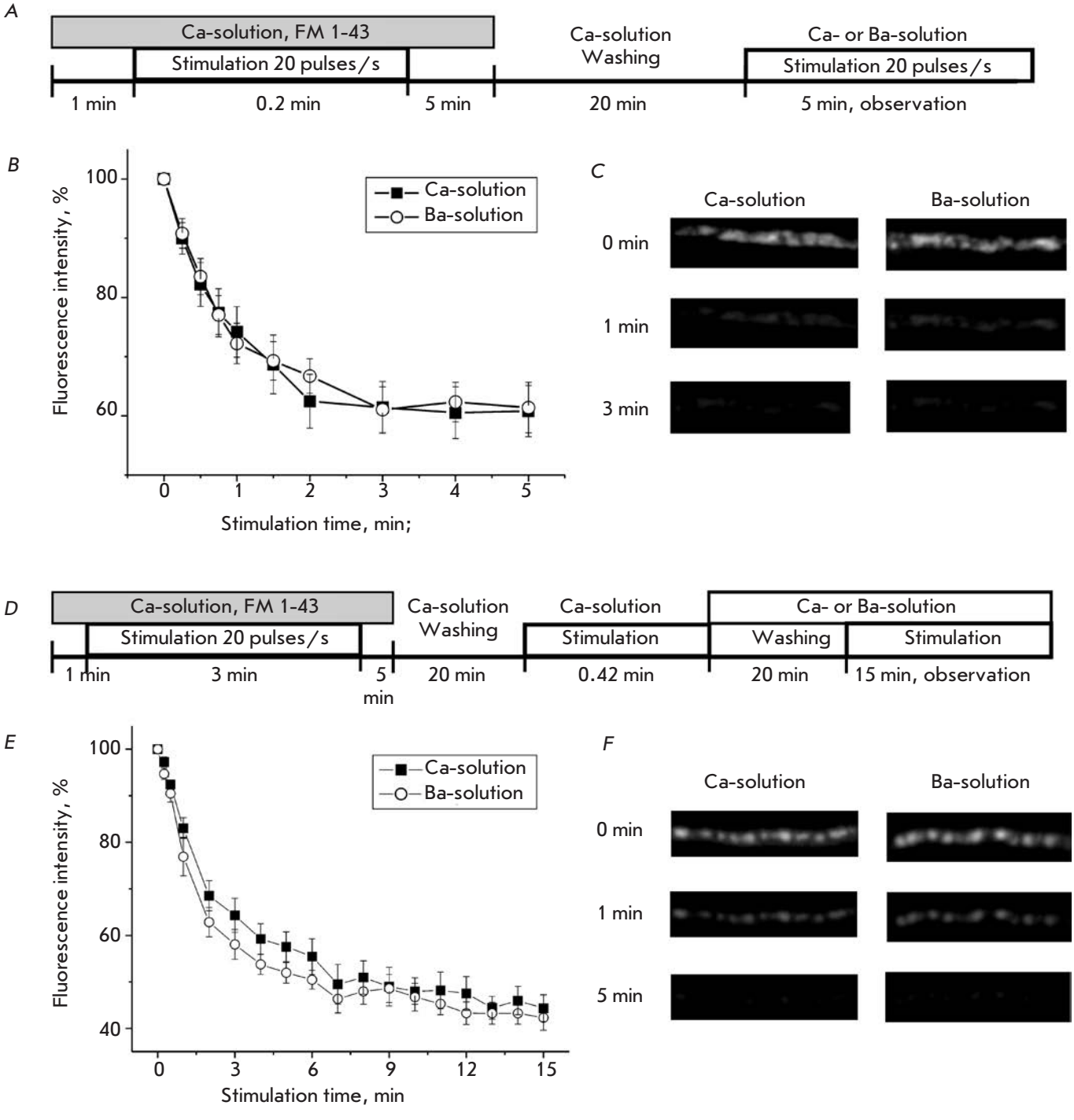

Fig. 4. Exocytosis of the recycling and reserve synaptic vesicle pools in Ca- and Ba- solutions. Scheme of the experiment involving isolated staining and investigation of exocytosis of the recycling synaptic vesicle pool (A). The dynamics of fluorescence intensity decay of nerve terminals with apreliminarily stained recycling synaptic vesicle pool under high-frequency stimulation in Ca- (black squares) and Ba- (white circles) solutions (B). Fluorescence image examples from B (C). Scheme of the experiment involving isolated staining and investigation of exocytosis of the reserve synaptic vesicle pool (D). The dynamics of fluorescence intensity decay of nerve terminals with a preliminarily stained reserve synaptic vesicle pool under high-frequency stimulation in Ca- (black squares) and Ba- (white circles) solutions (E). Fluorescence image examples from E (F)

of vesicles and subsequent formation of new vesicles by endocytosis. Synchronous and asynchronous exocytosis occur in the same areas of nerve endings at active zones, as evidenced by the complete identity of the topology and configuration of fluorescent spots under release stimulation in Ca-and Ba-solutions (*Fig. 2B*).

The ability of vesicles belonging to different functional pools of the nerve ending to become involved in asynchronous transmitter release was tested in experiments involving isolated staining of recycling and reserve vesicle pools. It was shown that the dynamics of dye-unloading from both the recycling and reserve vesicle pools in synchronous and asynchronous transmitter release is absolutely similar and that the fluorescence intensity decayed to the same level (*Figs. 4B, E*). Hence, both vesicle pools equally participated in both the synchronous and asynchronous transmitter release. Our study did not confirm the view of some authors that the nerve endings may contain a separate population of vesicles that would trigger asynchronous transmitter release [18, 19] but not be involved in the evoked synchronous release.

CONCLUSIONS

Our data suggest that the same synaptic vesicles originate both types of the evoked transmitter release in neuromuscular junction. It can be assumed that a synaptic vesicle contains the assembly of proteins required for both synchronous and asynchronous transmitter release. Probably the choice of the evoked release, in which the synaptic vesicle will participate, depends on the dynamics of the Ca^{2+} ions around the vesicles, vesicle arrangement with respect to a calcium channel, and the properties of the Ca-sensors of exocytosis. ●

The authors would like to thank A.V. Zakharov for his help in the analysis of the experimental data.

This work was supported by the Russian Foundation for Basic Research, grant №14-04-01232-a and the Russian Science Foundation (№14-15-00847).

REFERENCES

1. Katz B., Miledi R. // Proc. R. Soc. Lond. B. 1965. V. 161. P. 483–495.
2. Van der Kloot W., Molgó J. //Physiol. Rev. 1994. V. 74. № 4. P. 899–991.
3. Khuzakhmetova V., Samigullin D., Nurullin L., Vyskočil F., Nikolsky E., Bukharaeva E. //Int. J. Dev.Neurosci. 2014. V. 34. P. 9–18.
4. Rahamimoff R., Yaari Y.// J. Physiol. 1973. V. 228. P. 241–257.
5. Atluri P., Regehr W. // J. Neurosci. 1998. V. 18. P. 8214–8227.
6. Zefirov A.L., Moukhamedyarov M.A. // Ross. Fiziol. Zh. Im. I.M. Sechenova. 2004. V. 90. № 8. P. 1041–1059.
7. Zefirov A.L., Grigor'ev P.N. // Ross. Fiziol. Zh. Im. I.M. Sechenova. 2009. V. 95. № 3. P.262–272.
8. Bukharaeva E.A., Samigullin D., Nikolsky E.E., Magazanik L.G. // J. Neurochem. 2007. V. 100. № 4. P.939–949.
9. Kaeser P.S., Regehr W.G. // Annu. Rev. Physiol. 2014. V.76. P. 333–363.
10. Cummings D.D., Wilcox K.S., Dichter M.A. // J. Neurosci. 1996 V. 16. №17. P. 5312–5323.
11. Sun J., Pang Z.P., Qin D., Fahim A.T., Adachi R., Sudhof T.C. // Nature. 2007. V. 450. P. 676–682.
12. Zefirov A.L., Grigor'ev P.N. // Bull. Exp. Biol. Med. 2008.V. 146. № 12. P. 608–612.
13. Burgalossi A., Jung S., Meyer G., Jockusch W.J., Jahn O., Taschenberger H., O'Connor V.M., Nishiki T., Takahashi M., Brose N., Rhee J.S. // Neuron. 2010. V. 68. № 3. P. 473–87.
14. Rizzoli S.O., Betz W.J. // Nat. Rev. Neurosci. 2005 V.6 №1. P.57–69.
15. Zakharov A.V., Petrov A.M., Kotov N.V., Zefirov A.L.// Biofizika. 2012. V.57. № 4, P.42–50.
16. Ramirez D.M., Kavalali E.T. //Curr. Opin. Neurobiol. 2011 V.21 №2. P.275–82.
17. Sara Y., Virmani T., Deák F., Liu X., Kavalali E.T. // Neuron. 2005 V. 45 №4. P.563–73.
18. Otsu Y., Shahrezaei V., Li B., Raymond L.A., Delaney K.R., Murphy T.H. // J. Neurosci. 2004 V. 24. №2. P.420–33.
19. Peters J.H., McDougall S.J., Fawley J.A., Smith S.M., Andresen M.C. // Neuron. 2010. V. 65 №5. P.657–669.
20. Zefirov A.L., Zakharov A.V., Mukhametzianov R.D., Petrov A.M., Sitdikova G.F. // Ross. Fiziol. Zh. Im. I.M. Sechenova. 2008. V. 94 № 2. P. 129–141.
21. Silinsky E.M. // J. Physiol. 1978. V. 274 P. 157–171.
22. Betz W.J., Bewick G.S., Ridge R.M. // Neuron. 1992. V. 9. № 5. P. 805–813.
23. Zefirov A.L., Abdrakhmanov M.M., Mukhamedyarov M.A., Grigoryev P.N. // Neuroscience. 2006. V. 143, №4. P. 905–910.
24. Zefirov A.L., Abdrakhmanov M.M., Grigor'ev P.N.,Petrov A.M. // Tsitologiia. 2006. V. 48. № 1. P. 34–41.
25. Gaffield M.A., Rizzoli S.O., Betz W.J. // Neuron. 2006 V. 51. № 3. P.317–325.
26. Wen H., Linhoff M.W., Hubbard J.M., Nelson N.R., Stensland D., Dallman J., Mandel G., Brehm P. // J. Neurosci. 2013. V. 33. №17. P.7384–7392.
27. Raingo J., Khvotchev M., Liu P., Darios F., Li Y.C., Ramirez D.M., Adachi M., Lemieux P., Toth K., Davletov B., Kavalali E.T. // Nat. Neurosci. 2012. V. 15 P.738–745.
28. Sudhof T.C., Rothman J.E. // Science. 2009. V. 323. P. 474–477.
29. Medrihan L., Cesca F., Raimondi A., Lignani G., Baldelli P., Benfenati F. // Nat. Commun. 2013. V. 4:1512. P.1–13.

Genomic Study of Cardiovascular Continuum Comorbidity

O. A. Makeeva[1,2]*, A. A. Sleptsov[1], E. V. Kulish[1], O. L. Barbarash[2], A. M. Mazur[3], E. B. Prokhorchuk[3], N. N. Chekanov[3], V. A. Stepanov[1], V. P. Puzyrev[1,4]**

[1]Research Institute of Medical Genetics, Nab. Ushayki, 10, Tomsk, 634050, Russia

[2]Research Institute for Complex Issues of Cardiovascular Diseases, Sosnovy Blvd., 6, Kemerovo, 650000, Russia

[3]Genoanalitika, Leninskie Gory, 1/77, Off. 102, Moscow, 119234, Russia

[4]Siberian State Medical University, Moskovskiy Trakt, 2, Tomsk, 634050, Russia

*E–mail: oksana.makeeva@medgenetics.ru

**E–mail: valery.puzyrev@medgenetics.ru

Received: 14.01.2015

ABSTRACT **Comorbidity or a combination of several diseases in the same individual is a common and widely investigated phenomenon. However, the genetic background for non–random disease combinations is not fully understood. Modern technologies and approaches to genomic data analysis enable the investigation of the genetic profile of patients burdened with several diseases (polypathia, disease conglomerates) and its comparison with the profiles of patients with single diseases. An association study featuring three groups of patients with various combinations of cardiovascular disorders and a control group of relatively healthy individuals was conducted. Patients were selected as follows: presence of only one disease, ischemic heart disease (IHD); a combination of two diseases, IHD and arterial hypertension (AH); and a combination of several diseases, including IHD, AH, type 2 diabetes mellitus (T2DM), and hypercholesterolemia (HC). Genotyping was performed using the "My Gene" genomic service (www.i–gene.ru). An analysis of 1,400 polymorphic genetic variants and their associations with the studied phenotypes are presented. A total of 14 polymorphic variants were associated with the phenotype "IHD only," including those in the *APOB*, *CD226*, *NKX2–5*, *TLR2*, *DPP6*, *KLRB1*, *VDR*, *SCARB1*, *NEDD4L*, and *SREBF2* genes, and intragenic variants rs12487066, rs7807268, rs10896449, and rs944289. A total of 13 genetic markers were associated with the "IHD and AH" phenotype, including variants in the *BTNL2*, *EGFR*, *CNTNAP2*, *SCARB1*, and *HNF1A* genes, and intragenic polymorphisms rs801114, rs10499194, rs13207033, rs2398162, rs6501455, and rs1160312. A total of 14 genetic variants were associated with a combination of several diseases of cardiovascular continuum (CVC), including those in the *TAS2R38*, *SEZ6L*, *APOA2*, *KLF7*, *CETP*, *ITGA4*, *RAD54B*, *LDLR*, and *MTAP* genes, along with intragenic variants rs1333048, rs1333049, and rs6501455. One common genetic marker was identified for the "IHD only" and "IHD and AH" phenotypes: rs4765623 in the *SCARB1* gene; two common genetic markers, rs663048 in *SEZ6L* and intragenic rs6501455, were identified for the "IHD and AH" phenotype and a combination of several diseases (syntropy); there were no common genetic markers for the "syntropy" and "IHD only" phenotypes. Classificatory analysis of the relationships between the associated genes and metabolic pathways revealed that lipid–metabolizing genes are involved in the development of all three CVC variants, whereas immunity-response genes are specific to the "IHD only" phenotype. The study demonstrated that comorbidity presents additional challenges in association studies of disease predisposition, since the genetic profile of combined forms of pathology can be markedly different from those for isolated "single" forms of a disease.**

KEYWORDS **genetic polymorphism, multifactorial diseases, syntropy, comorbidity, association studies, cardiovascular continuum.**

ABBREVIATIONS **AH – arterial hypertension; HC – hypercholesterolemia; IHD – ischemic heart disease; HDLs – high density lipoproteins; LDLs – low density lipoproteins; ACS – acute coronary syndrome;T2DM – type 2 diabetes mellitus; CVD – cardiovascular disease; CVC – cardiovascular continuum.**

INTRODUCTION

Multiple, concurrent diseases have long been an issue in clinical practice [1, 2]. In developed countries, up to 80% of the healthcare budget is spent on patients with four or more diseases [3]. The most common term for this phenomenon is "comorbidity" [1]. However, only a portion of concurrent diseases with a common genetic basis and similar pathogenesis is referred to as "syntropies" or "attraction diseases" [4]. There are many clinically proven syntropic diseases, e.g., immunodependent diseases (allergic and autoimmune) [5, 6]; endocrine system diseases, including the combination of diabetes mellitus (T2DM), autoimmune thyroiditis, and the celiac disease [7]; some forms of mental illness [8]. Among them are cardiovascular diseases (CVDs), which are related to the concept of cardiovascular continuum (CVC).

The term "cardiovascular continuum" was proposed by Dzau and Braunwald in the early 1990s. The concept of CVC describes the development and progression of a disease over time and also reflects the essence of the relationships among various risk factors (genetic and environmental), highlighting their integrity [9–11]. The CVC hypothesis postulates that cardiovascular diseases (CVDs) are a specific chain of events that is triggered by numerous, interrelated or independent risk factors, progresses as a result of the activation of multiple signaling pathways and physiological processes, and, ultimately, leads to the end-stage heart disease. Cardiovascular risk factors include high cholesterol, arterial hypertension, diabetes mellitus, smoking, obesity, and physical inactivity. Cardiovascular disease continuum (continuum of clinical phenotypes) is based on the pathophysiologic continuum that includes progressive molecular and cellular changes manifesting themselves as a disease at the clinical level. Fundamentally, these processes are based on oxidative stress and endothelial dysfunction that, in turn, initiate a cascade of events, including disturbances in the system of vasoactive mediators, non-specific inflammatory response, and vascular remodeling. All the phenomenons mentioned above result in damage to target organs.

In clinical practice, comorbidity (combination of diseases) makes the use of genomic markers for predicting the risk of a disease more difficult. Do genetic variants that increase the risk of a certain single disease play the same pathogenic role in the case of complex phenotypes (combinations of diseases) or does their contribution change? How to account for the genetic pleiotropy and diverse effects of some genetic variants during the development of approaches to genetic testing? A genetic variant may be a risk factor for one disease and a protective factor for another.

This paper presents the results of a comparative analysis of a genetic component of three clinical phenotypes (a single disease, a combination of two diseases, and a combination of several CVDs) using a set of genomic markers provided by the "My gene" service (www.i-gene.ru). The main objective of the study was to identify common and specific genetic markers and perform a comparative analysis of the genetic component of various combinations of cardiovascular diseases.

MATERIALS AND METHODS

The study included three groups of patients with various combinations of CVDs and a control sample of relatively healthy individuals. Patients with various combinations of diseases were selected from a population of more than 800 patients admitted to a specialized cardiology hospital for acute coronary syndrome (ACS). All patients underwent a detailed clinical and laboratory examination for both primary diagnosis and concurrent pathologies. The inclusion criteria for the first sample group were as follows: patients with IHD (myocardial infarction) without any comorbidity ($n = 61$). This group of patients was diagnosed with IHD only, while other diseases, such as AH and T2DM, were excluded. The second sample group included patients with a combination of two diseases: IHD and AH ($n = 180$); patients with any other CVDs were excluded. The third sample group included patients with IHD, AH, T2DM, and HC ($n = 68$). The sample group with a combination of several diseases is hereafter referred to as "CVC syntropy." The remaining patients with a combination of IHD and some other pathology were excluded from the study.

The control group of relatively healthy individuals ($n = 131$) included subjects without CVD in their medical history, with normal blood pressure, and normal echocardiographic and lipid profile parameters. On the basis of these criteria, individuals of this group were selected from an epidemiologicaly collected sample formed for studying IHD risk factors.

Genomic DNA was isolated by standard method of phenol–chloroform extraction [12]. Genotyping was performed using Illumina Custom Genotyping Microarrays iSelectHD microarrays produced by an order of Genoanalitika for the "My gene" genomic service. A microarray comprised 4,416 genetic variants; of them, 2,121 were single nucleotide substitutions in 98 genes of monogenic diseases, 1,913 were polymorphic variants of the nuclear genome, and 382 were polymorphic variants of the mitochondrial genome.

In order to minimize technological errors during genotyping, polymorphic variants and DNA samples were collected using the following criteria:

1) proportion of genotyped single nucleotide variants in one sample should be no less than 98%;

2) proportion of genotyped samples for each polymorphic variant should be more than 98%;

Table 1. Polymorphic variants associated with the "IHD only" phenotype

Chromosome	Gene abbreviation	SNP Localization	SNP	Allele: MAF	Allele: *OR* (95% CI)	Fisher's exact test	Genotypes: *OR* (95% CI)	$P\chi^2$ perm.test
2p24	APOB	missense	rs1367117	A:0.29	A:1.76 (1.08–2.88)	0.022	AA:3.59 (1.25–10.85)	0.01
3q13.1			rs12487066	G:0.23	A:0.47 (0.28–0.79)	0.0026	AA:0.37 (0.18–0.74)	0.0031
4q32	TLR2	intron	rs1898830	G:0.34	A:0.51 (0.31–0.82)	0.0038	AA:0.43 (0.19–0.9)	0.021
5q34	NKX2–5	5'–ends	rs3095870	A:0.39	G:1.83 (1.1–3.12)	0.017	GG:2.09 (1.06–4.17)	0.024
7q36.1			rs7807268	C:0.45	C:1.96 (1.22–3.17)	0.0045	CC:2.73 (1.29–5.82)	0.0065
7q36.2	DPP6	intron	rs10239794	A:0.37	A:1.99 (1.24–3.2)	0.0029	AA:3.35 (1.4–8.26)	0.0041
11q13			rs10896449	G:0.46	A:0.57 (0.35–0.92)	0.016	AA:2.36 (1.16–4.8)	0.011
12p13	KLRB1	intron	rs4763655	A:0.34	G:0.56 (0.35–0.91)	0.014	GG:0.45 (0.21–0.94)	0.031
12q13.11	VDR	intron	rs7975232	A:0.54	A:0.57 (0.35–0.91)	0.013	AA:0.32 (0.11–0.8)	0.009
12q24.31	SCARB1	intron	rs4765623	A:0.25	G:0.57 (0.35–0.95)	0.025	GG:0.4 (0.2–0.8)	0.0068
14q13.3			rs944289	G:0.38	A:0.55 (0.34–0.88)	0.012	AA:0.42 (0.18–0.9)	0.017
18q22.3	CD226	missense	rs763361	A:0.39	A:1.79 (1.12–2.87)	0.012	AA:2.51 (1.11–5.7)	0.018
18q21	NEDD4L	intron	rs3865418	A:0.53	A:0.56 (0.35–0.91)	0.013	AA:0.36 (0.13–0.86)	0.017
22q13	SREBF2	intron	rs2267439	G:0.39	A:2.25 (1.33–3.92)	0.0018	AA:2.32 (1.17–4.67)	0.01

Note. Here and in *Tables 2* and *3*, MAF is the minor (rare) allele frequency; CI is the confidence interval; OR (95% CI) is the odds ratio (95% confidence interval); $P\chi^2$ is the level of significance of the chi–square test for an allele with one degree of freedom; $P\chi^2$ permutation test is the level of significance of the chi–square test for genotypes with two degrees of freedom.

3) genotype identity of any two samples should be less than 98%;
4) compliance of genotypic data of gender identity with an individual's gender;
5) compliance with the Hardy–Weinberg equilibrium in a pooled sample at a statistically significance level of $P > 10^{-8}$and in the control group at $P > 0.05$;
6) frequency of a rare allele is more than 5%; and
7) polymorphic variants are localized in autosomes.

A total of 407 genomic DNA samples and 1,400 polymorphism variants were selected for further analysis after genotyping quality control with subsequent exclusion of single nucleotide substitutions of monogenic disease genes and single nucleotide variants localized in sex chromosomes and mitochondria.

GenABEL software packages for the statistical environment R (version 2.14.2) were used to analyze associations. The statistical significance level calculated by random permutations with 10,000 replications (permutation test) was considered to be equal to $P<0.05$. The network analysis of intergenic interactions was performed using the Search Tool for the Retrieval of the Interacting Genes/Proteins platform [13]. The WEB–based Gene Set Analysis Toolkit was used for the annotation of metabolic and signaling pathways [14]. The predictive efficiency of the polymorphic variants that demonstrated a statistically significant association with the studied phenotypes was analyzed by standard AUC (Area Under Curve) calculations.

RESULTS

The main objective of the study was to identify common and specific genes for the studied phenotypes: a single disease (IHD), a combination of two diseases (IHD and AH), and a complex "syntropy" phenotype, which refers to a combination of several cardiovascu-

Table 2. Polymorphic variants associated with the "IHD and AH" phenotype

Chromosome	Gene abbreviation	SNP Localization	SNP	Allele: MAF	Allele: *OR* (95% CI)	Fisher's exact test	Genotypes: *OR* (95% CI)	$P\chi^2$ perm.test
1q42			rs801114	C:0.39	C:0.66 (0.46–0.95)	0.025	CC:0.3 (0.12–0.7)	0.0018
2q35	XRCC5	3'–end	rs2440	A:0.33	A:1.57 (1.1–2.26)	0.012	AA:2.48 (1.12–5.93)	0.017
6p21.3	BTNL2	missense	rs2076530	G:0.39	G:1.57 (1.1–2.23)	0.01	GG:1.96 (1.02–3.92)	0.034
6q23			rs10499194	A:0.35	G:1.52 (1.04–2.22)	0.026	GG:2.07 (1.25–3.44)	0.0037
6q23			rs13207033	A:0.35	G:1.49 (1.02–2.18)	0.033	GG:2.02 (1.22–3.36)	0.004
7p12	EGFR	intron	rs763317	A:0.42	G:0.67 (0.47–0.95)	0.022	GG:0.5 (0.29–0.88)	0.011
7q35	CNTNAP2	intron	rs7794745	T:0.36	A:0.69 (0.48–0.98)	0.032	AA:0.52 (0.31–0.87)	0.011
12q24.31	SCARB1	intron	rs4765623	A:0.25	A:0.63 (0.43–0.93)	0.017	AA:0.49 (0.3–0.82)	0.0038
15q26			rs2398162	G:0.4	A:0.68 (0.47–0.97)	0.033	AA:0.43 (0.19–0.93)	0.027
17cen–q21.3	HNF1A	intron	rs4430796	G:0.36	G:1.59 (1.12–2.28)	0.0077	GG:2.12 (1.09–4.3)	0.024
17q24.3			rs6501455	G:0.32	A:1.52 (1.05–2.19)	0.023	AA:2.4 (1.08–5.75)	0.024
20p11			rs1160312	G:0.42	G:1.56 (1.1–2.22)	0.011	GG:2.21 (1.16–4.38)	0.013
22q12.1	SEZ6L	missense	rs663048	A:0.19	C:0.57 (0.38–0.87)	0.0082	CC:0.53 (0.31–0.88)	0.011

Note. See Table 1 note.

lar diseases. To identify the genes associated with a particular phenotype (disease or combination of diseases), we compared the frequencies of the alleles and genotypes in patients and in the control group (case–control study), calculated odds ratios (OR), and evaluated the prognostic significance of genetic markers with statistically significant associations. All genetic markers/genes were classified according to association with a particular pathway or class of genes. The WebGestalt (WEB–based GEne SeT AnaLysis Toolkit) service was used to annotate signaling and metabolic pathways.

Tables 1–3 show the nomenclature and key statistics of the genetic variants whose allele frequencies were different in the study and control group: chromosomal localization, rs–number, rare allele frequency, location relative to the nearest genes, and OR value. *Table 4* shows predictive values of the polymorphic variants associated with a certain phenotype: disease or disease combination.

Below, we present the results obtained for each of the studied phenotypic groups.

Genetic markers associated with the IHD phenotype

A total of 14 polymorphic variants are associated with the "IHD only" phenotype (*Table 1*). Of them, two are missense substitutions: rs1367117 in the *APOB* gene and rs763361 in the *CD226* gene. One, rs3095870, is located near the 5'–end of the *NKX2–5* gene. Seven variants are located in intronic regions: rs1898830 in the *TLR2* gene, rs10239794 in *DPP6*, rs4763655 in *KLRB1*, rs7975232 in *VDR*, rs4765623 in *SCARB1*, rs3865418 in *NEDD4L*, and rs2267439 in *SREBF2*. Four genetic markers are located in intergenic spaces: rs12487066, rs7807268, rs10896449, and rs944289 (*Table 1*). The prognostic value of markers associated with this phenotype varied from 0.62 for rs12487066 to 0.57 for rs1367117 (*Table 4*).

On the basis of their primary biological function in the body, several groups of associated genes were selected to analyze the structure of a hereditary component of the studied phenotypes. For example, gene variants associated with the "IHD only" phenotype can be arbitrarily subdivided **into three groups**: 1) genes responsible for the lipid metabolism, 2) genes associat-

Table 3. Polymorphic variants associated with the "CVC syntropy" group

Chromosome	Gene abbreviation	Localization	SNP	Allele: MAF	Allele: *OR* (95% CI)	Fisher's exact test	Genotypes: *OR* (95% CI)	$P\chi^2$ perm. test
1q21	APOA2	5'–end	rs5082	G:0.47	A:1.83 (1.15–2.93)	0.0082	AA:2.42 (1.22–4.82)	0.007
2q31.3	ITGA4	synonymous substitution	rs1143674	A:0.39	A:1.76 (1.12–2.78)	0.011	AA:2.84 (1.27–6.47)	0.0069
2q32	KLF7	5'–end	rs7568369	A:0.28	C:0.45 (0.28–0.73)	0.00084	CC:0.34 (0.16–0.68)	0.0007
7q34	TAS2R38	missense	rs1726866	G:0.48	A:1.65 (1.04–2.63)	0.028	AA:2.42 (1.22–4.82)	0.0073
		missense	rs10246939	G:0.48	A:1.65 (1.04–2.63)	0.028	AA:2.42 (1.22–4.82)	0.0073
8q22.1	RAD54B	synonymous substitution	rs2291439	G:0.42	G:0.6 (0.37–0.97)	0.032	GG:0.25 (0.06–0.77)	0.011
9p21	MTAP	intron	rs7023329	G:0.52	A:1.95 (1.23–3.11)	0.0031	AA:2.38 (1.2–4.76)	0.0079
9p21.3			rs1333048	C:0.45	A:0.6 (0.38–0.94)	0.022	AA:0.37 (0.15–0.87)	0.018
9p21.3			rs1333049	G:0.44	C:0.61 (0.38–0.95)	0.028	CC:0.39 (0.16–0.88)	0.022
16q21	CETP	5'–end	rs183130	A:0.35	G:2.04 (1.21–3.51)	0.006	GG:2.19 (1.13–4.32)	0.013
17q24.3			rs6501455	G:0.32	G:2.06 (1.3–3.29)	0.0015	GG:3.91 (1.56–10.33)	0.0016
19p13.2	LDLR	intron	rs2738446	G:0.34	C:0.61 (0.38–0.97)	0.032	CC:0.38 (0.18–0.77)	0.0045
		synonymous substitution	rs688	A:0.34	G:0.61 (0.38–0.97)	0.032	GG:0.38 (0.18–0.77)	0.0048
22q12.1	SEZ6L	missense	rs663048	A:0.19	C:0.52 (0.31–0.88)	0.01	CC:0.49 (0.25–0.95)	0.027

Note. See Table 1 note.

ed with immunity, and 3) genes specific to the cardiac function.

The group of genes involved in the **lipid metabolism** includes *APOB*, *SREBF2*, and *SCARB1*. For example, the *APOB* gene product is the main apolipoprotein of chylomicron and LDLs. Polymorphic variants and some mutations of the *APOB* gene are known to be associated with HC and a high risk of IHD [15, 16].

The *SREBF2* gene product is a transcriptional activator required to maintain lipid homeostasis. In particular, this gene regulates the *LDLR* gene, which encodes the LDL receptor and also affects the cholesterol level and synthesis of fatty acids [17].

The *SCARB1* gene encodes a receptor of the various ligands involved in the lipid metabolism, including phospholipids, cholesterol esters, lipoproteins, and phosphatidylserine. Presumably, the product of this gene is also involved in the phagocytosis of apoptotic cells via its phosphatidylserine–binding activity, as well as in the uptake of cholesterol esters by HDLs [18].

The group of genes associated with **immunity** regulation includes *TLR2*, *KLRB1*, *CD226*, and *VDR*. The *TLR2* gene interacts with the *LY96* and *TLR1* genes and plays an important role in the formation of the innate immune response to bacterial lipoproteins and other components of the bacterial wall. It is activated by the MYD88 and TRAF6 factors, which leads to the activation of cytokines by NF–kB and an inflammatory response. The product of this gene may also play a role in apoptosis [19]. Structural polymorphisms in this gene are associated with susceptibility to leprosy and some infectious diseases [20].

The *KLRB1* gene inhibits natural killer cells (cytotoxicity cells). It is expressed in T–lymphocytes of peripheral blood, primarily in T–cells with antigenic memory [21].

The *CD226* gene encodes a receptor involved in intercellular adhesion, lymphocyte signaling, and cytotoxicity and secretion of lymphokines by cytotoxic T–lymphocytes and NK–cells [22].

Table 4. Predictive efficiency of polymorphic variants associated with the "IHD only," "IHD and AH," and "CVC syntropy" phenotypes

"IHD only"		"CVC syntropy"		"IHD and AH"	
SNP	AUC	SNP	AUC	SNP	AUC
rs1367117	0.57	rs801114	0.56	rs5082	0.60
rs12487066	0.62	rs2440	0.55	rs1143674	0.59
rs1898830	0.59	rs2076530	0.55	rs7568369	0.63
rs3095870	0.59	rs10499194	0.59	rs1726866	0.60
rs7807268	0.60	rs13207033	0.59	rs10246939	0.60
rs10239794	0.59	rs763317	0.57	rs2291439	0.57
rs10896449	0.60	rs7794745	0.58	rs7023329	0.60
rs4763655	0.61	rs4765623	0.59	rs1333048	0.58
rs7975232	0.59	rs2398162	0.55	rs1333049	0.58
rs4765623	0.61	rs4430796	0.56	rs183130	0.60
rs944289	0.59	rs6501455	0.58	rs6501455	0.59
rs763361	0.58	rs1160312	0.56	rs2738446	0.60
rs3865418	0.59	rs3843763	0.58	rs688	0.60
rs2267439	0.60	rs663048	0.58	rs663048	0.59

Note. AUC is the area under the curve.

The *VDR* gene encodes the nuclear vitamin D3 receptor; however, this protein is well known to function also as a receptor of secondary bile acid, lithocholic acid. The vitamin D3 receptor is involved in the mineral metabolism (calcium exchange), although it may also regulate a number of other metabolic pathways; in particular, the immune response [23].

The third group includes genes associated with various metabolic and signaling pathways; however, these genes are involved in specific cardiac functions. Two of them are associated with the transmembrane transport of electrolytes and the **cardiac conduction system** (*NEDD4L* and *DPP6*), and the third gene, *NKX2–5*, encodes the heart–specific **transcription factor**.

The *NEDD4L* gene plays an important role in the epithelial sodium transport via control of the expression of sodium channels on epithelial cells surface. The product of this gene was shown to be involved in the formation and transmission of the membrane potential along the cardiac conduction system [24]. Dunn *et al* [25] have demonstrated the association of some *NEDD4L* polymorphic variants with essential hypertension. The A–allele of the rs3865418 polymorphism is associated with high diastolic pressure in the Chinese population (OR = 1.31 (1.04–1.67), P = 0.025) [26]. In the present study, the A–allele and the AA genotype demonstrated a protective effect against IHD (*Table 2*).

The *DPP6* gene encodes a membrane protein (dipeptidyl aminopeptidase–likeprotein 6) which is a member of the S9B serine protease family. It can bind to specific voltage–dependent potassium channels, thereby affecting their expression, biophysical properties, and channel activity [27]. Defects in the *DPP6* gene lead to familial paroxysmal ventricular fibrillation type 2 [28].

The *NKX2–5* gene, which is expressed exclusively in the heart, encodes the homeobox–containing transcription factor. This factor is directly involved in the formation and development of the heart *in utero* [29]. Mutations in the *NKX2–5* gene cause various heart defects: from small anomalies to Fallot's tetralogy (MIM:108900,187500).

Genetic markers associated with the "IHD and AH" phenotype

Among the studied genetic markers, 13 were associated with the "IHD and AH" phenotype (*Table 2*). Two of them are missense substitutions (rs2076530 in the *BTNL2* gene and rs663048 in the *SEZ6L* gene), four are variants in introns (rs763317 in *EGFR*, rs7794745 in *CNTNAP2*, rs4765623 in *SCARB1*, rs4430796 in *HNF1A*), and six are located in intergenic regions (rs801114, rs10499194, rs13207033, rs2398162, rs6501455, and rs1160312).

The predictive value of the genetic markers evaluated by the AUC parameter (area under the ROC–curve) varied from 0.59 to 0.55 (*Table 4*).

Notably, it is difficult to associate this set of genes with any particular pathway and to classify it in a similar way as for the genes associated with the "IHD only" phenotype. However, it is noteworthy that several

genes are associated with **immunity and susceptibility to cancer and radiosensitivity**.

For example, the *BTNL2* gene is a regulator of immunity: its product, the butyrophilin–like protein 2, belongs to the family of B7 receptors, which function as T–cell–stimulating molecules by affecting the production of cytokines and regulating T–cell proliferation. Polymorphic variants of this gene are associated with an increased risk of prostate cancer, Kawasaki disease, as well as damage to coronary arteries in this disease [30]. The association of variants of this gene with susceptibility to tuberculosis was demonstrated [31]. According to the data of a genome–wide study [32], variations in *BTNL2* are also associated with the development of coronary atherosclerosis.

Genes in some way associated with the oncogenesis and immune system include *XRCC5*, *EGFR*, *HNF1A*, and *SEZ6L*. The *XRCC5* gene encodes an 80 kDa subunit of the Ku protein. The heterodimeric protein Ku is an ATP–dependent DNA helicase II, which is involved in DNA repair by non–homologous end joining. The Ku protein is involved in the recombination required to generate a diversity of antigen–binding sites of antibodies in mammals. In addition, Ku–proteins are involved in telomeric length maintenance and telomeric silencing [33]. A rare microsatellite polymorphism of this gene is known to be associated with oncopathology and radiosensitivity.

A protein encoded by the *EGFR* gene is a transmembrane glycoprotein, the epidermal growth factor receptor [34]. Defects in this gene lead to disruption of apoptosis; the association of this gene with carcinogenesis has been extensively studied [35]. The A–allele of rs763317, which is considered to be a lung cancer risk allele, is adverse to the "IHD and AH" phenotype.

The *HNF1A* gene product is a transcriptional activator that regulates the tissue–specific expression of several genes, particularly in pancreas and liver cells [36]. Defects in this gene lead to the familial form of liver adenomas (MIM:142330), MODY3–type diabetes mellitus (MIM:600496), and insulin–dependent type 2 diabetes mellitus (MIM:612520). We demonstrated that the G–allele, which is a T2DM risk factor, is unfavorable to the development of the combined IHD and AH pathology.

The *SEZ6L* gene function is poorly understood. It is assumed to be associated with specific functions of the endoplasmic reticulum. The gene has been extensively studied, because it is expressed in the brain tissue and lungs but not in lung cancer cells [37]. Data on an association between polymorphic variants of *SEZ6L* and IHD were reported [38], but the mechanism of this relationship is not known. Our data demonstrate that the lung cancer risk allele is also an unfavorable factor for IHD in combination with AH.

We found that the *CNTNAP2* gene is associated with the cardiovascular phenotype (which is unusual, given the known functions of the gene). The *CNTNAP2* gene encodes a transmembrane protein belonging to the family of neurexins, which act as cell–adhesion molecules and receptors in the nervous system. The CNTNAP2 protein performs its major functions in myelinated axons, enabling the interaction between neurons and glia. It is also responsible for the localization of potassium channels and differentiation of axons into separate functional subdomains. *CNTNAP2* gene variants are associated with a wide range of mental disorders, including autism, schizophrenia, mental retardation, dyslexia, and disruption of language functions [39]. The A–allele is a risk factor for schizophrenia but is a protective factor in the case of the "IHD and AH" phenotype.

As we have indicated, the *SCARB1* gene is associated with lipid metabolism. This gene is "common" for the "IHD" and "IHD and AH" phenotypes.

The functions of several genetic variants located in intergenic regions require further analysis. An association with a disease may be explained by a linkage disequilibrium with some other genes/variants directly involved in the formation of the disease or by an independent regulatory action. According to some studies, the intergenic variant rs1160312A is associated with hair loss, but at the same time, it is protective in the case of IHD combined with AH. According to a Wellcome Trust large–scale study conducted using the "case–control" approach, the A–allele of rs2398162 of this gene is a risk factor for essential hypertension; in our work, however, this allele is protective.

Genetic markers associated with the "CVC syntropy" phenotype

A total of 14 markers are associated with CVC syntropy (*Table 3*). Of these, three are missense substitutions: rs1726866 and rs10246939 in the *TAS2R38* gene and rs66048 in the *SEZ6L* gene; three are located near the 5'–region of genes: rs5082 of the *APOA2* gene, rs7568369 in the 5'–region of the *KLF7* gene, and rs183130 in the 5'–region of the *CETP* gene; three variants are synonymous substitutions: rs1143674 in the *ITGA4* gene, rs2291439 in the *RAD54B* gene, and rs688 in the *LDLR* gene; two variants are located in intronic regions: rs2738446 in the *LDLR* gene and rs7023329 in the *MTAP* gene; three markers are located in intergenic spaces: rs1333048 and rs1333049 in the 9p21.3 region and rs6501455 localized in 17q24.3 between the *KCNJ2* and *SOX9* genes, at approximately the same distance (*ca.* 1 million bp).

The genes associated with the "CVC syntropy" phenotype can be assigned to one of the following groups:

a) responsible for **lipid metabolism impairment**, b) genes of **immunity and inflammation**, c) **genes with miscellaneous functions**.

The genes *CETP*, *LDLR*, and *APOA2* are associated with the **lipid metabolism**. The *CETP* gene encodes a transporter of insoluble cholesterol esters. *CETP* polymorphic variants affect the level of high density lipoproteins (HDLs). In particular, mutations in this gene are associated with the development of hyper−α−lipoproteinemia, accompanied by high HDL levels (MIM:143470). The G−allele of rs183130 is associated with a low level of cholesterol in HDLs [40]. We demonstrated its involvement in the formation of the "CVC syntropy" phenotype.

The *LDLR* gene encodes a protein that functions as an intermediary of endocytosis of cholesterol−rich LDLs [41]. Variants of the *LDLR* gene, rs2738446 and rs688, are in linkage disequilibrium. In the Framingham study, rs688 is associated with IHD but is not directly related to such an important endophenotype as the level of lipoproteins [42]. According to some studies, rs688 in the *LDLR* gene may be associated with the onset of IHD via modulation of the coagulation factor VIII activity [43].

The *APOA2* gene encodes a HDL protein particle. Mutations in *APOA2* cause familial HC [44]. According to some reports, the AA genotype of rs5082 in the *APOA2* gene is associated with a high risk of IHD in males. In our work, the AA genotype was associated with a high risk of the "CVC syntropy" phenotype.

On the basis of their main functions, the genes *ITGA4*, *MTAP*, and *CDKN2V* may be assigned to a group of **immunity and inflammation** genes. The *ITGA4* gene encodes a protein of the integrinα−chain. Integrins are the most important intercellular adhesion molecules. They are heterodimeric membrane receptors consisting of α− and β−chains and functioning as cell−substrate and cell−cell adhesion receptors. Increased adhesion is known to be important in endothelial dysfunction in the case of inflammation, arteriosclerosis, and other pathological processes [45, 46]. There are no data on the association of rs1143674 in the *ITGA4* gene with cardiovascular phenotypes; however, it is known that this variant is associated with alternative splicing. The rs1143674 A−allele is associated with an increased risk of autism [47].

The MTAP gene is located in close proximity to *CDKN2A/2B* [48]. The *MTAP* and *CDKN2B* genes were shown to be expressed in cells and tissues involved in the development of atherosclerosis, including endothelial cells, macrophages, and smooth muscle cells of coronary arteries [49]. The *MTAP* gene was reported to be capable of acting as a tumor growth suppressor [50].

Four other genes, *RAD54B*, *SEZ6L*, *TAS2R38*, and *KLF7* are genes with miscellaneous functions. The product of *RAD54B* is involved in DNA repair and mitotic recombination. Mutations in this gene may be a cause of colon cancer and lymphomas [51]. Data on the functional role of the rs2291439 variant are limited, and there is no information on an association between this marker and diseases of the cardiovascular system.

The *TAS2R38* gene encodes a receptor responsible for bitter taste reception [52]. *TAS2R38* gene haplotypes define up to 85% of the variance in the sensitivity to flavors, from bitter to sweet [53]. Carriership of certain *TAS2R38* variants affects food preferences, for example, for carbohydrate−rich or lipid−rich food, which is considered a risk factor for the development of metabolic disorders and CVDs. Alleles of the gene that are associated with the syntropy phenotype are included in the haplotype responsible for the inability to feel the bitter taste; the same alleles are associated with the development of T2DM.

The *KLF7* gene product belongs to a group of transcriptional activators and is expressed in many body tissues. A study of animal models demonstrated that *KLF7* specifically regulates the expression of *TrkA*, which encodes the neurotrophic tyrosine kinase receptor type 1. A nonsense mutation of the *KLF7*gene leads to disruption of many nociceptive sensory receptors [54]. Investigation of *KLF7* gene polymorphisms revealed an association with T2DM risk in the Japanese

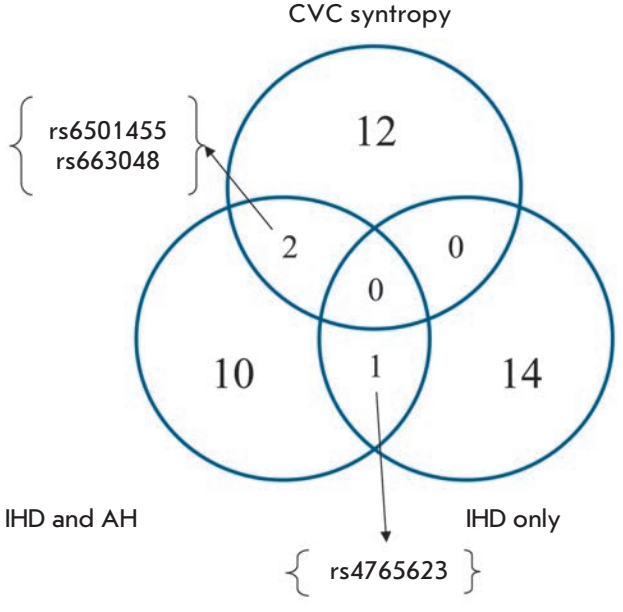

Fig. 1. Venn diagram of genetic markers associated with the studied phenotypes: common and specific variants

population and a protective effect against obesity in the Danish population [55, 56].

Characterization of the *SEZ6L* gene is provided above, since this gene is associated with the "IHD and AH" phenotype.

The functional significance of polymorphisms associated with the studied phenotype and located in intergenic regions remains unknown. According to [57], rs6501455 is associated with prostate cancer, but it is a protective allele for CVC syntropy. This gene is located on chromosome 17, *ca.* 1 million bp away from the *SOX9* and *CALM2P1* genes, with approximately more than 40,000 SNPs being identified in this same region. Importantly, almost all polymorphisms in this genomic region, which are present in the PubMed database, are associated with a particular CVD.

DISCUSSION

The objective of this study was to identify common and specific genes for three phenotypes: a single disease, a combination of two diseases, and a combination of CVDs. *Figure 1* shows the number of genes that are common and specific to the three phenotypes. For example, **two common genes** were identified for syntropy (a combination of several diseases: IHD, AH, T2DM, and HC in this study) and a combination of two diseases (IHD and AH); **one common gene** was identified between the "IHD and AH" and "IHD only" phenotypes; whereas there were **no common genes** between "IHD only" and "CVC syntropy" among the studied genes. A total of 14 specific genetic variants unique to the "IHD only" phenotype were identified: 12 were unique to "CVC syntropy," and 10 were unique to "IHD and AH."

In the case of comorbidities, it is important to know not only the proportion of common and specific genes, but also the profile of associated variants (their physiological role in the body), since the profile may indicate the most important pathways involved in the development of a pathology and define approaches to treatment. As seen from the associative profile provided for

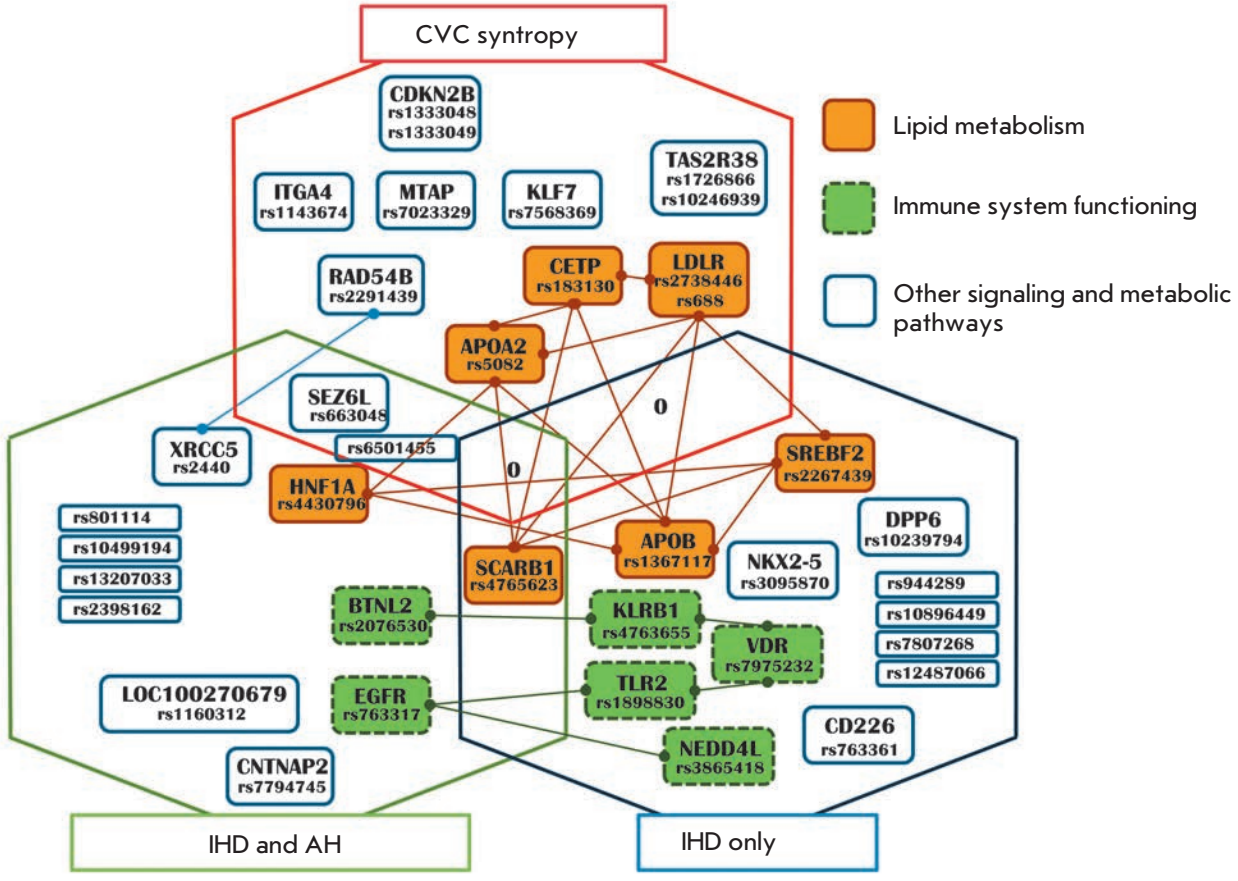

Fig. 2. Venn diagram of the relationships between all phenotype–associated genes and polymorphic variants with allowance for their association with a functional class. Intergenic relationships were developed based on the data of the SearchTool for the Retrieval of Interacting Genes/Proteins (STRING) online service

each studied phenotype, the "IHD only" phenotype is characterized by genes that regulate the lipid metabolism, genes associated with immunity, and genes specific to the heart function, such as the genes that control the cardiac conduction system.

Examination of the profile for a combination of two diseases, one of which is IHD, reveals a markedly different picture, and the gene variants associated with this phenotype seem rather unexpected; it is hard to relate a set of genes to a particular pathway and classify them similarly to the genes associated with the "IHD only" phenotype. Notably, several genes of immunity and predisposition to cancer are associated with the phenotype of a two–disease combination.

The genetic profile for the CVC syntropy phenotype appears to be logical in general; it includes genes responsible for lipid metabolism impairment and genes that control the immunity and inflammatory response (and genes with miscellaneous functions).

It should be noted that our analysis of a wide panel of markers (1,400) associated, according to the published data, with widespread diseases revealed previously unknown relationships (as it usually occurs in genome–wide studies); e.g., the association of the genes of cancer and neurological and psychiatric diseases with cardiovascular phenotypes.

A descriptive analysis of the functions of associated genes is supplemented by a classificatory network analysis of intergenic interactions that enables to retrace interaction chains for a set of genes, a STRING–analysis (*Fig. 2*). This analysis allows a formal assignment of particular genes to the most important metabolic pathways. This formal analysis revealed that the genes associated with immune function and lipid metabolism genes predominate among the IHD genes. In the case of the IHD and AH phenotype, two genes were related to the immune system, and two genes were associated with lipid metabolism. That is the *SCARB1* lipid metabolism gene that is common for these two pathologies. Among the CVC sintropy–associated genes, three genes were identified as genes related to lipid metabolism. According to the STRING analysis, the remaining genes were not related to a specific metabolic pathway.

CONCLUSION

Our findings indicate that lipid metabolism genes are involved in the formation of all variants of diseases (including various combinations) of the cardiovascular continuum, while the regulatory genes of the immune system are specific to IHD and do not participate in the development of CVC syntropy.

Coming back to the discussion of the role of syntropy (non–random combination of diseases) and the widespread phenomenon of comorbidity, we identified an additional complexity in the use of the data of genetic association studies in practical (diagnostic) tests for predisposition to common diseases. The genetic profile for a combination of several diseases can be markedly different from the profile for isolated forms. Identification of syntropic genes (influencing the development of a complex syntropyphenotype) is of interest not only for diagnostic purposes, but also, first and foremost, for predicting (or explaining present facts) the effect of some medications in the case of several, concurrent diseases. ●

This work was supported by Genoanalitika, the Russian Foundation for Basic Research (grant № 13–04–02162), and a grant from the President of the Russian Federation for Leading Scientific Schools (NSH–5096.2014.4).

REFERENCES

1. Feinstein A.R. The Pre–therapeutic classification of comorbidity in chronic disease. // J. Chronic Disease. 1970. V. 23. № 7. P.455–468.
2. Valderas J.M. Increase clinical, community and patient–centered health research. // J. Comorbidity. 2013 V. 3. № 2. P. 41–44.
3. Valderas J.M., Starfield B., Sibbald B., Salisbury C., Roland M. Defining comorbidity: implications for understanding health and health services. // Ann. Fam. Med. 2009. № 7. P. 357–363
4. Puzyrev V.P., Makeeva O.A., Freidin M.B. // Pers. Med. 2010. V. 7. P. 399–405.
5. Cookson W. The immunogenetics of asthma and ezema: a new focus on the epithelium. // Nat. Rev. Immunol. 2004. V. 4. P. 978–988.
6. Zhernakova A., van Diemen C.C., Wiymenda C. Detecing shared pathogenesis from shared genetics of immune–related desease. // Nat. Rev. Genet. 2009. V. 10. № 1. P. 43–55
7. Doolan A., Donaghue K., Fairchild J. Wong M., Williams A.J. Use of HLA Typing in diagnosing celiac disease in patients with type I diabetes. // Diabetes Care. 2005. V. 28. P. 806–809
8. Harvey M., Bellean P., Barden N. Gene interactions in depression: pathways out of darkness. // Trends Genet. 2007. V. 23. P. 547–556.
9. Dzau V., Braunwald E. // Am. Heart J. 1991. V. 121. P. 1244–1262.
10. Dzau V.J., Antman E.M., Black H.R., Hayes D.L., Manson J.E., Plutzky J., Popma J.J., Stevenson W. // Circulation. 2006. V. 144. P. 2850–2870.
11. Puzyrev V.P., Makeeva O.A., Golubenko M.V. // Vestnik VOGiS. 2006. V. 10. № 3. P. 479– 491.
12. Sambrook J., Russell D.W. Molecular cloning: a laboratory manual. 3rd ed. N.Y.: Cold Spring Harbor Laboratory Press. 2001. 2100 p.
13. http://string–db.org/
14. http://bioinfo.vanderbilt.edu/webgestalt/

15. Pullinger C.R., Hennessy L.K., Chatterton J.E., Liu W., Love J.A., Mendel C.M., Frost P.H., Malloy M.J., Schumaker V.N., Kane J.P. // J. Clin. Invest. 1995. V. 95. P. 1225–1234.
16. Soria L., Ludwig E., Clarke H., Vega G., Grundy S., McCarthy B. // Proc. Natl. Acad. Sci. U S A. 1989. V. 86. P. 587–591.
17. Irisawa M., Inoue J., Ozawa N., Mori K., Sato R. // J. Biol. Chem. 2009. V. 284. № 42. P. 28995–29004.
18. Scarselli E., Ansuini H., Cerino R., Roccasecca R.M., Acali S., Filocamo G,. Traboni C., Nicosia A., Cortese R., Vitelli A. // EMBO J. 2002. V. 21. № 19. P. 5017–5025.
19. Yang R.B., Mark M.R., Gray A., Huang A., Xie M.H., Zhang M., Goddard A, Wood W.I., Gurney A.L., Godowski P.J. // Nature. 1998. V. 395. № 6699. P. 284–288.
20. Bochud P.Y., Magaret A.S., Koelle D.M., Aderem A., Wald A. // J. Infect. Dis. 2007. V. 196. № 4. P. 505–509.
21. Lanier L.L., Chang C., Phillips J.H. // J. Immunol. 1994. V. 153. № 6. P. 2417–2428.
22. Shibuya A., Campbell D., Hannum C., Yssel H., Franz-Bacon K., McClanahan T., Kitamura T., Nicholl J., Sutherland G.R., Lanier L.L., et al. // Immunity. 1996. V. 4. № 6. P. 573–581.
23. Rochel N., Wurtz J.M., Mitschler A., Klaholz B., Moras D. // Mol. Cell. 2000. V. 5. № 1. P. 173–179.
24. van Bemmelen M.X., Rougier J.S., Gavillet B., Apothéloz F., Daidié D., Tateyama M., Rivolta I., Thomas M.A., Kass R.S., Staub O., et al. // Circ. Res. 2004. V. 95. № 3. P. 284–291.
25. Dunn D.M., Ishigami T., Pankow J., von Niederhausern A., Alder J., Hunt S.C., Leppert M.F., Lalouel J.M., Weiss R.B. // J. Hum. Genet. 2002. V. 47. № 12. P. 665–676.
26. Wen H., Lin R., Jiao Y., Wang F., Wang S., Lu D., Qian J., Jin L., Wang X. // Clin. Exp. Hypertens. 2008. V. 30. № 2. P. 87–94.
27. Strop P., Bankovich A.J., Hansen K.C., Garcia K.C., Brunger A.T. // J. Mol. Biol. 2004. V. 343. № 4. P. 1055–1065.
28. Alders M., Koopmann T.T., Christiaans I, Postema P.G., Beekman L., Tanck M.W., Zeppenfeld K., Loh P., Koch K.T., Demolombe S., et al. // Am. J. Hum. Genet. 2009. V. 84. № 4. P. 468–476.
29. Turbay D., Wechsler S.B., Blanchard K.M., Izumo S. // Mol. Med. 1996. V. 2. № 1. P. 86–96.
30. Hsueh K.C., Lin Y.J., Chang J.S., Wan L., Tsai F.J. // Eur. J. Pediatr. 2010. V. 169. № 6. P. 713–719.
31. Lian Y., Yue J., Han M., Liu J., Liu L. // Infect. Genet. Evol. 2010. V. 10. № 4. P. 517–521.
32. Lu X., Wang L., Chen S., He L., Yang X., Shi Y., Cheng J., Zhang L., Gu C.C. Huang J. et al. // Nat Genet. 2012. V. 44. № 8. P. 890–894.
33. Boulton S.J., Jackson S.P. EMBO J. 1998. V. 17. № 6. P. 1819–1828.
34. Galisteo M.L., Dikic I., Batzer A.G., Langdon W.Y., Schlessinger J. // J. Biol. Chem. 1995. V. 270. № 35. P. 20242–20245.
35. Rikova K., Guo A., Zeng Q., Possemato A., Yu J., Haack H., Nardone J., Lee K., Reeves C., Li Y., et al. // Cell. 2007. V. 14. №. 131. № 6. P.1190–1203.
36. Chi Y.I., Frantz J.D., Oh B.C., Hansen L., Dhe-Paganon S., Shoelson S.E. // Mol. Cell. 2002. V. 10. № 5. P. 1129–1137.
37. Suzuki H., Gabrielson E., Chen W., Anbazhagan R., van Engeland M., Weijenberg M.P., Herman J.G., Baylin S.B. // Nat. Genet. 2002. V. 31. № 2. P. 141–149.
38. Bressler J., Folsom A.R., Couper D.J., Volcik K.A., Boerwinkle E. // Am. J. Epidemiol. 2010. V. 171. № 1. P. 14–23.
39. Rodenas-Cuadrado P., Ho J., Vernes S.C. // Eur. J. Hum. Genet. 2014. V. 22. P. 171–178.
40. Spirin V., Schmidt S., Pertsemlidis A., Cooper R.S., Cohen J.C., Sunyaev S.R // Am J Hum Genet. 2007. V. 81. № 6. P. 1298–1303.
41. Francke U., Brown M.S., Goldstein J.L. // Proc. Natl. Acad. Sci. U S A. 1984. V. 81. № 9. P. 2826–2830.
42. Zhu H., Tucker H.M., Grear K.E., Simpson J.F., Manning A.K., Cupples L.A., Estus S. // Hum. Mol. Genet. 2007. V. 16. № 14. P. 1765–1772.
43. Martinelli N., Girelli D., Lunghi B., Pinotti M., Marchetti G., Malerba G., Pignatti P.F., Corrocher R., Olivieri O., Bernardi F. // Blood. 2010. V. 116. № 25. P. 5688–5697.
44. Takada D., Emi M., Ezura Y., Nobe Y., Kawamura K., Iino Y., Katayama Y., Xin Y., Wu L.L., Larringa-Shum S., et al. // J. Hum. Genet. 2002. V. 47. P. 656–664.
45. Vassiliadis E., Barascuk N., Didangelos A., Karsdal M.A. // Biomark. Insights. 2012. №7 P.45–57.
46. Brachtl G., Sahakyan K., Denk U., Girbl T., Alinger B., Hofbauer S.W., Neureiter D., Hofbauer J.P., Egle A., Greil R., et al. // PLoS One. 2011. V. 6. № 8. e23758.
47. Conroy J., Cochrane L., Anney R.J., Sutcliffe J.S., Carthy P., Dunlop A., Mullarkey M., O'hici B., Green A.J., Ennis S., et al. // Am. J. Med. Genet. B. Neuropsychiatr. Genet. 2009. V. 150B. № 4. P. 535–544.
48. Pasmant E., Laurendeau I., Heron D., Vidaud M., Vidaud D., Bieche I. // Cancer Res. 2007. V. 67. P. 3963–3969.
49. Broadbent H.M., Peden J.F., Lorkowski S., Goel A., Ongen H., Green F., Clarke R., Collins R., Franzosi M.G., Tognoni G., et al. // Hum. Mol. Genet. 2008. V. 17. P. 806–814.
50. Behrmann I., Wallner S., Komyod W., Heinrich P.C., Schuierer M., Buettner R., Bosserhoff A.K. // Am. J. Pathol. 2003. V. 163. P. 683–690.
51. Miyagawa K., Tsuruga T., Kinomura A., Usui K., Katsura M., Tashiro S., Mishima H., Tanaka K. // EMBO J. 2002. V. 21. №1–2. P. 175–180.
52. Zhang Y., Hoon M.A., Chandrashekar J., Mueller K.L., Cook B., Wu D., Zuker C.S., Ryba N.J. // Cell. 2003. V. 112. № 3. P. 293–301.
53. Kim U.K., Jorgenson E., Coon H., Leppert M., Risch N., Drayna D. // Science. 2003. V. 299(5610). P. 1221–1225.
54. Lei L., Laub F., Lush M., Romero M., Zhou J., Luikart B., Klesse L., Ramirez F., Parada L.F. // Genes. Dev. 2005. V. 19. № 11. P. 1354–1364.
55. Kanazawa A., Kawamura Y., Sekine A., Iida A., Tsunoda T., Kashiwagi A., Tanaka Y., Babazono T., Matsuda M., Kawai K., et al. // Diabetologia. 2005. V. 48. № 7. P. 1315–1322.
56. Zobel D.P., Andreasen C.H., Burgdorf K.S., Andersson E.A., Sandbaek A., Lauritzen T., Borch-Johnsen K., Jorgensen T., Maeda S., Nakamura Y., et al. // Eur. J. Endocrinol. 2009. V. 160. № 4. P. 603–609.
57. Gudmundsson J., Sulem P., Steinthorsdottir V., Bergthorsson J.T., Thorleifsson G., Manolescu A., Rafnar T., Gudbjartsson D., Agnarsson B.A., Baker A., et al. // Nat. Genet. 2007. V. 39. № 8. 977–983.

Regulation of Human Adenovirus Replication by RNA Interference

N. A. Nikitenko[1], T. Speiseder[2], E. Lam[2], P. M. Rubtsov[1], Kh. D. Tonaeva[3], S. A. Borzenok[3], T. Dobner[2], V. S. Prassolov[1*]

[1]Engelhardt Institute of Molecular Biology, Russian Academy of Sciences, Vavilova Str., 32, Moscow, 119991, Russia

[2]Heinrich Pette Institute – Leibniz Institute for Experimental Virology, Martinistrasse 52 D-20251, Hamburg, Germany

[3]S.N. Fedorov Eye Microsurgery Complex of the Ministry of Health of the Russian Federation, Beskudnikovskiy Blvd., 59A, Moscow, 127486, Russia

*E-mail: prassolov45@mail.ru

Received: 23.06.2015

ABSTRACT **Adenoviruses cause a wide variety of human infectious diseases. Adenoviral conjunctivitis and epidemic keratoconjunctivitis are commonly associated with human species D adenoviruses. Currently, there is no sufficient or appropriate treatment to counteract these adenovirus infections. Thus, there is an urgent need for new etiology-directed therapies with selective activity against human adenoviruses. To address this problem, the adenoviral early genes *E1A* and *E2B* (viral DNA polymerase) seem to be promising targets. Here, we propose an effective approach to downregulate the replication of human species D adenoviruses by means of RNA interference. We generated *E1A* expressing model cell lines enabling fast evaluation of the RNA interference potential. Small interfering RNAs complementary to the *E1A* mRNA sequences of human species D adenoviruses mediate significant suppression of the *E1A* expression in model cells. Furthermore, we observed a strong downregulation of replication of human adenoviruses type D8 and D37 by small hairpin RNAs complementary to the *E1A* or *E2B* mRNA sequences in primary human limbal cells. We believe that our results will contribute to the development of efficient anti-adenoviral therapy.**

KEYWORDS **RNA interference, human adenoviruses, small interfering RNAs, lentiviral vectors, small hairpin RNAs.**

ABBREVIATIONS **siRNA – small interfering RNA; shRNA – small hairpin RNA; HAdV – human adenovirus; FFU – focus forming unit; MFI– mean fluorescence intensity.**

INTRODUCTION

Adenoviral ocular infections are of great current concern in biomedicine due to the wide prevalence and high rate of adenovirus infection episodes. Adenoviruses commonly cause human respiratory and gastrointestinal infections, adenoviral conjunctivitis (inflammation of the conjunctiva) and epidemic keratoconjunctivitis (combined inflammation of the cornea and conjunctiva) [1]. In Russia, more than 300,000 people are annually diagnosed with epidemic keratoconjunctivitis [2]. The most serious eye infections are caused by human species D adenoviruses (HAdVs) types D8, D19, and D37 [3]. HAdV infection affects people of all age groups [4]. In Russia, about 18 million people visit the ophthalmologist for inflammatory eye diseases annually, which accounts for up to 80% of temporary disability due to eye diseases and 10–30% of visual acuity loss and blindness [5]. An epidemic spread, large loss due to temporary disability, a high likelihood of complications (temporary or permanent loss of vision), and a multitude of clinical manifestations define the medical and social significance of adenoviral eye diseases. Adenovirus infections present a serious health risk for immunocompromised individuals [6]. Obesity in children and nonalcoholic fatty liver disease in adults are known to be caused by human spicies D adenovirus type 36 (HAdV D36) [7].

Currently, the limited efficacy of therapies for the adenovirus infection [8] dictates the need for developing drugs with selective activity against adenovirus pathogens.

Human adenovirus early genes, such as the DNA polymerase *E2B* gene and *E1A* gene, which are involved in viral DNA replication, seem to be potential targets for antiviral therapy [9–11].

E1A gene products promote the G_0 to S phase cell cycle transition. Interaction between *E1A* gene products and the retinoblastoma protein (pRb) activates the E2F1 transcription factor, triggering expression of the

genes necessary for progression through the S phase. This enables the adenovirus to replicate in the infected cell using the host's replication machinery. One of the functions of the E2F1 transcription factor is transactivation of the p14/ARF protein that is accompanied by induction of p53-dependent apoptosis. During viral infection, the 55 kDa E1B protein inactivates p53, thereby preventing induction of apoptosis in the cell until the adenovirus replication cycle is completed [12, 13].

Small interfering RNAs (siRNAs), which are short 21–23 bp duplexes with 2–3 overhanging nucleotides at 3'-ends capable of suppressing gene expression at the post-transcriptional level, are commonly used in gene function studies [14, 15]. Interfering RNAs were shown to be capable of suppressing the expression of various target genes, including viral genes [16–18]. Interfering RNAs could be effectively delivered to cells by recombinant lentiviral vectors encoding small hairpin RNAs (shRNAs), which are precursors of small interfering RNAs [19–21].

We believe that this approach can be used for downregulation of the *E1A and E2B* expression [10, 11] of HAdVs causing ocular and respiratory tract infections.

This paper presents the results of *E1A* gene expression downregulation in human species D adenoviruses types D8, D19, D36, and D37 using siRNAs and shRNAs, as well as inhibition of HAdVs D8 and D37 replication upon simultaneous downregulation of *E1A* and *E2B* expression using shRNAs.

MATERIALS AND METHODS

Cell culture

Human embryonic kidney cells HEK293 [22], human lung adenocarcinoma epithelial cells A549 (DSMZ ACC107; Brauschweig, Germany), human nonsmall cell lung cancer cells H1299, A549 E1A and H1299 E1A model cells were grown in a DMEM medium (Life Technologies, UK) containing 10% fetal bovine serum (Life Technologies), 4 mM*L*-glutamine, 1 mM sodium pyruvate, and streptomycin/penicillin at a concentration of 100 μg/mL and 100 U/mL, respectively, at 37°C under 5% CO_2 atmosphere. Primary human limbal cells [24, 25] were cultured on a DMEM/F12 medium (Life Technologies) containing 10% fetal bovine serum (Life Technologies), 4 mM*L*-glutamine, 1 mM sodium pyruvate, 10 mM HEPES, 0.4 μM insulin, 10 nM dexamethasone, and streptomycin/penicillin at a concentration of 100 μg/mL and 100 U/mL, respectively, at 37°C under 5% CO_2.

Lentiviral vectors

Recombinant lentiviral vectors were constructed using standard genetic engineering techniques [26, 27]. Recombinant lentiviral virions were generated in the HEK293 cells by calcium phosphate co-transfection of lentiviral vector DNA and plasmids directing the synthesis of all the lentiviral proteins required to produce infectious lentiviral particles. Infectious pseudoviral particles were collected during 2 days with 12-h intervals. A549 and H1299 cells were used for lentivirus titer estimation. Viral stocks with titers of 5×10^5 to 5×10^6 were further used.

Model cell lines

Model cells expressing the *E1A* gene of the human adenovirus type 36 (*E1A-D36*) were produced by transduction of A549 and H1299 cells with LeGO-iGT-Puro-opt-based pseudolentiviral particles E1A-LeGO-iGT containing an expression cassette "promoter–*E1A* gene of HAdV D36–IRES–*dTomato* marker gene –puromycin resistance gene."

In order to generate a H1299 shE1A model cell line, the initial H1299 cells were transduced with lentiviral particles containing a sequence encoding shE1A, the *Cerulean* fluorescent protein gene, and the blasticidin (BSD) resistance gene. 48 h post transduction, the cells were placed into a selective medium with 5 μg/mL blasticidin. Selection was conducted for 10 days. H1299 shE1A cells were then analyzed by flow cytometry.

Limb shE2B, Limb shE1A, and LimbshE2B/shE1A model cell lines were prepared by transduction of primary human limbal cells with pseudolentiviral particles encoding shE2B [10, 11] or shE1A.

siRNAs

We designed siRNAs complementary to different regions of the *E1A* mRNA sequences of HAdVs types 8, 19, 36, and 37. xpression. To suppress the target gene expression the following 21 bp siRNAs were synthesized (Sintol, Russia): siE1A-1 (sense strand 5'-GGAGGACUUUGUGAAUACAUU-3', antisense strand 5'-UGUAUUCACAAAGUCCUCCUU-3');siE1A-2(sense strand 5'-GAGGCUGUGAAUUUAAUAUUU-3', antisense strand 5'-AUAUUAAAUUCACAGCCUCUU-3'), and siE1A-3 (sense strand 5'-GCUCUGUGUUACAUGAAAUUU-3', antisense strand 5'-AUUUCAUGUAACACAGAGCUU-3'). siScr having no homology with known viral mRNAs as well as human, mouse, and rat mRNAs (sense strand 5'-CAAGUCUCGUAUGUAGUGGUU-3', antisense strand 5'-CCACUACAUACGAGACUUGUU-3') were used as a control. The siRNAs were designed using the Whitehead Institute siRNA Selection Program [28].

siRNA transfection

Cells in the exponential growth phase were seeded into 24-well plates, 3×10^4 cells per well, 1 day prior to the experiment and transfected with siRNAs at a

concentration of 200 nM using a Lipofectamine® 2000 Transfection Reagent (Life Technologies) according to the manufacturer's protocol.

shRNAs

We constructed shE1A-LeGO-Cer/BSD and shScr-LeGO-Cer/BSD lentiviral vectors encoding shRNAs: shE1A, which corresponds to siE1A-1 (sense strand 5'-p-aacgATATTAAATTCACAGCCTCct-tcctgcaaGAGGCTGTGAATTTAATATtttttc-3', antisense strand 5'-p-tcgagaaaaaATATTAAAT-TCACAGCCTCttgcaggaagGAGGCTGTGAAT-TTAATATcgtt-3') and a control shScr (sense strand 5'-p-gatccgCCACTACATACGAGACTTcttcctgt-caCAAGTCTCGTATGTAGTGGtttttg-3', antisense strand 5'-p-aattcaaaaaCCACTACATACGA-GACTTGtgacaggaagCAAGTCTCGTATGTAGTGG-cg-3'). In this work, we also used lentiviral vectors shE2B-LeGO-G (encoding shRNA targeting the DNA polymerase mRNA of HAdVs D8, D19, D36, and D37) and shScr-LeGO-G, which were described previously in [10, 11].

Flow cytometry

The cell fluorescence intensity was measured by an Epics 4XL flow cytometer (Beckman Coulter, USA). Obtained results were analyzed with WinMDI software, version 2.8

Real-time PCR

Total RNA was isolated from cell cultures using a TRIzol® reagent (Life Technologies) according to the manufacturer's protocol. Reverse transcription was carried out using ImProm-II™ Reverse Transcriptase (Promega, USA). *E1A-D36* mRNA levels were assessed in real-time PCR using specific primers : sense sequence 5'-GCATCCAGAGCCATTTGAGC-3'; antisense sequence 5'-TTAGGGTCGTCATCATGGGC-3'. Resulting values for each sample were normalized to the β-actin housekeeping gene expression. The β-actin expression level was quantified using the following primers: sense sequence 5'-ATGGATGATGATATC-GCCGC-3'and antisense sequence 5'-CTTCT-GACCCATGCCCAC-3'. Real-time PCR was performed in 96-well plates using a MiniOpticon system (Bio-Rad, USA) and an iQ SYBR Green Supermix reagent (Bio-Rad) in accordance with the manufacturer's recommendations. PCR products were analyzed using the MiniOpticon system software (Bio-Rad).

Quantification of the human adenovirus genome copy number

HAdV D8 (ATCC® VR-1085AS/RB™ ATCC® VR-1085AS/RB™) and HAdV D37 (ATCC® VR-929™) were purchased from the American-Type-Culture-Collection (ATCC). Replication of species D human adenoviruses was evaluated 6 days post infection. For this, HAdV D8 and D37 infected cells were harvested, and total DNA was isolated using a QIAamp DNA Mini Kit (QIAGEN, Germany) according to the manufacturer's recommendations. Quantitative PCR was performed as described in [29] on a Rotor Gene Q cycler (QIAGEN) using a TaqMan® Universal PCR Master Mix reagent (Life Technologies). PCR products were analyzed using the Rotor Gene Q cycler software (QIAGEN).

Statistical data processing

All data are presented as a mean ± standard deviation (SD). The statistical significance was determined using the unpaired two sample t-test and GraphPad Prism software 6 (GraphPad Software, USA). The value of $p<0.05$ was considered statistically significant.

RESULTS AND DISCUSSION

Derivation of model cell lines expressing the HAdV D36 *E1A* gene

Model cell lines A549 E1A and H1299 E1A expressing the E1A gene of human species D adenovirus type 36 (*E1A-D36*) were obtained in order to analyze the functional activity of synthetic siRNAs and lentiviral vectors directing the synthesis of shRNAs in transduced cells.

The *E1A* expression in cells is known to induce p53-dependent apoptosis [30]. *E1A* expression products promote the G_0 to S phase transition and disturbance of the mechanisms controlling DNA synthesis. This increases the likelihood of DNA damage during replication. In response to heavy DNA damage, the p53 protein triggers a cascade of reactions leading to apoptosis. Therefore, A549 and H1299 cells were first transfected with siRNAs complementary to various fragments of the *E1A* mRNA and with control siScr. After 24 h, the cells were transduced by pseudolentiviral particles (*Fig. 1A*) containing the expression cassette "promoter– target *E1A-D36* gene–IRES–dTomato fluorescent protein gene–puromycin resistance gene." The marker gene encoding the dTomato fluorescent protein and the target *E1A* gene are separated by the IRES sequence (internal ribosome entry site). IRES allows for the synthesis of several proteins from a single mRNA in eukaryotic cells. Thus, the target and marker genes are expressed with a comparable efficiency [31]. This enables indirect estimation of the *E1A* expression level via measuring dTomato fluorescence by flow cytometry.

The efficiency of the introduced genes, expression was evaluated by flow cytometry detection of dTomato fluorescence and real-time PCR. The flow cytometry

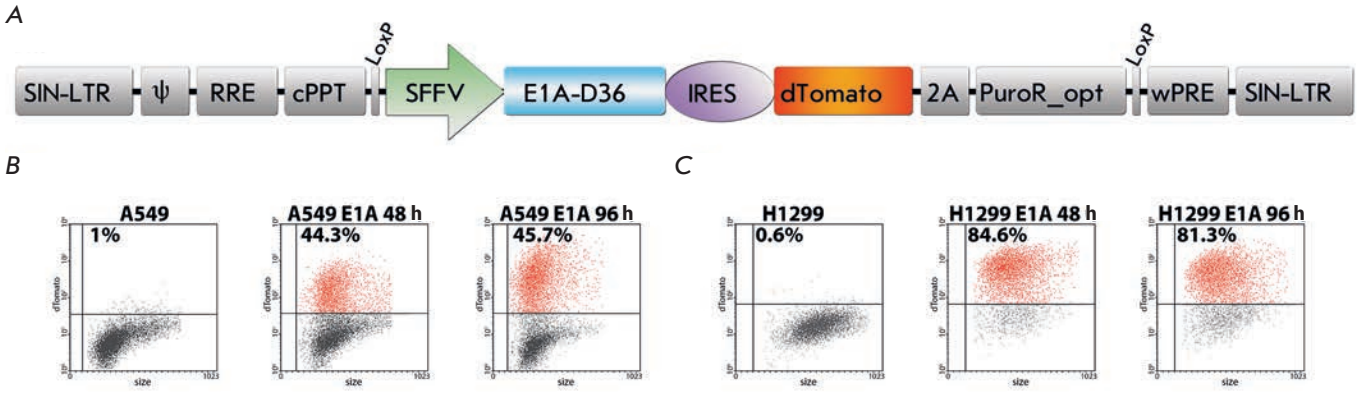

Fig. 1. Model cell lines. A – Lentiviral vector containing the *E1A-D36* gene of HAdV D36 and the dTomato/puromycin-resistance fusion gene separated by an IRES sequence. The vector is based on the LeGO-iGT-Puro-opt vector. SIN-LTR– self-inactivating-long-terminal repeat ; ψ – packaging signal; RRE– rev-responsive element; cPPT– central polypurine tract; SFFV– spleen focus-forming virus U3 promoter; *E1A-D36*– *E1A* gene of HAdV D36; IRES– internal ribosome entry site; dTomato – dTomato fluorescent protein; 2A– self-cleaving peptide of the porcine teschovirus-1; PuroR_opt– codon optimized cDNA of puromycin resistance; wPRE– Woodchuck hepatitis virus post-transcriptional regulatory element. B – Flow cytometry assay of A549 E1A cells expressing the dTomato fluorescent protein. C – The number of H1299 E1A cells expressing the dTomato fluorescent protein measured by flow cytometry

data for evaluation of the transduction and subsequent transgene expression efficiency are shown in *Figs. 1B* and *C*.

The number of cells of the A549 E1A and H1299 E1A model lines in which dTomato protein fluorescence was registered amounted to 44 and 85% of the total cell population, respectively, compared to a control (non-transduced A549 and H1299 line cells).

These findings indicate that the produced A549 E1A and H1299 E1A transgenic model cells express the introduced target gene and *dTomato* marker gene with a high efficiency.

According to the obtained results, the number of fluorescent cells in A549 E1A and H1299 E1A model lines is significantly different. The heterogeneity of A549 E1A and H1299 E1A cells in the *dTomato* expression level may be caused by individual properties of the cells. The different number of lentiviral provirus molecules is integrated in the genome of transgenic cells. The viral DNA integrates into different regions of the genome, which may provide varying transgene expression levels. Despite the similarity of the morphology and origin of A549 and H1299 cells, differences between these two lines may be one of the causes. The *E1A* gene expression is known to result in p53-dependent apoptosis. H1299 cells are p53-deficient. Hence, the likelihood of apoptosis in H1299 E1A cells is significantly lower than in A549 E1A cells. It may be assumed that A549 cells are transduced with the same efficiency as H1299 cells, but p53-dependent apoptosis occurs in most of the transduced A549 E1A cells, enabling detection of dTomato fluorescence in a smaller number of A549 E1A cells compared to H1299E1A model cells.

siRNA-mediated downregulation of *E1A-D36* gene expression

The structure of the expression cassette "promoter–*E1A-D36* gene–IRES–*dTomato* marker gene –puromycin resistance gene" enables rapid assessment of the silencing activity of siRNAs and the lentiviral vectors directing the synthesis of shRNAs (precursors of siRNAs).

Because of degradation of a mRNA common to both genes due to the inhibitory activity of interfering RNAs targeting *E1A-D36* mRNA, the cell stops producing both the *E1A-D36* gene products and the dTomato fluorescent protein, which can be quantified by flow cytometry.

Since the *E1A* gene expression results in induction of apoptosis, the experiment was performed as follows: siRNAs complementary to various regions of the *E1A-D36* mRNA were transfected into A549 and H1299 cells; after 24 h, the cells were transduced with pseudolentiviral particles containing an expression cassette "promoter SFFV–*E1A-D36* gene–IRES–dTomato fluorescent protein gene–puromycin resistance gene." The efficiency of siRNAs was evaluated by flow cytometry and real-time PCR 48 and 96 h post transduction.

The activity of siRNAs complementary to the *E1A-D36* mRNA caused a significant decrease in the *dTomato* expression level (*Fig. 2*). In the population of

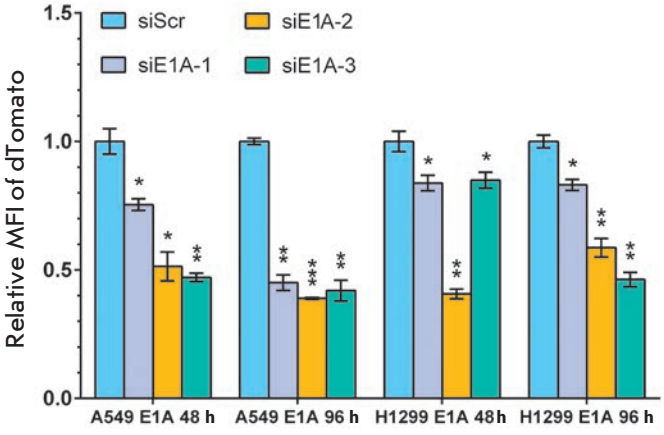

Fig. 2. Silencing activity of siRNAs complementary to the *E1A-D36* mRNA sequence. The silencing activity of siRNAs targeted against the *E1A-D36* mRNA resulted in a reduction in the dTomato MFI in A549 E1A and H1299 E1A cells. 1 corresponds to the dTomato MFI value in cells transfected with siScr. All reported values are a mean ± standard deviation of three independent experiments. The differences between siScr and targeting siRNAs were statistically significant in all cases (*$p<0.05$, **$p<0.01$, ***$p<0.001$)

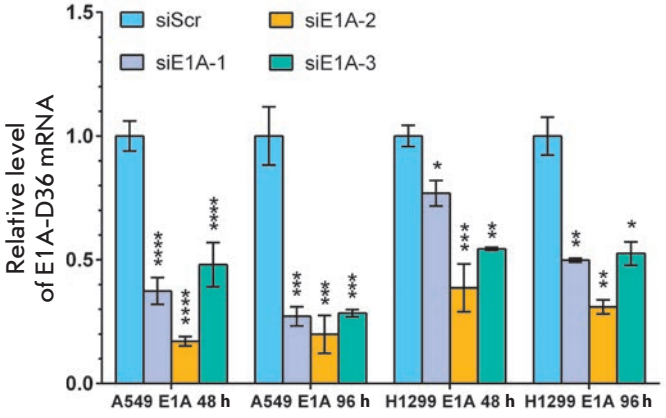

Fig. 3. siRNA-induced downregulation of *E1A-D36* expression. Levels of *E1A-D36* mRNA in A549 E1A and H1299 E1A model cells were analyzed by RT-qPCR. 1 corresponds to values for the cells transfected with siScr. Results were normalized to the endogenous b-actin mRNA level. All reported values are a mean ± standard deviation of three independent experiments. The differences between siScr and targeting siRNAs were statistically significant in all cases (*$p<0.05$, **$p<0.01$, ***$p<0.001$, ****$p<0.0001$)

A549 E1A cells transfected with siE1A-1, siE1A-2, and siE1A-3, the mean fluorescence intensity (MFI) of dTomato was decreased by 25, 49, and 53% after 48 h and by 55, 61, and 58% after 96 h, respectively, compared to control A549 E1A cells transfected with siScr. A siRNA biological activity assay showed that MFI of the dTomato fluorescent protein in the H1299 E1A model cell population was decreased by 18, 60, and 17% under the action of siE1A-1, siE1A-2, and siE1A-3 as early as after 48 h and by 18, 44, and 56% after 96 h, respectively, compared to control H1299 E1A cells transfected with siScr. All the presented data were obtained in three independent experiments ($p<0.05$).

Results obtained by flow cytometry are consistent with the real-time PCR data. The effect of siRNAs on the *E1A-D36* mRNA expression level in model cells was assessed 48 and 96 h post transduction with pseudolentiviral particles encoding the target gene (*Fig. 3*). The *E1A-D36* mRNA expression level in A549 E1A cells transfected with siE1A-1, siE1A-2, and siE1A-3 was reduced by 58, 83, and 63% and 69, 88, and 72% 48 h and 96 h post transduction, respectively, compared to control cells. The *E1A-D36* mRNA level in H1299 E1A model cells transfected with siE1A-1, siE1A-2, and siE1A-3 was reduced by 28, 71, and 46% and 50, 69, and 47% 48 h and 96 h post transduction, respectively, compared to control cells.

A reduction in the mean fluorescence intensity of the dTomato marker protein occurs more slowly and less effectively than suppression of target gene expression at the mRNA level. These data may be explained by the fact that the fluorescent protein is quite stable, and its half-life is about 72 h.

According to the flow cytometry and real-time PCR data, the *E1A-D36* gene expression was mostly affected by siE1A-2. The siRNA silencing activity depends on several factors. These include the secondary structure of a target mRNA, siRNA sequence uniqueness, and stability and the thermodynamic asymmetry of siRNA duplexes. The secondary structure of a target mRNA or the proteins bound to it are known to be capable of hindering access for siRNAs [15, 32].

Downregulation of *E1A-D36* gene expression by a lentiviral vector encoding shRNA

We constructed lentiviral vectors encoding shRNAs corresponding to siE1A-2 (with the highest suppression of *E1A-D36* expression) and control siScr. Lentiviral vectors ensure integration of a sequence encoding shRNA into the cell genome, providing long-term suppression of the target gene expression. These lentiviral vectors were constructed based on the LeGO-Cerulean/BSD (*Fig. 4A*) carrying the Cerulean fluorescent protein gene and blasticidin resistance gene.

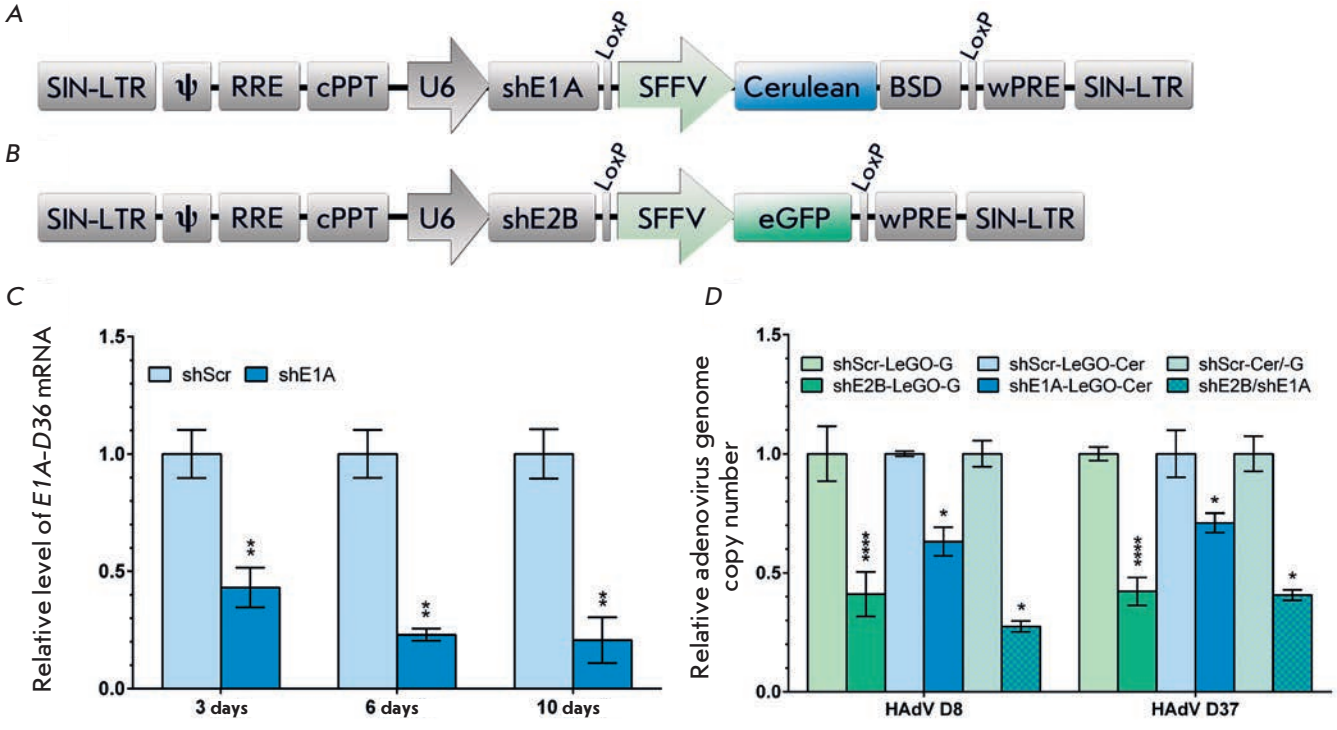

Fig. 4. Silencing activity of shRNAs targeting *E1A* and *E2B* (DNA-polymerase) mRNAs of human species D adenoviruses. A – LeGO-Cerulean/BSD-based lentiviral vector encoding shE1A complementary to *E1A* of HAdVs D8, D19, D36, and D37. B – LeGO-G-based lentiviral vector encoding shE2B complementary to *E2B* of HAdVs D8, D19, D36, and D37. SIN-LTR– self-inactivating-long-terminal repeat; ψ– packaging signal; RRE– rev-responsive element; cPPT– central polypurine tract; U6– murine U6 pol-III promoter; SFFV– spleen focus-forming virus U3 promoter; Cerulean– fluorescent protein Cerulean; eGFP– enhanced green fluorescent protein; BSD– blasticidin resistance gene; wPRE– Woodchuck hepatitis virus post-transcriptional regulatory element. C – RT-PCR quantification of E1A-D36 mRNA levels in H1299 cells expressing shE1A 3, 6, and 10 days post transduction with a lentiviral vector encoding E1A-D36. Results were normalized to the endogenous b-actin mRNA level. 1 corresponds to values for the control cells expressing shScr. All reported values are a mean ± standard deviation of three independent experiments. The differences between shScr and shE1A were statistically significant in all cases (**$p<0.01$). D – Downregulation of HAdV D8 and D37 genome replication in primary human limbal cells. Viral genome replication was measured via RT-qPCR. 1 corresponds to values for the control cells. All reported values are a mean ± standard deviation of three independent experiments. The differences between shScr and targeting shRNAs were statistically significant in all cases (*$p<0.05$, ****$p<0.0001$)

The shScr-LeGO-Cerulean/BSD vector encoding a hairpin structure having no homology with known viral mRNAs as well as rat, mouse, and human mRNAs was used as a control to demonstrate the absence of a nonspecific activity of shRNAs.

These lentiviral vectors were transduced into the genome of H1299 cells. Ten days after selection on blasticidin, the transduction efficiency of the H1299 shE1A and H1299 shScr cells was evaluated by flow cytometry of Cerulean reporter protein fluorescence. The number of fluorescent cells amounted to 92–98% of the total cell number in the population compared to control cells (non-transduced H1299 cells).

Then, H1299 shE1A model cells were transduced with E1A-LeGO-iGT pseudolentiviral particles. The biological activity of shE1A was evaluated 3, 6, and 10 days post transduction using real-time PCR in three independent experiments ($p<0.05$). The expression level of the *E1A* target gene was down by 57, 77, and 80% under the action of shE1A after 3, 6, and 10 days, respectively, compared to the control (*Fig. 4C*).

We demonstrated that lentiviral vectors encoding shRNAs significantly suppress the *E1A-D36* target gene expression. It should be noted that persistent suppression of the *E1A-D36* expression mediated by shRNA-expressing lentiviral particles was preserved

in model cells for 10 days. This demonstrates the high efficiency of the constructed lentiviral vectors.

Downregulation of human species D adenoviruses replication by shRNAs in primary human limbal cells

We evaluated the ability of shRNAs targeting mRNAs of the *E1A* and *E2B* HAdV early genes to suppress viral replication. Primary human limbal cells (Limb) were transduced with shE2B-LeGO-G (*Fig. 4B*) and shE1A-LeGO-Cerulean/BSD lentiviral vectors encoding shE2B and shE1A, respectively. Limbal cells transduced with pseudolentiviral particles carrying shScr (whose sequence has no homology with known viral mRNAs and mouse, rat, and human mRNAs) were used as a control.

Cells of the derived lines were infected with HAdV D8 and HAdV D37, which cause epidemic keratoconjunctivitis, at a multiplicity of infection of 20 fluorescence-forming units (FFU)/cell. The cells were cultured for 6 days post infection, which is sufficient to complete the full replication cycle of a human adenovirus. Six days post infection, the efficiency of shRNAs was assessed via qPCR to detect HAdV D8 and HAdV D37 genomes. We observed a significant downregulation of human adenovirus replication in primary human limbal cells. The copy number of HAdV D8 and HAdV D37 genomes was reduced by 59 and 58% under the action of shE2V, 37 and 30% under the action of shE1A, and 73 and 60% under the simultaneous action of shE2B and shE1A, respectively, compared to control cells (*Fig. 4D*).

We suppose that downregulation of expression of human species D adenoviral early genes results in premature termination of the adenovirus replication cycle. This explains the significant reduction in the adenovirus genome copy number. Nevertheless, we have not achieved a complete suppression of viral replication. This may be associated with the high multiplicity of infection (20 FFU/cell), the sample analysis time (6 days post infection, while maximum suppression of target gene expression by shRNAs is observed on the 9^{th}–10^{th} day (*Fig. 4C*) [10, 11]), as well as the low transduction efficiency of primary human limbal cells (50–70% fluorescent cells in the population according to fluorescence microscopy).

In the experiment, we used primary human limbal cells derived from the human cornea, which is affected in epidemic keratoconjunctivitis. We also used HAdVs D8 and D37 that are the main causative agents of the disease. Thus, we developed an *in vitro* model system of adenovirus ocular infection and demonstrated the high efficiency of shRNAs targeted against early genes of human spicies D adenoviruses.

CONCLUSIONS

We developed an approach to efficiently suppress replication of human species D adenoviruses via RNA interference. In order to evaluate the silencing activity of siRNAs specific to the *E1A* gene of HAdVs D8, D19, D36, and D37, as well as lentiviral vectors that direct the synthesis of an analogous shRNA in cells, we produced model cell lines whose genome contains the expression cassette "promoter–*E1A-D36* gene–IRES–*dTomato* marker gene– puromycin resistance gene." These model cell lines enable rapid evaluation of the efficiency of interfering RNAs complementary to different regions of the target gene mRNA.

The high efficiency of these vectors in downregulation of human species D adenoviruses D8 and D37 replication was shown in primary human limbal cells. The simultaneous action of shE1A and shE2B led to a decrease in the adenovirus genome copy number by 70%, on average.

We believe that our findings will be helpful for the design and development of novel medicinal agents against human diseases caused by adenoviruses. ●

This study was supported by the Russian Foundation for Basic Research (grant № 14-04-00821 A) and program of the Presidium of the Russian Academy of Sciences "Basic Research in Nanotechnologies and Nanomaterials".

REFERENCES

1. Gonzalez-Lopez J.J., Morcillo-Laiz R.,Munoz-Negrete F.J. // Arch Soc Esp Oftalmol. 2013. V. 88. № 3. P. 108–115.
2. Alexeev V.N., Martynova E.B.,Zhukova E.A. // Clinical Ophtalmology. Russian Medical Journal. 2005. V. 4. P. 146–149.
3. Meyer-Rusenberg B., Loderstadt U., Richard G., Kaulfers P.M.,Gesser C. // Dtsch Arztebl Int. 2011. V. 108. № 27. P. 475–480.
4. Langley J.M. // Pediatrics in Review. 2005. V. 26. № 7. P. 244–249.
5. Maychuk Y.F. // Russian Ophthalmological Journal. 2008. V. 3. P. 18-25.
6. Myers G.D., Krance R.A., Weiss H., Kuehnle I., Demmler G., Heslop H.E.,Bollard C.M. // Bone Marrow Transplant. 2005. V. 36. № 11. P. 1001–1008.
7. Trovato G.M., Martines G.F., Pirri C., Trovato F.M., Castro A., Garozzo A.,Catalano D. // J Clin Gastroenterol. 2012. V. 46. № 6. P. e46–54.
8. Skevaki C., Galani I., Pararas M., Giannopoulou K.,Tsakris A. // Drugs. 2011. V. 71. № 3. P. 331–347.
9. Kneidinger D., Ibrisimovic M., Lion T.,Klein R. // Antiviral Res. 2012. V. 94. № 3. P. 195–207.
10. Nikitenko N.A., Speiseder T., Groitl P., Spirin P.V., Prokofjeva M.M., Lebedev T.D., Rubtsov P.M., Lam E., Riecken K., Fehse B., et al. // Biochimie. 2015. V. 113. P. 10–16.

doi:10.1016/j.biochi.2015.03.010
11. Nikitenko N.A., Speiseder T., Groitl P., Spirin P.V., Prokofjeva M.M., Lebedev T.D., Rubtsov P.M., Lam E., Riecken K., Fehse B., et al. // Biochimie 2015. V. 116. P.166. doi:10.1016/j.biochi.2015.05.008
12. Isobe T., Hattori T., Kitagawa K., Uchida C., Kotake Y., Kosugi I., Oda T.,Kitagawa M. // J Biol Chem. 2009. V. 284. № 41. P. 27766–27779.
13. Yousef A.F., Fonseca G.J., Pelka P., Ablack J.N., Walsh C., Dick F.A., Bazett-Jones D.P., Shaw G.S.,Mymryk J.S. // Oncogene. 2010. V. 29. № 33. P. 4693–4704.
14. Bantounas I., Phylactou L.A.,Uney J.B. // Journal of Molecular Endocrinology. 2004. V. 33. № 3. P. 545–557.
15. Vilgelm A.E., Chumakov S.P.,Prassolov V.S. // Molecular Biology. 2006. V. 40. № 3. P. 339–354.
16. Spirin P.V., Baskaran D., Orlova N.N., Rulina A.V., Nikitenko N.A., Rubtsov P.M., Chumakov P.M., Prassolov V.S., Chernolovskaya E.L., Zenkova M.A., et al. // Molecular Biology. 2010. V. 44. № 5. P. 776–786.
17. Spirin P.V., Nikitenko N.A., Lebedev T.D., Rubtsov P.M., Prassolov V.S.,Stocking C. // Molecular Biology. 2011. V. 45. № 6. P. 950–958.
18. Elbashir S.M., Harborth J., Lendeckel W., Yalcin A., Weber K.,Tuschl T. // Nature. 2001. V. 411. № 6836. P. 494–498.
19. Lebedev T.D., Spirin P.V.,Prassolov V.S. // Acta Naturae. 2013. V. 5. № 2. P. 7–18.
20. Singer O.,Verma I.M. // Curr Gene Ther. 2008. V. 8. № 6. P. 483–488.
21. Manjunath N., Wu H., Subramanya S.,Shankar P. // Adv Drug Deliv Rev. 2009. V. 61. № 9. P. 732–745.
22. Graham F.L., Smiley J., Russell W.C.,Nairn R. // J Gen Virol. 1977. V. 36. № 1. P. 59–74.
23. Mitsudomi T., Steinberg S.M., Nau M.M., Carbone D., D'Amico D., Bodner S., Oie H.K., Linnoila R.I., Mulshine J.L., Minna J.D., et al. // Oncogene. 1992. V. 7. № 1. P. 171–180.
24. Borzenok S.A., Onishchenko N.A., Tonaeva K.D., Komakh Y.A., Kovshun Y.V.,Strusova N.A. // Russian Journal of Transplantology and Artificial Organs. 2014. V. 16. № 1. P. 12–20.
25. Borzenok S.A., Onischenko N.A., Tonaeva K.D., Komakh Y.A., Suskova V.S., Suskov S.I., Didenko L.V., Shevlyagina N.V.,Kost E.A. // Russian Journal of Transplantology and Artificial Organs. 2012. V. 14. № 2. P. 78–85.
26. Weber K., Bartsch U., Stocking C.,Fehse B. // Mol Ther. 2008. V. 16. № 4. P. 698–706.
27. Weber K., Mock U., Petrowitz B., Bartsch U.,Fehse B. // Gene Ther. 2010. V. 17. № 4. P. 511–520.
28. Yuan B., Latek R., Hossbach M., Tuschl T.,Lewitter F. // Nucleic Acids Res. 2004. V. 32. № Web Server issue. P. W130–134.
29. Heim A., Ebnet C., Harste G.,Pring-Akerblom P. // J Med Virol. 2003. V. 70. № 2. P. 228–239.
30. Debbas M.,White E. // Genes Dev. 1993. V. 7. № 4. P. 546–554.
31. Zhou Y., Aran J., Gottesman M.M.,Pastan I. // Hum Gene Ther. 1998. V. 9. №3. P. 287-293.
32. Nikitenko N.A.,Prassolov V.S. // Acta Naturae. 2013. V. 5. № 3. P. 35–53.

The Novel Dipeptide Translocator Protein Ligand, Referred to As GD-23, Exerts Anxiolytic and Nootropic Activities

P. Yu. Povarnina*, S. A. Yarkov, T. A. Gudasheva, M. A. Yarkova, S. B. Seredenin
V.V. Zakusov Research Institute of Pharmacology of RAMS, ul. Baltiyskaya, 8, Moscow, 125315, Russia
*E-mail: povarnina@gmail.com
Received: 11.11.2014

ABSTRACT **The translocator protein (TSPO) promotes the translocation of cholesterol to the inner mitochondrial membrane and mediates steroid formation. In this study, we first report on a biological evaluation of the dipeptide GD-23 (N-carbobenzoxy-L tryptophanyl-L isoleucine amide), a structural analogue of Alpidem, the principal TSPO ligand. We show that GD-23 in a dose range of 0.05 to 0.5 mg/kg (i.p.) exhibits anxiolytic activity in the elevated plus maze test and nootropic activity in the object recognition test in scopolamine-induced amnesia in rodents. It was shown that GD-23 did not affect spontaneous locomotor activity, holding promise as a nonsedative anxiolytic agent. The anxiolytic and nootropic activities of GD-23 were abrogated by the TSPO specific ligand PK11195, which thus suggests a role for TSPO in mediating the pharmacological activity of GD-23.**
KEYWORDS **translocator protein, dipeptide, GD-23, anxiolytic activity, nootropic activity.**
ABBREVIATIONS **TSPO – translocator protein, GABA – gamma aminobutyric acid, EPM – elevated plus maze, i.p. – intraperitoneally, s.c. – subcutaneous.**

INTRODUCTION

There has been an increase in the incidence of anxiety disorders over the past several years [1]. Benzodiazepines are used to manage anxiety, binding the GABA(A) receptor α- and γ subunits and allosterically modulating GABA(A)-ergic transmission [2]. Although benzodiazepines are highly effective for the relief of anxiety, they carry the risk of negative side effects such as sedation, muscle relaxation, cognitive impairment, as well as tolerance and dependence after repeated treatment.

Promising candidates for fast-acting anxiolytic drugs free of side effects could be selective antagonists of the GABA(A) receptor α2- and α3 subunits, mediating the anxiolytic effects [2], or ligands of the translocator protein (TSPO), previously known as the peripheral benzodiazepine receptor [1].

TSPO is primarily expressed in steroid-producing cells, including central and peripheral nervous system cells, and localizes in the outer mitochondrial membrane [3]. TSPO is involved in the first steroidogenic reaction by regulating cholesterol transport into mitochondria [4]. Neurosteroids are known as endogenous GABA(A) ligands that modulate neuronal excitability, whose anxiolytic effects, for example, pregnenolone, have been described in detail [5]. TSPO and neurosteroids have been implicated in the etiology of anxiety disorders. Recent work has reported that patients suffering from symptoms of clinical anxiety have reduced levels of TSPO in blood cells and neurosteroids in the spinal fluid [6, 7]. Neurosteroids and benzodiazepines recognize different GABA(A) receptor epitopes [1], which accounts for their pharmacological properties. Numerous *in vitro* and *in vivo* studies have shown that TSPO ligands stimulate neurosteroidogenesis [5]. For this reason, TSPO ligands have emerged as fast-acting agents for the pharmacological treatment of anxiety-like disorders [5, 8].

This study extends our previous work in which we engineered a structurally similar analog of Alpidem (anxiolytic), the primary member of the pyrazolopyrimidine TSPO ligands, by synthesizing short peptides with tailored functionalities based on the chemical scaffolds of nonpeptide drug compounds [9]. The novel peptide, a substituted dipeptide amid N-carbobenzoxy-L-tryptophanyl-L-isoleucine, (GD-23) and Alpidem share structural homology with two aromatic and one aliphatic pharmacophores. GD-23 was chemically synthesized using activated N-oxysuccinimide ethers.

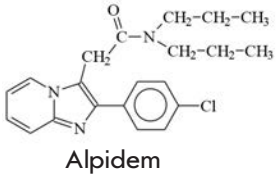
Alpidem

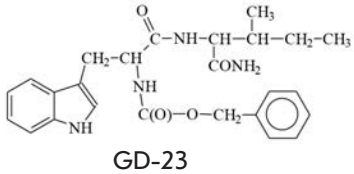
GD-23

The objective of this study was to assess the pharmacological activity of GD-23 in terms of anxiolytic and nootropic effects. To confirm the role of TSPO in modulating GD-23 action, we undertook an analysis of GD-23 antagonism in the context of PK11195, the TSPO specific ligand.

EXPERIMENTAL SECTION

Compounds

In a previous study of our scientific group, an amid N-carbobenzoxy -L-tryptophanyl-L-isoleucine (GD-23) was designed[10]. The detailed data are given below: $T_{m.}$ 214–216°C, $[a]_D^{20}$ -23° (s 1; DMF); 1H NMR spectrum (DMSO-d_6) δ:0.80 (3 H, t, $C^{\delta}H_3$ Ile), 0.83 (3 H, d, $C^{\gamma'}H_3$ Ile), 1.07 and 1.44 (2 H, 2 m, $C^{\gamma}H_2$ Ile), 1.72 (1 H, m, $C^{\beta}H$ Ile), 2.92 and 3.11 (2 H, 2d, $C^{\beta}H$ Trp), 4.17 (1 H, dd, $C^{\alpha}H$ Ile), 4.34 (1 H, m, $C^{\alpha}H$ Trp), 4.93 and 4.98 (2 H, 2 d, -OC$\underline{H}_2C_6H_5$), 6.95–7.28 (10 H, m, -$OCH_2C_6\underline{H}_5$, indole), 7.46 (1 H, d, NH Trp), 7.77 (1 H, d, NH Ile), 7.41 and 7.13 (2 H, 2s, NH_2amide), 10.80 (1 H, s, NH indole). The empirical formula established as $C_{25}H_{30}N_4O_4$ by elementary analysis showed less than 0.4% variation from the theoretical formula. Chromatographic purity was estimated by TLC/HPLC. Scopolamine and the PK11195 inhibitor (N-butan-2-yl-1-(2-chlorophenyl)-N-methylisoquinoline-3-carboxamide) were obtained from Sigma-Aldrich (USA).

GD-23 dipeptide and PK11195 were dissolved in a 0.05% water Tween-80 solution for intraperitoneal administration (IA) of 2 ml per kg of rat body weight. GD-23 was injected at doses of 0.05, 0.5, 0.1, 1 and 5 mg per kg of body weight (mice and rats); PK11195 at a dose of 10 mg per kg of mouse body weight and 3 mg per kg of rat body weight [5]. Scopolamine was diluted to give 1 ml per kg of rat body weight and administered subcutaneously (SC) at 2 mg/kg. Control animals were sham-inoculated with 0.05% water Tween-80 as PK11195 and GD inoculates, and with saline as scopolamine inoculates, by the same route and in the same volume.

Animals

Experiments were run with 107 outbred male rats (weighing 195–215 g) obtained from the animal nursery filial SCBMT Stolbovaya (Russia) and 80 CD1 male mice (weighing19–25 g) obtained from the animal breeding center at the Putschino filial of the M.M. Shemyakin and Yu.A. Ovchinnikov Institute of Bioorganic Chemistry of the RAS. The animals were housed under controlled temperature, 20–22°C, and maintained on a reversed 12:12 hour light/dark cycle, with ad libitum access to water and food. All handling and experimental procedures took place during the light phase of the cycle between 10:00 and 14:00 pm. All animals were randomly assigned into groups, balanced for weight. The animals were habituated to the test room in home cages 24 h prior to experimentation. All experimental procedures followed the guidelines for animal care of the European Community Council (86/609/CEE), and they were approved by the Bioethical Committee of the Institution (protocol № 115.09.2014).

GD-23 ANXIOLYTIC ACTIVITY

"Elevated plus maze test" (EPM)

The elevated plus maze is a widely used behavioral assay for rodents [11].The EPM apparatus was constructed of grey polyvinylchloride, consisting of two open arms connected perpendicular to two closed arms. The open arms had no walls (open arms; 65 × 5 cm). The other two arms were enclosed by opaque side walls (15 cm high). The apparatus was elevated 40 cm above ground. All arms extended from a common central platform (5 × 5 cm). The animals were placed in the center of the platform. The number of entries into the open and closed arms, the total time spent in the open and closed arms were recorded within a 5-min period. The anxiolytic activity of GD-23 was assessed using the following criteria: open arm time, open arm entries, as well as the most appropriate parameter (regardless of the activity level and time spent in the center of the apparatus) – the ratio of open arm time/entries to the total open and closed arm time/ open and closed arm entries [11].

Experimental design

The animals received GD-23 30 min before maze exposure. To study the antagonistic effect of GD-23 on the TSPO antagonist PK11195 was injected 30 min prior to GD-23 administration.

NOOTRIPIC ACTIVITY OF GD-23

Object recognition test

The exploration of new objects in animals is based on preference for novelty and could be used to evaluate working memory [12]. The rats were housed singly in a T4 cage, similar to their home cage, lined with sawdust and were allowed 5 min to explore. Metal and glass cans filled to a volume of 0.33 ml with liquid were used as objects. Metal cans were yellow-orange, glass cans were green. All cans were tightly closed with lids. The cans used in the study were sized-matched but were visually and texturally unique. The cans were heavy enough to resist tipping and dragging inside the cage; a simple shape excluded preference for one object over an other.

The test consisted of object familiarization and test phases. During the familiarization session, the rats

Table 1. GD-23 effects on CD1 mouse behavior in the EPM test

GD-23, dose, mg/kg	Open arm time, s	Closed arm time, s	Open arm entries	Closed arm entries	Total time spent on open arms to total time spend on open and closed arms , %	Total Open arm entries to/ total open and closed arm entries, %
Control	14.25 (7.21)	232.88 (38.16)	1.88 (1.46)	7.50 (2.07)	6.06 (3.56)	19.43 (12.56)
0.1	81.88* (32.40)	146.75* (43.57)	4.38* (1.51)	9.25 (3.62)	36.58* (15.71)	33.69 (13.17)
0.5	77.25* (42.53)	198.13 (50.87)	4.13* (2.36)	10.00 (3.85)	28.48* (16.51)	27.79 (7.39)
1.0	20.50 (6.05)	235.25 (19.51)	1.88 (1.46)	7.75 (2.05)	8.00 (2.36)	18.03 (7.75)
5.0	14.25 (7.21)	232.88 (38.16)	1.88 (1.46)	7.50 (2.07)	6.06 (3.56)	19.43 (12.56)

Note. Data are given as a mean±(SD); each group included eight animals;*$p < 0.01$versus control animals.

Table 2. The effect of the selective TSPO antagonist PK11195 on the anxiolytic effect of GD-23

Group	Open arm time, s	Closed arm time, s	Open arm entries	Closed arm entries	Total time spent on open arms to total time spend on open and closed arms , %	Total Open arm entries to/ total open and closed arm entries , %
Control	41.50 (15.99)	131.00 (18.02)	3.13 (2.23)	8.25 (1.91)	23.87 (7.58)	25.78 (13.16)
PK11195 (10 mg/kg)	30.13 (26.82)	167.25 (13.92)*	3.00 (2.98)	8.63 (2.39)	14.43 (11.82)	22.20 (17.77)
GD-23 (0.5 mg/kg)	105.50* (27.93)	106.88* (9.51)	7.38* (1.06)	7.63 (1.41)	48.99** (7.87)	49.33** (7.59)
PK11195 (10.0 mg/kg) + GD-23 (0.5mg/kg)	50.00# (26.60)	125.13 (22.92)	5.38 (2.88)	9.38 (3.11)	27.15## (11.08)	35.11# (9.35)

Note. Data are given as a mean±(SD); each group included eight animals; *$p < 0.01$versus control animals; #$p < 0.05$, $p < 0.01$ as compared with GD-23 group (0.5 mg/kg).

were exposed to two new objects in adjacent corners of the cage. Object exploration time was recorded for 4 min, followed by object removal. The break time between the phases was 3 min, while the rat was still in the same cage. During the test phase, the rat was presented with two objects in the same corners; one object was familiar from the familiarization phase, whereas the other was novel. Object exploration time was recorded for 4 min. Left and right positions of familiar and unfamiliar objects were counter-balanced across rats to avoid location bias. The objects were cleaned with ethanol to remove olfactory cues between each testing session.

Exploration of an object was defined as pointing the nose to the object at a distance of <2 cm. For evaluation of working memory, we used the discrimination index calculated as the difference in time exploring the novel and familiar objects, expressed as the ratio of the total time spent exploring both objects [i.e., (Time Novel − Time Familiar/Time Novel + Time Familiar) × 100%], where Time Novel and Time Familiar are exploration times for novel and familiar objects, respectively .

Experimental design

The model of impaired cognition by scopolamine has been extensively validated to study the amnesic effects of nootropic drugs [14, 15]. GD-23 was administered 1 h before scopolamine inoculation. Thirty minutes post scopolamine inoculation, the rats were exposed to the objects. When studying the antagonistic action of GD-23 towards the TSPO inhibitor, the rats received PK11195 30 min after GD-23 administration. Thirty minutes post scopolamine inoculation, the rats were allowed to explore novel objects.

Statistics

Intergroup differences were analyzed with the Mann-Whitney U test with Bonferroni correction. Significance was set at $p < 0.05$. Data were expressed as the mean and standard deviation or median and interquartile range, as appropriate.

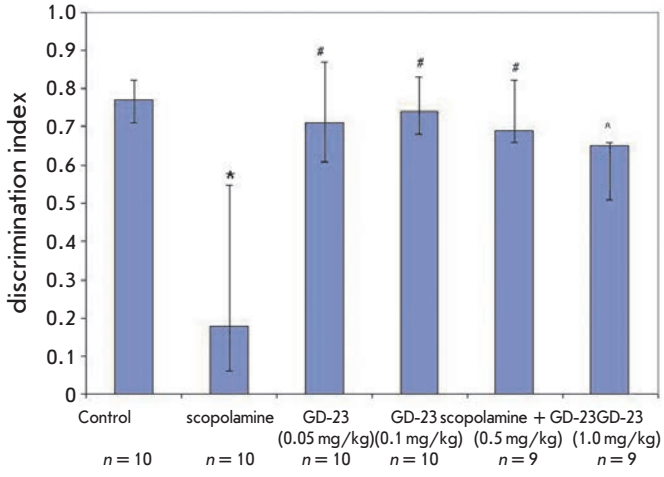

Figure 1. GD-23 antagonizes scopolamine-induced amnesia during exploration of novel objects. Rats received GD-23(IA) 1 h prior to scopolamine administration (0.2 μg/k, SC). Rats were allowed to explore novel objects 30 min post-scopolamine. The discrimination index showing the difference in the exploration time of a novel object and a familiar one to the total exploration time of a novel object and a familiar one during the test phase was calculated by the equation: D = (Time Novel – Time Familiar/Time Novel + Time Familiar). Data are given as median and interquartile ranges. n –number of animals in each group;*$p < 0.01$ as compared wiith control animals, #$p < 0.05$ versus scopolamine animals

Table 3. Antagonistic activity of PK11195 against the nootropic effect of GD-23 in scopolamine-induced amnesia in rats during exploration of familiar objects

Group	n	Discrimination index
Control	8	0.8 (0.75–0.9)
Scopolamine	9	0.08 (0.03–0.24)*
Scopolamine+GD23	10	0.66 (0.52–0.95)#
Scopolamine+GD23+PK11195	9	0.14 (-0.1–0.42)^
Scopolamine+PK11195	7	0.4 (0.23–0.44)
PK 11195	6	0.8 (0.64–0.99)

Note. Rats received GD-23 (0.1 mg/kg, IA) 1 h before scopolamine administration (0.2 mg/kg, SC). PK11195 (3 mg/kg, IA) was injected 30 min after GD-23 inoculation and 30 min prior to scopolamine exposure. Rats were allowed to explore novel objects 30 min post-scopolamine. The discrimination index showing the difference in the exploration time of a novel object and a familiar one to the total exploration time of a novel object and familiar objects during the test phase was calculated by the equation: D = (Time Novel – Time Familiar/Time Novel + Time Familiar). n –number of animals in each group,*$p < 0.05$ versus control animals, #$p < 0.01$ versus scopolamine animals, ^ – $p < 0.01$ as compared with "GD+scopolamine" animals. Data are given as median and interquartile ranges.

RESULTS

GD-23 exerts anxiolytic effects in EPM

GD-23 dipeptide at a dose of 0.1 and 0.5 mg/kg significantly increased the open arm time (5- to 6–fold increase versus control group ($p<0.01$)) and the number of open arm entries (2- to 3-fold increase versus control group ($p<0.01$)) in mice. In addition, GD-23 demonstrated a 5- to 6-fold increase in the time (%) in the open arms to the total time spent in open and closed arms, which serves as an appropriate indicator of anxiolytic effects (*Table 1*). These results indicate that GD-23 displays marked anxiolytic-like effects when administered at a dose of 0.1 or 0.5 mg/kg.

GD-23 anxiolytic effects are dependent on TSPO interaction

Prior inoculation of PK11195, a TSPO antagonist, at a dose of 10.0 mg/kg nearly completely abrogated the anxiolytic effects of GD-23 in the EPM test ($p<0.05$) (*Table 2*). The animals receiving PK11195 before GD-23 exhibited an open arm time and a percentage of time spent in open arms similar to the control. PK11195 at a dose of 10.0 mg/kg did not affect anxiety behavior; that is, the time and number of open arm entries, as well as the percentage of time and open arm entries, did not change. PK11195 seems to have antagonized GD-23 due to the competition for the same binding site. This finding indicates a role for the TSPO receptor in modulating GD-23 anxiolytic effects.

GD-23 reverses scopolamine-induced memory impairment in rats

No intergroup differences were detected in the total object exploration time between the object familiarization and test phases ($p>0.05$). Alternatively, the exploration rate was not significantly different. During the test phase, the animals took more time to explore unfamiliar objects than familiar ones ($p<0.05$). Scopolamine administration significantly reduced the ability to explore objects, as shown by a 4-fold decrease in the discrimination index when compared to the control ($p<0.01$, *Fig.1*).

GD-23 at doses of 0.05, 0.1, and 0.5 mg/kg significantly alleviated scopolamine-induced amnesia with a pronounced effect at a dose of 0.1 mg/kg, whereas at a dose of 1.0 mg/kg GD-23 abolished it.

The nootropic activity of GD-23 in amnesic rats is related to TSPO interaction

When administered, PK11195 completely antagonized the nootropic effect of GD-23 ($p<0.01$). The discrimination indices (indicators of working memory) in rats treated with scopolamine alone, and scopolamine rats that had received GD-23 and PK11195, showed no significant difference (*Table 3*). PK11195 did not affect

animal behavior in this test. Overall, similar to the anxiolytic affect of GD-23, the nootropic effect appears to be also associated with TSPO interaction.

DISCUSSION

In this study, we extended our previous findings by demonstrating that the dipeptide GD-23, which was engineered based on the scaffold of Alpidem [9], the prototype compound from the imidazopyridine family of TSPO ligands, has prominent anxiolytic and nootropic effects in a dose range of 0.05–0.5 mg/kg via intraperitoneal injection. However, both activities were completely abrogated by PK11195, which indicates a role for TSPO in the pharmacological potency of GD-23.

TSPO ligands have been pursued as anxiolytic agents. Recently, a scientific group from the Beijing Institute of Pharmacology and Toxicology (Beijing, China) reported the construction of a selective TSPO ligand, YL-IPA08 [N-ethyl-N-(2-pyridinylmethyl)-2-(3,4-ichlorophenyl)-7-methylimidazo [1,2-a] pyridine-3-acetamide hydrochloride], capable of producing anxiolytic- and antidepressant-like effects in stress-induced mice exposed to oral doses. Moreover, this study presented data that YL-IPA08 could elevate the level of allopregnanolone in the prefrontal cortex and blood plasma of mice [8]. This compound is currently in preclinical investigation.

Japanese scientists [5] reported on the anti-anxiety and antidepressant-like effects of N-benzyl-N-ethyl-2-(7,8-dihydro-7-methyl-8-oxo-2-phenyl-9H-purin-9-yl)acetamide (AC-5216) upon oral administration in rats. Furthermore, AC-5216 had no myorelaxant effects nor did it affect the memory [5]. However, clinical trials of XBD173 were terminated in Phase II for lack of therapeutic efficacy [ClinicalTrials.gov identifier: NCT00108836].

There are several classes of TSPO ligands available encompassing isoquinolinecarboxamides, indoleacetamides, imidazopyridines, pyrazolopyrimidines, benzoxazepines, and phenoxyphenylacetamide derivatives [16]. Our literature search failed to identify any publications reporting the design of TSPO ligands other than those listed above. Consequently, this is believed to be the first study to report on a peptide TSPO ligand which could hold promise as a highly effective and low-toxic agent producing little or no tolerance and dependence.

GD-23 exhibits both anxiolytic and nootropic-like effects in the scopolamine induced amnesia model. These activities seem to be associated with neorosteroid stimulation, which is intrinsic to TSPO agonists. Neorosteroids such as allopregnanolone, dehydroepiandrosterone, cortisol, and corticosterone promote memory and learning; an insufficient hormone supply due to pathology or aging correlate with cognitive impairment [17]. In conclusion, in contrast to benzodiazepines, whose side effects include cognitive impairment, GD-23 exerts nootropic effects, within dose ranges optimal for anti-anxiety action. In addition, GD-23 does not affect spontaneous activity in mice (data not shown) and thus supports the lack of sedative potential in GD-23 at the doses evaluated.

Our findings lend credence to the potential of peptide TSPO ligand GD-23 as a promising fast-acting agent for anti-anxiety therapy without the side-effects associated with benzodiazepine anxiolytics. ●

This work was financially supported by the Fundamental Research Program of the Presidium of the RAS "Fundamental research on biomedical technologies 2014," project "Construction, synthesis and evaluation of pharmacological activity of novel mitochondrial translocator protein (TSPO) ligands."

REFERENCES

1. Nothdurfter C., Baghai T.C., Schüle C., Rupprecht R. // Eur. Arch. Psychiatry Clin. Neurosci. 2012. V. 262. № 2. P. 107–112.
2. Rudolph U., Knoflach F. // Nat. Rev. Drug Discov. 2011. V. 10. № 9. P. 685–697.
3. Rupprecht R., Papadopoulos V., Rammes G., Baghai T.C., Fan J., Akula N., Groyer G., Adams D., Schumacher M. // Nat. Rev. Drug Discov. 2010. V. 9. № 12. P. 971–988.
4. Lacapère J.J., Papadopoulos V. // Steroids. 2003. V. 68. № 7–8. P. 569–585.
5. Kita A., Kohayakawa H., Kinoshita T., Ochi Y., Nakamichi K., Kurumiya S., Furukawa K., Oka M. // Br. J. Pharmacol. 2004. V. 142. № 7. P. 1059–1072.
6. Nothdurfter C., Rammes G., Baghai T.C., Schüle C., Schumacher M., Papadopoulos V., Rupprecht R. // J. Neuroendocrinol. 2012. V. 24. № 1. P. 82–92.
7. Pinna G., Rasmusson A.M. // J. Neuroendocrinol. 2012. V. 24. № 1. P. 102–116.
8. Zhang L.M., Qiu Z.K., Zhao N., Chen H.X., Liu Y.Q., Xu J.P., Zhang Y.Z., Yang R.F., Li Y.F. // Int. J. Neuropsychopharmacol. 2014. V. 17. № 10. P. 1659–1669.
9. Gudasheva T.A. // Vestn. Ross. Akad. Med. Nauk. 2011. № 7. P. 8–16.
10. Gudasheva T.A., Deeva O.A., Mokrov G.V., Yarkov S.A., Yarkova M.A., Seredenin S.B. // Dokl. Biochem. Biophys. 2015. V. 464. № 3. P. 290–293.
11. File S.E. // Behav. Brain Res. 2001. V. 125. № 1–2. P. 151–157.
12. Ennaceur A., Delacour J. // Behav Brain Res. 1988. V. 31. № 1. P. 47–59.
13. Barsegyan A., McGaugh J.L., Roozendaal B. // Front. Behav. Neurosci. 2014. № 8. P. 160.
14. Verloes R., Scotto A.M., Gobert J., Wülfert E. // Psychopharmacology (Berl.). 1988. V. 95. № 2. P. 226–230.
15. Gorelov P.I., Ostrovskaya R.U., Sazonova N.M. // Eksp. Klin. Farmakol. 2013. V. 76. № 7. P. 3–5.
16. James M.L., Selleri S., Kassiou M. // Curr. Med. Chem. 2006. V. 13. № 17. P. 1991–2001.
17. Vallee M., Mayo W., Koob G.F., Le Moal M. // Int. Rev. Neurobiol. 2001. № 46. P. 273–320.

5-Arylaminouracil Derivatives as Potential Dual-Action Agents

E. S. Matyugina[1], M. S. Novikov[2], D. A. Babkov[2], V. T. Valuev-Elliston[1], C. Vanpouille[3], S. Zicari[3], A. Corona[4], E. Tramontano[4], L. B. Margolis[3*], A. L. Khandazhinskaya[1**], S. N. Kochetkov[1].
[1]Engelhardt Institute of Molecular Biology, Vavilova Str., 32, Moscow, 119991, Russia
[2]Department of Pharmaceutical & Toxicological Chemistry, Volgograd State Medical University, Pavshikh Bortsov Sq., 1, Volgograd, 400131, Russia
[3]Eunice Kennedy-Shriver National Institute of Child Health and Human Development, National Institutes of Health, Bethesda, MD 20892, USA
[4]Department of Life and Environmental Sciences, University of Cagliari, Monserrato, 09042, Italy
*E-mail: margolil@helix.nih.gov
**E-mail: khandazhinskaya@bk.ru
Received 27.01.2015

ABSTRACT **Several 5-aminouracil derivatives that have previously been shown to inhibit *Mycobacterium tuberculosis* growth at concentrations of 5–40 μg/mL are demonstrated to act also as noncompetitive non-nucleoside inhibitors of HIV-1 reverse transcriptase without causing toxicity *in vitro* (MT-4 cells) and *ex vivo* (human tonsillar tissue).**
KEYWORDS **5-(phenylamino)uracil derivatives, 5'-norcarbocyclic nucleoside analogs, HIV and *Mycobacterium tuberculosis* co-infection, dual action.**
ABBREVIATIONS **HIV, human immunodeficiency virus; TB, tuberculosis; WHO, World Health Organization; AIDS, acquired immunodeficiency syndrome; HIV NNRTIs, non-nucleoside inhibitors of HIV-1 reverse transcriptase.**

INTRODUCTION

Currently, HIV infection and TB are believed to be the major causes of infectious deaths worldwide. According to the latest WHO statistics, 9 million people were newly diagnosed with TB in 2013 and 1.5 million people died of TB (in 360,000 of these cases, TB was associated with HIV) [1]. In 2013, there were 35 million AIDS patients worldwide; 2.1 million cases of HIV infection were detected in 2013, and 1.5 million people died of AIDS, with TB remaining the main cause of death with dual infection (66.5%) [2]. HIV-infected patients are at an increased risk of latent tuberculosis reactivation (50% with TB vs. 10% without), and HIV-infected TB patients face a high risk of death. HIV patients receiving anti-TB drugs during a standard 6-month regimen are at a higher risk of recurrence than TB patients receiving a longer course of therapy [3]. Thus, TB and HIV co-infection is a very serious issue requiring a search for dual-action drugs.

Recently, we demonstrated that some 5-arylaminouracil derivatives are capable of affecting active division of *Mycobacterium tuberculosis* cells. Total inhibition of mycobacterium growth by compounds (**2**), (**3**), (**6**), (**7**), (**10**), (**15**)–(**17**), and (**19**) (*Fig. 1*) was observed at concentrations of 5–40 μg/mL, with compound (**19**) exhibiting a higher activity against the MS-115 strain with multiple-drug resistance (including five major first-line anti-TB drugs: isoniazid, rifampicin, streptomycin, ethambutol, and pyrazinamide) than against the sensitive H37Rv laboratory strain [4].

This paper is devoted to the evaluation of 5-arylaminouracil derivatives as HIV NNRTIs and to a more detailed investigation of the toxicity of these compounds.

EXPERIMENTAL

Compounds (**1**)–(**20**) were synthesized as previously described [4].

1-(4'-Hydroxy-2'-cyclopenten-1'-yl)-3-benzyl-5-(phenylamino) uracil (21)

K_2CO_3 (36 mg, 0.26 mM) and BnBr (42 μL, 0.35 mM) were added to a compound (**11**) solution (50 mg, 0.18 mM) in 5 mL of dimethylformamide (DMF). The reaction mixture was stirred at room temperature for 24 h. The reaction progress was monitored by means of TLC. We removed the solvent in an oil pump vacuum, purified the residue using column chromatography on silica gel, and eluted it with the system $CHCl_3$–CH_3OH (98:2). In total, 43 mg of the product (**21**) (yield of 66%) was obtained as a yellowish powder. R_f = 0.32 ($CHCl_3$–

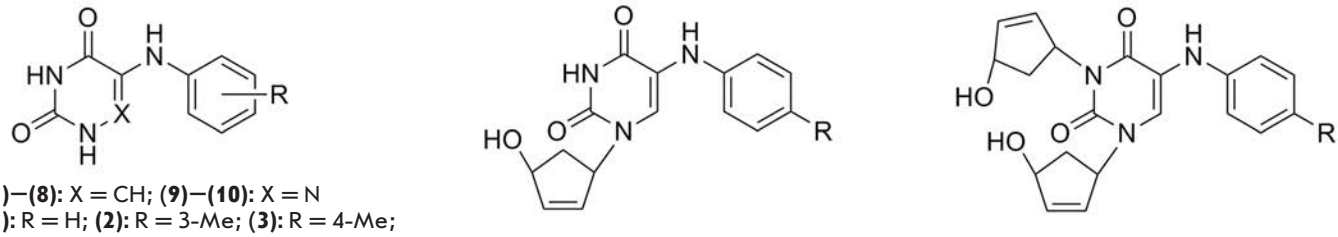

(1)–(8): X = CH; **(9)–(10):** X = N
(1): R = H; **(2):** R = 3-Me; **(3):** R = 4-Me;
(4): R = 2,3-Me_2; **(5):** R = 2,5-Me_2;
(6): R = 4-*n*Bu; **(7):** R = 4-*n*BuO;
(8): R = 4-PhO; **(9):** R = H; **(10):** R = 4-*n*Bu

(11): R = H; **(12):** R = Me; **(13):** R = *n*Bu;
(14): R = *n*BuO; **(15):** R = PhO

(16): R = H; **(17):** R = Me; **(18):** R = *n*Bu;
(19): R = *n*BuO; **(20):** R = PhO

Fig. 1

CH_3OH, 98 : 2). ^{1}H-NMR ($CHCl_3$): 7.50–7.49 (2H, m, H_3,H_5-Bn), 7.32–7.23 (6H, m, $H_{2''}$, $H_{3''}$, $H_{5''}$, $H_{6''}$, H_2,H_6-Bn), 6.95–6.93 (2H, m, H_5, H_4-Bn), 6.90–6.88 (1H, t, $H_{4''}$), 6.20–6.18 (1H, m, $H_{2'}$), 6.01 (1H, s, NH), 5.84–5.82 (1H, m, $H_{3'}$), 5.61–5.58 (1H, m, $H_{1'}$), 5.23–5.16 (2H, d, J = 13.70, CH_2), 4.84–4.83 (1H, m, $H_{4'}$), 2.86–2.85 (1H, m, $H_{a5'}$), 1.70–1.66 (1H, m, $H_{b5'}$). ^{13}C-NMR ($CHCl_3$): 160.80, 149.73 (C-4, C-2), 142.34 (C-4"), 139.24 (C-2'), 138.19 (C-4 Bn), 132.40 (C-3'), 129.63 (C-3", C-5"), 129.34 (C-3, C-5 Bn), 128.63 (C-2", C-6"), 127.91 (C-1"), 121.18 (C-1 Bn), 119.50 (C-5), 117.19 (C-6), 113.11 (C-2, C-6, Bn), 74.99 (C-1'), 61.05 (C-4'), 45.49 (C-5'), 39.94 (CH_2).

1-(4'-Hydroxy-2'-cyclopenten-1'-yl)-3-benzyl-5-(*p*-methylphenylamino) uracil(22)

The synthesis was carried out as for (**21**), with (**12**) used as a starting compound. Of the product (**22**), 35 mg (yield of 68%) was obtained as a white-yellow powder. R_f = 0.43 ($CHCl_3$–CH_3OH, 98 : 2). ^{1}H-NMR ($CHCl_3$): 7.50–7.48 (2H, m, H_3,H_5-Bn), 7.31–7.23 (4H, m, H_2, H_4, H_6-Bn, H_5), 7.06–7.04 (2H, m, $H_{3''}$,$H_{5''}$), 6.87–6.85 (2H, m, $H_{2''}$, $H_{6''}$), 6.18–6.16 (1H, m, $H_{2'}$), 5.94 (1H, s, NH), 5.83–5.81 (1H, m, $H_{3'}$), 5.58–5.56 (1H, m, $H_{1'}$), 5.23–5.16 (2H, d, J = 13.76, CH_2), 4.84–4.82 (1H, m, $H_{4'}$), 2.87–2.83 (1H, m, $H_{a5'}$), 2.26 (3H, s, CH_3), 1.69–1.65 (1H, m, $H_{b5'}$). ^{13}C-NMR ($CHCl_3$): 160.75, 149.66 (C-4, C-2), 139.57 (C-4"), 139.14 (C-2'), 138.19 (C-4 Bn), 132.40 (C-3'), 130.14 (C-3", C-5"), 129.33 (C-3, C-5, Bn), 128.67 (C-2", C-6"), 127.88 (C-1"), 120.23 (C-1, Bn), 117.86 (C-2, C-6, Bn), 117.66 (C-5), 114.39 (C-6), 75.02 (C-1'), 61.12 (C-4'), 45.45 (C-5'), 39.94 (CH_2), 20.76 (CH_3).

Anti-HIV activity

Isolation of recombinant HIV-1 reverse transcriptase (p66/p51 heterodimer) and determination of its activity were performed as described earlier [5, 6]. The inhibition constant (K_i), calculated according to Dixon's method for noncompetitive inhibitors [7], was used as a quantitative measure of the inhibitory activity of the compounds. Nevirapine, a first-generation HIV NNRTI, was used as a control.

Cytotoxicity in vitro

We tested the compounds for potential cytotoxicity in the MT-4 cell line using an automatic cell counter (ChemoMetec). The number of live and dead cells was counted in the control cultures, and the cultures were treated with compound (**6**), (**7**), or (**19**). Compounds (**6**) and (**7**) were tested at concentrations of 0.136–33 μM (0.035–9 μg/mL), and compound (**19**) was tested at concentrations of 0.272–66 μM (0.119–28 μg/mL).

We discriminated live from dead cells by evaluating propidium iodide uptake according to the manufacturer's instructions. We collected and analyzed data using the Nucleoview software (version 1.0,ChemoMetec).

Toxicity *ex vivo*

The cytotoxicity of compounds (**6**), (**7**), and (**19**) was determined in human tonsillar tissues. A total of 27 tissue blocks were incubated with compound (**19**) (20 μg/mL) or with compound (**6**) or (**7**) (5 μg/mL) for each experimental point. Tissue blocks were cultured for 12 days. Then, the cells were isolated from the control and treated and stained with combinations of fluorescence-labeled antibodies against CD3-QD605, CD4-QD655, CD8-QD705, CD25-APC, CD38-PE, HLA-DR-APC-Cy7, CXCR4-Brilliant violet 421, CCR5-PR-Cy5 CD45RA-FITC, and CCR7-PE-Cy7 (Caltag Laboratories; Biolegend). We determined the numbers of cells of different phenotypes in isolated suspensions using flow cytometry as previously described. The volume of an analyzed suspension was controlled by means of Trucount beads (Becton Dickinson); the number of counted cells was normalized to the weight of the tissue fragments used for cell isolation.

RESULTS AND DISCUSSION

The structural similarity of compounds (**1**)–(**20**) to uracil derivatives previously synthesized in our laboratory, together with their action as HIV NNRTIs [8, 9], suggested that these compounds might have similar properties. Compounds (**1**)–(**20**) belong to two groups: (**1**)–(**10**) are 5-arylaminouracil derivatives, while (**11**)–(**20**)

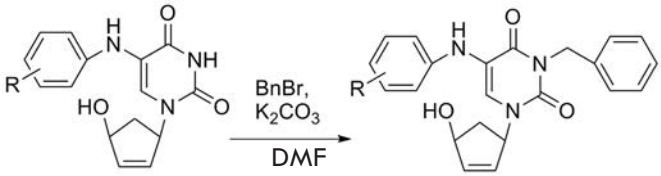

(11): R = H
(12): R = Me

(21): R = H
(22): R = Me

Fig.2

contain one or two additional 4'-hydroxycyclopentene moieties and thus can be considered as 5'-norcarbocyclic analogs of 2',3'-dideoxy-2',3'-uridine. Despite the known structural similarity to nucleosides, the 5'-norcarbocyclic analogs are able to inhibit HIV reverse transcriptase through a non-competitive mechanism, binding at the so-called hydrophobic "non-nucleoside inhibitor binding center" [8, 9]. However, those among compounds (**1**)–(**20**) that inhibit the growth of *M. tuberculosis* did not possess the ability to inhibit HIV-1 reverse transcriptase (K_i>> 200 μM). The only exception was compound (**15**) (K_i = 119 μM), which belongs to the class of 5'-norcarbocyclic analogs of uridine.

N^3-benzyl derivatives (**21**) and (**22**) (*Fig. 2*) were synthesized to enhance the anti-HIV activity of compounds of this class by increasing their hydrophobicity. These compounds were obtained in acceptable yields (61–69%) through a reaction of the initial carbocyclic analogs (**11**) and (**12**) with benzyl bromide in the presence of potassiumcarbonate. We confirmed the structures and purity of the synthesized compounds using ^{1}H- and ^{13}C-NMR-spectroscopy and TLC. The inhibitory activity of the derivative (**22**) against HIV-1 reverse transcriptase appeared to be slightly higher than those of compound (**21**) (K_i= 60 and>100 μM, respectively) and the initial compounds (**11**) and (**12**).

Previously, we had assessed the cytotoxicity of the synthesized compounds on Vero, A_{549}, and Huh7 cell lines and demonstrated that they were nontoxic at concentrations of up to 50 μg/mL (CD_{50} >> 100 μM). The toxicity of compounds (**6**), (**7**), and (**19**), which exhibited the most pronounced anti-TB properties, was further investigated *in vitro* on the MT-4 cell line and *ex vivo* on human tonsillar tissue.

Neither the cytotoxic nor the cytostatic effect of the compounds in MT-4 cells were observed at concentrations up to the maxima of 66 μM for (**19**) and 33 μM for (**6**) and (**7**).

Cytotoxicity assessment of the compounds (20 μg/mL for (**19**) and 5 μg/mL for (**6**) and (**7**)) on different cell types in the tissue system showed a lack of significant death rates of T cells (CD3+), B cells (CD3–), CD4+ and CD8+ T lymphocytes, and similarly for the CD4+ lymphocyte subgroups naive (CD45RA+/CCR7+), central memory cells (CD45RA–/CCR7+), effector memory cells CD45RA–/CCR7–), differentiated effector memory cells (Temra, CD45RA+/CCR7–), and activated CD4+ T-lymphocytes as well, with the last being identified as CD4+/CD25+, CD4+/CD38+T-cells, or CD4+/HLA-DR+. In all of these groups, the number of cells in the control and treated tissues was the same.

Thus, despite the fact that the new 5-arylaminouracil derivatives showed no significant anti-HIV-activity, even the low activity of compounds (**15**) and (**22**) is indicative of their affinity for HIV-1 reverse transcriptase. The structural similarity of compounds of this type to many highly active antiviral agents of non-nucleoside nature which are used in HIV infection as components of complex, highly intensive antiretroviral therapy [10], in combination with their profound antituberculosis activity, makes them attractive targets for further modifications. ●

This work was supported by joint project № 13-04-91441 of the Intramural Program of the National Institute of Child Health and Human Development, National Institutes of Health (NIH, USA) and the Russian Foundation for Basic Research, as well as by a project of the Russian Foundation for Basic Research № 13-04-00742.

REFERENCES

1. Global tuberculosis report 2014. WHO. http://www.who.int/tb/publications/global_report/gtbr14_executive_summary.pdf?ua=1
2. Global HIV report 2014. WHO. http://www.who.int/hiv/data/epi_core_dec2014.png?ua=1.
3. Nahid P., Gonzalez L.C., Rudoy I., de Jong B.C., Unger A., Kawamura L.M., Osmond D.H., Hopewell P.C., Daley C.L. // Am. J. Respir. Crit. Care Med. 2007. V. 175. P. 1199–1206.
4. Matyugina E.S., Novikov M.S., Babkov D.A., Ozerov A.A., Chernousova L.N., Andreevskaya S.A., Smirnova T.G., Karpenko I.L., Chizhov A.O., Muthu P., et al. // Chem. Biol. Drug Design. 2015. Accepted article: DOI: 10.1111/cbdd.12603.
5. Novikov M.S., Valuev-Elliston V.T., Babkov D.A., Paramonova M.P., Ivanov A.V., Gavryushov S.A., Khandazhinskaya A.L., Kochetkov S.N., Pannecouque C., Andrei G., et al. // Bioorg. Med. Chem. 2013. V. 21. P. 1150–1158.
6. Le Grice S.F., Grüninger-Leitch F.R. // Eur. J. Biochem. 1990. V. 187. P. 307.
7. Dixon M. // Biochem. J. 1953. V. 55. № 1. P. 170–171.
8. Matyugina E.S., Valuev-Elliston V.T., Babkov D.A., Novikov M.S., Ivanov A.V., Kochetkov S.N., Balzarini J., Seley-Radtke K.L., Khandazhinskaya A.L. // Med. Chem. Commun. 2013. V. 4. P. 741–748.
9. Matyugina E.S., Valuev-Elliston V.T., Geisman A.N., Novikov M.S., Chizhov A.O., Kochetkov S.N., Seley-Radtke K.L., Khandazhinskaya A.L. // Med. Chem. Commun. 2013. V. 4. P. 1443–1451.
10. Tanaka H., Baba M., Saito S., Miyasaka T., Takashima H., Sekiya K., Ubasawa M., Nitta I., Walker R.T., Nakashima H., et al. // J. Med. Chem. 1991. V. 34. № 4. P. 1508–1511.

Clonal Rearrangements and Malignant Clones in Peripheral T-cell Lymphoma

Yu. V. Sidorova[1], N. G. Chernova[1], N. V. Ryzhikova[1], S. Yu. Smirnova[1], M. N. Sinicina[1], Yu. E. Vinogradova[2], H. L. Julhakyan[1], A. M. Kovrigina[1], E. E. Zvonkov[1], A. B. Sudarikov[1]*
[1]National Hematology Research Center of the Ministry of Health, Novy Zykovski lane 4a, 125167, Moscow, Russia
[2]I.M. Sechenov Moscow State Medical University, Department of Hospital Therapy №2, B. Pirogovskaya, 4, 119435 Moscow, Russia
*E-mail: dusha@blood.ru
Received: 24.03.2015

ABSTRACT **Aim: To assess the feasibility and informative value of T-cell clonality testing in peripheral T-cell lymphoma (PTCL). Patients and methods: Biopsies of involved sites, blood, and bone marrow samples from 30 PTCL patients are included in the study. Rearranged *TCRG* and *TCRB* gene fragments were PCR-amplified according to the BIOMED-2 protocol and analyzed by capillary electrophoresis on ABI PRISM 3130 (Applied Biosystems). Results: *TCRG* and *TCRB* gene clonality assay was valuable in confirming diagnosis in 97% of PTCL patients. T-cell clonality assay performed on blood or bone marrow samples reaffirmed lymphoma in 93% of cases, whereas morphological methods were informative in 73% of cases only. We observed multiple *TCRG* and *TCRB* gene rearrangements, loss of certain clones in the course of the disease, as well as acquisition of new clones in 63% of PTCL cases, which can be attributed to the genetic instability of the tumor. Conclusion: *TCRG* and *TCRB* gene clonality assay is beneficial for the diagnosis of PTCL. However, the presence of multiple clonal rearrangements should be considered. Clonal evolution in PTCL, particularly acquisition of new clones, should not be treated as a second tumor. Multiple *TCRG* and *TCRB* gene rearrangements may interfere with minimal residual disease monitoring in PTCL.**
KEYWORDS **peripheral T-cell lymphoma, PCR, gene rearrangement of T cell receptor, T-lymphocytes clonality.**
ABBREVIATIONS **PTCL-NOS, peripheral T-cell lymphoma, not otherwise specified; TCR, T-cell receptor; TCRG, T-cell receptor gamma; TCRB, T-cell receptor beta; TCRD, T-cell receptor delta; CD, cluster of differentiation.**

INTRODUCTION

Peripheral T-cell lymphoma, not otherwise specified (PTCL-NOS) is a heterogeneous group of lymphomas with a mature immunophenotype of peripheral (post-thymic) T-lymphocytes. This diagnosis covers more than 29% of T-cell lymphomas that do not belong to other nosological forms and is a diagnosis by exclusion [1, 2]. Clinically, the disease is aggressive (five-year overall survival rate is less than 32%), often advanced (69% of patients are diagnosed at stages III/IV) with extranodal sites being involved (bone marrow, skin, subcutaneous tissue, and lungs) [3]. It is believed that the morphological substrates of the tumors are T-lymphocytes of mature T-cells immunophenotype with a αβ-variant of the T-cell surface receptor (TCRαβ) and CD2+, CD3+, CD5+, CD7+, CD4+ or CD8+ markers, whose expression displays signs of aberrance (loss of one or more of them). Most often, PTCL-NOS has a CD4+/CD8-immunophenotype, less commonly a CD4-/CD8+ one. In some peripheral T-cell lymphomas, the expression of T-cell markers on the surface is limited, e.g. only CD2 or CD3. In addition, a small number of PTCL-NOS are γδ-T-lymphocytes lymphomas that cannot be classified as hepatolienal γδ-lymphomas or γδ-variant of large granular lymphocytes leukemia based on clinical and morphological data [3–6]. A study of clonal rearrangements of T-cell receptor genes in PTCL-NOS confirms T-cell clonality in complex diagnostic cases and proves the presence of a tumor [7–11]. The method consists of PCR amplification and analysis of the genes of the V-D-J-segments junction region of the T-cell receptors δ (*TCRD*), γ (*TCRG*), and β (*TCRB*). This region has a unique nucleotide sequence in each normal T-lymphocyte. A fragment analysis of amplification products derived from healthy tissue reveals a lot of peaks with a Gaussian distribution of their lengths (*Fig.1A*). Monoclonal samples with the same length of PCR products are present as a single peak (monoallelic rearrangement, *Fig. 1B*) or as two peaks (biallelic rearrangement, *Fig. 1B*).

The length of the monoclonal PCR product is unique for the tumor clone and is identical in all affected tissues of a patient. Detection of a clone, for example, in bone marrow aspirate, indicates bone marrow involvement. Furthermore, the nature of rearrangements can reveal the degree of a lymphoid tumor maturity. Rearrangements during normal maturation of T-lymphocytes occur in sequence: *TCRD* (Vδ–Dδ, Dδ–Dδ, Dδ–Jδ, Vδ–Jδ) gene locus is rearranged first, followed by *TCRG* (Vγ–Jγ) and incomplete rearrangement of *TCRB* (Dβ–Jβ). Complete rearrangements of *TCRB* (Vβ–Jβ) and *TCR*α-locus (Vα–Jα) (*Fig. 2*) occur later [12, 13]. Since *TCR*δ (TCRD) genes are located inside *TCR*α-locus, they are cut out during *TCR*α rearrangement. Therefore, the entire range of clonal rearrangements observed in lymphomas can be divided into early and more mature ones. If a tumor contains *TCRD* and *TCRG* loci clonal products, incomplete rearrangement of Dβ–Jβ, and no complete Vβ-Jβ rearrangements of *TCRB* genes, this indicates an early nature of the rearrangements, which corresponds to a tumor of γδ-T-lymphocytes. More commonly, a tumor has a more mature spectrum of rearrangements: Vγ–Jγ, Dβ–Jβ, and Vβ–Jβ rearrangements present simultaneously, which is typical of most TCRαβ-lymphomas, including PTCL-NOS. According to published data, clonal rearrangements of the *TCRG* and *TCRB* genes are present in 81–94% and 96% of PTCL-NOS, respectively [7, 8].

MATERIALS AND METHODS

A retrospective analysis of clonality studies results in PTCL-NOS over the last 10 years (2005-2015) has

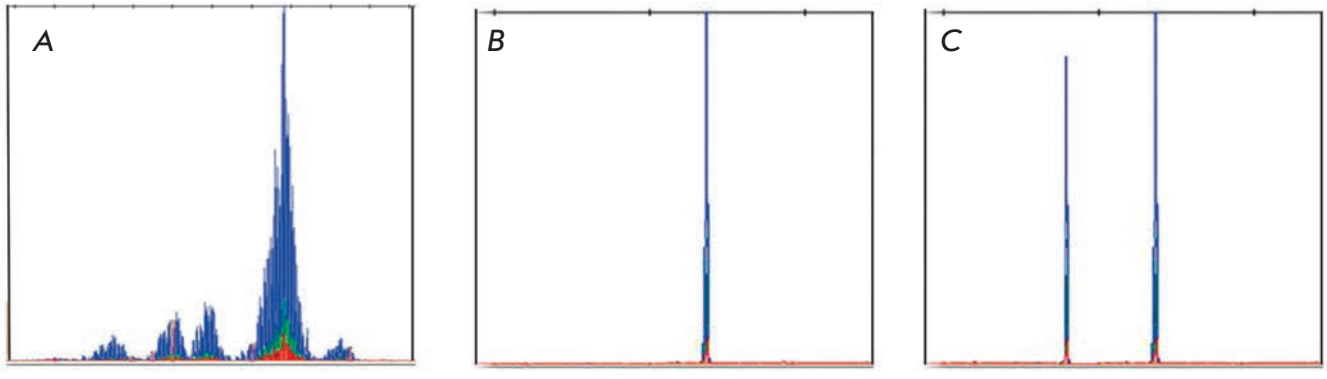

Fig. 1. Example of TCRG clonality testing: a) polyclonal, b) monoclonal (monoallelic rearrangement), c) monoclonal (biallelic rearrangement)

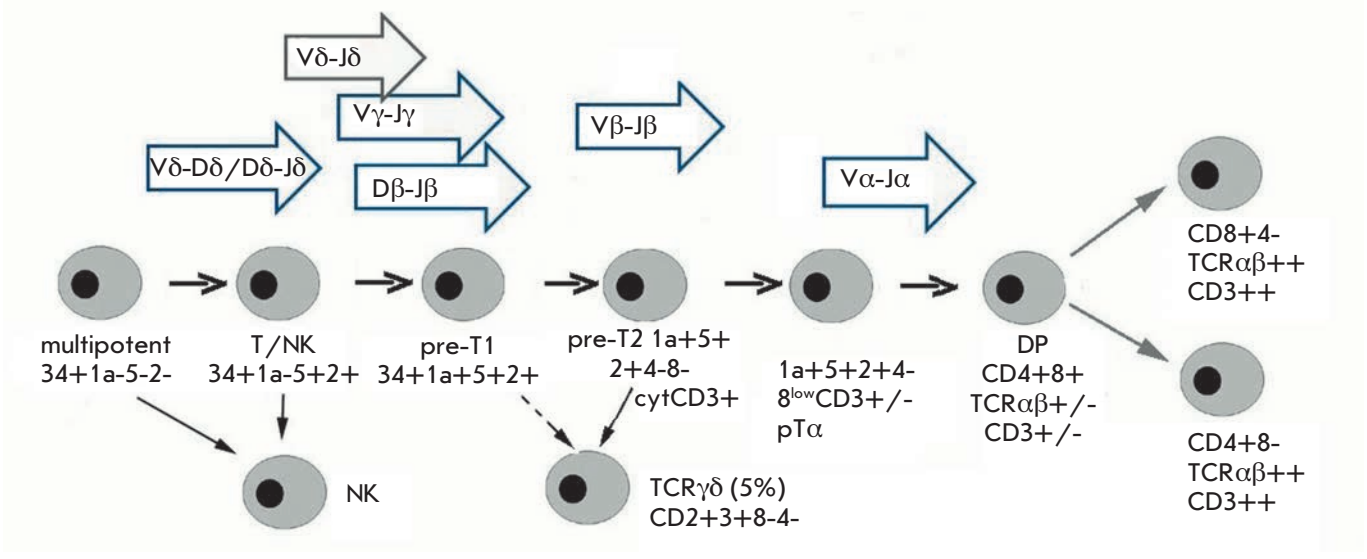

Fig. 2. Early stages of T-cell development. Sequential rearrangements in δ, γ, β, and α chains of TCR genes. DP – double positive cells

Table 1. Data of laboratory diagnostics

№	Major immunophenotypical characteristics of the tumor	Lesion volume	Stage	BM PCR	Total number of clonal rearrangements ***			Qty clones**	Qty tissues studied
					TCRG, *TCRD**	TCRB Dβ–Jβ	TCRB Vβ–Jβ		
1	LN CD3m+CD4+CD8-CD30-GranzB-CD5-CD57-CXCL13-CD7+	LN	I	nm	3 Vγ–Jγ	3 Dβ–Jβ	0	2	1
2	Spl CD3m+CD4+CD8+CD5+TIA-1+GranzB+CD7+CD56+	BM Liv Spl GI	IV	+	2 Vγ–Jγ	3 Dβ–Jβ	1Vβ–Jβ	3	5
3	Spl CD3m+CD4-CD8+CD2+CD7+CD30-CD10-CD5+	BM Spl	IV	+	1 Vγ-Jγ 3*TCRD*	2 Dβ–Jβ	5 Vβ–Jβ	4	2
4	BM CD3m+CD4+CD8+CD10-CD1a-CD5+CD7+	BM Spl	IV	+	6 Vγ–Jγ	4 Dβ–Jβ	5 Vβ–Jβ	4	2
5	BM CD3e-CD4-CD8+(part)CD7-CD2-CD1a-CD5-CD56-CD30- Spl CD3e+CD4-CD8-CD7-CD2-CD1a-CD5-CD30-ALK-GranzB-	BM Spl	IV	+	3 Vγ–Jγ	3 Dβ–Jβ	3Vβ–Jβ	3	3
6	LN CD3m+CD4+CD8-CD45RO+CD2+CD7-CD30-ALK-	BM LN	IV	+	3 Vγ–Jγ	nd	nd	2	1
7	LN CD3m+CD4-CD8+CDRO+CD30-CD15-CD23-CD56-	BM LN Spl Sto	IV	+	3 Vγ–Jγ	1 Dβ–Jβ	2Vβ–Jβ	2	5
8	LN CD3m+CD4+CD8-CD 5+CD10-CD23-	BM LN Skin Ton	III	+	5Vγ–Jγ	1 Dβ–Jβ	3Vβ–Jβ	4	9
9	LN CD3m+CD4-CD8+CD2+CD5+CD30+	BM LN Skin Lar Ton	IV	+	8Vγ–Jγ	3 Dβ–Jβ	3Vβ–Jβ	7	6
10	LN CD3m+CD4-CD8+CD5+TIA-1+	BM LN GI MG Lung	IV	+	2Vγ–Jγ	3 Dβ–Jβ	3Vβ–Jβ	3	6
11	LN CD3m+CD4+CD8-CD2+CD5+CD7+CD15-CD1a-	BM LN Lung Sto Skin Liv Spl NL	III	+	4Vγ–Jγ	2 Dβ-Jβ	2 Vβ–Jβ	5	7
12	LN CD3m+CD4+CD8-CD30+GranzB-EMA+	BM LN MG Lung Ton NL	IV	+	3 Vγ–Jγ	2 Dβ-Jβ	1 Vβ–Jβ	2	2
13	Spl CD3m+CD4-CD8-TIA-I+	BM Spl Liv	IV	+	8Vγ–Jγ	2 Dβ–Jβ	4Vβ–Jβ	4	4
14	LN CD3m+CD4+CD8+CD7+CD2+CD30-NK-	BM LN Skin	IV	+	2 Vγ–Jγ	3 Dβ–Jβ	1 Vβ–Jβ	2	2
15	Med CD3m+CD4+CD8-CD30-ALK-	Mediastinum	IE	nm	2 Vγ–Jγ	1Dβ–Jβ	1 Vβ–Jβ	1	1
16	Lung CD3m+CD4+CD8-CD45RO+CD5+CD7+CD30-CD10-CD23-	LN Lung	IE	+	3Vγ–Jγ	1Dβ–Jβ	2Vβ–Jβ	2	3
17	LN CD3m+CD4+CD8-CD30+CD33+CD56-	Med LN	III	+	3Vγ–Jγ	2Dβ–Jβ	1Vβ–Jβ	2	2
18	LN CD3m+CD4-CD8+CD5+CD7+	LN	III	+	2Vγ–Jγ	0	2Vβ–Jβ	1	2
19	LN CD3m+CD4+CD8-CD5+CD4+CD10-ALK-	LN Spl	III	+?	2Vγ–Jγ	0	1Vβ–Jβ	1	2
20	Spl CD3c+CD4-CD8-CD1a-CD2+CD5-CD7-CD4-CD8-CD16+CD56+	BM Spl	IV	+	2Vγ–Jγ	1Dβ–Jβ	2Vβ–Jβ	2	2
21	LN CD3m+CD4-CD8-CD30-CD15-CD5+CD7+NK-CD2+GranzB-	BM LN	IV	+	2Vγ–Jγ	1Dβ–Jβ	2Vβ–Jβ	2	2
22	LN CD3m+CD4-CD8+CD30-CD10-CD15-CD23-	BM LN	IV	+	1Vγ–Jγ	0	2Vβ–Jβ	1	1
23	Orbit CD3m+CD4+CD8+CD5+CD7+TIA-1+CD10-CD30-CD56-LPM-1-CD23-ALK-	Soft tissues of the orbirt	IE	Nm	1Vγ–Jγ	1Dβ–Jβ	1Vβ–Jβ	1	1
24	Spl CD3m+CD4+CD8-CD2+CD5+CD7+CD56+TIA-1+	BM Spl	IV	+	2Vγ–Jγ	1Dβ–Jβ	2Vβ–Jβ	1	2

25	LN CD3m+CD4+CD8-CD2+CD7+GranzB+CD30-CXCL13-PD1−LMP1-	Spl LN	III	-	0	0	0	0	2
26	LN CD3m+CD4+CD8-CD2+CD5+CD7+CD30-ALK−GranzB-EMA-CD56-CD57-	BM LN	IV	-	0	2 Dβ–Jβ (doubt)	1Vβ–Jβ (doubt)	1	2
27	LN CD3e-CD4-CD8-CD10-CD5-CD23-CD30-ALK-JICA+CD2+CD7+GranzB-	BM LN Skin	IV	+	0	1Dβ–Jβ (BM)	0	1	3
28	BM CD2+CD3+CD5-CD7+-CD4-CD8-CD16+56+cytCD3TCRγδ+ Spl CD3e+ (m+cyt) CD4-CD8-CD5-CD7-TIA-I+CD56+	BM Spl	IV	+	2Vγ–Jγ 3*TCRD*	2Dβ–Jβ	0	1	2
29	Blood CD3+TCRαβ+CD4+CD8+CD5+CD7+	BM Spl	IV	+	1Vγ–Jγ	0	2Vβ–Jβ	1	1
30	BM 30% cellsCD3+CD4-CD8-CD5-CD2+	BM Spl	IV	+	3 Vγ–Jγ	2Dβ–Jβ	1Vβ–Jβ	2	2

Note. LN, lymph node; Spl, spleen; BM, bone marrow; GI, intestine; Sto, stomach, Lar, larynx, Liv, liver; Ton, tonsils; Lung, lung; MG, mammary gland; NL, neuroleukemia; Med, mediastinum. TCRD*, the study of TCRD genes was conducted in two patients with suspicion of γδ-T-cell lymphoma. Number of clones**, the minimum number of tumor clones in a patient, based on the number of clonal rearrangements in a single locus and the appearance (changing) of clonal products in various tissues. Cases with appearance (change) of clonal products are underlined. For explanation, see Results and Discussion sections. The total number of clonal rearrangements***, total number of clonal rearrangements (peaks) observed in all tissues examined; nm, no material, nd, no data; doubt, an uncertain picture.

been conducted in the National Hematology Research Center of the Russian Ministry of Health (hereinafter the NHRC).

Patients and samples

The set of patients consisted of 30 people (15 men and 15 women, median age 56 years (32−75)). The disease stage was determined according to the Ann-Arbor classification (1971); bone marrow involvement was considered to be stage IV. Four patients were diagnosed with stage I; four, with stage III; and 22, with stage IV. Lymph nodes were involved in 18 (60%) patients; bone marrow, in 22 (73%); spleen, in 14 (47%); skin, in 5 (17%); gastrointestinal tract, in 4 (13%); lungs, in 4 (13%); tonsils, in 3 (10%); liver, in 3 (10%); mediastinum, in 2 (7%); meninges (neuroleukemia), in 2 (7%); mammary gland, in 2 (7%); and soft tissues of the orbit, in 1 (3%) (*Table 1*). Histological and immunohistochemical studies were performed in the NHRC Department of Pathology; and molecular and genetic studies of clonality, in the NHRC Laboratory of Molecular Hematology.

Isolation of DNA from tissues

Leukocytes and DNA from blood and bone marrow samples were isolated as described [14]. For isolation of DNA from tissue embedded into a paraffin block, five 5-μm sections were collected in Eppendorf tubes. The tissue was dewaxed by heating [15, 16]. Freshly frozen tissue for DNA extraction was thawed, and a 1×1×1 mm piece was cut out. DNA was isolated by the method based on tissue dissolution in concentrated ammonia with subsequent neutralization with glacial acetic acid and salting-out of proteins [17]. DNA concentration was determined using a UV spectrophotometer. DNA samples were stored at −20°C.

Studies of TCR gene rearrangements by PCR and fragment analysis

T-cell clonality was assessed using multiplex BIOMED-2 primers systems for fragment analysis [13] based on the rearrangements of the *TCRG* (Vγ−Jγ) and *TCRB* (Vβ−Jβ, Dβ−Jβ) genes. In the case of γδ-T-cell lymphomas, *TCRD* genes rearrangements were also analyzed. Multiplex amplification of *TCRD* genes was performed in duplicate tubes according to the BIOMED-2 protocol, Tube A and Tube B, and *TCRB* gene amplification, in three tubes, Tube A, Tube B, and Tube C (see description of the reactions in *Table 2*). Primers produced by Syntol (Russia) were used for amplification of the *TCRD*, *TCRG* genes. The reaction mixture in a final volume of 20 μl included 100 ng of DNA, 10 μl of a 2 × PCR mixture (PCR Master Mix Promega), and 5 pmol of each primer. *TCRB* genes were amplified using a commercial TCRB Gene Clonality Assay ABI Fluorescence Detection kit (Invivoscribe Technologies) and AmpliTaq Gold DNA polymerase (Applied Biosystems) according to the manufacturers' instructions. PCR conditions were as follows: pre-dena-

Table 2. Sets of PCR primers used for the BIOMED-2 protocol for the *TCRD*, *TCRG*, *TCRB* genes

Set of primers (the name of the tubes)	Forward primers	Reverse primers	Length of the product, bp
TCRD Tube A	Dδ2,Vδ1,Vδ2,Vδ3,Vδ4, Vδ5,Vδ6	Jδ1FAM Jδ2R6G Jδ3TAMRA Jδ4ROX	130–280
TCRD Tube B	Dδ2,Vδ1,Vδ2,Vδ3,Vδ4, Vδ5, Vδ6	Dδ3FAM	190–280
TCRG	Vγ1f, Vγ9, Vγ10, Vγ11	Jγ1/2FAM Jp1/2FAM	100–250
TCRB Tube A	Vβ2–Vβ24 (23 primers)	Jβ1.1–Jβ1.6HEX (6 primers) Jβ2.2, Jβ2.6, Jβ2.7 FAM (3 primers)	240–280
TCRB TubeB	Vβ2–Vβ24 (23 primers)	Jβ2.1, Jβ2.3, Jβ2.4, Jβ2.5 FAM (4 primers)	240–280
TCRB TubeC	Dβ1,Dβ2	Jβ1.1–Jβ1.6HEX Jβ2.1–Jβ2.7FAM (13 primers)	170–210 (Dβ2) 290–310 (Dβ1)

turation at 95˚C (5 min); 35 cycles at 92˚C (35 seconds), 60˚C (35 seconds), 72˚C (35); and final elongation at 72˚C (10 min). PCR was performed using an automated DNA Engine thermocycler (BioRad, Hercules, USA).

An automatic ABI PRISM 3130 Genetic Analyzer (Applied Biosystems, USA) was used for the fragment analysis of PCR products. To perform it, 2 μL of a 20-fold diluted PCR product was mixed with 10 μL of formamide (Applied Biosystems) and 0.04 μL of GeneScan 500-LIS Size Standard (Applied Biosystems). After denaturation at 95˚C for 3 minutes and subsequent cooling, 10 μL of the mixture was added to a well of a 96-well plate and high resolution capillary electrophoresis was performed on a POP-4 polymer (Applied Biosystems). The fluorescence of the amplificates and their profile (length distribution) were analyzed by the GeneMapper software v. 4.0 (Applied Biosystems).

Statistical analysis

To compare the results obtained by the two methods, the Spearman rank correlation coefficient was calculated using the following formula: $r_s = 1 - 6\sum d^2/(N^3 - N)$, where N is the sample size; d is the difference between the ranks for each member of the sample; and r_s is the Spearman coefficient.

RESULTS

TCR gene clonality was detected in 29 of the 30 patients (97%): for *TCRG* genes, in 27 of the 30 (90%); and for *TCRB* genes, in 29 of the 30 (97%). In some PTCL samples, the rearrangement was detected in only one of the loci, *TCRG* or *TCRB*, which is due to abnormal differentiation of tumor cells and is often associated with an immature and aberrant immunophenotype. For example, in patient 27, whose bone marrow had only one clonal Dβ–Jβ rearrangement, the surface of the tumor cells did not have CD3, CD5, CD4, or CD8, but only CD2 and CD7. The most likely explanation for the lack of clonal peaks in the study of *TCR* genes (patient 25) is the small number of tumor cells in the sample (many reactive T-lymphocytes). PCR detected bone marrow involvement or the presence of clonal lymphocytes in the blood in 93% (25 out of 27) of patients (*Table 1*). The clonal rearrangements in bone marrow were not detected only in patients 25 and 26, for whom clonal peaks were also absent or doubtful in the lymph nodes. Morphological methods failed to detect bone marrow involvement in four patients (№ 16–19), whereas PCR detected clonal cells in their bone marrow. Detection of clonal rearrangements of *TCRG* genes in the bone marrow or blood is considered to be a poor prognostic factor in PTCL [18]. In most patients, we observed multiple (more than two) clonal rearrangements in one locus. Tumor lymphocytes clone may have a rearrangement on one chromosome (monoallelic rearrangement) or on two homologous chromosomes (biallelic rearrangement). Therefore, only one or two clonal peaks can be detected for each gene (*TCRD* or *TCRG* or *TCRB*) in one tumor clone.

Additional Dβ2–Jβ rearrangement (*Fig. 3*) is described as an exception [19, 20]. In this case, an additional clonal peak in a range from 170–210 bp was observed in Tube C during fragment analysis after amplification of *TCRB* genes (*Table 2*).

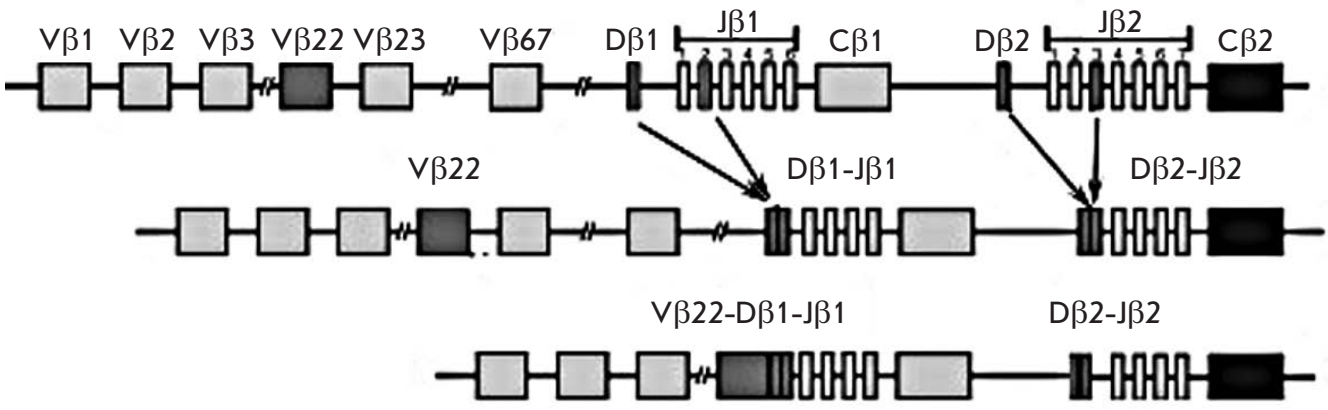

Fig. 3. Additional Dβ2–Jβ rearrangement acquisition diagram. Figure shows TCRB locus withVβ22–Dβ1-Jβ1 and Dβ2–Jβ2 fusions

In 13 out of the 30 (43%) patients, three or more clonal peaks were detected in one *TCR* gene locus in at least one tissue (10 patients, in the *TCRG* locus; 11, in the *TCRB* locus). Multiple (three or more) clonal peaks were detected at the same frequency in bone marrow, lymph nodes, and/or spleen (in 10 out of 13 patients). In theory, the "extra" peaks can be attributed to reactive T-cells, but we faced a completely different situation. In 63% of the patients (15 out of 24) in whom we had analyzed several tissues, we observed the appearance of new clonal peaks and new clones in various tissues. The clonal rearrangements reported earlier were either not detected or partially preserved. There was a correlation between observations for the *TCRG* and *TCRB* genes: i.e., the appearance of a new clonal peak of *TCRG* genes was usually accompanied by the identification of a new clonal rearrangement of *TCRB* genes. This pattern can only be explained by the presence of several tumor clones and their different representations in the tissues and organs. In total, several clones were detected in 19 of the 30 patients (63%). The number of clones ranged from two to seven (*Table 1*). There was no correlation with age ($p = 0.43$) or the stage of the disease ($p = 0.29$). Identification of several clones correlated with the number of analyzed tissues ($r_s = 0.6$, $p<0.0005$). This phenomenon might have been overlooked in other patients due to the low number of investigated tissues. The most representative examples of clonality studies in PTCL are given below.

Patient 11 (*Fig. 4*). At the time of the diagnosis, Patient 11 displayed a pattern typical of mature T-cell lymphoma: biallelic rearrangement of *TCRG* genes (212 and 224 bp) and complete rearrangement of *TCRB* genes (Tube B, 262 bp). Bone marrow examination revealed two more clones with incomplete rearrangement of *TCRB* genes (Tube C 187 and 193 bp). Progression of the disease leads to skin lesions, which were accompanied by one or two new clonal rearrangements of *TCRG* genes (201 bp) and complete rearrangement of *TCRB* genes (Tube A 254 bp). Further progress leads to the development of neuroleukemia. The cerebrospinal fluid (CSF) lacked the clones previously detected in the tumor (*TCRG* 212 and 224 bp) but contained a clone with rearrangement of *TCRG* genes, 201 bp in length, and a new clone with rearrangement of *TCRG* genes, 174 bp in length. After 11 months, the patient underwent splenectomy and liver biopsy due to growing cytopenia. The clonal rearrangement pattern in spleen and liver is identical to the original one in the stomach and lymph node. Therefore, Patient 11 has a total of four rearrangements of the *TCRG* gene: two full rearrangements of *TCRB* genes and two incomplete rearrangements of the *TCRB* gene. The dynamics of appearance of new rearrangements during the progression of the disease indicates five or more different tumor clones.

Patient 9 (*Fig. 5*). Patient 9 had multiple clonal rearrangements of the *TCRG* and *TCRB* genes with a varying presence of clones in different tissues and organs. The primary diagnosis included examination of the blood, bone marrow, tonsil biopsy and lymph node 1. Five or more rearrangements of the *TCRG* and *TCRB* genes were detected in the blood and bone marrow. Tonsil and lymph node 1 contained three and four clonal rearrangements of *TCRG*, respectively, and four rearrangements of the *TCRB* gene. Lymph node 2 and skin biopsies were performed with progression of the disease. The lymph node biopsy revealed five rearrangements of the *TCRG* gene and eight of the *TCRB* genes. Except for the rearrangements of *TCRB* (A), 267

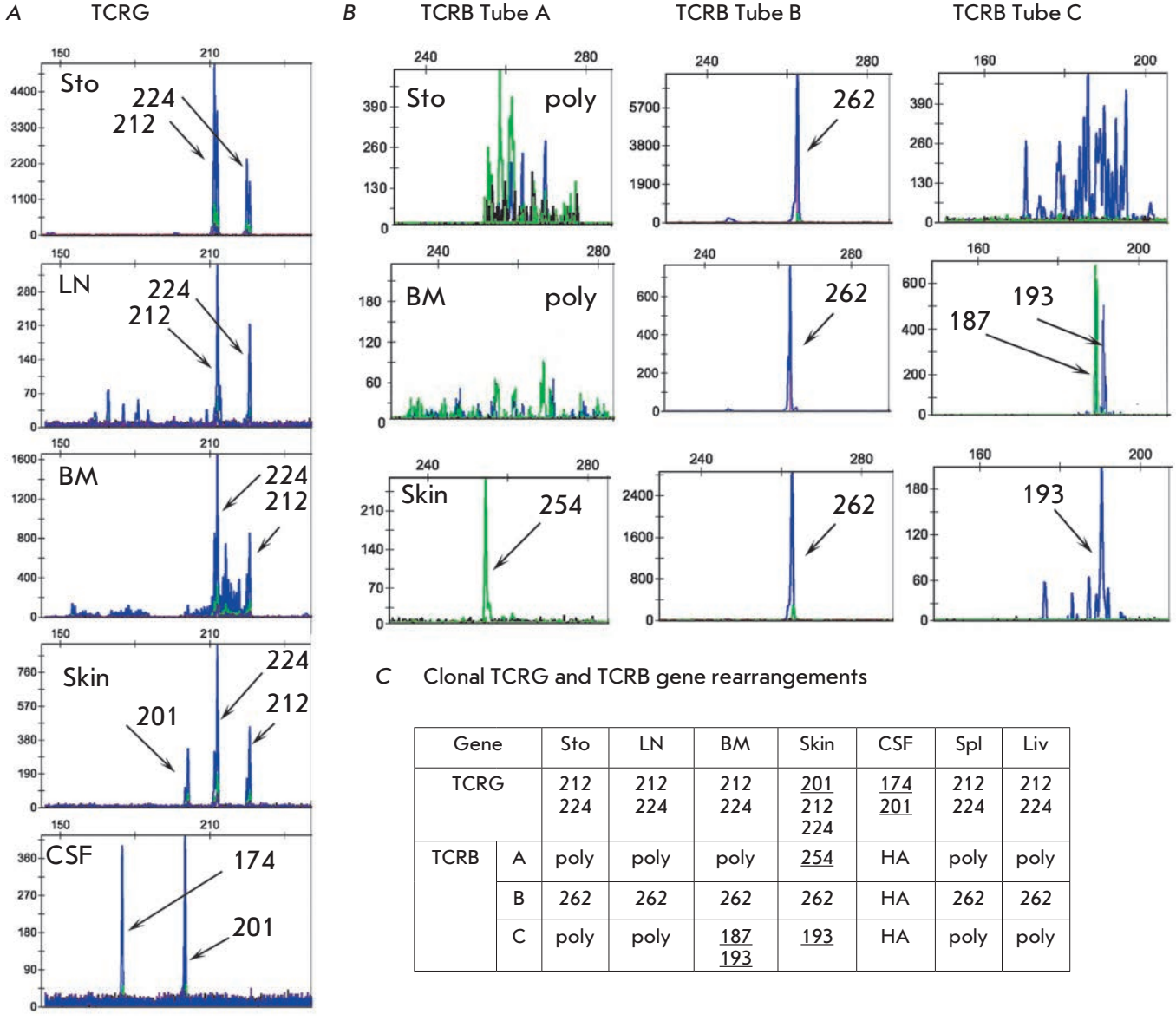

C Clonal TCRG and TCRB gene rearrangements

Gene		Sto	LN	BM	Skin	CSF	Spl	Liv
TCRG		212 224	212 224	212 224	<u>201</u> 212 224	<u>174</u> <u>201</u>	212 224	212 224
TCRB	A	poly	poly	poly	<u>254</u>	HA	poly	poly
	B	262	262	262	262	HA	262	262
	C	poly	poly	<u>187</u> <u>193</u>	<u>193</u>	HA	poly	poly

Fig. 4. Clonal TCR rearrangements found in case 11.A, TCRG pattern; B, TCRB pattern; C, Summary Table. Sto, stomach, BM, bone marrow, LN, lymph node, CSF, poly, polyclonal case, NA, no amplification. New clonal products are underlined

bp, and *TCRB* (B), 262 bp, that are present in most tissues simultaneously, other rearrangements of *TCRB* genes were randomly distributed and belonged to different tumor clones. The data of molecular clonality studies indicate the presence of seven or more tumor clones in this patient.

Patient 8 (*Fig. 6*). Patient 8 had five different rearrangements of *TCRG* genes (177, 183, 204, 225, 248 bp) with different clones present in different studied tissues. We found four rearrangements of *TCRB*: three complete rearrangements (Tubes A and B) and one incomplete Dβ2–Jβ2 (Tube C). In this case, there was no clear connection between the *TCRG* and *TCRB* genes rearrangements. For example, the lymph node 1 and skin predominantly had *TCRG* gene rearrangements, 183 and 248 bp in size, however, the pattern for *TCRB* was different. The number of clones in this patient was four or higher, but it is possible that the number of clones could be much higher. For example, the clones with only a *TCRG* or *TCRB* rearrangement, or clones with rearrangements of *TCRG* 177 bp and *TCRB* 260 bp, *TCRG* 177 bp and *TCRB* 189 bp, etc.

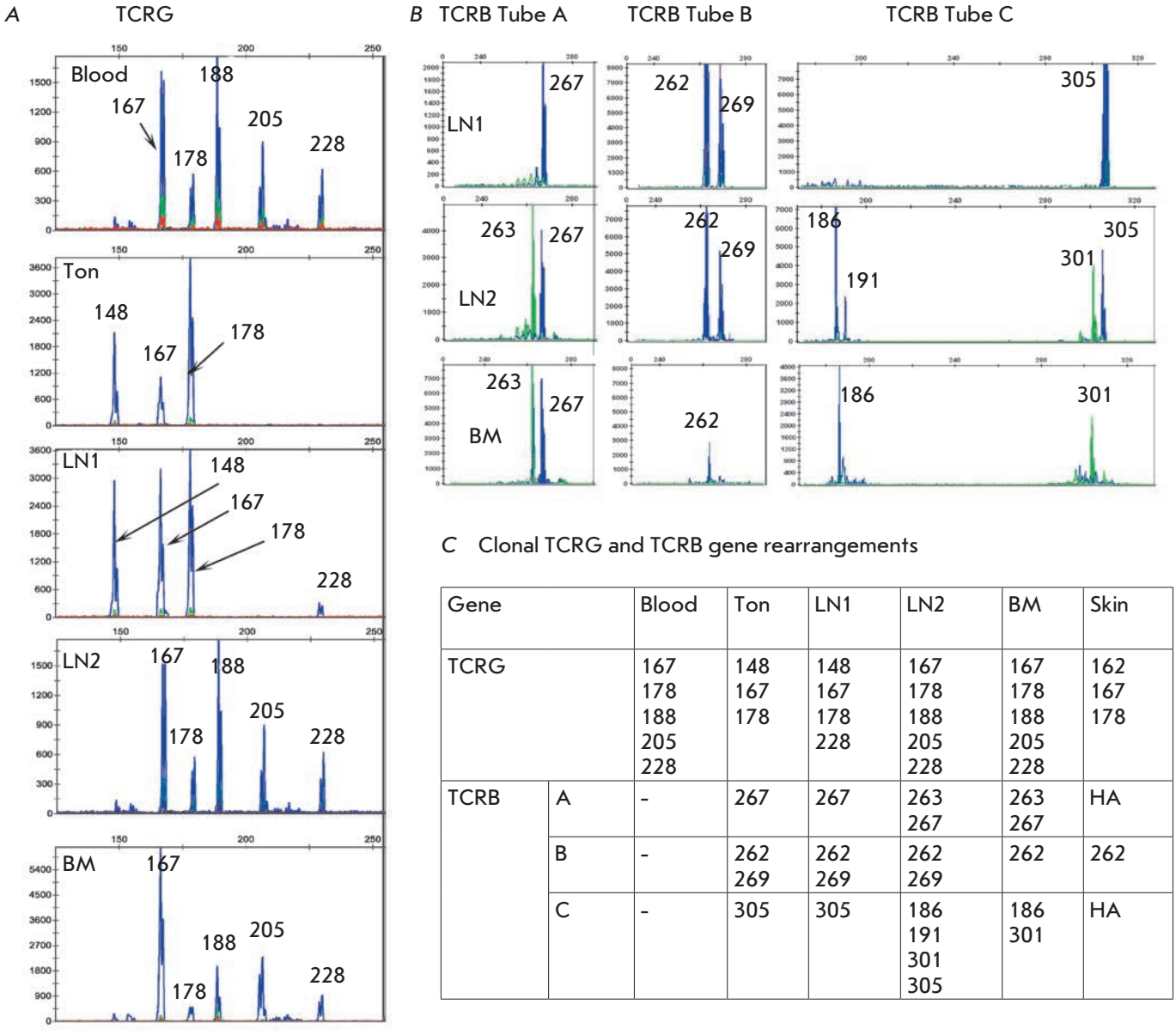

C Clonal TCRG and TCRB gene rearrangements

Gene		Blood	Ton	LN1	LN2	BM	Skin
TCRG		167 178 188 205 228	148 167 178	148 167 178 228	167 178 188 205 228	167 178 188 205 228	162 167 178
TCRB	A	-	267	267	263 267	263 267	HA
	B	-	262 269	262 269	262 269	262	262
	C	-	305	305	186 191 301 305	186 301	HA

Fig. 5. Clonal TCR rearrangements found in case 9.A, TCRG pattern; B, TCRB pattern; C, Summary table. Ton, tonsil; BM, bone marrow; LN, lymph node; NA, no amplification

DISCUSSION

The presence of several tumor clones described in acute lymphoblastic leukemia (ALL) is attributed to an "ongoing" process of rearrangement of immunoglobulins and *TCR* genes in early progenitor cells [21–24]. Clonal products sequencing during ALL manifestation and in relapse showed that clones with incomplete rearrangements of the *TCRD* and *TCRB* genes and their derivatives with complete clonal rearrangements are simultaneously present in ALL. Furthermore, in some cases complete rearrangement is modified. The *V* gene is replaced with another (upstream) gene or the rearrangement is completely replaced by another one of the upstream *V* and downstream *J* genes, i.e. by the genes that are distal to the previous rearrangement. In some cases, there is a deletion and disappearance of the *TCR* gene rearrangement in relapse.

We believe that the molecular events that occur in ALL can also occur in PTCL. In tumor cells, the control mechanisms which are responsible for preventing further restructuring of a locus after a productive rearrangement are disrupted, which leads to increased

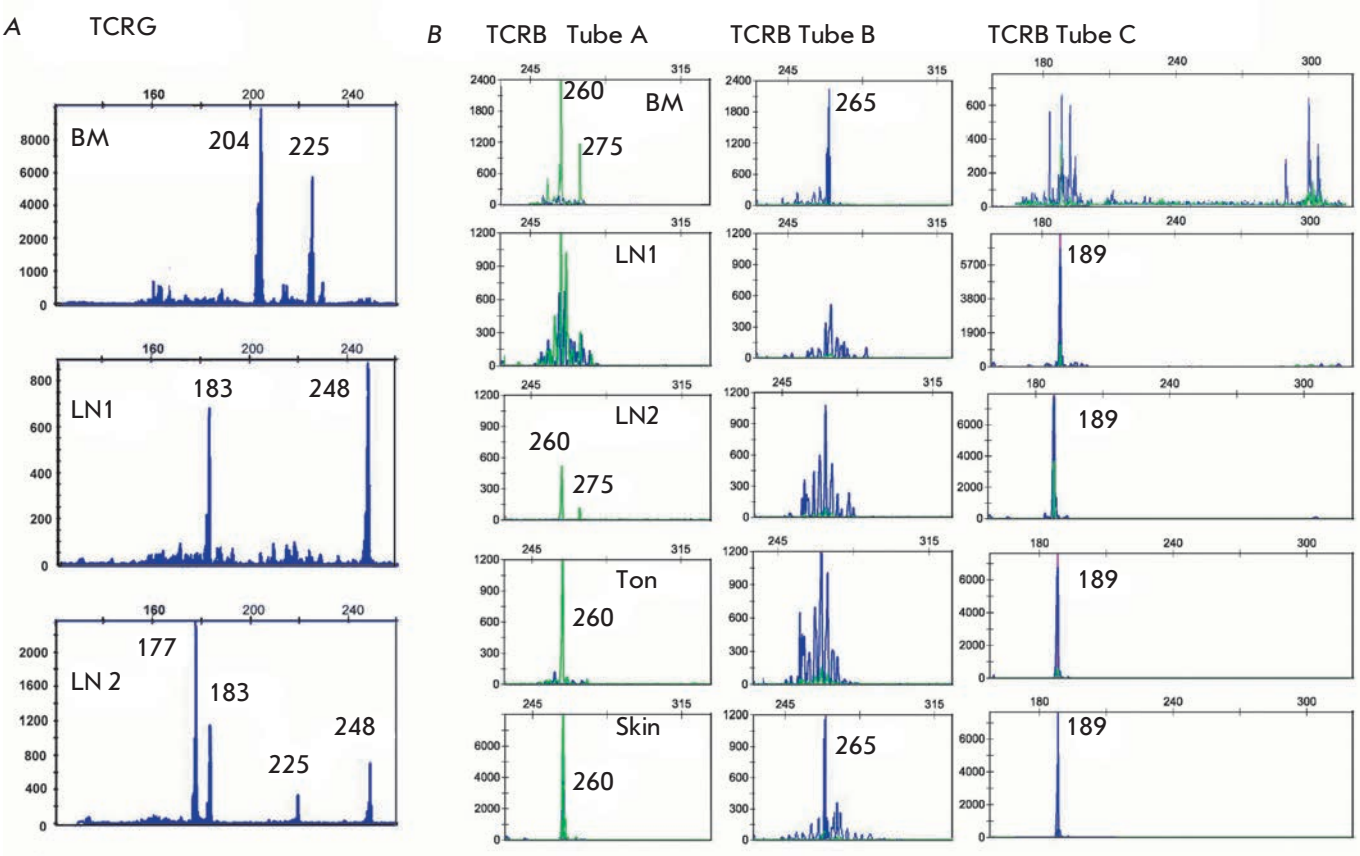

C Clonal TCRG and TCRB gene rearrangements

Gene		BM	LN1	LN2	Ton	LN3	Skin
TCRG		204 225	183 248	177 183 225 248	177	177	183 248
TCRB	A	260 275	poly	260 275	260	260	260
	B	265	poly	poly	poly	poly	265
	C	poly	189	189	189	189	189

Fig. 6. Clonal TCR rearrangements found in case 8.A, TCRG pattern; B, TCRB pattern; C, Summary table. Ton, tonsil; BM, bone marrow; LN, lymph node; poly, polyclonal case

activity of the *RAG1* and *RAG2* enzymes, changes in chromatin organization, etc. It is possible that in PTCL rearrangements can be replaced with new ones and/or that an incomplete Dβ–Jβ one can be replaced with a complete Vβ–Jβ one. In addition, there is general chromosomal instability, which can lead to deletions or duplications of the *TCR* genes locus. The deletion of the locus may trigger further rearrangements on homologous chromosomes. Complex chromosomal changes, including triploidy, tetraploidy, loss of chromosomes, 7q trisomy, and translocations involving *TCR* genes loci (14q11, 7q34-35, 7p13-21) are described in various pe-

ripheral T-cell lymphomas [25–27]. In any case, clonal rearrangements are common markers that indicate the heterogeneity of the tumor and clonal evolution during the progression of the disease. We have observed "multiclonality" in most patients, but it is unclear whether this phenomenon is present only in PTCL. It is possible that some other lymphomas also have high clonal heterogeneity, but their "visualization" requires different approaches and methods.

CONCLUSIONS

Studies of *TCRG* and *TCRB* genes clonality effectively prove the presence of a tumor in the majority (97%) of PTCL patients. PCR revealed bone marrow involvement and/or presence of clonal lymphocytes in the blood in the majority (93%) of patients, whereas in morphological studies bone marrow involvement was confirmed only in 73% of the patients. A specific pattern of rearrangements in PTCL (multiple rearrangements of the *TCRG* and *TCRB* genes, loss and gain of new ones, presence of several clones of a tumor) was observed in the majority of patients (63%) and should certainly be taken into account when using this method for diagnostic purposes. The emergence of new clonal peaks (clones) should not be considered to be the emergence of a new tumor. In addition, multiple rearrangements may interfere with minimal residual disease monitoring in PTCL. ●

REFERENCES

1. Swerdlow S.H., Campo E., Harris N.L., Jaffe E.S., Pileri S.A., Stein H., Thiele J., Vardiman J.W. WHO Classification of Tumors of Hematopoietic and Lymphoid Tissues. Lyon: IARC, 2008. V. 2. 439 p.
2. Vose J., Armitage J., Weisenburger D., Savage K., Connors J., Gascoyne R., Chhanabhai M., Wilson W., Jaffe E., Armitage J., et al. // J. Clin. Oncol. 2008. V. 26. № 25. P. 4124–4130.
3. Weisenburger D.D., Savage K.J., Harris N.L., Gascoyne R.D., Jaffe E.S., MacLennan K.A., Rüdiger T., Pileri S., Nakamura S., Nathwani B., et al. // Blood. 2011. V. 117. № 12. P. 3402–3408.
4. De Leval L., Gaulard P. // Histopathology. 2011. V. 58. № 1. P. 49–68.
5. Vinogradova Yu. E., Lutsenko I.N., Samoilova R.S., Selivanova E.I., Zamulaeva I.A., Gretsov E.M., Vorobyov I.A., Kaplanskaya I.B., Ryzhikova N.A., Al-Radi L.S., Gabeeva N.G., Dzhulakyan U.L., Egorova E.K., Margolin O.V., Kremenetskaya A.M., Vorobyov A.I. // Gematologiya i Transfuziologiya. 2009. V. 54. №2. P. 14–18.
6. Vinogradova Y.E., Kaplanskaya I.B., Samoilova R.S., Vorobiev I.A., Zingerman B.V., Sidorova Y.V., Shklovskiy-Kordi N.E., Aitova L.G., Maryin D.C., Vorobiev A.I., et al. // Clin. Med. Insights: Blood Disorders. 2012. № 5. P. 1–13.
7. Brüggemann M., White H., Gaulard P., Garcia-Sanz R., Gameiro P., Oeschger S., Jasani B., Ott M., Delsol G., Orfao A., et al. // Leukemia. 2007. V. 21. № 2. P. 215–221.
8. Tan B.T., Warnke R.A., Arber D.A. // J. Mol. Diagn. 2006. V. 8. № 4. P. 466–475.
9. Sidorova Yu. V., Nikitin E.A., Peklo M., Vlasik T.N., Samoilova R.S., Kravchenko S.K., Melikyan A.L., Vinogradova Yu. E., Pivnik A.V., Sudarikov A.B. // TerArkh. 2003. V. 75. № 7. P. 48–52.
10. Nikitin E.A., Sidorova Yu. V., Ryzhikova N.V., Biderman B.V., Melikyan A.L., VinogradovaYu.E., Al-Radi L.S., Sudarikov A.B. // TerArkh. 2006. V. 78. № 7. P. 52–57.
11. Sidorova Yu. V., Nikitin E.A., Biderman B.V., Groznova A. A., Sorokina T.V., Sudarikov A.B. // Spravochnik Zaveduyushchego KDL 2009. № 6. P. 13–21.
12. Rothenberg E.V., Moore J.E., Yui M.A. // Nat. Rev. Immunol. 2008. V. 8. № 1. P. 9–21.
13. Dongen J.J., Langerak A.W., Bruggemann M., Evans P.A., Hummel M., Lavender F.L., Delabesse E., Davi F., Schuuring E., García-Sanz R., et al. // Leukemia. 2003. V. 17. № 12.P. 2257–2317.
14. Sidorova Yu. V., Sorokina T.V., Biderman B.V., Nikulina Ye. Ye., Kisilitchina D.G., Naumova Ye. V., Potchar M. Ye., Lugovskaya S.A., Ivanova V.L., Kovaleva L.G., Ptuschkin V.V., Nikitin Ye. A., Sudarikov A.B. // Klin Lab Diagn. 2011. № 12. P. 22–35.
15. Wu L., Patten N., Yamashiro C.T., Chui B. // Appl. Immunohistochem. Mol. Morphol. 2002. V. 10. № 3. P. 269–274.
16. Coombs N.J., Gough A.C., Primrose J.N. // Nucl. Acids-Res. 1999. V. 27. № 16. e12.
17. Sidorova J.V., Biderman B.V., Nikulina E.E., Sudarikov A.B. // Exp. Dermatol. 2012. V. 21. № 1. P. 57–60.
18. Schützinger C., Esterbauer H., Hron G. // Leuk. Lymphoma. 2008. V. 49. № 2. P. 237–246.
19. Langerak A.W.,Wolvers-Tettero I.L.M.,Van Dongen J.J.M. // Leukemia. 1999. V. 13. № 6. P. 965–974.
20. Groenen P.J., Langerak A.W., van Dongen J.J., van Krieken J.H. // J. Hematop. 2008. V. 1. № 2. P. 97–109.
21. Szczepański T., van der Velden V.H., Raff T., Jacobs D.C., van Wering E.R., Brüggemann M., Kneba M., van Dongen J.J. // Leukemia. 2003. V. 17. № 11. P. 2149–2156.
22. de Haas V., Verhagen O.J., von dem Borne A.E., Kroes W., van den Berg H., van der Schoot C.E. // Leukemia. 2001. V. 15. № 1. P. 134–140.
23. Szczepański T., Willemse M.J., Brinkhof B., van Wering E.R., van der Burg M., van Dongen J.J. // Blood. 2002. V. 99. № 7. P. 2315–2323.
24. Germano G., del Giudice L., Palatron S., Giarin E., Cazzaniga G., Biondi A., Basso G. // Leukemia. 2003. V. 17. № 8. P. 1573–1582.
25. Boehm T., Rabbitts T.H. // FASEB J. 1989. V. 3. № 12. P. 2344–2359.
26. Schlegelberger B., Himmler A., Godde E., Grote W., Feller A.C., Lennert K. // Blood. 1994. V. 83. №2. P. 505–511.
27. Gesk S., Martín-Subero J.I., Harder L., Luhmann B., Schlegelberger B., Calasanz M.J., Grote W., Siebert R. // Leukemia. 2003. V. 17. № 4. P. 738–745.

Internalization and Recycling of the HER2 Receptor on Human Breast Adenocarcinoma Cells Treated with Targeted Phototoxic Protein DARPin-miniSOG

O. N. Shilova*, G. M. Proshkina, E. N. Lebedenko, S. M. Deyev
Shemyakin/Ovchinnikov Institute of Bioorganic Chemistry, Russian Academy of Sciences, Miklukho-Maklaya Str., 16/10, Moscow, 117997, Russia
*E-mail: olga.shilova.n@gmail.com

ABSTRACT **Design and evaluation of new high-affinity protein compounds that can selectively and efficiently destroy human cancer cells are a priority research area in biomedicine. In this study we report on the ability of the recombinant phototoxic protein DARPin-miniSOG to interact with breast adenacarcinoma human cells overexpressing the extracellular domain of human epidermal growth factor receptor 2 (HER2). It was found that the targeted phototoxin DARPin-miniSOG specifically binds to the HER2 with following internalization and slow recycling back to the cell membrane. An insight into the role of DARPin-miniSOG in HER2 internalization could contribute to the treatment of HER2-positive cancer using this phototoxic protein.**

KEYWORDS **internalization, recycling, scaffold proteins, DARPin, targeted phototoxic protein, HER2.**

ABBREVIATIONS **DARPin – Designed Ankyrin Repeat Protein, HER2 – human epidermal growth factor receptor 2, IPTG – isopropyl β-D-1-thiogalactopyranoside, PBS – phosphate buffered saline, PI – propidium iodide, scFv – single-chain variable antibody fragment.**

INTRODUCTION

Monoclonal antibodies and their derivatives are widely used in clinical application for selective destruction of human tumors [1, 2]. At the same time, the development of new approaches (such as fully synthetic libraries, phage and ribosomal display) for *in vitro* generation of non-natural proteins with high affinity for a given target has led to the creation of non-immunoglobulin scaffold proteins with one whole framework, carrying altered amino acids that confer on protein variants specificity to different targets [3–5]. Scaffold proteins, having the same affinity and specificity, surpass their corresponding monoclonal antibodies in physical and chemical properties. They possess such desired properties as a small size, which enables efficient tissue penetration, rapid folding, high chemical, proteolytic and thermal stability and they do not tend to aggregate. A scaffold protein can be engineered to have a unique cysteine that facilitates further chemical conjugation to cytotoxic molecules, fluorophores and nanoparticles. Moreover, the absence of disulfides allows to expresse proteins in the cytoplasm of *Escherichia coli* and produce proteins with high affinity to selective target without animal immunization. These features give scaffold proteins advantages over antibodies being used as binding moieties in multifunctional compounds for the diagnosis and treatment of human diseases.

Alternative binding molecules include adnectins, affibodies, anticalins and proteins based on naturally occurring repeat proteins (ankyrin and tetratricopeptide repeats) [3–5].

In the laboratory of Dr. Plückthun set-designed ankyrin repeat proteins (DARPins) with high affinity for human epidermal growth factor receptor 2 (HER2 or ERBB2) have been developed [6].

The transmembrane receptor HER2 is overexpressed in 20–30% of breast and ovary tumors [7, 8]. High level of HER2 expression usually correlates with aggressive tumor phenotype and enhanced metastasis [9]. Because HER2 is expressed at relatively low levels in normal epithelial cells, it makes this receptor an attractive target in cancer therapy. In summary, the design and evaluation of novel, highly specific molecules

capable of selectively killing cancer cells overexpressing HER2 remain an important task.

In this work, we used DARPin_9-29 as a targeting module to deliver the phototoxic protein miniSOG [10] to human breast adenocarcinoma HER2-positive cells.

The objective of this study was to assess the binding of the fusion protein DARPin-miniSOG to a HER2 overexpressing tumor cells and to investigate the possibility of internalization of the HER2/DARPin-miniSOG complex.

EXPERIMENTAL SECTION

Cell lines and cultivation conditions

Human breast adenocarcinoma HER2 overexpressing SK-BR-3 cells and Chinese hamster ovary CHO cells were grown at 37°C in 5% CO_2 in a McCoy's 5A medium (Life technologies, USA) supplemented with 10% fetal bovine serum (HyClone, Belgium).

Production of DARPin-miniSOG protein

The coding sequence of the targeting module DARPin_9-29 was amplified from plasmid pCG-Hnse-DARPin-d18-9-29 (kindly provided by Dr. Plückthun, University of Zurich). The amplified fragment was digested by NdeI and HindIII endonucleases and inserted into the pET22b expression vector digested with the same enzymes. The coding sequence of the cytotoxic module miniSOG was amplified from plasmid pSD-4D5scFv-miniSOG [11], digested with HindIII and XhoI endonucleases and cloned into a pET22b vector in the same reading frame with a DARPin_9-29 coding sequence. The resulting expression cassette consists of inducible promoter T7 and polynucleotide sequences encoding DARPin_9-29, miniSOG, and hexahistidine tag.

The DARPin-miniSOG protein was produced in *E. coli* strain BL21(DE3). Protein expression was induced with 1 mM IPTG at OD_{600}= 0.5–0.7. Cell culture was grown at 25°C for 8 h. DARPin-miniSOG was isolated from a soluble fraction by metal affinity chromatography according to the manufacturer's instructions.

Flow cytometry

Flow cytometry analysis was performed on a BD Accuri C6 cytometer (Becton Dickinson, USA). Adherent cells were detached by incubation in a Versen solution ("PanEko", Russia) and washed with PBS ("PanEko", Russia). To determine live and dead cell subpopulations, the samples were incubated in 100 μl PBS with propidium iodide (PI, Sigma-Aldrich, USA) in final concentration 2.5 mg/ml on ice for 5 min in the dark. A minimum of 10,000 events were collected for each sample. Cells were gated on single cell populations followed by gating on viable cells (PI negative). The following detection parameters were used: 20 mV laser power, 533/30 nm band pass filter (FL1-channel) for DARPin-miniSOG, and 585/40 nm band pass filter (FL2-channel) for PI. Data were analyzed using the BD Accuri C6 software.

Competitive binding assay

The binding specificity of the fusion protein DARPin-miniSOG to HER2 was tested by flow cytometry. HER2 overexpressing SK-BR-3 cells were treated with DARPin-miniSOG in the presence or in the absence of a competitive agent, and the fluorescence intensity was measured. Confluent SK-BR-3 cells were detached by incubation in Versen solution, washed twice in PBS. Each sample included ~10^5cells. The cells were incubated with DARPin-miniSOG (500 nM) on ice for 30 min and washed twice with cold PBS to remove the unbound protein. Fluorescence intensity was detected in the FL1 channel (green fluorescence). All data were obtained as means of FL1 fluorescence intensities. DARPin_9-29 was used as a competitive agent in equimolar concentration. The anti-HER2 4D5-scFv, specific for a different HER2 epitope, was used as a negative control.

Internalization of HER2 upon interaction with DARPin-miniSOG

SK-BR-3 cells were grown in a McCoy's 5A medium (Life technologies, USA) with 1% fetal bovine serum (HyClone, Belgium) for 14 h. The culture medium was removed, the cells harvested and washed twice with PBS. A cell suspension of 4 × 10^5 cells was incubated with 250 μl of 1 μM DARPin-miniSOG in PBS on ice for 30 min, harvested by centrifugation at 4°C for 5 min at 800g, washed once with cold PBS, and aliquoted into four portions. The first portion was subjected to detection of the level of DARPin-miniSOG fluorescence on the surface of SK-BR-3 cells at 4°C. The level of cellular autofluorescence was established on untreated cells (control).

The other three portions (1 × 10^5 cells each), treated with DARPin-miniSOG at 4°C, were incubated in a McCoy's medium with 1% serum in a 24-well plate in 5% CO_2 at 37°C until needed. After 4, 8, and 12 h following the first measurement, the cells were detached with a Versen solution, washed twice with PBS, and divided in half. The first half of cells was used for measuring background fluorescence; the second half was incubated in 50 μl of 1 μM DARPin-miniSOG on ice for 30 min. After incubation, the cells were once washed with cold PBS. DARPin-miniSOG fluorescence was measured for each pair of samples at each time point.

Time course of fluorescence intensity of HER2-truncated SK-BR-3 cells treated with DARPin-miniSOG

SK-BR-3 cells were grown in a McCoy's 5A medium (Life technologies, USA) with 1% fetal bovine serum (HyClone, Belgium) for 14 h. The culture medium was removed, the cells harvested and washed twice with sterile PBS. To remove the extracellular domain of the HER2 receptor, a suspension of 1.5×10^6 cells was incubated with 1% papain (AppliChem, Germany) at 37°C for 15min. The cells were washed with cold PBS and divided into seven portions. The first portion (the starting time point) was divided in half: the first half (~12.5×10^4 cells) was stained with DARPin-miniSOG (1 μM) at 4°C, the second half was used for autofluorescence normalization. The other six portions were incubated in a McCoy's medium with 1% serum in a 24-well plate in 5% CO_2 at 37°C and evaluated for fluorescence at the time points of 2, 4, 8, 12, 24 and 72 h. At each time point, the cells were detached with a Versen solution, washed with cold PBS, and divided in half. The first half was treated with DARPin-miniSOG, as described above, and the second half was left untreated. Green fluorescence was measured for each pair of samples at each time point.

RESULTS AND DISCUSSION

A targeted protein DARPin-miniSOG for selective elimination of human cancer cells under light irradiation was engineered at the laboratory of Dr. Deyev (IBCh RAS). A nonimmunoglobulin protein DARPin_9-29 recognizing HER2 with high affinity [6] was used as a targeting module in fusion protein DARPin-miniSOG. In contrast to the anti-HER2 4D5scFv that binds subdomain IV of the HER2 extracellular domain, DARPin_9-29 binds to subdomain I of HER2 [12]. The recombinant flavoprotein miniSOG, which is known to generate reactive oxygen species under blue light irradiation [10], was used as a cytotoxic module in fusion protein DARPin-miniSOG. Being in activated state, miniSOG emits green fluorescence (λ_{max}= 500 nm). So binding of DARPin-miniSOG to cells can be directly detected by flow cytometry.

Photoactivated toxin DARPin-miniSOG exerts a specific cytotoxic effect on HER2-positive cells, causing necrosis of irradiated cells *in vitro*.

In this study, we investigated DARPin-miniSOG interaction with HER2-overexpressing cancer cells and established if the cytotoxic module miniSOG in the fusion protein DARPin-miniSOG influenced the HER2-binding specificity of the targeted domain DARPin_9-29.

The binding specificity of targeting module DARPin_9-29 in the fusion protein was analyzed in a competitive inhibition assay by labeling SK-BR-3 cells expressing ~10^6 HER2 molecules per cell with the fluorescent fusion protein DARPin-miniSOG. Parental DARPin_9-29 was used as a competitive agent. SK-BR-3 cells were treated with DARPin-miniSOG (500 nM) or with an equimolar mixture of DARPin-miniSOG (500nM) and competitive agent DARPin_9-29 (500 nM). To quantify the fluorescence level, SK-BR-3 cells were incubated with the protein at 4°C: incubation at low temperature prevents the internalization of the complex receptor-protein.

We found that the mean fluorescence intensity of the cells treated with DARPin-miniSOG was 2-fold higher than that of the cells incubated with DARPin_9-29 and DARPin-miniSOG (*Fig. 1A*, red and green lines, respectively); i.e., DARPin_9-29 competes with DARPin-miniSOG for binding to SK-BR-3 cells. Importantly, the use of 4D5scFv, which recognizes a HER2 epitope different from that of DARPin_9-29, does not result in fluorescence decline (*Fig. 1A*, blue line). HER2-negative CHO cells show no fluorescence signal following incubation with DARPin-miniSOG (*Fig. 1B*). Overall, we showed that the targeted fusion protein DARPin-miniSOG selectively binds to human breast adenocarcinoma HER2 overexpressing cells. The presence of the cytotoxic module miniSOG in the fusion protein does not affect the functional qualities of the HER2 targeting module.

To gain insight into the interactions of the targeted phototoxin DARPin-miniSOG with tumor cells, we tracked the pathway of the receptor-protein complex following binding of DARPin-miniSOG with HER2-positive cells. We were concerned as to whether the bound HER2 would be internalized. If so, what is the post endocytic traffic of HER2 after ligand binding: recycling or degradation in late lysosomes?

Internalization of HER2 has become the focus of intense research. In general, internalization mechanisms of activated receptors of the epidermal growth factor receptor family (EGFR/HER1 and HER3) have been described in detail: receptor mediated endocytosis occurs after ligand binding [13]. After internalization the complex of receptor-ligand can undergo sorting in early endosomes (fast recycling) or in multivesicular bodies (slow recycling). In both cases the receptor recycles back to the cell surface. But there exists a third pathway for the receptor-ligand complex: degradation in lysosomes. The receptor pathway is determined by the sensitivity of a receptor-ligand complex to acidic degradation during traffic from endosomes to lysosomes. Less stable complexes dissociate early, which is followed by receptors recycling to the cell membrane. More stable complexes dissociate later, and receptors in a complex with ligands degrade in lysosomes [14].

In the current literature two different points of view on HER2 internalization exist. While several studies in-

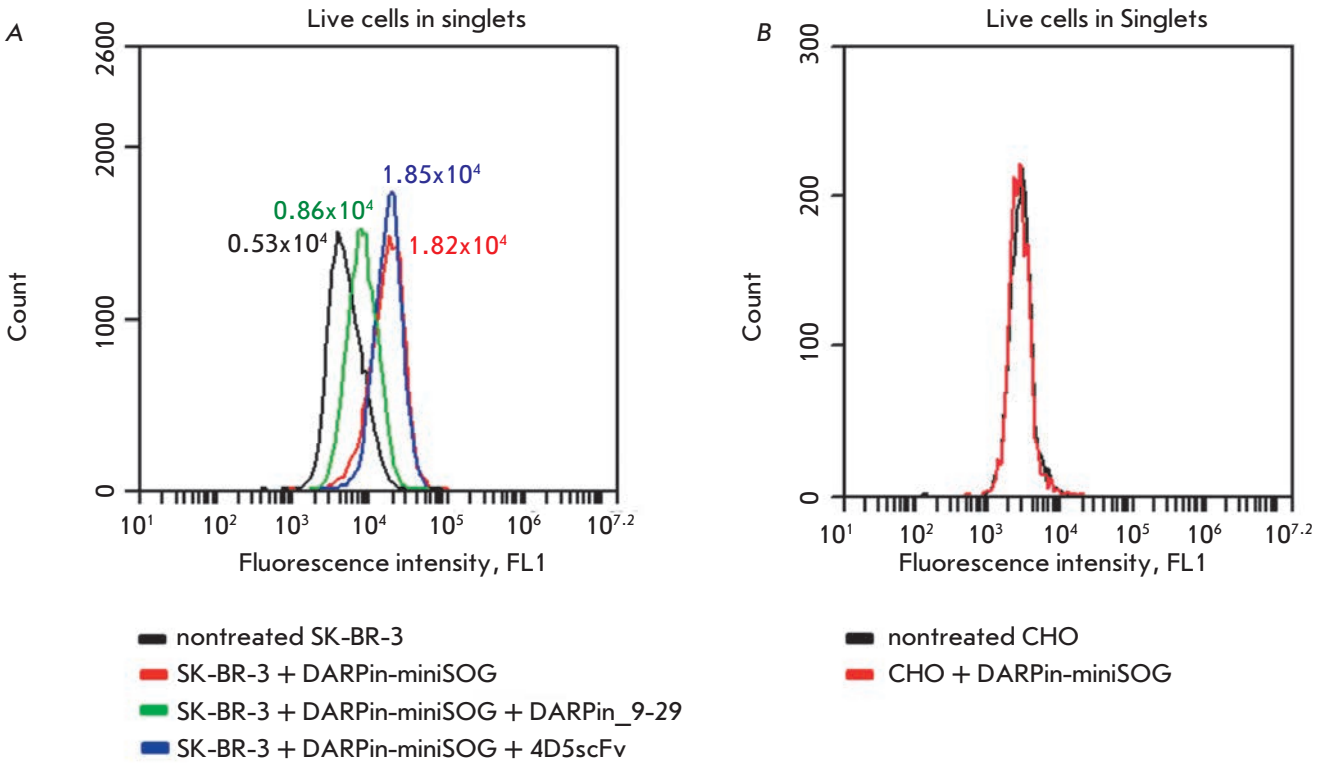

Fig. 1. DARPin-miniSOG specific interaction with human breast adenocarcinoma HER2 overexpressing SK-BR-3 cells. **A.** Flow cytometry analysis of HER2-positive SK-BR-3 cells. Cells were treated with: DARPin-miniSOG protein (red), DARPin-miniSOG protein in combination with competitive agent DARPin_9-29 (green), and DARPin-miniSOG protein in combination with non-competitive HER2-specific mini antibody 4D5scFv (blue). The autofluorescence of untreated SK-BR-3 cells is indicated with a black line. The means of fluorescence in the green channel (Mean FL1-A) for each sample are shown in the corresponding color near the peak. **B.** Flow cytometry analysis of HER2-negative CHO cells treated with DARPin-miniSOG (red line) and not treated cells (black line)

dicate that HER2 is endocytosis-resistant [15, 16], other studies indicate that HER2 is internalized and recycled back to the cell surface via an early endosome [17–19].

It is well established that, unlike other family members, HER2 has no natural ligands and lacks an internalization signal in its intracellular domain [20]. Therefore, it is impossible to study ligand-induced endocytosis of homodimers. There is evidence suggesting that HER2 expression inhibits formation of clathrine-coated pits [16, 21]. It was shown that upon ligand-induced heterodimerization with the other members of the EGFR family, HER2 inhibits down-regulation of the dimerization partners [22]. Trastuzumab (Herceptin), a humanized monoclonal antibody widely used in targeted therapy for HER2 positive breast cancer, is not able to promote HER2 internalization alone [23], as presumed previously. However, Trastuzumab induces HER2 internalization and intracellular degradation when combined with Pertuzumab (Perjeta), another noncompetitive anti-HER2 antibody, or L26 antibody that, similar to Pertuzumab, inhibits HER2 heterodimerization with the other members of the EGFR family [24–26].

Not only full-size antibodies, but also single-chain fragments (scFvs) have been shown to promote HER2 internalization. Ivanova and colleagues [27] reported that incubation of HER2-positive BT-474 cells with the recombinant protein 4D5scFv–dibarnase, consisting of two barnase molecules (a cytotoxic ribonuclease from *Bacillus amyloliquefaciens*) and the single-chain variable fragment of humanized anti-HER2-antibody 4D5, leads to receptor removal from the cell surface at 37°C. The internalized receptor is localized in endosomes and multivesicular bodies [27]. HER2 internalization can also occur following exposure to the fusion protein DARPin-mCherry, recognizing the extracellular domain of HER2 [28].

In this work we studied HER2 internalization induced by DARPin-miniSOG binding.

The overview of the experiment is illustrated in *Fig. 2A*. The fluorescence levels of cells treated with DARPin-miniSOG at 4°C (conditions abolishing in-

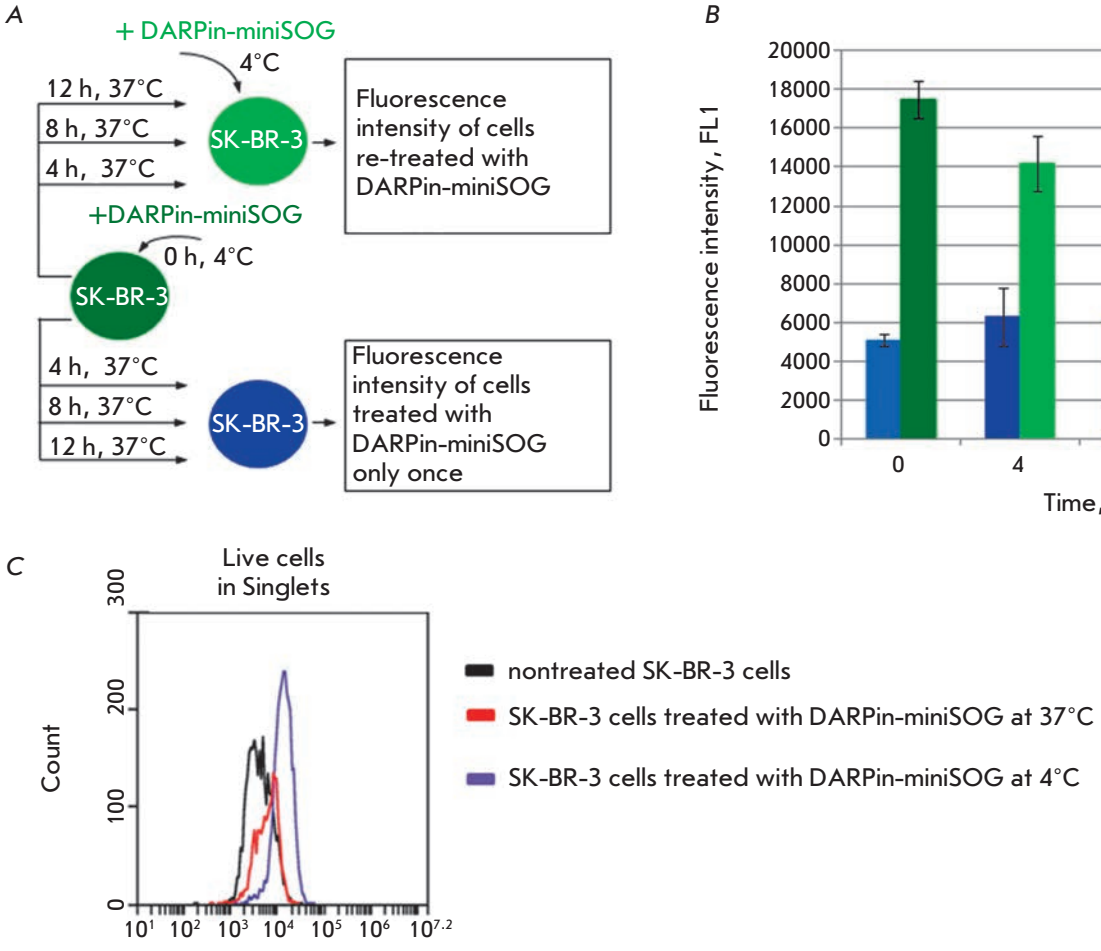

Fig. 2. DARPin-miniSOG interaction with the HER2 on SK-BR-3 cells. **A.** Overview of the experiment. **B.** Histogram showing fluorescence of HER2-positive SK-BR-3 cells labeled with the targeted protein DARPin-miniSOG. The light blue column shows the mean autofluorescence of control SK-BR-3 cells, the deep green column shows the mean fluorescence of SK-BR-3 cells once treated with DARPin-miniSOG at 4°C. The blue columns show the means fluorescences of cells treated with DARPin-miniSOG at 4°C, followed by incubation at 37°C for 4, 8 and 12 h, respectively. The light green columns show the means fluorescences of SK-BR-3 cells treated with DARPin-miniSOG at 4°C, followed by incubation at 37°C for 4, 8 and 12 h and re-treated with DARPin-miniSOG at 4°C. The error bars indicate the standard deviations calculated from two independent experiments. **C.** Flow cytometry analysis of SK-BR-3 cells incubated with DARPin-miniSOG under different conditions

ternalization) were analyzed (*Fig. 2B*, dark green column, time point 0 h) compared to autofluorescence (*Fig. 2B*, blue column, time point 0 h). Then these cells were incubated at 37°C in a CO_2-incubator (internalization conditions). After incubation at time points 4, 8 and 12 h the fluorescence levels were measured (*Fig. 2B*, dark blue columns, time points 4, 8 and 12 h, respectively) and re-analyzed after re-treatment of cells with DARPin-miniSOG on ice (*Fig. 2B*, light green columns, time points 4, 8 and 12 h, respectively). It should be noted that the concentration of DARPin-miniSOG was in excess of the receptor molecules on the cell surface.

The internalization of the complex HER2/DARPin-miniSOG is suggested by a reduction in the SK-BR-3 cell fluorescence after treatment with DARPin-miniSOG at 37°C as compared to the fluorescence of cells exposed to DARPin-miniSOG at 4°C: a 10-min incubation at 37°C leads to a 2-fold decrease in fluorescence intensity (*Fig. 2C*). The mean fluorescence of SK-BR-3 cells pre-treated with DARPin-miniSOG at 4°C and further incubated at 37°C (internalization

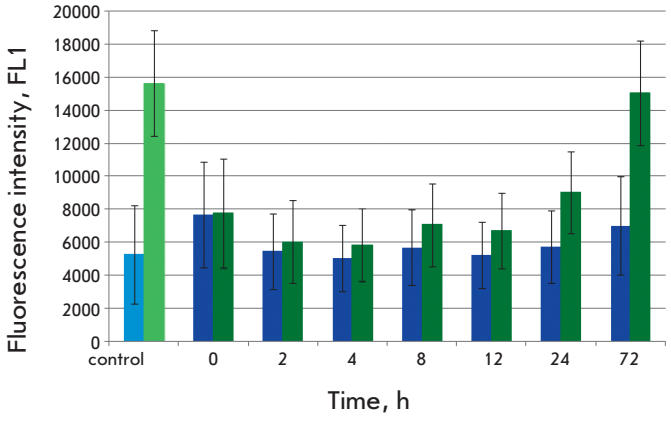

Fig. 3. Time course of fluorescence intensity of HER2-truncated SK-BR-3 cells treated with DARPin-miniSOG. SK-BR-3 cells nontreated with papain were used as a control: the light blue column shows the mean autofluorescence of the control SK-BR-3 cells, the light green column shows the mean fluorescence of SK-BR-3 cells treated with DARPin-miniSOG at 4°C. The blue columns show the means fluorescences of SK-BR-3 cells treated with papain at each time point. The dark green columns show the means fluorescences of SK-BR-3 cells treated with papain at time point 0 h and treated with DARPin-miniSOG at 4°C at time points 2, 4, 8, 12, 24, and 72 h respectively. The error bars show the standard deviations

conditions) is 1.4-fold higher at time point 4 h and 1.3-fold higher at time point 8 h compared to the mean background autofluorescence but returns to the initial autofluorescence at time point 12 h (*Fig. 2B*, blue columns).

The ability of SK-BR-3 cells to rebind DARPin-miniSOG at 4°C compared to control SK-BR-3 cells, once treated with DARPin-miniSOG at 4°C (dark green column), declines by 1.2-fold at time point 4 h and by 1.4-fold at time point 8 h (*Fig. 2B*, light green columns). At time point 12 h the ability of SK-BR-3 cells to bind DARPin-miniSOG at 4°C completely recovers.

The ability of SK-BR-3 cells to rebind DARPin-miniSOG after incubation at 37°C could result from a dissociation of the complex HER2/DARPin-miniSOG and HER2 recycling to the membrane, as well as from *de novo* synthesis of new receptor molecules.

To estimate the contribution of *de novo* receptor biosynthesis we studied the kinetics of staining SK-BR-3 cells with DARPin-miniSOG if the extracellular domain of HER2 was truncated by papain from the cell surface. The fluorescence level of HER2-truncated SK-BR-3 cells treated with DARPin-miniSOG was 43% after 12 h and 57% after 24 h compared to the fluorescence level of HER2-positive SK-BR-3 cells treated with DARPin-miniSOG. The fluorescence level of HER2-truncated SK-BR-3 cells returned to the initial level only after 72 h (*Fig. 3*). This observation suggests that in 12 h time HER2-truncated SK-BR-3 cells fail to completely recover the HER2 receptor density on their surface (*Fig. 3*).

The results from this study show that the HER2 density on SK-BR-3 cells changes in response to stimulation: when DARPin-miniSOG interacts with HER2, the HER2/DARPin-miniSOG complex internalizes, which leads to a decrease in the number of HER2 molecules on the cell surface and, accordingly, to a decrease in the fluorescence intensity of cells re-treated with DARPin-miniSOG (*Fig. 2*). After ~12 h, the mean fluorescence intensity of re-treated cells returns to its initial level. In conclusion, taking into account the experiments and dynamics of *de novo* biosynthesis of HER2 we conclude that after internalization of the HER2/DARPin-miniSOG complex, its dissociation occurs and the HER2 receptor returns slowly on the cell membrane. The pool of *de novo* synthesized HER2 receptors is not significant and does not noticeably affect the mean fluorescence values of the stained cells.

CONCLUSION

In this work, we have reported on the interaction of the fusion protein DARPin-miniSOG with HER2 receptors. It was found that DARPin-miniSOG induced HER2 internalization followed by recycling of HER2 back to the cell surface. These findings are important for the further development of treatment for HER2-positive cancer using a novel phototoxic protein DARPin-miniSOG. ●

This work was supported by the Russian Science Foundation (grant 14-24-00106).

REFERENCES

1. Deyev S.M., Lebedenko E.N. // Acta Naturae. 2009. V. 1. № 1. P. 32–50.
2. Deyev S.M., Lebedenko E.N. // Bioessays. 2008. V. 30. № 9. P. 904–918.
3. Boersma Y.L., Plückthun A. // Curr. Opin. Biotechnol. 2011. V. 22. № 6. P. 849–857.
4. Löfblom J., Frejd F.Y., Ståhl S. // Curr. Opin. Biotechnol. 2011. V. 22. № 6. P. 843–848.
5. Deyev S.M., Lebedenko E.N., Petrovskaya L.E., Dolgikh D.A., Gabibov A.G., Kirpichnikov M.P. // Russ. Chem. Rev. 2015. V. 84. № 1. P. 1–26.
6. Steiner D., Forrer P., Plückthun A. // J. Mol. Biol. 2008. V. 382. № 5. P. 1211–1227.
7. Slamon D.J., Clark G.M., Wong S.G., Levin W.J., Ullrich A., McGuire W.L. // Science. 1987. V. 235. № 4785. P. 177–182.
8. Slamon D.J., Godolphin W., Jones L.A., Holt J.A., Wong S.G., Keith D.E., Levin W.J., Stuart S.G., Udove J., Ullrich A.

// Science. 1989. V. 244. № 4905. P. 707–712.
9. Holbro T., Hynes N.E. // Annu. Rev. Pharmacol. Toxicol. 2004. V. 44. P. 195–217.
10. Shu X., Lev-Ram V., Deerinck T.J., Qi Y., Ramko E.B., Davidson M.W., Jin Y., Ellisman M.H., Tsien R.Y. // PLoS Biol. 2011. V. 9. № 4. e1001041.
11. Mironova K.E., Proshkina G.M., Ryabova A.V., Stremovskiy O.A., Lukyanov S.A., Petrov R.V., Deyev S.M. // Theranostics. 2013. V. 3. № 11. P. 831–840.
12. Jost C., Schilling J., Tamaskovic R., Schwill M., Honegger A., Plückthun A. // Structure. 2013. V. 21. № 11. P. 1979–1991.
13. Sorkin A., Goh L.K. // Exp. Cell Res. 2009. V. 315. № 4. P. 683–696.
14. Sorkin A., Waters C.M. // Bioessays. 1993. V. 15. № 6. P. 375–382.
15. Hommelgaard A.M., Lerdrup M., van Deurs B. // Mol. Biol. Cell. 2004. V. 15. № 4. P. 1557–1567.
16. Haslekas C., Breen K., Pedersen K.W., Johannessen L.E., Stang E., Madshus I.H. // Mol. Biol. Cell. 2005. V. 16. № 12. P. 5832–5842.
17. Harari D., Yarden Y. // Oncogene. 2000. V. 19. № 53. P. 6102–6114.
18. Hendriks B.S., Opresko L.K., Wiley H.S., Lauffenburger D. // Cancer Res. 2003. V. 63. № 5. P. 1130–1137.
19. Austin C.D., de Maziere A.M., Pisacane P.I., van Dijk S.M., Eigenbrot C., Sliwkowski M.X., Klumperman J., Scheller R.H. // Mol. Biol. Cell. 2004. V. 15. № 12. P. 5268–5282.
20. Sorkin A., Di Fiore P.P., Carpenter G. // Oncogene. 1993. V. 8. № 11. P. 3021–3028.
21. Cortese K., Howes M.T., Lundmark R., Tagliatti E., Bagnato P., Petrelli A., Bono M., McMahon H.T., Parton R.G., Tacchetti C. // Mol. Biol. Cell. 2013. V. 24. № 2. P. 129–144.
22. Wang Z., Zhang L., Yeung T.K., Chen X. // Mol. Biol. Cell. 1999. V. 10. № 5. P. 1621–1636.
23. Longva K.E., Pedersen N.M., Haslekas C., Stang E., Madshus I.H. // Int. J. Cancer. 2005. V. 116. № 3. P. 359–367.
24. Ben-Kasus T., Schechter B., Lavi S., Yarden Y., Sela M. // Proc. Natl. Acad. Sci. USA. 2009. V. 106. № 9. P. 3294–3299.
25. Nahta R., Hung M.C., Esteva F.J. // Cancer Res. 2004. V. 64. № 7. P. 2343–2346.
26. Friedman L.M., Rinon A., Schechter B., Lyass L., Lavi S., Bacus S.S., Sela M., Yarden Y. // Proc. Natl. Acad. Sci. USA. 2005. V. 102. № 6. P. 1915–1920.
27. Ivanova J.L., Edelweiss E.F., Leonova O.G., Balandin T.G., Popenko V.I., Deyev S.M. // Biochimie. 2012. V. 94. № 8. P. 1833–1836.
28. Mironova K.E., Chernykh O.N., Ryabova A.V., Stremovkiy O.A., Proshkina G.M., Deyev S.M. // Biochemistry (Mosc). 2014. V. 79. № 12. P. 1698–1704.

Apigenin Inhibits Growth of Breast Cancer Cells: The Role of ERα and HER2/neu

A. M. Scherbakov*, O. E. Andreeva
Blokhin N. N. Russian Cancer Research Center, Kashirskoye Shosse, 24, Moscow, 115478, Russia
*E-mail: alex.scherbakov@gmail.com
Received: 18.03.2015

ABSTRACT **Phytoestrogens are a group of plant-derived compounds with an estrogen-like activity. In mammalians, phytoestrogens bind to the estrogen receptor (ER) and participate in the regulation of cell growth and gene transcription. There are several reports of the cytotoxic effects of phytoestrogens in different cancer cell lines. The aim of this study was to measure the phytoestrogen activity against breast cancer cells with different levels of ER expression and to elucidate the molecular pathways regulated by the leader compound. Methods used in the study include immunoblotting, transfection with a luciferase reporter vector, and a MTT test. We demonstrated the absence of a significant difference between ER+ and ER− breast cancer cell lines in their response to cytotoxic stimuli: treatment with high doses of phytoestrogens (apigenin, genistein, quercetin, naringenin) had the same efficiency in ER-positive and ER-negative cells. Incubation of breast cancer cells with apigenin revealed the highest cytotoxicity of this compound; on the contrary, naringenin treatment resulted in a low cytotoxic activity. It was shown that high doses of apigenin (50 μM) do not display estrogen-like activity and can suppress ER activation by 17β-estradiol. Cultivation of HER2-positive breast cancer SKBR3 cells in the presence of apigenin resulted in a decrease in HER2/neu expression, accompanied by cleavage of an apoptosis substrate PARP. Therefore, the cytotoxic effects of phytoestrogens are not associated with the steroid receptors of breast cancer cells. Apigenin was found to be the most effective phytoestrogen that strongly inhibits the growth of breast cancer cells, including HER2-positive ones.**
KEYWORDS **breast cancer, phytoestrogens, estrogen receptor, HER2/neu.**

INTRODUCTION

Breast cancer is the most common cancer in females, ranking second in the incidence rate after skin neoplasms in the Russian population [1–4]. The search for new prospective compounds that could inhibit the development of breast cancer and the analysis of their impact on tumor cells is one of the priorities in oncology. Given the important role of hormones in the development of reproductive system tumors, compounds structurally similar to estrogens, e.g., phytoestrogens, are of particular interest. Phytoestrogens are plant-derived compounds with steroid-like structures [5]. Because of their "hormonal" properties, phytoestrogens are also referred to as "food hormones." Phytoestrogens are unique in their paradoxical effect on cells: depending on the conditions, they can either inhibit tumor growth or act as cell protectors [5–7].

Initially, interest in phytoestrogen research arose from the analysis of epidemiological data showing a reduced rate of tumor incidence and cancer mortality in a number of geographical areas with high consumption of fruits and vegetables [8–10]. A study by Knekt *et al.* [8], which was conducted in Finland, included 9,959 individuals who were followed from 1967 to 1991 and whose individual consumption of phytoestrogens with food was analyzed. A total of 997 cases of cancer (ca. 10% of the complete sample) were identified over the entire period of the study, including 151 cases of lung cancer. A statistical analysis showed that the relative risk of cancers (all localizations) in a group with high consumption of phytoestrogens was reduced to 0.8 (the risk level in a group with low consumption of phytoestrogens was taken as 1). The most significant results were obtained upon analysis of the incidence rate of lung cancer; the risk dropped to 0.54 in the group with high consumption of phytoestrogens [8]. Similar tendencies were found upon examination of 1,031 ovarian cancer females and 2,411 healthy donors in Italy over a period between 1992 and 1999 [11]. According to Rossi *et al.* [11], the risk of ovarian cancer dropped to 0.63 in the group with high consumption of flavonols (in particular, quercetin) and to 0.51 in the group with high

consumption of foods rich in isoflavones (e.g., genistein). Therefore, the epidemiological data indicate the advisability of increased consumption of foods rich in phytoestrogens to prevent cancer.

However, the epidemiological data do not reveal the molecular mechanisms by which phytoestrogens affect tumor cells and/or protect normal cells from malignant transformation. This is why an extensive search for the main intracellular targets of these compounds is currently underway in *in vitro* models [12–17]. The key targets of phytoestrogens in tumor cells are believed to be receptor tyrosine kinases, including the epidermal growth factor receptor (EGFR) [18–20], fibroblast growth factor receptor 2 (FGFR2) [21], HER2/neu [22], vascular endothelial growth factor receptor 3 (VEGFR3) [21, 23], the platelet-derived growth factor receptor alpha and beta (PDGFRα and ß) [21], etc. In addition to receptors, some members of the phytoestrogen class effectively inhibit the intracellular kinases involved in the regulation of cell proliferation and cell survival, such as p21-activated kinase 3 (PAK3), phosphatidylinositol 3-kinase (PI3K), Akt, PIM1, Aurora-A, Janus kinase 3 (JAK3), etc. [15, 16, 21]. The wide range of the potential targets of phytoestrogens makes these compounds promising for further experimental and clinical studies.

Is the estrogen receptor (ER) required for the antiproliferative effect of phytoestrogens on tumor cells, and is the hormone-like effect of phytoestrogens concentration-dependent? There is no definite answer to these questions [5, 6, 17]. The aim of this study was to investigate the effect of members of the main groups of phytoestrogens on breast cancer cells with various ER statuses and to analyze the molecular pathways responsible for the antiproliferative and cytotoxic effects of a leader compound. Using human breast cancer cell lines, we demonstrated that the antiproliferative effect of high doses of phytoestrogens (apigenin, genistein, quercetin, naringenin) did not depend on the status of steroid hormone receptors. *In vitro* experiments revealed a similar efficacy of these compounds in a ER-positive MCF-7 cell line and ER-negative SKBR3 model. The maximum antiproliferative effect was observed for flavone apigenin that was analyzed in more detail as the leader compound. An increase in apigenin concentrations from 5 to 50 μM in MCF-7 cells was demonstrated to result in a "switch" from estrogen-like (similar to the effect of 17β-estradiol, a natural ligand of ERα) to anti-estrogenic effects (similar to the effect of antiestrogen drugs): a high apigenin dose inhibited activation of estrogen receptors by 17β-estradiol. ER-negative SKBR3 breast cancer cells are known to be characterized by a high level of HER2/neu, one of the key receptors defining the high aggressiveness and

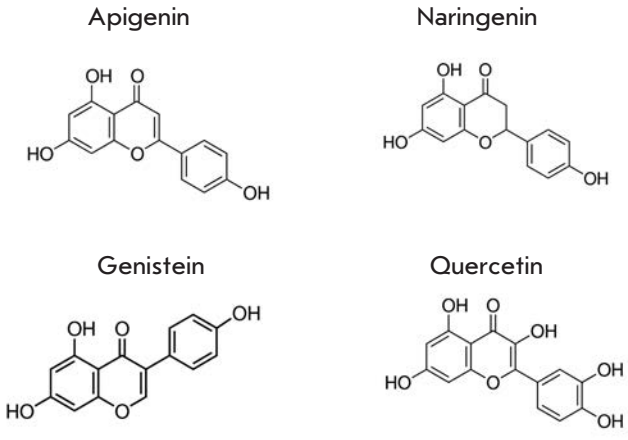

Fig. 1. Chemical structures of phytoestrogens (apigenin, naringenin, genistein, quercetin)

survival of tumor cells [24]. Immunoblotting demonstrated that apigenin at a dose of above 25 μM reduces the expression of HER2/neu in SKBR3 cells, with a simultaneous degradation of the apoptosis effect or substrate poly ADP-ribose polymerase (PARP). Apigenin was the most promising among the tested compounds, demonstrating significant inhibition of growth of breast cancer cells with various ERα statuses, including HER2-positive ones.

MATERIALS AND METHODS

Phytoestrogens from various groups were studied: apigenin (flavone), naringenin (flavanone), genistein (isoflavone), and quercetin (flavonol). Quercetin, genistein, and naringenin were purchased from Sigma-Aldrich (USA), apigenin was from Enzo Biochem (USA); the chemical purity of each compound was at least 97%. The chemical structures of the compounds are shown in *Fig. 1*. The compounds were dissolved in dimethylsulfoxide at a concentration of 50 mM, and the solutions were stored until use at −20°C.

Human breast cancer cells MCF-7 (ERα+/HER2−) and SKBR3 (ERα−/HER2+) were obtained from the collection of the Blokhin N.N. Russian Cancer Research Center. The cell lines were cultured *in vitro* in a standard DMEM medium (Biolot, Russia) with 10% fetal calf serum (HyClone, USA) and gentamycin (50 U/mL, PanEco, Russia) at 37 °C, 5% of CO_2, and a relative humidity of 80–90%. The cell growth rate was determined using a MTT assay, based on the uptake of the MTT reagent (3-[4,5-dimethylthiazol-2]-2,5-diphenyltetrazolium bromide) by the living cells [25, 26].

To determine the transcriptional activity of ERα, the cells were transfected with a plasmid containing the luciferase reporter gene under the control of an ER-sensitive promoter (ERE/Luc); the plasmid was a kind

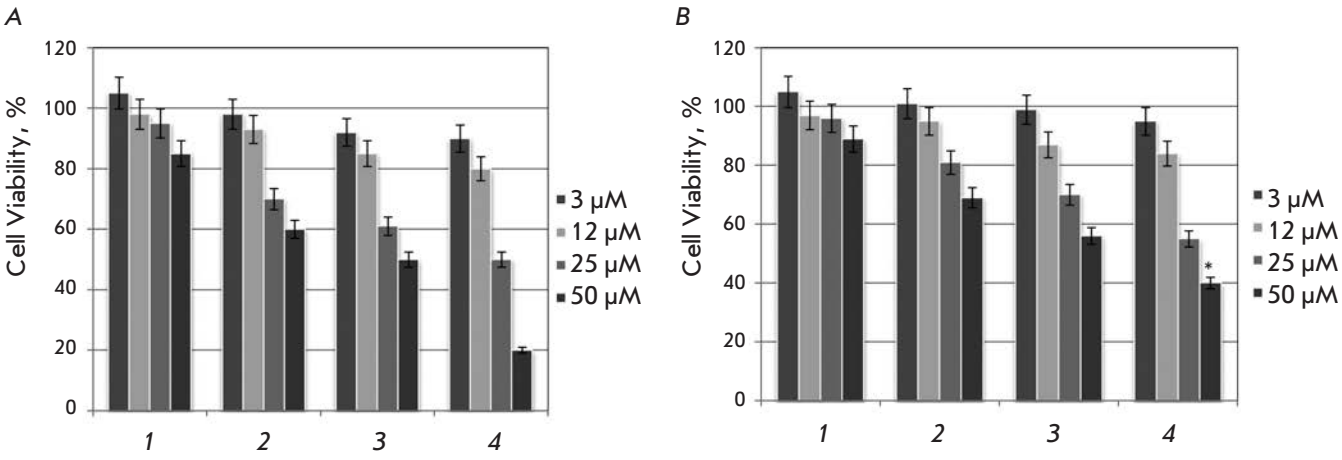

Fig. 2. Cytostatic effect of phytoestrogens on breast cancer cells MCF-7 (A) and SKBR3 (B). Data of a MTT test conducted after 3-day cell growth in the presence of phytoestrogens: 1 – naringenin, 2 – genistein, 3 – quercetin, 4 – apigenin. The chart shows the number of living cells after treatment with phytoestrogens. The number of control cells of an appropriate cell line is taken as 100%. * $p<0.05$ compared to the number of MCF-7 cells survived at an apigenin dose of 50 μM

IC_{50} of phytoestrogens

IC_{50}, μM	Naringenin	Genistein	Quercetin	Apigenin
MCF-7	> 50	> 50	50	25
SKBR3	> 50	> 50	> 50	30

gift from George Reid (European Molecular Biology Laboratory, Germany) [27]. The cells were transfected using a Metafectene® PRO reagent according to the manufacturer's recommendations (Biontex Laboratories, Germany). The efficacy and potential toxicity of the transfection was monitored by co-transfection of the cells with a plasmid containing the β-galactosidase gene. The luciferase activity was calculated in arbitrary units (ratio of the total luciferase activity to the galactosidase activity in samples).

For immunoblotting purposes, the cells at 80% confluency were detached from the dishes (60 mm, Corning, USA) into 1 mL of a phosphate buffer. To obtain a total cell extract, samples were added with 130 μL of the following buffer: 50 mM Tris-HCl pH 7.4, 1% SDS (sodium dodecyl sulfate), 1% Igepal CA-630, 0.25% Na deoxycholate, 150 mM NaCl, 1 mM EDTA (ethylenediaminetetraacetic acid), 1 mM PMSF (phenylmethanesulfonyl fluoride); 1 μg/mL of aprotinin, leupeptin, and pepstatin; and 1 mM Na orthovanadate and 1 mM NaF. Total cell extracts were sonicated on a SoniPrep 150 Plus disintegrator (MSE) (five cycles of 10 s each with an amplitude of 3.2) to reduce the viscosity of a solution. Cell extract samples were then centrifuged (10,000 *g*, 10 min, +4°C, Eppendorf 5417R centrifuge, Germany), and standard electrophoresis and immunoblotting procedures were performed. The levels of HER2/neu and PARP were determined by primary antibodies (Cell Signaling Technology, USA). Antibodies to β-actin (Cell Signaling Technology, USA) were used to monitor the effectiveness of immunoblotting and to normalize the results. Detection was performed using secondary horseradish peroxidase-conjugated antibodies (Jackson ImmunoResearch, USA) in the LAS 4000 system (GE HealthCare, USA). DATAPLOT software (USA) was used for statistical analysis. In all cases, the statistical criteria were considered to be significant at $p<0.05$; each experiment was performed at least in triplicate.

RESULTS AND DISCUSSION

Comparison of the cytotoxic properties of various groups of phytoestrogens with respect to breast cancer cells: selection of the leader compound

At the first stage of the study, the antiproliferative effect of high doses of phytoestrogens was evaluated

in the MTT test. ERα-positive cells of the MCF-7 line were seeded onto culture plates, and phytoestrogens apigenin (flavone), naringenin (flavanone), genistein (isoflavone), and quercetin (flavonol) were added after 24 h. 3-day incubation of cells with naringenin was found to have almost no antiproliferative effects. Genistein had a stronger proliferative effect and at the dose of 50 μM caused a 40% reduction in the number of living cells. Quercetin, a member of the flavonol group, exhibited a genistein-like activity. The highest antiproliferative effect was observed for apigenin (*Fig. 2A*) at a concentration of 50 μM (according to the MTT test data, 20% of MCF-7 cells compared with the control).

The ERα-negative SKBR3 cell line was used to answer the question of the possible impact of ERα expression on cell sensitivity to the antiproliferative action of phytoestrogens (at high concentrations). The distribution of SKBR3 cells by sensitivity to various phytoestrogens was similar to the distribution of ERα-positive MCF-7 cells. Naringenin was the least cytotoxic. Genistein and quercetin had a moderate antiproliferative effect. The highest antiproliferative activity was observed for apigenin: at a concentration of 50 μM, it caused the death of 60% of SKBR3 cells (3-day incubation with phytoestrogens, *Fig. 2B*). It should be noted that only quercetin (MCF-7 cells) and apigenin (MCF-7 and SKBR3 cells) reached the IC_{50} level (*Table*) after incubation of the cells with the phytoestrogens in the given range of concentrations (up to 50 μM). Therefore, naringenin and genistein are rather "weak" antiproliferative agents, and they should be tested in combination with compounds from other classes, e.g., antiestrogens of the SERM group (tamoxifen, etc.) and specific inhibitors of tyrosine kinases. Comparison of the number of viable MCF-7 and SKBR3 cells after 3-day incubation with 50 μM apigenin demonstrated that the SKBR3 line is more resistant to the cytostatic effect of apigenin than MCF-7 (40 and 20% of cells compared to the control, respectively, $p<0.05$). On the basis of this observation, we presumed that high doses of apigenin could inhibit both the estrogen receptor signaling pathway (important factor for the growth of MCF-7 cells) and receptor tyrosine kinases, in particular HER2/neu (overexpression of this receptor was detected in SKBR3 cells).

The results of this series of experiments indicate that apigenin has the maximum antiproliferative effect among the tested phytoestrogens. Therefore, we further examined the molecular mechanisms of the action of high doses of this phytoestrogen on breast cancer cells.

Effect of apigenin on the estrogen receptor activity

The tendencies discussed in the previous section indicate that the antiproliferative effect of phytoestrogens on breast cancer cells increases as their concentration increases. It is important to note that this effect is independent of the hormonal status of cells; however, the ERα-positive MCF-7 line is more sensitive to the antiproliferative action of high doses of apigenin (50 μM) than the ERα-negative SKBR3 line. We assumed that the increase in the concentration of apigenin is accompanied by a "switching-off" of the hormonal component of its action on breast cancer cells. To test this hypothesis, MCF-7 cells were transfected with a plasmid containing a reporter construct with the luciferase gene under the control of an estrogen-sensitive promoter. The cells were then transferred to a DMEM medium without phenol red (PanEco, Russia) and cultivated with addition of a 10% steroid-free fetal calf serum (HyClone, USA) for 24 h. The luciferase activity was measured after 7 h of cell growth in the presence of 17β-estradiol and apigenin. As shown in *Fig. 3*, low-dose apigenin had an estrogen-like effect and enhanced the inducing effect of 17β-estradiol on the estrogen receptor. A 10-fold increase in the apigenin concentration (to 50 μM) had the opposite effect: the phytoestrogen inhibited the estrogen receptor activity and prevented

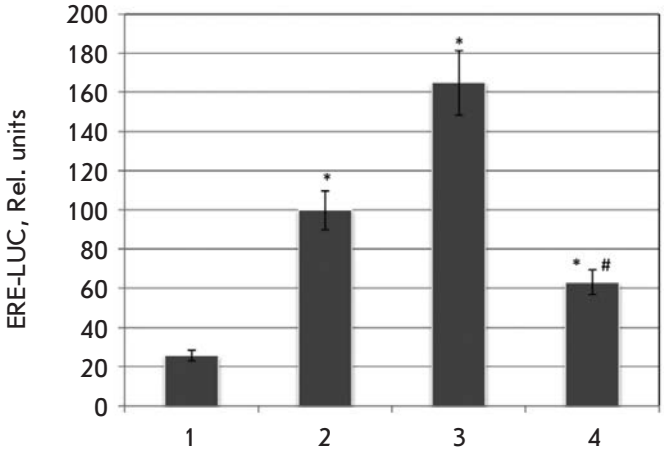

Fig. 3. The effect of apigenin on the 17β-estradiol-induced activity of the estrogen receptor. After transfection with a reporter plasmid, MCF-7 cells were seeded onto 24-well plates and after 24 h were treated with 17β-estradiol and apigenin (1 – control MCF-7 cells; 2 – 10 nM 17β-estradiol; 3 – 10 nM 17β-estradiol and 5 μM apigenin; 4 – 10 nM 17β-estradiol and 50 μM apigenin). The luciferase activity was measured after 7 h of cultivation in the presence of the phytoestrogens according to the standard protocol by the reagent's manufacturer (Promega, USA). * $p<0.05$ compared with control cells; # $p<0.05$ for comparing columns 4 and 3

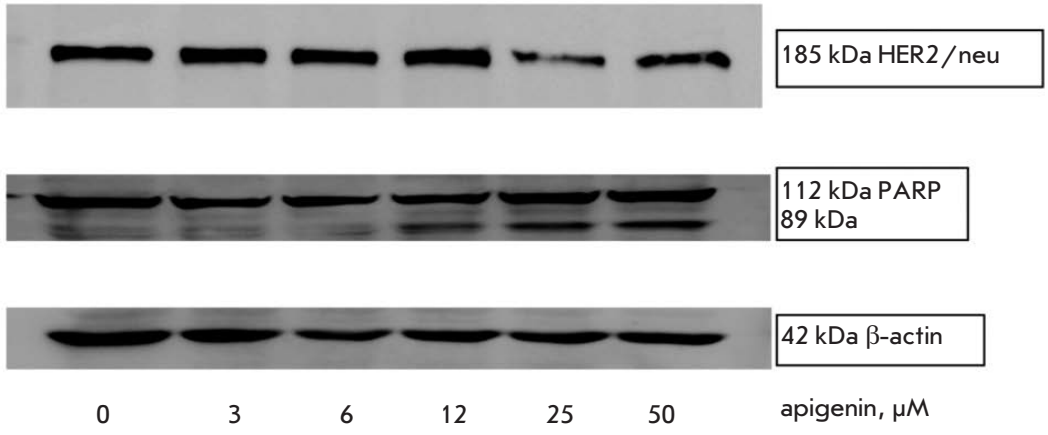

Fig. 4. The effect of apigenin on HER2/neu expression and PARP degradation in SKBR3 cells. SKBR3 cells were treated with the apigenin concentrations shown in the figure for 3 days. The results of one of three independent experiments are shown

the action of 17β-estradiol. Thus, the anti-estrogenic properties of apigenin may be one of the explanations for the cytostatic effects of its high (50 μM) doses. These findings partly explain the effect of apigenin on MCF-7 cells: apigenin blocks the main proliferative stimulus for this tumor line. Which "target" does apigenin block in a ERα-negative SKBR3 breast cancer cell line? This issue was examined in the next series of experiments.

Changes in the HER2/neu level during incubation of breast cancer cells with apigenin

The expression of HER2/neu is known to be detected in 10–30% of breast cancers, which is regarded as a marker of poor prognosis [28, 29]. We analyzed the effect of apigenin on the HER2/neu expression in SKBR3 cells that produce this protein in sufficient quantities. As seen in *Fig. 4*, apigenin at concentrations from 3 to 12 μM does not affect the HER2/neu level in SKBR3 cells. However, incubation of the cells with higher doses of apigenin (25 and 50 μM) results in significant inhibition of the HER2/neu expression. Immunoblotting with antibodies to the apoptosis effector substrate, PARP, revealed partial degradation of PARP (identified as accumulation of a truncated 89 kDa form of PARP) upon increasing the apigenin concentration in SKBR3 cells.

The ability of phytoestrogens to lower the HER2/neu level in tumor cells was discovered by Mai *et al.* [30] during incubation of the human breast cancer BT-474 cell line (HER2/neu+, ERα+) with 25 μM genistein. In addition, cultivation of BT-474 cells with genistein and an antiestrogen tamoxifen led to a further decrease in the expression of HER2/neu. A similar effect was observed for another member of the HER receptor family, EGFR (HER1) [30]. The phosphorylation level of HER2/neu and EGFR kinases was not analyzed, because the biological effect of genistein in this case was caused by a decrease in the level of its target protein (rather than by its activity). Sakla *et al.* [31] confirmed the data on the reduction in the HER2/neu level [30] and also showed that even at low doses (1 μM) genistein decreases the level of HER2/neu phosphorylation in BT-474 cells. Our data on a decrease in the HER2/neu level in SKBR3 cells upon incubation with apigenin are consistent with the results obtained in another cell model (MDA-MB-453 breast cancer line) [32]. It was shown that the phytoestrogens apigenin, luteolin, naringenin, eriodictyol, and hesperetin at high doses (40 μM) cause degradation of HER2/neu in MDA-MB-453 cells. Initiation of apoptosis upon incubation of the cells with apigenin was found to occur through the release of cytochrome *c* and activation of caspase 3. Summarizing our findings and published data, we conclude that high doses of apigenin reduce the expression of one of the major tyrosine kinases supporting the growth of HER2-positive cells and simultaneously initiate apoptotic processes.

CONCLUSION

The cytotoxic and antiproliferative effects of phytoestrogens on malignant cells are being extensively studied today [14, 33–38]. The interest in phytoestrogens is largely based on their natural origin and the relatively low cost of their synthesis and purification. In addition, there are data that support the prospects of their use for the prevention of cancer [38, 39]. Our work focuses on the investigation of the properties of flavone apigenin that exhibits a high antiproliferative activity in cells with various statuses of estrogen receptors. At high doses, apigenin was demonstrated to prevent the activation of the estrogen receptor by 17β-estradiol and cause inhibition of the HER2/neu expression, accompanied by a degradation of PARP in HER2-positive breast cancer cells. Other apigenin targets were iden-

tified in breast cancer cells, including proteins supporting the growth and survival of the tumor: PI3K/Akt [40], STAT3 [33], NF-κB [34], p53 [34, 41], p21 [41], JAK3 [42], cyclins D1, D3, and Cdk4 [43]and VEGF [44]. Apparently, apigenin is a multi-target compound that triggers breast cancer cell death through the inhibition of receptor tyrosine kinases, decreased expression of growth factors, activation of p53, and suppression of key transcription factors. In 2008, a phase II clinical trial (NCT00609310) of a drug containing 20 mg of apigenin and 20 mg of epigallocatechin gallate in patients with colorectal cancer was registered on the ClinicalTrials.gov database. The first batch of data from this study, regarding changes in the disease relapse rate in patients treated with a mixture of these phytoestrogens, is expected in 2016. No other clinical trials of apigenin (as an antitumor agent) are currently registered on ClinicalTrials.gov. Further investigation of the antitumor activity of apigenin and its synthetic derivatives is quite promising, particularly in relation to HER2-positive breast tumors. ●

The authors would like to thank M.A. Krasil'nikov for the discussion of the experimental results and the article and George Reid for providing the ERE/LUC plasmid.

This work was funded by grants from the Russian Science Foundation (№ 14-15-00362, experiments in section #2) and the Russian Foundation for Basic Research (№ 15-04-02172, experiments in sections #1 and 3).

REFERENCES

1. Merabishvili V.M. // Voprosy Onkologii. 2013. V. 59. № 3. P. 314–319.
2. DeSantis C.E., Lin C.C., Mariotto A.B., Siegel R.L., Stein K.D., Kramer J.L., Alteri R., Robbins A.S., Jemal A. // CA Cancer J. Clin. 2014. V. 64. № 4. P. 252–271.
3. DeSantis C., Ma J., Bryan L., Jemal A. // CA Cancer J. Clin. 2014. V. 64. № 1. P. 52–62.
4. Malignant tumors in Russia in 2013 (incidence and mortality). Eds.: A.D. Kaprin, V.V. Starinskiy, G.V. Petrova, 2015, Moscow: Herzen Moscow Oncology Research Institute. (In Russian).
5. Bilal I., Chowdhury A., Davidson J., Whitehead S. // World J. Clin. Oncol. 2014. V. 5. № 4. P. 705–712.
6. Patisaul H.B., Jefferson W. // Front Neuroendocrinol. 2010. V. 31. № 4. P. 400–419.
7. Bhukhai K., Suksen K., Bhummaphan N., Janjorn K., Thongon N., Tantikanlayaporn D., Piyachaturawat P., Suksamrarn A., Chairoungdua A. // J. Biol. Chem. 2012. V. 287. № 43. P. 36168–36178.
8. Knekt P., Jarvinen R., Seppanen R., Hellovaara M., Teppo L., Pukkala E., Aromaa A. // Am. J. Epidemiol. 1997. V. 146. № 3. P. 223–230.
9. Mourouti N., Panagiotakos D.B. // Maturitas. 2013. V. 76. № 2. P. 118–122.
10. Qu X.L., Fang Y., Zhang M., Zhang Y.Z. // Asian Pac. J. Cancer Prev. 2014. V. 15. № 21. P. 9085–9091.
11. Rossi M., Negri E., Lagiou P., Talamini R., Dal Maso L., Montella M., Franceschi S., La Vecchia C. // Internat. J. Cancer. 2008. V. 123. № 4. P. 895–898.
12. Spoerlein C., Mahal K., Schmidt H., Schobert R. // J. Inorg Biochem. 2013. V. 127. P. 107–115.
13. Harrison M.E., Power Coombs M.R., Delaney L.M., Hoskin D.W. // Exp. Mol. Pathol. 2014. V. 97. № 2. P. 211–217.
14. Bai H., Jin H., Yang F., Zhu H., Cai J. // Scanning. 2014. V. 36. № 6. P. 622–631.
15. Maurya A.K., Vinayak M. // Nutr. Cancer. 2015. V. 67. № 2. P. 354–363.
16. Li S.Z., Qiao S.F., Zhang J.H., Li K. // Anticancer Agents Med. Chem. 2015. V. 15 (9). P. 1185–1189.
17. Chen F.P., Chien M.H., Chern I.Y. // Climacteric. 2015. V. 18 (4). P. 574–581.
18. Gruca A., Krawczyk Z., Szeja W., Grynkiewicz G., Rusin A. // Molecules. 2014. V. 19. № 11. P. 18558–18573.
19. Gadgeel S.M., Ali S., Philip P.A., Wozniak A., Sarkar F.H. // Cancer. 2009. V. 115. № 10. P. 2165–2176.
20. Firdous A.B., Sharmila G., Balakrishnan S., RajaSingh P., Suganya S., Srinivasan N., Arunakaran J. // Food Funct. 2014. V. 5. № 10. P. 2632–2645.
21. Boly R., Gras T., Lamkami T., Guissou P., Serteyn D., Kiss R., Dubois J. // Internat. J. Oncol. 2011. V. 38. № 3. P. 833–842.
22. Huang C., Lee S.Y., Lin C.L., Tu T.H., Chen L.H., Chen Y.J., Huang H.C. // J. Agric. Food Chem. 2013. V. 61. № 26. P. 6430–6445.
23. Yu Z.J., He L.Y., Chen Y., Wu M.Y., Zhao X.H., Wang Z.Y. // Chinese journal of cellular and molecular immunology. 2009. V. 25. № 8. P. 678–680.
24. Longva K.E., Pedersen N.M., Haslekas C., Stang E., Madshus I.H. // Int. J. Cancer. 2005. V. 116. № 3. P. 359–367.
25. Iselt M., Holtei W., Hilgard P. // Arzneimittelforschung. 1989. V. 39. № 7. P. 747–749.
26. Merlin J.L., Azzi S., Lignon D., Ramacci C., Zeghari N., Guillemin F. // Eur. J. Cancer. 1992. V. 28A. № 8–9. P. 1452–1458.
27. Reid G., Hubner M.R., Metivier R., Brand H., Denger S., Manu D., Beaudouin J., Ellenberg J., Gannon F. // Mol. Cell. 2003. V. 11. № 3. P. 695–707.
28. Brufsky A.M. // Breast Cancer (Auckl). 2014. V. 8. P. 109–118.
29. Carey L.A., Perou C.M., Livasy C.A., Dressler L.G., Cowan D., Conway K., Karaca G., Troester M.A., Tse C.K., Edmiston S., et al. // JAMA. 2006. V. 295. № 21. P. 2492–2502.
30. Mai Z., Blackburn G.L., Zhou J.R. // Mol. Carcinogenesis. 2007. V. 46. № 7. P. 534–542.
31. Sakla M.S., Shenouda N.S., Ansell P.J., Macdonald R.S., Lubahn D.B. // Endocrine. 2007. V. 32. № 1. P. 69–78.
32. Way T.D., Kao M.C., Lin J.K. // FEBS Lett. 2005. V. 579. № 1. P. 145–152.
33. Seo H.S., Ku J.M., Choi H.S., Woo J.K., Jang B.H., Shin Y.C., Ko S.G. // Anticancer Res. 2014. V. 34. № 6. P. 2869–2882.
34. Seo H.S., Choi H.S., Kim S.R., Choi Y.K., Woo S.M., Shin I., Woo J.K., Park S.Y., Shin Y.C., Ko S.G. // Mol. Cell Biochem. 2012. V. 366. № 1–2. P. 319–334.

35. Sak K. // Pharmacogn. Rev. 2014. V. 8. № 16. P. 122–146.
36. Shukla S., Gupta S. // Pharm. Res. 2010. V. 27. № 6. P. 962–978.
37. Bilal I., Chowdhury A., Davidson J., Whitehead S. // World J. Clin. Oncol. 2014. V. 5. № 4. P. 705–712.
38. Kim S.H., Kim C.W., Jeon S.Y., Go R.E., Hwang K.A., Choi K.C. // Lab. Anim. Res. 2014. V. 30. № 4. P. 143–150.
39. Douglas C.C., Johnson S.A., Arjmandi B.H. // Anticancer Agents Med. Chem. 2013. V. 13. № 8. P. 1178–1187.
40. Lee W.J., Chen W.K., Wang C.J., Lin W.L., Tseng T.H. // Toxicol. Appl. Pharmacol. 2008. V. 226. № 2. P. 178–191.
41. Seo H.S., Ju J.H., Jang K., Shin I. // Nutr. Res. 2011. V. 31. № 2. P. 139–146.
42. Ye Q., Kantonen S., Gomez-Cambronero J. // J. Mol. Biol. 2013. V. 425. № 4. P. 755–766.
43. Way T.D., Kao M.C., Lin J.K. // FEBS Lett. 2005. V. 579. № 1. P. 145–152.
44. Mafuvadze B., Benakanakere I., Hyder S.M. // Menopause. 2010. V. 17. № 5. P. 1055–1063.

GENERAL RULES

Acta Naturae publishes experimental articles and reviews, as well as articles on topical issues, short reviews, and reports on the subjects of basic and applied life sciences and biotechnology.

The journal is published by the Park Media publishing house in both Russian and English.

The journal *Acta Naturae* is on the list of the leading periodicals of the Higher Attestation Commission of the Russian Ministry of Education and Science

The editors of *Acta Naturae* ask of the authors that they follow certain guidelines listed below. Articles which fail to conform to these guidelines will be rejected without review. The editors will not consider articles whose results have already been published or are being considered by other publications.

The maximum length of a review, together with tables and references, cannot exceed 60,000 symbols (approximately 40 pages, A4 format, 1.5 spacing, Times New Roman font, size 12) and cannot contain more than 16 figures.

Experimental articles should not exceed 30,000 symbols (20 pages in A4 format, including tables and references). They should contain no more than ten figures. Lengthier articles can only be accepted with the preliminary consent of the editors.

A short report must include the study's rationale, experimental material, and conclusions. A short report should not exceed 12,000 symbols (8 pages in A4 format including no more than 12 references). It should contain no more than four figures.

The manuscript should be sent to the editors in electronic form: the text should be in Windows Microsoft Word 2003 format, and the figures should be in TIFF format with each image in a separate file. In a separate file there should be a translation in English of: the article's title, the names and initials of the authors, the full name of the scientific organization and its departmental affiliation, the abstract, the references, and figure captions.

MANUSCRIPT FORMATTING

The manuscript should be formatted in the following manner:

- Article title. Bold font. The title should not be too long or too short and must be informative. The title should not exceed 100 characters. It should reflect the major result, the essence, and uniqueness of the work, names and initials of the authors.
- The corresponding author, who will also be working with the proofs, should be marked with a footnote *.
- Full name of the scientific organization and its departmental affiliation. If there are two or more scientific organizations involved, they should be linked by digital superscripts with the authors' names. Abstract. The structure of the abstract should be very clear and must reflect the following: it should introduce the reader to the main issue and describe the experimental approach, the possibility of practical use, and the possibility of further research in the field. The average length of an abstract is 20 lines (1,500 characters).
- Keywords (3 – 6). These should include the field of research, methods, experimental subject, and the specifics of the work. List of abbreviations.
- INTRODUCTION
- EXPERIMENTAL PROCEDURES
- RESULTS AND DISCUSSION
- CONCLUSION

  The organizations that funded the work should be listed at the end of this section with grant numbers in parenthesis.
- REFERENCES

  The in-text references should be in brackets, such as [1].

RECOMMENDATIONS ON THE TYPING AND FORMATTING OF THE TEXT

- We recommend the use of Microsoft Word 2003 for Windows text editing software.
- The Times New Roman font should be used. Standard font size is 12.
- The space between the lines is 1.5.
- Using more than one whole space between words is not recommended.
- We do not accept articles with automatic referencing; automatic word hyphenation; or automatic prohibition of hyphenation, listing, automatic indentation, etc.
- We recommend that tables be created using Word software options (Table → Insert Table) or MS Excel. Tables that were created manually (using lots of spaces without boxes) cannot be accepted.
- Initials and last names should always be separated by a whole space; for example, A. A. Ivanov.
- Throughout the text, all dates should appear in the "day.month.year" format, for example 02.05.1991, 26.12.1874, etc.
- There should be no periods after the title of the article, the authors' names, headings and subheadings, figure captions, units (s – second, g – gram, min – minute, h – hour, d – day, deg – degree).
- Periods should be used after footnotes (including those in tables), table comments, abstracts, and abbreviations (mon. – months, y. – years, m. temp. – melting temperature); however, they should not be used in subscripted indexes (T_m – melting temperature; $T_{p.t}$ – temperature of phase transition). One exception is mln – million, which should be used without a period.
- Decimal numbers should always contain a period and not a comma (0.25 and not 0,25).
- The hyphen ("-") is surrounded by two whole spaces, while the "minus," "interval," or "chemical bond" symbols do not require a space.
- The only symbol used for multiplication is "×"; the "×" symbol can only be used if it has a number to its right. The "·" symbol is used for denoting complex compounds in chemical formulas and also noncovalent complexes (such as DNA·RNA, etc.).
- Formulas must use the letter of the Latin and Greek alphabets.

- Latin genera and species' names should be in italics, while the taxa of higher orders should be in regular font.
- Gene names (except for yeast genes) should be italicized, while names of proteins should be in regular font.
- Names of nucleotides (A, T, G, C, U), amino acids (Arg, Ile, Val, etc.), and phosphonucleotides (ATP, AMP, etc.) should be written with Latin letters in regular font.
- Numeration of bases in nucleic acids and amino acid residues should not be hyphenated (T34, Ala89).
- When choosing units of measurement, SI units are to be used.
- Molecular mass should be in Daltons (Da, KDa, MDa).
- The number of nucleotide pairs should be abbreviated (bp, kbp).
- The number of amino acids should be abbreviated to aa.
- Biochemical terms, such as the names of enzymes, should conform to IUPAC standards.
- The number of term and name abbreviations in the text should be kept to a minimum.
- Repeating the same data in the text, tables, and graphs is not allowed.

GUIDENESS FOR ILLUSTRATIONS

- Figures should be supplied in separate files. Only TIFF is accepted.
- Figures should have a resolution of no less than 300 dpi for color and half-tone images and no less than 500 dpi.
- Files should not have any additional layers.

REVIEW AND PREPARATION OF THE MANUSCRIPT FOR PRINT AND PUBLICATION

Articles are published on a first-come, first-served basis. The publication order is established by the date of acceptance of the article. The members of the editorial board have the right to recommend the expedited publishing of articles which are deemed to be a priority and have received good reviews.

Articles which have been received by the editorial board are assessed by the board members and then sent for external review, if needed. The choice of reviewers is up to the editorial board. The manuscript is sent on to reviewers who are experts in this field of research, and the editorial board makes its decisions based on the reviews of these experts. The article may be accepted as is, sent back for improvements, or rejected.

The editorial board can decide to reject an article if it does not conform to the guidelines set above.

A manuscript which has been sent back to the authors for improvements requested by the editors and/or reviewers is reviewed again, after which the editorial board makes another decision on whether the article can be accepted for publication. The published article has the submission and publication acceptance dates set at the beginning.

The return of an article to the authors for improvement does not mean that the article has been accepted for publication. After the revised text has been received, a decision is made by the editorial board. The author must return the improved text, together with the original text and responses to all comments. The date of acceptance is the day on which the final version of the article was received by the publisher.

A revised manuscript must be sent back to the publisher a week after the authors have received the comments; if not, the article is considered a resubmission.

E-mail is used at all the stages of communication between the author, editors, publishers, and reviewers, so it is of vital importance that the authors monitor the address that they list in the article and inform the publisher of any changes in due time.

After the layout for the relevant issue of the journal is ready, the publisher sends out PDF files to the authors for a final review.

Changes other than simple corrections in the text, figures, or tables are not allowed at the final review stage. If this is necessary, the issue is resolved by the editorial board.

FORMAT OF REFERENCES

The journal uses a numeric reference system, which means that references are denoted as numbers in the text (in brackets) which refer to the number in the reference list.

For books: the last name and initials of the author, full title of the book, location of publisher, publisher, year in which the work was published, and the volume or issue and the number of pages in the book.

For periodicals: the last name and initials of the author, title of the journal, year in which the work was published, volume, issue, first and last page of the article. Must specify the name of the first 10 authors. Ross M.T., Grafham D.V., Coffey A.J., Scherer S., McLay K., Muzny D., Platzer M., Howell G.R., Burrows C., Bird C.P., et al. // Nature. 2005. V. 434. № 7031. P. 325–337.

References to books which have Russian translations should be accompanied with references to the original material listing the required data.

References to doctoral thesis abstracts must include the last name and initials of the author, the title of the thesis, the location in which the work was performed, and the year of completion.

References to patents must include the last names and initials of the authors, the type of the patent document (the author's rights or patent), the patent number, the name of the country that issued the document, the international invention classification index, and the year of patent issue.

The list of references should be on a separate page. The tables should be on a separate page, and figure captions should also be on a separate page.

The following e-mail addresses can be used to contact the editorial staff: vera.knorre@gmail.com, actanaturae@gmail.com, tel.: (495) 727-38-60, (495) 930-87-07

Russian NanoTechnologies journal turns 10 this year